A STUDY ON MECHANISTIC-EMPIRICAL DESIGN OF FLEXIBLE ROAD PAVEMENT AND OVERLAY USING METHOD OF EQUIVALENT THICKNESS

Thesis submitted

by

MANOJ KUMAR SAHIS

Doctor of Philosophy (Engineering)

DEPARTMENT OF CONSTRUCTION ENGINEERING
FACULTY COUNCIL OF ENGINEERING AND TECHNOLOGY
JADAVPUR UNIVERSITY
KOLKATA-700032, INDIA
2024

JADAVPUR UNIVERSITY
KOLKATA-700032, INDIA

1. Title of The Thesis: **A Study on Mechanistic - Empirical Design of Flexible Road Pavement and Overlay Using Method of Equivalent Thickness**

2. **Name , Designation & Institution of Supervisor : Dr. Partha Pratim Biswas**

Professor,
Department of Construction Engineering,
Jadavpur University, Salt Lake Campus, Sector-III, Block –LB, Plot-8
Kolkata-700106, India
Phone: 9830404294 (Mob), (033) 2335-5211 (O)
Fax: (033) 2335-7254
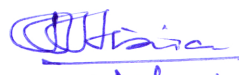
3. **List of Publications**

Papers published in International journal

1. Sahis, M. K., Biswas, P. P., Sadhukhan, S., & Saha, G. (2023). Mechanistic-Empirical Design of Perpetual Road Pavement Using Strain-based Design Approach. Periodica Polytechnica Civil Engineering, 67(4), 1105-1114.

2. Sahis, M. K., Biswas, P. P., & Saha, G. (2021). Mechanistic-Empirical Design of Overlay Based on Vertical Interface Stress and Curvature Index of Deflection Basin. Jordan Journal of Civil Engineering, 15(3).

3. Sahis, M. K., & Biswas, P. P. (2021). Optimization of Bituminous Pavement Thickness Using Mechanistic-Empirical Strain-Based Design Approach. Civil Engineering Journal, 7(5), 804-815.

4. Sahis, M. K., Biswas, P. P., Paul, S., & Banerjee, A. (2023, January 20). Determination of Compacted Subgrade Thickness to achieve an Effective CBR Based on Subgrade Deflection Using Odemark's Method. International Journal of Civil Engineering, 11(1), 9–17. https://doi.org/10.14445/23488352/ijce-v11i1p102

5. Purakayastha, S., Biswas, P. P., & Sahis, M. K. (2020). Determination Of Bituminous Overlay Thickness of Flexible Pavement by Mechanistic-Empirical Approach Based on Concentration Factor. International Journal of Pavement Research and Technology, 13, 222-227.

6. Biswas, P.P & Sahis, M.K & Mondal, G.C & Majumdar, D. (2016). Design of Low Volume Rural Roads with Unbound Granular Materials using Odemark's Method. International Journal of Engineering Research and Technology, V5. 10.17577/IJERTV5IS060520.

Papers published in International and National conference

1. Purakayastha, S., Biswas, P. P., Sahis, M. K., & Mondal, G. C. (2022). Characterization of Layer Index in Bituminous Pavement Using Mechanistic-Empirical Approach Based on Concentration Factor in a Layered System. In Proceedings of the RILEM International Symposium on Bituminous Materials: ISBM Lyon 2020 *1* (pp. 347-354). Springer International Publishing.

2. Biswas, P. P., Sahis, M. K., Mandal, G & Majumder, D. (2017). A Mechanistic-Empirical Design Concept for Low Volume Flexible Pavement Using Unbound Granular Materials with Application of Concentration Factor in a Layered System.531-536. 10.1201/9781315100333-76.

3. Biswas, P. P., Sahis, M. K., & Sengupta, A. (2021). Determination of Compacted Subgrade Thickness on Weak Subgrade Using Odemark's Method Based on Mechanistic-Empirical Design Approach. In Proceedings of the Indian Geotechnical Conference 2019: IGC-2019 Volume V (pp. 79-87). Springer Singapore,

4. Biswas, P.P., Sahis, M. K., Mondal, G.C & Sengupta, A (2019). Prediction of Residual Life of Pavement by Surface Deflection using Odemark's Approach, International Airfield and Highway Pavements Conference (Pavement Performance and Condition Assessment), Chicago, Illinios, July 21-24, 2019.

5. Sahis, M. K., Biswas, P. P., & Mondal, G.C Paul,S "A Mechanistic – Empirical design of bituminous overlay on flexible road pavement using vertical interface deflection as design parameter", Proceedings of 10th international conferences on maintenance and rehabilitation of pavements- Mairepave10 – Volume 2 (accepted for publication), Guimarães, Portugal, July 24-26, 2024.

6. Paul,S Sahis, M. K., Biswas, P. P., & Mondal, G.C "Mechanistic-Empirical Design of Low Volume Flexible Road Pavement by limiting Vertical Interface Stress and Strain on Subgrade", Proceedings of 10th international conferences on maintenance and rehabilitation of pavements- Mairepave10 – Volume 2 (accepted for publication), Guimarães, Portugal, July 24-26, 2024.

05/06/24

Manoj Kumar Sahis
BE, ME, MIGS, MIE, MICI, Chartered Engineer
Associate Professor
Department of Construction Engineering
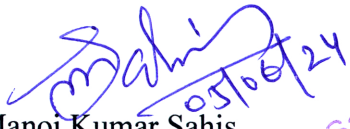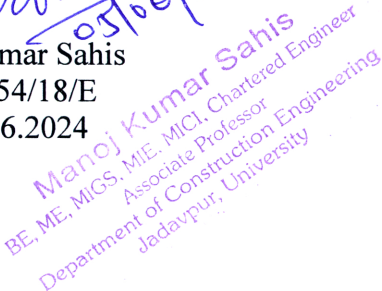Jadavpur, University

H6/24

Dr. Partha Pratim Biswas
Professor
Department of Construction Engineering
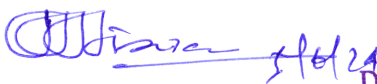Jadavpur University
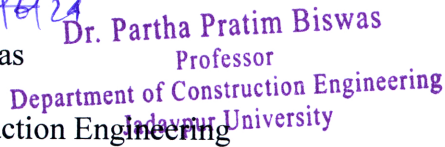
STATEMENT OF ORIGINALITY

I, Manoj Kumar Sahis, registered on the 04th day of July'2018 do hereby declare that this thesis entitled "**A Study on Mechanistic-Empirical Design of Flexible Road Pavement and Overlay Using Method of Equivalent Thickness**" contains literature survey and original research work done by the undersigned candidate as part of Doctoral studies.

All information in this thesis has been obtained and presented in accordance with existing academic rules and ethical conduct. I declare that, as required by these rules and conduct, I have fully cited and referred all materials and results that are not original to this thesis.

I also declare that I have checked the thesis as per the " Policy on Anti Plagiarism, Jadavpur University, 2019" and the level of similarity as checked by iThenticate software is 5%.

Manoj Kumar Sahis
Index No.54/18/E
Date: 05.06.2024
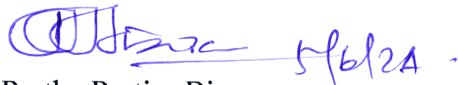
Certified by Supervisor

Dr.Partha Pratim Biswas
Professor
Department of Construction Engineering
Jadavpur University, Saltlake Campus
Block- LB, Sector-III, Plot No. 8
Kolkata -700106, India

III

CERTIFICATE FROM THE SUPERVISOR

Date: 05.06.2024

This is to certify that the thesis entitled "**A Study on Mechanistic-Empirical Design of Flexible Road Pavement and Overlay Using Method of Equivalent Thickness**" submitted by Shri Manoj Kumar Sahis, who got his name registered on 04th day of July'2018, for the award of Ph.D (Engg.) degree of Jadavpur University is absolutely based upon his own work under the supervision of Dr. Partha Pratim Biswas and that neither his thesis nor any part of the thesis has been submitted for any degree/ Diploma or any other academic award anywhere before.

Dr.Partha Pratim Biswas

Professor,

Department of Construction Engineering

Jadavpur University, Saltlake Campus

Block- LB, Sector-III, Plot No. 8

Kolkata -700106, India

Dr. Partha Pratim Biswas
Professor
Department of Construction Engineering
Jadavpur University

DEDICATED

TO

LATE FATHER, MOTHER AND ELDER BROTHER

ACKNOWLEDGEMENTS

I'd like to take this opportunity to thank my supervisor, Prof. Partha Pratim Biswas, for his invaluable direction, motivation, and consistent encouragement, without which my thesis would not have taken shape. In addition to my thesis work, he has been incredibly supportive of my efforts to publish technical papers and advance my career. I would also want to thank Prof. Gokul Chandra Mondal for accepting to be a part of my committee and for his constant advice during this thesis work. I'd like to thank Prof. Subhajit Saraswati, the head of the department, in particular. He has taught me more than I could ever give him credit for as my teacher and mentor.

I am grateful to my teachers, especially Prof. Debasish Bandyopadhyay, Prof. Kaushik Bandyopadhyay, Prof. Sayan Nandi, Prof. Partha Ghosh, Prof. J.J. Mondal, Prof. Tathagata Roy and Prof. Himadri Guha, for their encouragement and support. I want to thank Dr. Dipesh Majumder for providing me the strength to overcome all of the problems I've faced.

I am also grateful to everyone I have had the pleasure of working with on this and other similar initiatives. Each member of my thesis Committee has provided me with considerable personal and professional guidance, as well as teaching me a great deal about research and life in general.

Nobody has meant more to me in the pursuit of this undertaking than the members of my family. I'd like to thank my late parents, whose love and advice are with me no matter what I do. Most significantly, I want to thank my supportive wife, Sonali, and my wonderful son, Nilax, who are constant sources of inspiration for me.

Special thanks are due to my students, Mr.Sourav Paul, Mrs.Nabina Shyam, Mr.Arghya Banerjee and Mr. Shreyan Ganguly for their encouragement and support all through my studies.

ABSTRACT

Present thesis employs a stress and strain based Mechanistic-Empirical principles to estimate the optimal thickness of compacted subgrade on top of a weak natural subgrade to enhance subgrade strength under specific axle load repetitions. Yoder and Witczak's CBR-depth relationship determines allowed vertical stress, while the IRC-37:2018 specifies vertical compressive strain on the natural subgrade. The findings indicate that the thickness of the compacted subgrade increases with increase in axle load repetitions and decrease in natural subgrade strength. In both the approaches, the increase in compacted subgrade thickness is significant up to 50 msa load repetitions, beyond which it becomes less significant. Moreover, a comparative analysis of stress and strain-based methods highlight that the strain-based criteria yields thicker compacted subgrade than stress-based methods.

Furthermore, the study includes determination of compacted subgrade thickness and effective CBR of the soil subgrade in a two-layered system using layer transformation theory and Boussinesq' method. It has been assumed that the summation of deflection of natural and compacted subgrade in a layered system under a wheel load is the total deflection in a two layered subgrade system. In present model, an equivalent homogeneous subgrade has been considered which will produce the same deflection of two layered subgrade system. The findings reveal substantial variations in the thickness of compacted subgrade up to a CBR of 20% for borrowed soil, beyond which the variations are less significant. In this context, recommendation for selection of a specified thickness of 500 mm compacted subgrade by IRC/MORD may be revisited.

A stress based Mechanistic –Empirical technique has been proposed in present thesis to formulate a design approach for determination of unbound granular layer thickness for low volume road pavement considering the pavement as three layered system. In a three-layer pavement system, vertical compressive stress at the interface of granular unbound layers has been determined using Boussinesq's equation. It has been found that, the results of proposed model shows good convergence with existing design guidelines. In present analysis, a concentration factor has been used in a model for determination of vertical stress in a layered system to design a low volume road pavement. The proposed model shows good correlation between pavement thickness and CBR which matches closely with other design approaches.

One of the objectives of present study is to develop a suitable optimization approach for determination of bituminous and granular layer thickness to withstand required axle load repetitions. The analytical approach for determination of pavement thickness proposed in this study is based on the influence of different pavement layer thicknesses on allowable radial tensile strain and vertical compressive strain at different layer interface. The flexible pavement section in present study has been modelled as a three-layered system, with the binder base (bituminous layer) on top, followed by the granular layer, which rests on soil subgrade as its foundation. Odemark's method has been used to transform the three-layered system into a homogeneous one. The radial tensile strain at the bottom of the bituminous layer and the vertical compressive strain on the top of the subgrade were estimated by Boussinesq's theory. The strain value thus obtaned has been made equal to the allowable strain from IRC:37-2018 to determine the thickness of constituent pavement layer thickness for anticipated axle load repetitions. It has been found that the variation of granular layer thickness is more sensitive than the bituminous layer thickness on pavement performance in terms of rutting. The deflection values for the optimized pavement section using present method has been compared with the deflection obtained using the IITPAVE and KENPAVE which exhibits reasonable good convergence.

In present study, a Mechanistic-Empirical model of the strain-based design for perpetual road pavement has been proposed. In this analysis , the perpetual pavement has been primarily characterised as a three layered bituminous pavement that can withstand a minimum design traffic of 300 msa or thickness corresponding to a fatigue strain of 80 $\mu\varepsilon$ or the rutting strain of 200 $\mu\varepsilon$. It has been observed that the thickness of the binder base required to withstand fatigue is generally more than that required to withstand rutting under a specified axle load repetition. The performance of perpetual pavement was found to be governed by its failure under fatigue. The modified fatigue and rutting strain for perpetual road pavement design have been obtained as 95 $\mu\varepsilon$ and 185 $\mu\varepsilon$ respectively.

A Mechanistic-Empirical apprpoach has been proposed to determine bituminous overlay thickness on the top of an existing flexible road pavement by limiting the vertical interface stress at pavement -overlay interface . In prsent analysis, a new overlay with old pavement has been considered as a two-layered system. The modulus of existing pavement has been estimated based on surface deflection on existing road

pavement. The vertical stress at pavement-overlay interface due to wheel load has been determined using Boussinesq's theory after the required transformation of the layered system by Odemark's method.

The vertical stress thus obtained has been made equal to allowable vertical stress found from Danish and Huang's empirical correlation to estimate the overlay thickness for different axle load and pavement deflection. Comprative results between two stress based methods and the Asphalt Institute method have been found reasonably close. Base layer Index as a measure of the curvature of overlay under wheel load has also been considered as a performance criterion. In this backdrop, comparative analysis of Base layer index as obtained from overlay thickness with stress-based and deflection-based criteria has been presented in this study. It has been found that the overlay thickness estimated using the stress-based methods are reliable and safe against cracking. Sensitivity analysis of data used in present analysis shows that the modulus of the bituminous layer as most sensitive parameter in comparison to axle load repetition.

Furthermore, the overlay thickness has also been obtained by limiting vertical interface deflection for different axle loads repetitions and compared with the thickness of overlay estimated using the Asphalt Institute (AI) method. Convergence in the rate of change of overlay thickness with deflection proves the sensitivity of pavement deflection on overlay thickness is comparable between two deflection-based methods. In this study, the effect of overloading has also been analysed in terms of increased wheel load on overlay thickness. The reduced service life of overlay due to overloading has been estimated by back-calculation of vertical interface deflection. It has been found that, when the pavement is badly damaged with higher deflection, the reduction in overlay life for both in high and low-volume roads are comparable and significant.

An attempt has also been made in this study to develop a method for predicting the residual life of flexible pavement using surface deflection as a design parameter. The pavement structure has been considered as a three-layered system with bituminious binder base, granular unbound layers and subgrade soil. Relationships between surface deflection, pavement subgrade CBR, and axle load repetitions has been used to calculate residual life and determine terminal surface deflection.

The outcome of this study establishes significant correlations between surface deflection, pavement subgrade CBR and axle load repetitions. The correlations have

been used to estimate the residual life of pavement based on its surface deflection. The model presented in present analysis may also be used to estimate the terminal surface deflection of pavement beyond which the need of repair becomes urgent.

Finally, the study also combines PYTHON, MATHEMATICA, and JAVA to develop algorithms to create Graphical User Interfaces (GUIs). These developed GUI provides a reliable and user friendly platform for design of flexible road pavement and overlay.

Keywords: Compacted subgrade, natural subgrade, binder base, California Bearing Ratio , Boussinesq's, Mechanistic-Empirical, interface stress, Odemark's Method, Boussinesq, fatigue, rutting, perpetual pavement, overlay thickness, Interface-deflection, Base layer index , residual life.

CONTENTS

Description	Page No.

CONTENTS

Description	Page No.

CONTENTS

	Description	Page No.

CONTENTS

	Description	Page No.

CONTENTS

FIGURES

FIGURES

FIGURES

FIGURES

FIGURES

FIGURES

FIGURES

FIGURES

FIGURES

FIGURES

FIGURES

FIGURES

FIGURES

FIGURES

TABLES

TABLES

TABLES

TABLES

TABLES

TABLES

LIST OF ABBREVIATIONS/SYMBOLS

Abbreviation/Symbols	Description
δ	Interface deflection
μ	Poisson's ratio
σ_z	Vertical compressive stress
a	Radius of contact
q	Tyre pressure
N	Axle load repetitions
CBR	California Bearing Ratio
f	Odemark's correction factor
h_{eq}	Equivalent layer thickness
h_{cs}	Depth of compacted subgrade
δ	Interface deflection
μ	Poisson's ratio
ε_z	Vertical compressive strain
ϵ_t	Radial tensile strain
z	Vertical compressive stress
a	Radius of contact
N	Axle load repetitions
CBR	California Bearing Ratio
CBR$_{eff}$	Effective CBR
E$_{ns}$	Modulus of elasticity of subgrade materials
E$_{eff}$	Effective layer modulus
VCS	Vertical compressive strain
RTS	Radial tensile strain
M$_R$	Resilient modulus of bituminous layer
V$_{be}$	Volume of effective bitumen in bituminous mix
V$_a$	Volume of air void in bituminous mix
CVPD	Cumulative vehicle per day
MDD	Maximum dry density
OMC	Optimum moisture content
PMGSY	Pradhan Mantri Gram Sarak Yojna
ODR	Other District road
MDR	Major District Road

AASHO	American Association of State Highway Officials
LVR	Low Volume Road
AASHTO	The American Association of State Highway and Transportation Officials
σ_{zper}	Permissible vertical stress
E_3	Elastic Modulus of subgrade
ESAL	Equivalent standard axle load
WMM	Wet Mix Macadam
WBM	Water Bound Macadam
CRMB	Crumb rubber modified bitumen
MET	Method of equivalent thickness
RBDO	Reliability Based Design Optimization
FOSM	First Order-Second Moment
MEPDG	Mechanistic Empirical Pavement Design Guide
AADT	Annual average daily temparature
PMA	Polymer modified asphalt
AAPT	Annual average pavement temparature
RSM	Response Surface method
SRBDO	System Reliability Based Design Optimization
FFP	Futuristic Flexible Pavement
FC	Fatigue Cracking
FRL	Fatigue Resistance Layer
FEL	Fatigue Endurance Limit
NCAT	National Center for Asphalt Technology
HMA	Hot Mix Ashphalt
AI	Asphalt Institute
LE	Limit Equilibrium
LEFM	Linear Elastic Fracture Mechanics
BBD	Benkelman Beam Deflection
FWD	Falling weight Defelectometer
BLI	Base layer index
MLI	Middle layer Index
LLI	Lower layer Index
ELT	Equivalent layer thickness

SCI	Surface curvature index
RSL	Residual service life
PSI	Pavement serviceability index
GUI	Graphical user Interface

CHAPTER 1
INTRODUCTION

1.1   Introduction

The interconnected network of expressways and highways that link cities and support economic interchange are essential to a nation's infrastructure. One of the most significant infrastructural elements influencing production and economic activity is believed to be transportation. Despite the lack of land, the need for paved roads is rising significantly to alleviate the need for basic transportation and to boost economic activity. Therefore, there is a lot of pressure to invest in the transportation industry. However, according to many Empirical design guidelines, estimation of optimum pavement section is not acceptable as it is difficult to evaluate and fails to examine the intricate interactions of the materials in the various layers. Through the use of finite elements [9] and Mechanistic-Empirical [26, 27-32,135,149-151, 44-47] fundamental analysis, an affordable and effective pavement system can be constructed.

The behavior of a flexible pavement may be considered as a homogenous half-space [34] to describe it in the simplest possible terms. The extent and depth of a half-space are both limitless, and the top plane is where the loads are applied. An elastic half-space was/is subjected to a concentrated load according to the original Boussinesq's [34] theory. It is possible to combine the stresses, strains, and deflections caused by a concentrated load to find those caused by a circular loaded area. Boussinesq's [34] solutions received a lot of attention prior to Burmister's [37-41] invention of layer-based theory since they were the only ones accessible. If the theory is used, stresses, strains, and deflections of all pavement layers can be estimated.

With the advancement of our understanding of building materials, techniques, and equipment, pavement design is continually changing. The conventional empirical method for designing pavements has changed to a more mechanistic approach, leading to the global adoption of the Mechanistic-Empirical [26, 27-32,135,149-151, 44-47] methodology. The goal of this innovative strategy is to reduce stress, strain, and deflection in the different pavement structure layers, which are arranged from top to bottom in decreasing order of elastic modulus. As the pavement's foundation, the subgrade is essential

to the structure's overall stability since it carries weight and transfers load stress to the underlying soil.

Enhancing the strength of other pavement layers, including the granular base, sub base, binder base, and wearing course, which can be reinforced by adding more overlay thickness, is not the same as improving the subgrade. Over the course of the pavement's service life, strengthening the subgrade after it has been laid becomes quite difficult. Rutting is one of the most frequent reasons in which bituminous pavement fails. It usually happens as a consequence of soft subgrade failure, but it can also happen as a result of binder base failure from high axle loads and elevated tire pressure.

Although there are ways to limit rutting [26, 27-32,135,149-151, 44-47], by applying bituminous layers that are resistant to rutting, these approaches can be expensive over the course of the pavement's life. As a result, during the first stages of construction, it is essential to determine the type and strength of the natural subgrade and to put strengthening measures in place. The most common method is to add a thick compacted subgrade [31-32,145-146] on the top of comparatively soft natural subgrade to increase the strength of the composite subgrade. To resist excessive deflection of granular sub-base during construction phase, the subgrade strength must be increased to withstand pavement deterioration under static and dynamic traffic pressures,.

Stronger subgrades minimize the need for thick pavement crusts, which lowers construction costs. Increased natural subgrade strength can be achieved in highway construction by a number of methods which have been investigated earlier and are frequently utilized, such as soil stabilization using additives, admixtures, and fibers, geotextiles, and sand drains. The use of a compacted subgrade [31-32] layer on top of a poor natural subgrade has been recommended in different Indian guidelines for flexible pavement design in order to improve subgrade strength and decrease pavement thickness.

The failure of bituminous road pavement is primarily influenced by subgrade failure, which is the softest and weakest layer in a multi-layer pavement system. Damage to any constituent layer increases vertical stress, strain, and deflection on the natural subgrade, which acts as the pavement foundation. Therefore, subgrade strength [145-146] is crucial to ensure the durability of the road pavement since there is limited opportunity for subgrade

repair or strengthening once the pavement is constructed. For roads built on poor subgrade, subgrade improvement has become a major concern during the pre-construction phase. The most common method of subgrade improvement involves placing suitable soil from a borrow pit on top of the natural subgrade and compacting it to the desired density and depth.

The pavement's resistance to rutting is improved by this compacted subgrade depth, which also reduces the requirement for thicker pavement layers, thereby reducing project costs. The California Bearing Ratio (CBR) of the two-layered system, also known as effective CBR (CBR_{eff}), [145-146] has been determined in this work using a Mechanistic - Empirical approach. CBR_{eff} is dependent on the thickness of the compacted subgrade and the CBR values of the borrowed soil and natural subgrade.

Over the past ten years, India's economy has become one of the fastest-growing in the world. Its economic policy is currently focused on increasing employment possibilities through direct and indirect means, such as by developing its road network to improve surface connectivity. With a population of over 1.4 billion people, India has launched the Pradhan Mantri Gram Sarak Yojana (PMGSY) [86], a comprehensive plan for rural road connectivity, with the goal of connecting every village in the country by roads in all weather conditions. Approximately two thirds of India's total road length is comprised of this rural road network.

Nonetheless, the majority of these rural roads are categorized as low volume roads, and depending on the amount of traffic they actually receive over the course of their service life, they can be upgraded to level like Other District Roads (ODR) or Major District Roads (MDR). In India, a road is considered low volume if it carries less than 450 commercial vehicles per day or has design traffic of less than two million standard axles (msa) during its service life.

India boasts the second-longest total road network in the world, but the quality of its road surfaces has caused several questions on its durability. About 33% of India's road network is made up of unsurfaced roads, which urgently need to be repaired and upgraded in order to make those safe and functional.

Utilizing waste materials and locally accessible resources are becoming more and more important in the effort to promote sustainable road construction. India produces 960 million tons of solid waste a year as a result of industrial,

mining, municipal, agricultural, and other processes producing byproducts. Inorganic elements from the mining and industrial sectors, such as blast furnace slag, building and demolition waste, and mill tailings, which can be utilized as sub-base or granular base in road pavement to utilize around 30% of this waste. Furthermore, elements that can be employed as fillers in bituminous mixtures or for soil stabilization include fly ash, rice husk ash, cement kiln dust, and marble dust. The cost of building a pavement can be reduced by using alternative resources, such as waste materials, in the base and sub-base layers, particularly for unbound granular materials in low volume roads. In this background, design method has been developed to estimate the layer thickness of low volume roads.

For a country like India, which struggles to link its vast and isolated areas, the early deterioration of bituminous road pavements is a serious problem. The majority of India's vast road network which handles largely both freight and passenger traffic is made up of flexible pavements. Therefore, keeping these pavements durable it is essential to lower total maintenance expenses. In this regard, developing a trustworthy technique for determining the thickness of the different layers in a multilayered bituminous road is crucial. Reliability analysis [56-57,73] of the methodology is also crucial for developing pavements resistant to cracking as well as rutting. It is important to remember that although bituminous layers (which are used as wearing courses or binder) can be readily replaced by adding an overlay to an already-existing road, whereas it is much more difficult to enhance the mechanical strength and thickness of the granular layer once the road has been built to the full depth of granular layers and is in use.

In light of this, the current study aims to establish a methodology for estimating the thickness of the granular and bituminous layers in a flexible road pavement using a mechanistic-empirical approach. In this context, Odemark's method [52,126,181], also referred as the method of equivalent thickness (MET) [52,126,181], is presented as an transformation technique for design of pavement thickness in a three-layer conventional flexible pavement. It is important to note that the idea of perpetual pavement has emerged as a result of notable rise in traffic volume, unforeseen axle loads, and the expanding need for freight lanes. Currently, the process of designing a flexible pavement usually entails considering the pavement structure as a multi-layered system. Flexible

pavement design started with a two-layered system assumption and developed into a more intricate multi-layered design approach over time. The pavement's design is mainly dependent on the methodology that is selected and the boundary conditions those are considered in the design.

Perpetual pavements [147,149,152,154,156,157,158,165,171-172] is essentially made of an impermeable, wear and rut resistant top layer of asphalt, a base layer that is durable and fatigue-resistant, and an intermediate layer which is also rut resistance and have the property of resistance against moisture susceptibility. It is occasionally required to restrict strain distribution and optimize fatigue ratios in design in order to prevent fatigue cracking from the bottom up.

Although a number of endurance limits for perpetual pavements have been proposed, none have been established with high degree of reliability. Based on laboratory testing, Monismith and McLean established a Fatigue Endurance Limit (FEL) [135,147,149,152,154,156,157,158,165,171-172] value in the range of 70 to 100 $\mu\epsilon$ for most perpetual pavement designs. This value has since been proposed by the National Center for Asphalt Technology (NCAT) [135,147,149,152,154,156,157,158,165,171-172] for these designs. However, based on data from various pavement sections in use, some researchers have proposed that the Fatigue Resistance Layer (FRL) [135, 147, 149, 152, 154, 156, 157,158,165,171-172] can sustain up to 150 $\mu\epsilon$, depending on the type of bituminous mixture used. One of the major portion of the present study is focused on developing a Mechanistic-Empirical flexible pavement design method based on the MET [52,126,181] methodology in light of the background information provided. This approach provides a straightforward and useful pavement design option.

The necessity of restoring road and airport pavements has grown dramatically over time. Over the past 20 years, road connection has become increasingly important in India when it comes to infrastructure development. The demand for pavement repairs has increased as a result of the road network's expansion, particularly in light of the unanticipated effects of climate change and high traffic volumes that have negatively impacted the service life of road pavements. As a result, pavement needs maintenance and scheduling of repairs

with appropriate materials, which have taken precedence in pavement maintenance plans.

In this ambit an effective and useful overlay design is essential to improve the serviceability and usability of road pavements. Based on stress, strain, or deflection criteria [10,137,151], overlay design can include expected axle load repetitions during the pavement's service life. Many researchers have used empirical, mechanistic, and Mechanistic-Empirical approaches [26, 27-32,135,149-151, 44-47] to estimate the thickness of bituminous overlay for damaged flexible road pavement. Present study considers a mechanistic-empirical approach to design bituminous overlay thickness based on interface deflection as a design criterion.

Applying an overlay [10,137-151] on top of an existing bituminous layer is the most sustainable method of pavement rehabilitation in the modern world. The modulus of the various pavement layers, Poisson's ratio, the thickness of the constituent layers, and the anticipated volume of traffic are some of the factors that affect the thickness of the overlay.

The semi-empirical and semi-mechanistic approach have been used in present overlay design approaches, such as the Asphalt Institute (AI) method [10], can occasionally lead to premature failure or over estimated pavement thickness, which is economically unfeasible. Thus, the goal of this study is to add some value to the existing overlay design methodology while offering a thorough and critical comparison with the popular AI approach.

An essential part of managing and maintaining infrastructure is to estimate the pavement's residual life. When deciding whether and how to replace or repair deteriorated road surfaces, the remaining service life information (RSL) [20, 26, 58, 64,69,155] assists the engineers and transportation authorities in making well-informed judgments. Surface deflection analysis, especially when using Odemark's [126] method is a useful technique for determination of how long a pavement will be functional for use. In general, there are three RSL estimation procedures: namely, functional failure, structural failure and combination of both [188]. Deflection testing has become a commonly used technique for assessing the structural strength of pavements. The deflection as a reaction to a known load applied at the pavement surface is measured using current deflection testing equipment. Surface-deflection testing is widely

acknowledged by highway agencies as a routine procedure because of its rapid and reliable results, while processing of deflection data remains an area of ongoing study.

The structural assessment gives a variety of information on how pavements should behave. However, due to the costs of data collection and analysis, many agencies do not currently analyze structural capacity at the network level of pavement management, though it is required to be done frequently at the project level. In this backdrop, analytical method of estimation of remaining service life of bituminous road pavement can be an effective approach in pavement management system.

Futuristic Flexible Pavement (FFP) [86] is now considered necessary for maximizing soil strength through comprehensive and effective technology, eliminating re-work during rehabilitation, improving overall performance, reducing pavement composition for cost savings, decreasing aggregate consumption, lowering bitumen burning to reduce Greenhouse Gas (GHG) emissions, and enhancing overall cost-effectiveness, durability, and environmental sustainability. In that backdrop, the broad objectives of present study may partially supplement the need of FFP.

1.2 Broad objective of the study

The main objective of this study is to formulate a Mechanistic-Empirical approach for the estimation of compacted subgrade, pavement thickness for low, high volume and perpetual road pavement, Moreover the thickness of bituminous overlay and remaining life assessment of road pavements have also been included as the objective of study. The study includes use of vertical interface stress, strain and deflection as design criteria using method of equivalent thickness.

1.3 Scope of work
- Transformation of a multi layered pavement system into a homogenous system using Odemark's (MET) method.
- Determination of vertical compressive stress and strain using Boussinesq's method.

- Determination of allowable vertical compressive stress using correlation from Huang and Ullidtz and consideration of regional factor as per Alaska Flexible Pavement Design guidelines.

- Determination of fatigue strain, rutting strain, modulus of sub base, and base as per the criteria outlined in IRC: 37-2018.

- Determination of the concentration factor variation considering different elastic moduli of pavement materials.

- Determination of the depth and effective CBR of the borrow material using a deflection-based approach.

- Estimation of constituent layer thickness of a perpetual road pavement as specified using provisions of IRC: 37-2018.

- Determination of BLI value for comparison with stress-based and deflection-based (AI) overlay design methods.

- Estimation of elastic modulus of the existing pavement using a deflection-based approach.

- Determination of interface deflection for the purpose of designing an overlay design on an existing pavement.

- Estimation of total deflection in a three-layer flexible pavement using Odemark's–Boussinesq's approach.

- Validation of results obtained from stress, strain, and deflection-based methods using IITPAVE.

- Developing Graphical User Interface (GUI) for all algorithms adopted in the study.

1.4   Organization of dissertation

This dissertation is divided into eight chapters. Chapter 1 covers a brief introduction, including problem statement, study objectives, and outline of the dissertation. Chapter 2 includes determination of compacted subgrade thickness. Chapter 3 includes design of low volume rural road pavement with unbound materials. Chapter 4 includes optimization of bituminous pavement thickness using strain based design criteria by Odemark's approach. Chapter 5 includes Mechanistic- Empirical design of perpetual road pavement using strain based

design approach. Chapter 6 covers mechanistic empirical design of bituminous overlay. Chapter 7 includes prediction of residual life of pavement by surface deflection using method of equivalent thickness. Chapter 8 includes conclusions and future scope of work.

CHAPTER 2
DETERMINATION OF COMPACTED SUBGRADE THICKNESS

2.1   Introduction

The approach of pavement design conceptually dynamic and is changing with the advancement of knowledge in construction material, methodology and equipment. Empirical approach of pavement design has been changed in association with Mechanistic approach to evolve the Mechanistic – Empirical [26, 27-32,135,149-151, 44-47] approach, which is now being widely practiced worldwide. The basic mechanism of design of pavement thickness is based on the concept of limiting the stress, strain and deflection of constituents paving layers. Such layers are arranged in order of decreasing magnitude of elastic modulus from top to bottom. Subgrade is the foundation of pavement structure and therefore stability of pavement structure largely depends on the performance of the foundation on which it is supposed to transfer the load to the soil.

Improvement of subgrade is qualitatively different from the approach of improvement of strength of other paving layers. The paving layers include granular base and sub base, binder base and wearing course which are frequently strengthened by putting additional thickness of overlay. But once the pavement is laid on subgrade, it becomes very difficult to strengthen the subgrade during the service life of pavement. The most frequent types of failure in Bituminous pavement failure is in the form of rutting caused by failure of soft subgrade. However, rutting may also be caused due to failure of binder base due to higher axle load with increased tyre pressure.

The repair to prevent rutting by rut resistant bituminous layer is done but that is expensive in terms of life cycle cost of pavement. Therefore, it is important to study the type and strength of natural subgrade and to decide upon the strengthening measures at initial stage of construction. The most widely used method in this context is to put compacted subgrade with adequate thickness to achieve a better strength of composite subgrade with a stiffer layer on top, followed by the soft natural subgrade . The strength of the subgrade need to be increased to withstand excessive deflection of granular subbase which may cause pavement deterioration under static and dynamic stresses generated by traffic.

The better is the strength of subgrade, the requirement of pavement crust becomes less which results saving in cost of construction. Keeping this in view,

improvement of natural subgrade by various techniques including soil stabilization by adding different additives, admixtures and fibres, use of geotextiles, use of sand drains etc. have already been explored by the engineers and used frequently in highway construction. The guidelines for the design of flexible pavements in India, has also recommended the provision of using compacted subgrade layer on the top of weak natural subgrade to increase subgrade strength to reduce the pavement thickness.

The failure of bituminous road pavement is largely guided by the failure of subgrade, which is the softest as well as weakest layer in a multi-layer pavement system. Damage in any of the constituent layers in a flexible pavement increases the vertical stress, strain, or deflection on the top of the natural subgrade, which acts as foundation of the pavement structure. The most popular method of strength improvement of subgrade is to place a suitable type of soil from a borrow pit on the top of the natural subgrade and to compact it with the required target density and depth. The depth of compacted subgrade, thus prepared, primarily increases the durability of the road against rutting and on the other hand the increased CBR of compacted subgrade reduces the requirement of pavement layer thickness, thereby reducing the project cost. In the present study, a Mechanistic-Empirical [26, 27-32,135,149-151, 44-47] approach has been developed to determine the CBR of the two-layered system often known as effective CBR (CBR_{eff}) [145,146] which depends on the thickness of compacted subgrade and CBR of both natural subgrade and borrowed soil.

2.2   Literature review

Nataatmadja et al. (2019) [121] proposed a study on the performance of soil subgrade under the traffic condition. The study focused on the fact that good subgrade can prevent premature failures of the pavement during the service life of the pavement. Odemark's layer transformation has been used to transform a multi-layered system in to homogenous one with or without any layer correction factor. The study focuses on a two-layered subgrade which consists of a relatively thick layer as capping on top of an semi-infinite layer. Aust Road sublayer analysis has been used in the study. This paper also explores various

techniques for determining the effective subgrade CBR to be used in designing flexible pavements. It compares results from different methods like the Odemark Transformation Method and multi-layered elastic analyses, proposing a new validated approach based on the performance of typical pavement structures. The study concludes that without the usual correction factor in Odemark's method, the study underestimates the necessary thickness of the capping layer if anisotropy and nonlinearity is considered.

Biswas et al. (2019) [33] proposed a methodology to evaluate the optimum thickness of compacted subgrade in a two layered system using Mechanistic-Empirical design approach. The study calculates the allowable vertical stress on the compacted subgrade based on CBR-depth relationships and axle load specifications. Additionally, it evaluates the vertical compressive strain on the natural subgrade according to rutting criteria. By transforming the two-layered system into a homogeneous one, the study applies mechanistic formulations to determine the compacted subgrade thickness needed to withstand design load repetitions while limiting vertical compressive strain on the natural subgrade. The study also finds that the thickness of compacted subgrade required to achieve the specified CBR over weak natural subgrade varies significantly depending on the ratio of elastic modulus in the two-layered system. Results suggest revisiting the concept of effective CBR and fixed thickness provisions in existing specifications for rural roads.

Tarefder et al. (2008, 2012) [172,173] analyzed the impact of a weak subgrade with varying strength and stiffness on pavement design and performance. The subgrade's strength and stiffness were represented by its soil resistance R-value, evaluated using data from US 550, a rural highway in Northwest New Mexico. Calculated subgrade R-values were compared to those used in the actual design of US 550. Pavement design simulations were conducted using the Mechanistic-Empirical Pavement Design Guide (MEPDG) and elastic analysis. The MEPDG simulations indicated potential failure of the existing design due to top-down longitudinal cracking, consistent with field observations. Top-down cracking was found to be less affected by subgrade strength, while rutting was sensitive to low R-values or weak subgrade. An R-value of 17 was identified as a threshold for distinguishing good subgrade from

poor, based on resistance to rutting and roughness degradation. Elastic analysis showed that increasing subgrade R-values could significantly reduce compressive strain at the subgrade surface. Subgrade treatment effectively reduced stress and strain in weak subgrade. This study provides valuable insights for designing and predicting the performance of pavements built on weak subgrade.

Putri et al. (2017) [139] proposed a study to introduces a method for determining pavement thickness based on establishing a threshold stress. This approach aims to keep the maximum deviator stress caused by traffic loads on the subgrade below a critical threshold by providing an appropriate pavement layer thickness. Its goal is to maintain stable subgrade deformation behavior under repeated loads, thus minimizing plastic deformation. Unlike existing methods, this approach is versatile, suitable for various soil types, surface conditions, and base qualities. It allows for the separate consideration and assessment of surface and base qualities, facilitating straightforward determination. The paper proposes a simple laboratory test procedure for quickly assessing the subgrade soil's threshold stress and provides a systematic formation design flowchart along with a practical example. Emphasis is placed on the importance of drainage conditions for the method's success. The effectiveness of the design approach is demonstrated through observations of actual formation performance under repeated loadings.

IRC:37-2018 [51] IRC:37-2018 is a comprehensive guideline provided by the Indian Roads Congress (IRC) regarding the design of flexible pavements. It offers detailed insights into the various aspects of flexible pavement design, catering to the diverse conditions encountered in India's road network. The document covers the design methodology, materials selection, construction techniques, and maintenance considerations for flexible pavements. It emphasizes the importance of considering factors such as traffic volume, climate conditions, subgrade strength, and pavement layer properties to ensure long-lasting and cost-effective road infrastructure. IRC:37-2018 outlines the design process, which typically involves determining the traffic loads, estimating the pavement's structural capacity, and selecting appropriate pavement layers and thicknesses. It provides equations, charts, and tables to aid engineers in these

calculations, taking into account factors like vehicle types, axle loads, and design life. Moreover, the guideline discusses the selection and characterization of materials such as aggregates, bitumen, and additives, emphasizing their suitability for the specific traffic and environmental conditions. It also covers construction techniques, quality control measures, and guidelines for pavement maintenance to ensure durability and performance over the pavement's design life. In summary, IRC:37-2018 serves as a valuable resource for engineers, contractors, and policymakers involved in the design, construction, and maintenance of flexible pavements in India, offering a comprehensive framework to ensure the quality, safety, and sustainability of road infrastructure. Additionally the guideline for design of bituminous road pavement, recommends at least 500 mm thickness as compacted sub grade on the top of weak natural subgrade. But the guideline does not recommend any correlation with axle load repetition and thickness of the compacted sub grade. The respective code proposed certain equations for subgrade CBR with modulus and also for traffic load repetitions with different strains generated within different layer interfaces. These empirical strain equations can be used to generate Mechanistic-Empirical pavement design models.

Reddy et al. (1993, 2001) [145,146] analyzed that the subgrade for flexible pavement can be defined as a combination of two layers. The upper layer is compacted and having higher stiffness placed on relatively weak soil making total thickness of 500mm in cutting or embankment. The study concludes that for the design of flexible pavement composite strength of the subgrade which is the combined strength of borrow as well as natural soil must take in to consideration. The study also concludes that design CBR of subgrade is very low as compared to borrow material and only CBR of borrow must alone not taken in to consideration for pavement design.

C.A.Booth (2022) [16] investigated that the pavement failures attributed to low California bearing ratio (CBR) and high swelling potential. The study explores the use of sustainable waste materials like brick dust waste (BDW), ground granulated blast furnace slag (GGBS), recycled plastic (RP), and recycled glass (RG) as partial replacements for cement and lime in treating clay. Road pavement design was carried out using the Design Manual for Road and

Bridges (DMRB) to evaluate treated clay's performance with different CBR values. Failure analysis of road pavements supported by eco-friendly treated clay was conducted to understand defect formation. The study calculated the embodied carbon of treated clay and performed a life cycle cost analysis (LCCA) comparing flexible pavements with treated clay to those with imported materials. Results showed significant improvements in CBR values and reductions in swelling, leading to thinner pavements and reduced stress, thereby enhancing resistance to fatigue, rutting, and permanent deformation. Eco-friendly treated clay exhibited low embodied carbon and lower life cycle costs compared to imported materials. The study concludes that using waste materials in road construction can reduce carbon emissions and construction costs, benefiting owners and operators by saving money compared to removing and replacing clay with imported materials.

A. Gediket et al. (2020) [15] illustrated that the majority of global highways feature flexible pavements composed of multiple layers, including asphaltic and granular, over a foundational layer known as the subgrade. A structurally sound subgrade is crucial for withstanding construction stresses and preventing later deformations under traffic loads. Weak subgrades can be reinforced with modifications like a capping layer to reduce stress on the pavement. This study aims to enhance understanding of optimal pavement functionality by examining key design parameters such as material properties, layer count, and thickness. Using KENLAYER software, design of flexible pavements based on specific Equivalent Single Axle Load (ESAL) requirements. Cost-effectiveness was also considered in selecting the best-performing composition. Results suggest that pavements utilizing high modulus asphalt are ideal for subgrades with CBR of at least 3%, while weaker subgrades benefit from a capping layer to meet high ESAL application designs.

Mishra, D., et al. (2019) [141] described that pavement construction becomes very much expensive when the pavement builds on weak soil. The choice and application of pavement rehabilitation methods often rely on data regarding the pavement's functional and structural condition. Agencies commonly conduct visual distress surveys and Falling Weight Deflectometer (FWD) testing as part of pavement preservation programs. While back

calculating layer moduli from FWD data is standard, it requires accurate layer thickness estimates, which can be challenging to obtain without coring, a time-consuming process. To address this, Boise State University's ongoing research proposes using Deflection Basin Parameters (DBPs) derived from FWD tests to infer individual layer conditions, offering an alternative to traditional methods. Through Finite-Element Modeling, the study verified the adequacy of DBPs by assigning typical modulus values to layers and calculating corresponding DBPs, which mostly aligned with literature ranges. Subsequently, four pavement sections in Idaho were assessed using this approach, and the results compared favorably with visual distress assessments. This research suggests DBPs as viable alternatives for network-level pavement condition evaluation.

M. John. N (2015) [119] mentioned that the subgrade acts as a load-bearing layer of the entire pavement system. Models are generated to evaluate the structural contribution of the subgrade layer and also the effective layer thickness. The study further concludes that the performance of pavement structure is highly dependent on the stiffness and thickness of the subgrade and accordingly the traffic should also be categorized based on the geotechnical properties of the subgrade.

M. Nazari et al. (2012) [115] investigated a study on a two layered system based on CBR test. Seventy-two CBR tests were conducted on two-layered samples, including both unreinforced and reinforced configurations. These samples consisted of a sand base layer over a cohesive soil subgrade layer. Three reinforcement scenarios were examined: unreinforced, reinforced with nonwoven geotextile, and reinforced with geogrid, with four different compaction moisture contents (CMC) for the subgrade layers. CBR tests were carried out on sand base layers of varying thicknesses under soaked and unsoaked conditions. The results revealed that the critical thickness of the sand layer depended on the strength of the subgrade clayey soil, influenced by compaction moisture and soaking conditions. Threshold thicknesses were observed in certain samples: those with 8%, 12%, and 16% CMC in unsoaked conditions, and those with 8% and 12% CMC in soaked conditions. However, in some cases, the critical thickness for the sand base layer was not evident.

El-Badway et al. (2011) [60] proposed a study for a two layered flexible pavement system. Flexible pavement has been considered a complex multi-layer system of structure with varying layer modulus and poisson's ratio. Odemark's layer transformation has been applied for transformation of this multi layered complex system in to simple one layer system for stress and strain. The study showed that the correction factor in Odemark's method is a function of several parameters of the layers such as layer thickness, modular ratio. Study also showed that good relationship can be established between vertical stress obtained using Odemark's method and layer elastic analysis for correction factor of 0.8 and 0.9. Finally the study concludes that the correction factor is not constant but varies according with the depth of pavement.

J.Mukabi (2016) [118] suggested that he subgrade serves as the foundational ground for the pavement and is crucial for its overall performance. However, existing models do not accurately quantify the structural thickness and stiffness that contribute effectively to the pavement's performance. This paper proposes models to precisely delineate the structural contribution of the subgrade layer and determine the necessary effective layer thickness. It further analyzes the impact of subgrade stiffness and structural layer thickness on various geotechnical engineering aspects, particularly concerning optimal base-subbase layer stiffness and thickness. The practical demonstration of how the effective performance of pavement structures depends on subgrade stiffness and structural layer thickness is also presented.

M.Zhang et al. (2020) [194] mentioned that determination of appropriate pavement layer thickness is crucial for pavement design, especially in areas with poor soil foundations where effective subgrade treatment enhances durability. However, finding the optimal thickness for subgrade treatment poses challenges for designers. A thicker treatment increases project costs significantly, while a thinner treatment may not improve pavement structure mechanics significantly. This study utilized the finite-element method to analyze real field pavement mechanical responses with subgrade treatments at varying depths. By employing orthogonal design and gray relational theory, it analyzed design indicators to optimize pavement structure for an expressway. Results revealed that subgrade treatment depth significantly affects stresses in asphalt

pavement structures and bottom tensile strains of asphalt layers. Hence, for a cost-effective solution with equal structural strength, using a reasonable depth for cement-treated subgrade instead of increasing asphalt layer thickness is preferable.

M.Alzaim et al. (2020) [14] mentioned that most highways worldwide feature flexible pavements comprised of multiple layers, including asphaltic and granular, over a subgrade foundation. A satisfactory bearing capacity in the subgrade is crucial to mitigate immediate construction stresses and later deformations under traffic loads. If the subgrade is weak, modifications like a capping layer can support the flexible pavement, reducing stress. This study aims to enhance understanding of optimal pavement functionality by examining key design parameters: material properties, layer count, and thickness, considering financial aspects. Using KENLAYER software, flexible pavement designs were aligned with specific Equivalent Single Axle Load (ESAL) targets. Results revealed that for high ESAL applications, pavements with high modulus asphalt are suitable for subgrades with CBR of at least 3%, while weaker subgrades benefit from a capping layer. Cost-effectiveness was considered in selecting the most suitable designs.

2.3   Determination of compacted subgrade thickness based on subgrade deflection

The most popular method of strengthening of subgrade is to place suitable type of soil from borrow pit on the top of natural subgrade and to compact it with required depth and density. The depth of compacted subgrade, thus prepared, primarily increases the durability of road against rutting and on the other hand the increased CBR of compacted subgrade reduces the requirement of pavement layer thickness, thereby reducing the project cost.

2.3.1   Objective

The objective of the present study is to formulate a Mechanistic-Empirical approach for the estimation of compacted subgrade thickness on the top of weak natural subgrade which may require to resist failure of pavement under rutting. The thickness of compacted subgrade thus obtained may be used to recommend an effective CBR in a two layered system of soil subgrade based on layer deflection.

2.3.2   Methodology

In this study compacted subgrade with specified thickness on top of natural subgrade has been considered as a two layered system as shown in Figure 2.1. The thickness of compacted subgrade has been determined in this chapter is based on layer deflection in a two layered system. The top layer in such a system consists of compacted subgrade soil with higher CBR collected from borrow pit followed by the weak natural subgrade. Present guidelines of bituminous pavement design advocates the use of effective CBR of subgrade when compacted subgrade is used for improvement of subgrade. Therefore, effective CBR may be used for the estimation of pavement thickness needs to be determined suitably which characterizes the strength of two different layers of subgrade in a multi-layered pavement system. In this backdrop, it has been proposed in this study to estimate the deflection of compacted and natural subgrade under a standard wheel load. In order to determine the deflection of compacted and natural subgrade using Boussinesq's [34] equation, it is necessary to transform the two-layered system into a homogeneous layer using Odemark's[52,126,170] method, which has been illustrated below.

Compacted subgrade
E_1, v_1
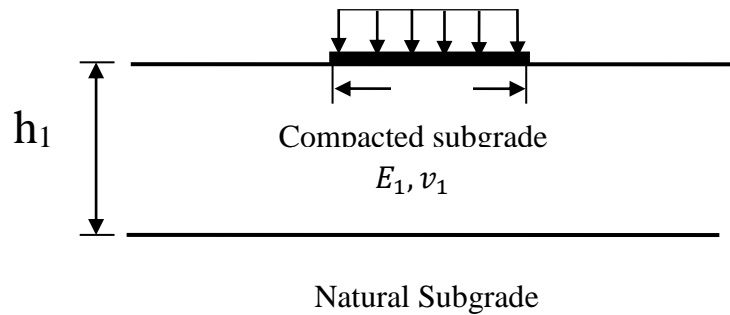
Natural Subgrade

Figure.2.1: Two-layer system with compacted subgrade on natural subgrade

2.3.3   Odemark's Method

In this method, a two-layered system with compacted subgrade on top with thickness h_1, followed by the natural subgrade may be transformed into a homogeneous half-space for application of Boussinesq's[34] equation to determine the vertical stress, strain, or deflection at the required depth. Transformation of a two-layered system into a homogeneous system can be done by Odemark's [126] method with a concept of equivalent layer thickness (h_e) which has been shown in Figure 2.2.

Odemark's [126] method is based on the assumption that the stresses and strains below a layer depend on the stiffness of that layer only. If the thickness, modulus, and Poisson's ratio of a layer are changed, but the stiffness remains unchanged, the stresses and strains below the layer should also remain unchanged.

So, the two-layer system with a modulus of top layer (E_1) with thickness h_1 and Poisson ratio v_1 when rests on bottom layer with a modulus of (E_2) and Poisson ratio v_2, may be represented by an equivalent thickness (h_e) as shown in Equation 2.1.

$$h_e = f\, h_1 \sqrt[3]{\frac{E_1(1-v_2{}^2)}{E_2(1-v_1{}^2)}} \tag{2.1}$$

Where, f is the Odemark's [126] correction factor, which depends on the type of layer interface and varies between 0.8-1.0. In present analysis, the value of Odemark's [126] correction factor has been considered as 0.9.

If the Poison's ratios of the layers are assumed approximately the same for the two layers under consideration, the equivalent thickness corresponding to the two-layered system may be expressed as

$$h_e = 0.9\, h_1 \sqrt[3]{\frac{E_1}{E_2}} \tag{2.2}$$

The deflection at a depth (z) for a circular load of radius 'a', with load intensity 'q', Modulus 'E" and Poisson's ratio "v" in a homogeneous section may be expressed as [34,181] as shown in
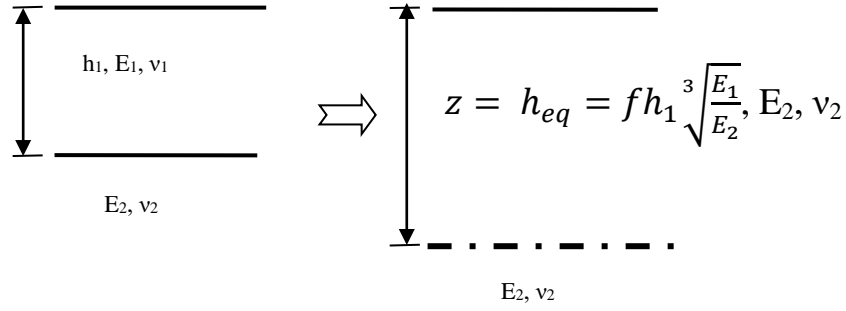
Figure 2.2 Transformation of a two-layered system by Odemark's approach

2.3.4   Model for estimation of effective subgrade CBR

In this chapter a mathematical model with two layered system of soil subgrade has been presented which consists a top layer of compacted subgrade with higher resilient modulus followed by the natural subgrade with lower resilient modulus. So, it is pertinent to mention that the equivalent modulus of such two layered systems will largely depend on the moduli of respective layers in a layered system as well as the thickness of the compacted subgrade. In this study, it has been assumed that the summation of deflection of natural and compacted subgrade in a layered system under a wheel load is the total deflection in a two layered subgrade system. In present model, an equivalent homogeneous subgrade has been considered which will produce the same deflection of two layered subgrade system. The modulus of such homogeneous system has been derived by transformation of two-layered systems which produces the same deflection of layered subgrade system and has been defined as equivalent modulus in this analysis. The concept of equivalent modulus thus explained in the present analysis for estimation of compacted subgrade thickness has been used for determination of effective CBR, which has been explained in subsequent paragraphs in this chapter.

In order to calculate the deflection following input parameters have been used in Equation 2.3.

$$\delta_z = \frac{(1+v)qa}{E}\left[2(1-v) - \left\{\frac{1}{\left\{\sqrt{1+\left(\frac{z}{a}\right)^2}\right\}^2} + (1-2v)\left\{\sqrt{1+\left(\frac{z}{a}\right)^2} - \frac{z}{a}\right\}\right\}\right] \tag{2.3}$$

A wheel load (P) of 40 kN with tyre pressure (q) 0.56 MPa with contact radius (a) = 150.8 mm and the Poisson's ratio (v) = 0.40 , have been considered in present analysis for both the layers of subgrade.

However, for calculation of deflection of compacted subgrade (δ_I),

$z = h_{cs}$ and $E = E_{cs}$, have been substituted in Equation 2.3 to get Equation 2.4.

$$\delta_I = \frac{(1+v)qa}{E_{cs}}\left[2(1-v) - \left\{\frac{1}{\left\{\sqrt{1+\left(\frac{h_{cs}}{a}\right)^2}\right\}^2} + (1-2v)\left\{\sqrt{1+\left(\frac{h_{cs}}{a}\right)^2} - \frac{h_{cs}}{a}\right\}\right\}\right] \tag{2.4}$$

Where, h_{cs} = Thickness of compacted subgrade (mm), E_{cs} = Modulus of compacted subgrade (MPa).

Similarly, for estimation of the deflection of natural subgrade (δ_{II}) ,

$z = h_{eq} = 0.9\, h_{cs} \sqrt[3]{\frac{E_{cs}}{E_{ns}}}$, $E = E_{ns}$, has been substituted in Equation 2.3 to obtain equation 2.5.

$$\delta_{II} = \frac{(1+v)qa}{E_{ns}}\left[\left\{\frac{1}{\left\{\sqrt{1+\left(\frac{h_{eq}}{a}\right)^2}\right\}^2} + (1-2v)\left\{\sqrt{1+\left(\frac{h_{eq}}{a}\right)^2} - \frac{h_{eq}}{a}\right\}\right\}\right] \tag{2.5}$$

Where E_{ns} = modulus of natural subgrade (MPa)

Therefore total deflection in subgrade may be considered as a summation of deflection of compacted subgrade in Equation 2.4 and natural subgrade in Equation 2.5.

So, total deflection in subgrade (δ) = $\delta_I + \delta_{II}$ (2.6)

It has to be noted that the top layer with compacted subgrade layerwith higher CBR rests on the natural subgrade which is semi-infinite in nature with

comparatively lower CBR. In such two-layered system, the equivalent modulus of a homogeneous system may be obtained from Equation 2.7 [37-41].

$$E_{eff} = \frac{2(1-v^2)qa}{\delta_I + \delta_{II}} \tag{2.7}$$

In this study, the effective CBR has been estimated from effective modulus of two different subgrade layers as obtained from Equation 2.7. The effective layer modulus thus obtained (E_{eff}) has been used for estimation of effective CBR (CBR_{eff}) by back calculation using the empirical correlations as shown in Equations 2.8 and 2.9 (IRC:37-2018) [51].

$$E_{eff} = 17.6(CBR_{eff})^{0.64} \tag{2.8}$$
$$E_{eff} = 10(CBR_{eff}) \tag{2.9}$$

In present model, the effective CBR has been considered as an input parameter for the estimation of compacted subgrade layer thickness where other input variables are the CBR of compacted and natural subgrade. Therefore, when the CBR of borrowed soil for compacted subgrade and the CBR of in situ natural subgrade are known, the thickness of compacted subgrade may be determined using present analytical approach to achieve an effective CBR of layered subgrade for design of pavement. The flow diagram of the adopted methodology has been shown in Figure 2.3.

```
┌─────────────────────────────────────────┐
│  Determination of deflection based       │
│  compacted subgrade thickness            │
└─────────────────────────────────────────┘
                    │
                    ▼
        ┌───────────────────────────┐
        │  CBR of natural and        │
        │  compacted subgrade as     │
        │  input parameter           │
        └───────────────────────────┘
                    │
                    ▼
    ┌───────────────────────────────────┐
    │  Transformation of layered system  │
    │  in to a homogenous system using   │
    │  Odemark's method                  │
    └───────────────────────────────────┘
                    │
                    ▼
    ┌───────────────────────────────────┐
    │  Estimation of deflection under    │
    │  wheel load on compacted subgrade  │
    │  (δᵢ) and natural subgrade (δᵢᵢ)   │
    └───────────────────────────────────┘
```

Estimation of deflection under wheel load on compacted subgrade (δ_I) and natural subgrade (δ_{II})

Total subgrade deflection $\delta = \delta_I + \delta_{II}$

Deflection in a homogenous system
$$\delta = \frac{1.5qa}{E_{eff}}$$

$$E_{eff} = \frac{1.5qa}{(\delta)}$$

$$E_{eff} = 10(CBR)$$
$$E_{eff} = 17.6(CBR)^{0.64}$$

OUTPUT
The thickness of compacted subgrade with required effective CBR

Figure 2.3 Flow diagram for determination of deflection based effective subgrade CBR and compacted subgrade thickness.

2.3.5   Results and Discussion

The effective CBR is an important parameter for characterization of subgrade when subgrade improvement is done by placing compacted borrowed soil over natural subgrade from the borrow pit. Increase in effective CBR improves significantly the service life of flexible pavement against rutting and therefore, it is important to study the influence of factors which may affect the effective CBR as design parameter. Moreover, it is also important to identify the most sensitive parameter out of various other factors which may influence the effective CBR of a layered subgrade. In present chapter, depth of compacted subgrade has been determined using natural subgrade CBR and compacted subgrade CBR as input variable with a target of achieving an effective CBR of compacted subgrade using borrowed soil. The natural subgrade CBR between 2-7% has been considered in present analysis whereas the borrowed soil CBR for compacted subgrade has been considered between 5-30%.In this study , natural subgrade CBR values has been considered in lower range which characterizes the strength of comparatively weak subgrade But , the strength of borrowed soil CBR for compacted subgrade has been considered relatively in a higher range which is needed for strength improvement of weak subgrade .In this context , it is relevant to mention that if the insitu subgrade CBR is less than 5%, IRC-37-2018 [51] recommends for subgrade improvement by placing borrowed soil on the top of weak natural subgrade.

In this backdrop, the effective CBR of subgrade has been considered in present study from 5- 15 %. It is to be noted that the thickness design of bituminous road pavement is now based on the effective CBR of the subgrade when the natural subgrade requires to be strengthened by compacted subgrade. Variation of thickness of compacted subgrade with effective CBR obtained from present analysis using the present model have been presented in this chapter from Figure 2.4 to Figure 2.19 and inTable 2.1 to Table 2.6 (Appendix 1A). It has been observed that the thickness of compacted subgrade decreases sharply with increase in CBR of borrowed soil. However, such rate of change of compacted subgrade thickness varies with the variation in effective CBR, the CBR of borrowed soil and natural subgrade. Moreover, such a change in

thickness of the compacted subgrade becomes significant when the requirement for effective CBR is higher.

In this study effective CBR between 5-10% has been characterized as lower range and whereas 10-15% has been considered as higher range of effective CBR. It has been observed in present analysis that the rate of change of thickness of compacted subgrade is significant up to 20% CBR of borrow materials when effective CBR lies in lower range. Moreover, the thickness change of compacted subgrade becomes less significant beyond the threshold of 20% CBR of borrow materials. However, the same was found to vary significantly up toa CBR of 30% when effective CBR lies in higher range. The requirement of compacted subgrade thickness becomes higher with a borrow material of comparatively lower CBR. But when the borrow material strength is higher with higher CBR value, the thickness of compacted subgrade becomes less. Moreover, the variation of compacted subgrade thickness was also found to vary with natural subgrade strength. However, the effect of variation of natural subgrade CBR on compacted subgrade thickness is less sensitive than the variation of CBR of borrow material. In present analysis MATHEMATICA programming language has been used to solve all the equations.
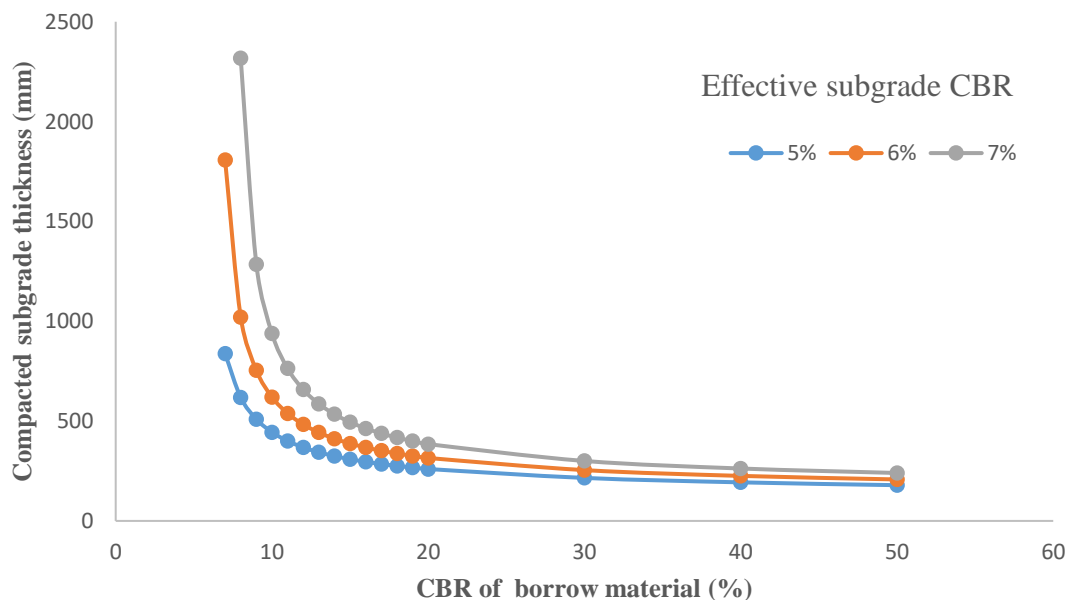
Figure 2.4: Variation of compacted subgrade thickness with change in CBR of borrow material for natural subgarde CBR of 2%
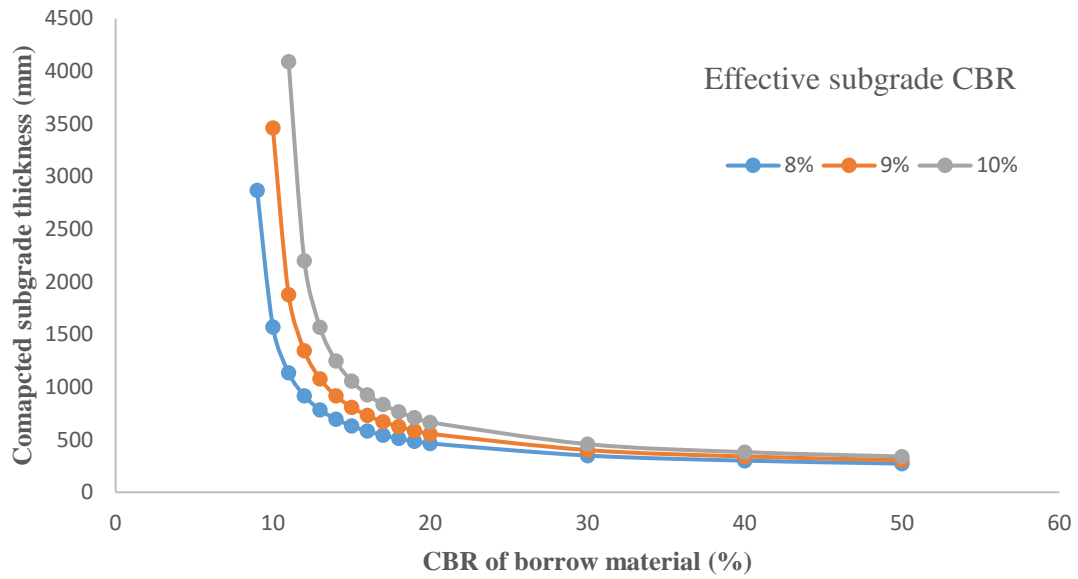
Figure 2.5: Variation of compacted subgrade thickness with change in CBR of borrow material for natural subgarde CBR of 2%
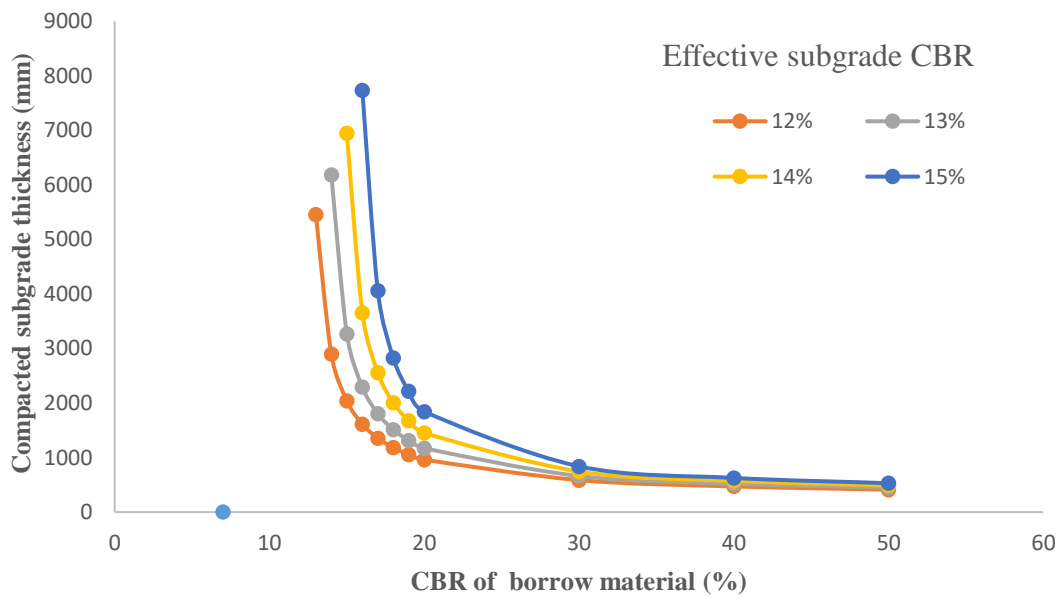
Figure 2.6: Variation of compacted subgrade thickness with change in CBR of borrow material for natural subgarde CBR of 2%
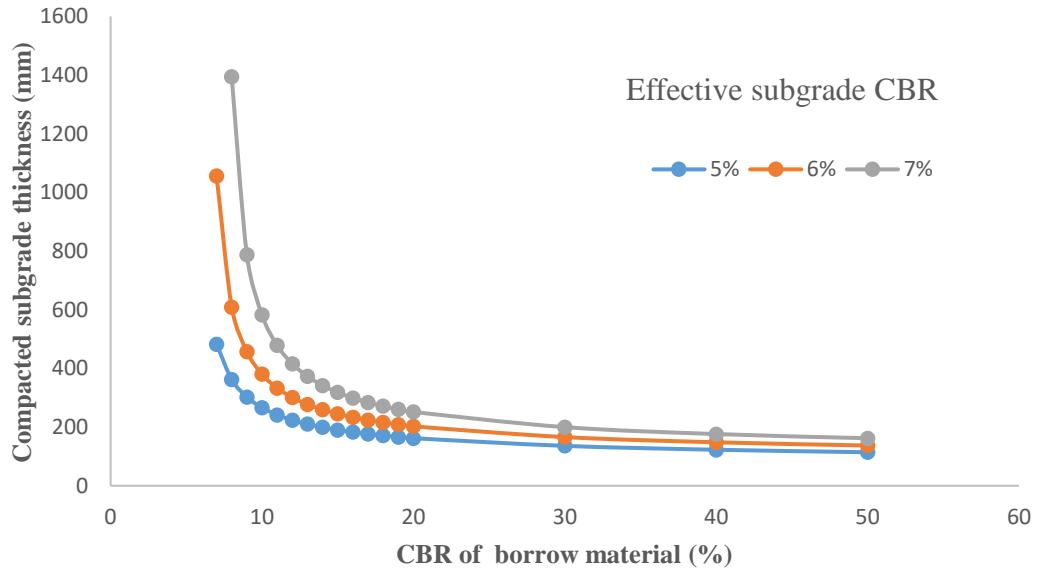
Figure 2.7: Variation of compacted subgrade thickness with change in CBR of borrow material for natural subgarde CBR of 3%
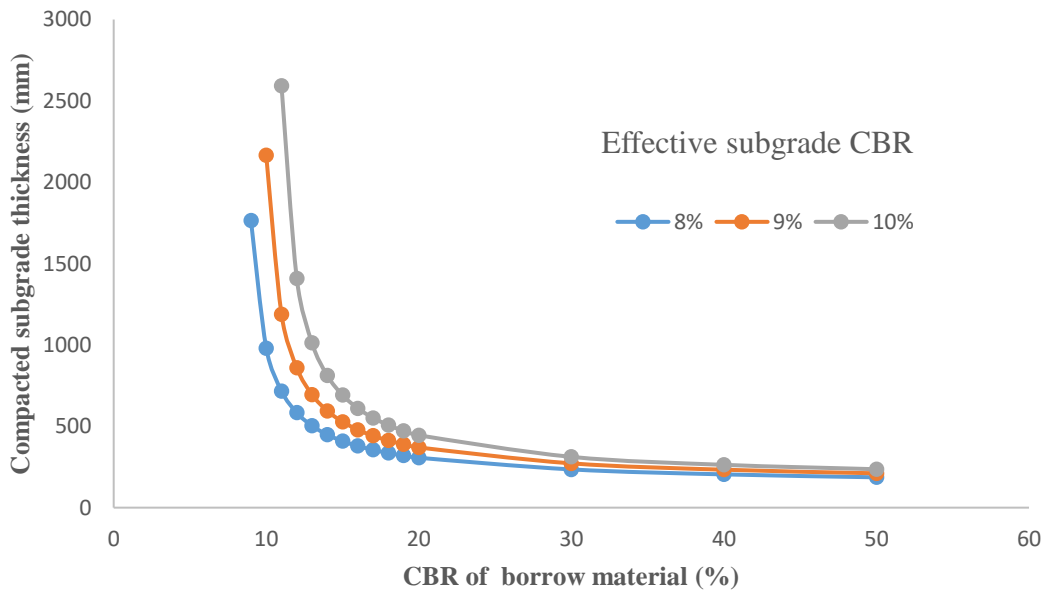
Figure 2.8: Variation of compacted subgrade thickness with change in CBR of borrow material for natural subgrade CBR of 3%
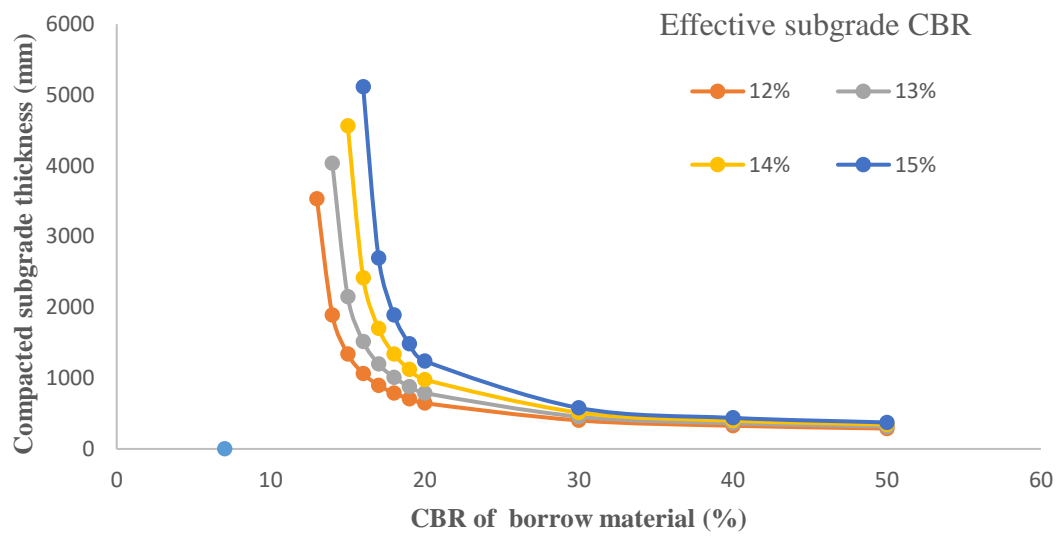
Figure 2.9: Variation of compacted subgrade thickness with change in CBR of borrow material for natural subgrade CBR of 3%
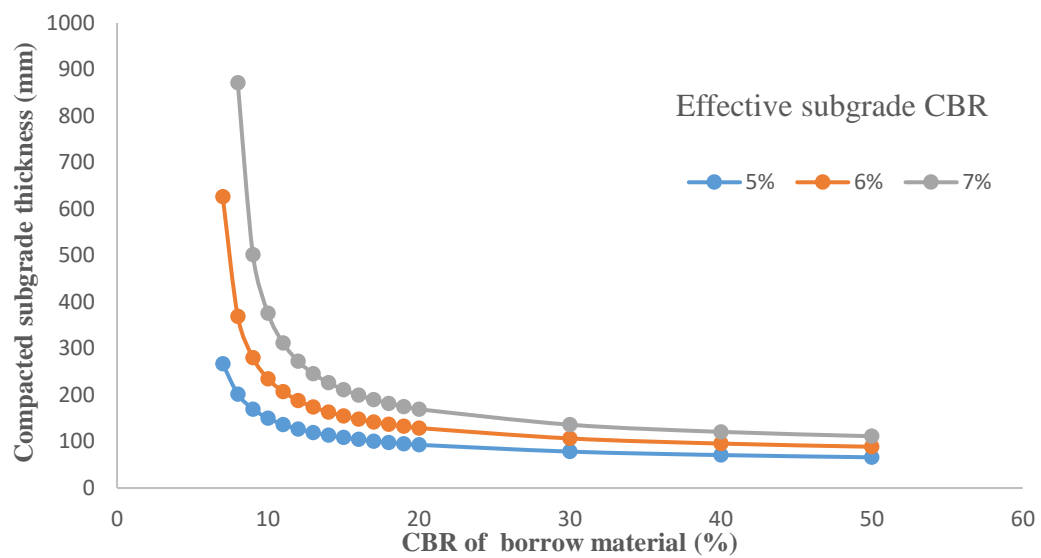
Figure 2.10: Variation of compacted subgrade thickness with change in CBR of borrow material for natural subgrade CBR of 4%

29
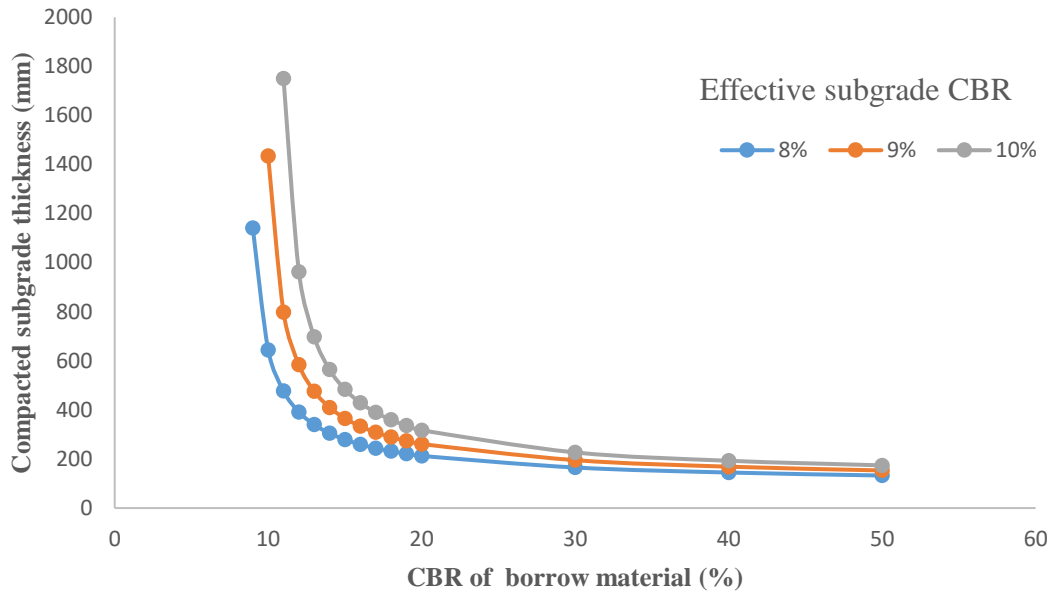
Figure 2. 11: Variation of compacted subgrade thickness with change in CBR of borrow material for natural subgrade CBR of 4%
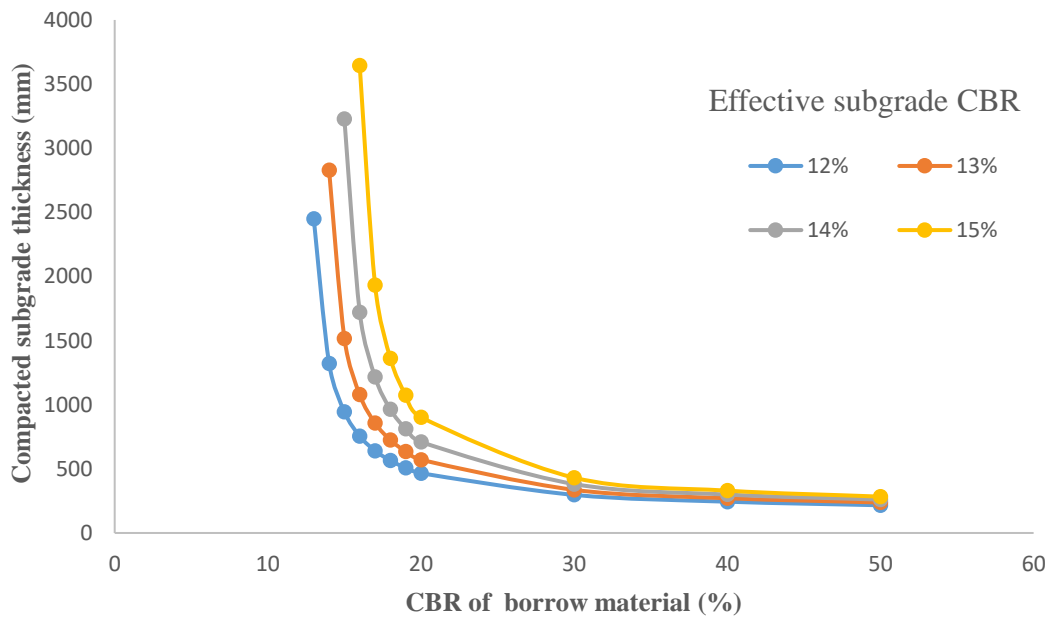
Figure 2.12: Variation of compacted subgrade thickness with change in CBR of borrow material for natural subgrade CBR of 4%
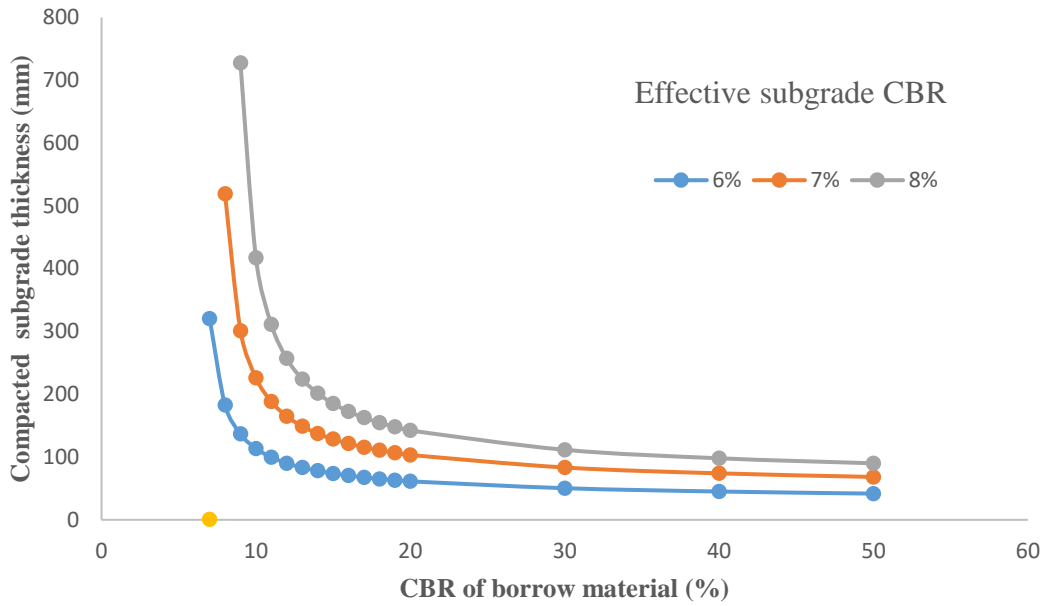
Figure 2.13: Variation of compacted subgrade thickness with change in CBR of borrow material for natural subgrade CBR of 5%
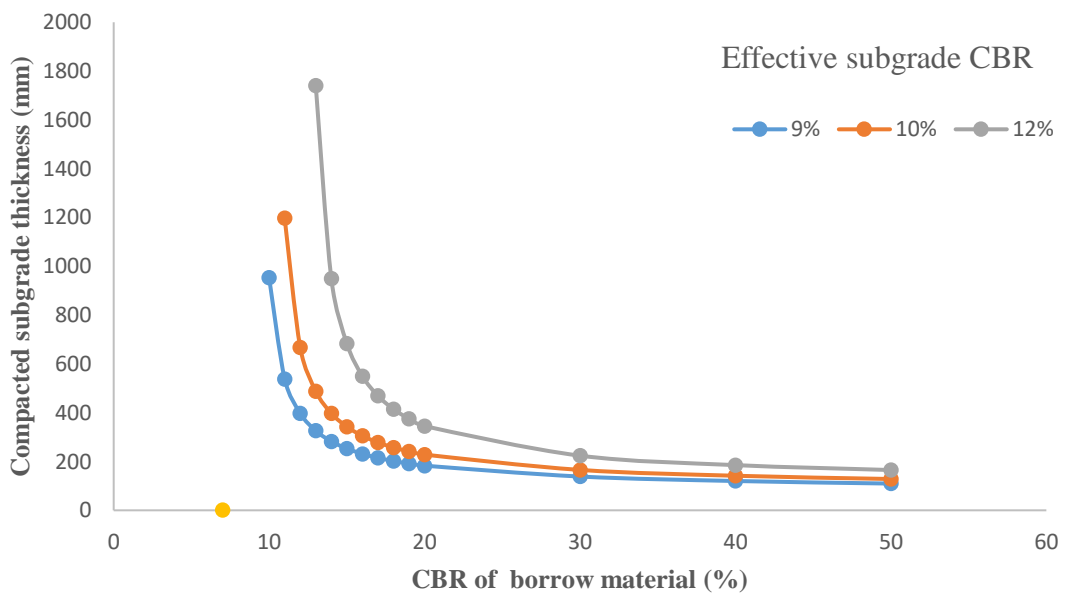
Figure 2.14: Variation of compacted subgrade thickness with change in CBR of borrow material for natural subgrade CBR of 5%
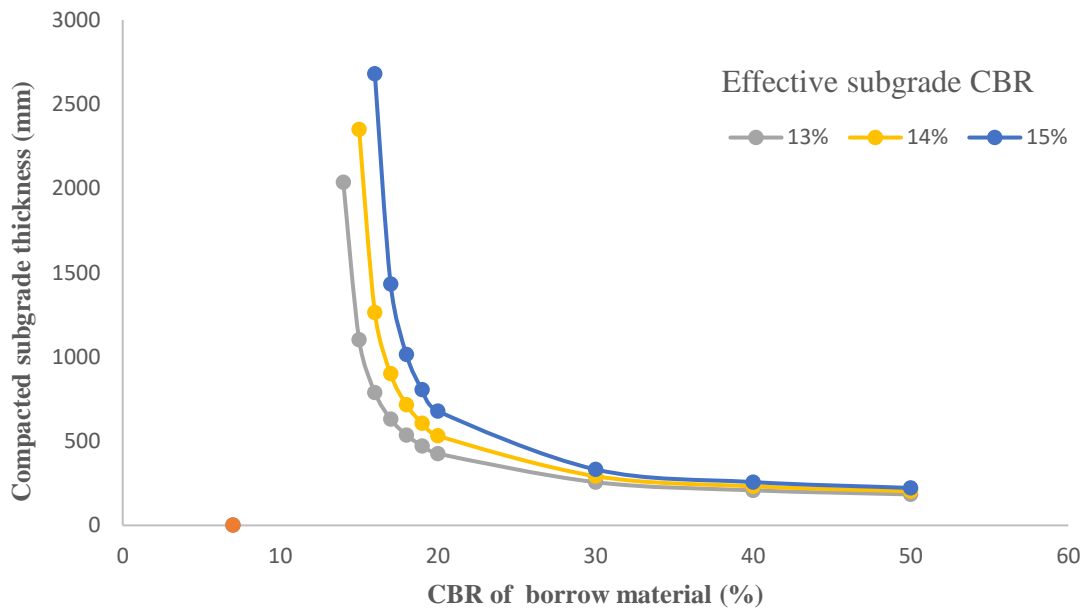
Figure 2.15: Variation of compacted subgrade thickness with change in CBR of borrow material for natural subgrade CBR of 5%
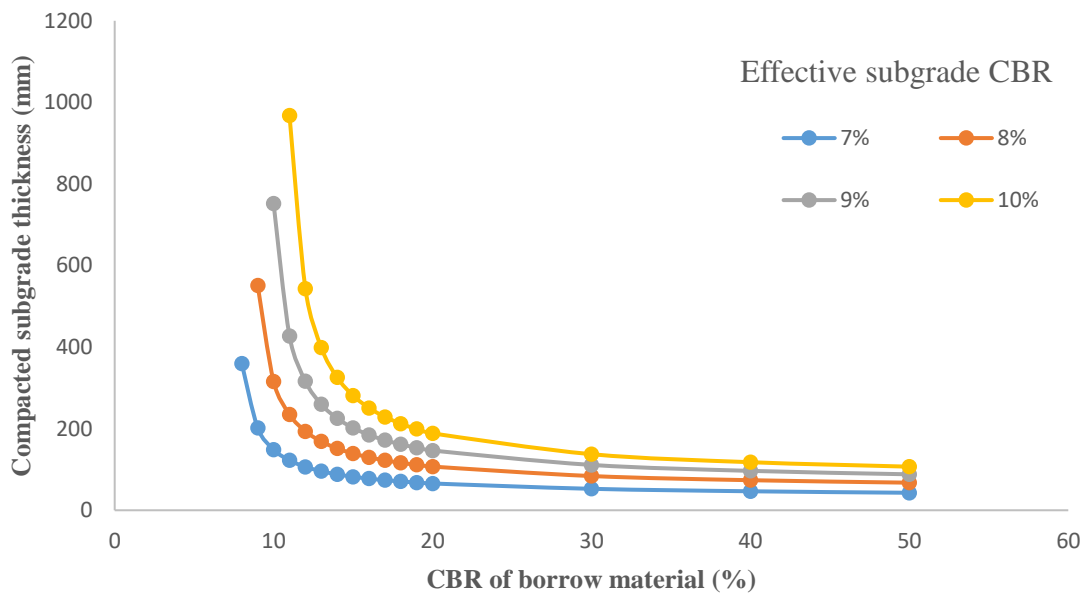
Figure 2.16: Variation of compacted subgrade thickness with change in CBR of borrow material for natural subgrade CBR of 6%
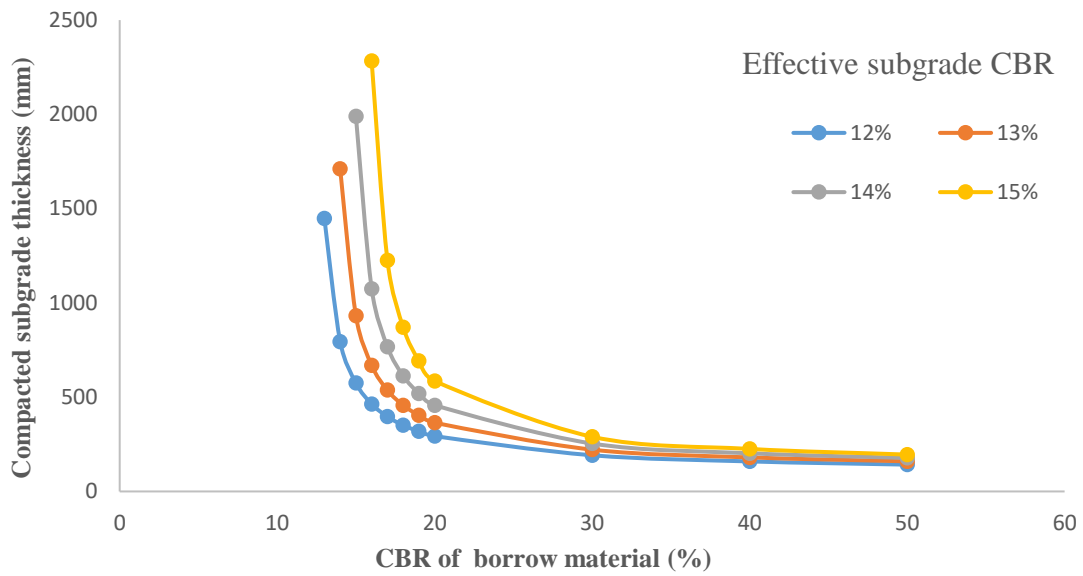
Figure 2.17: Variation of compacted subgrade thickness with change in CBR of borrow material for natural subgrade CBR of 6%
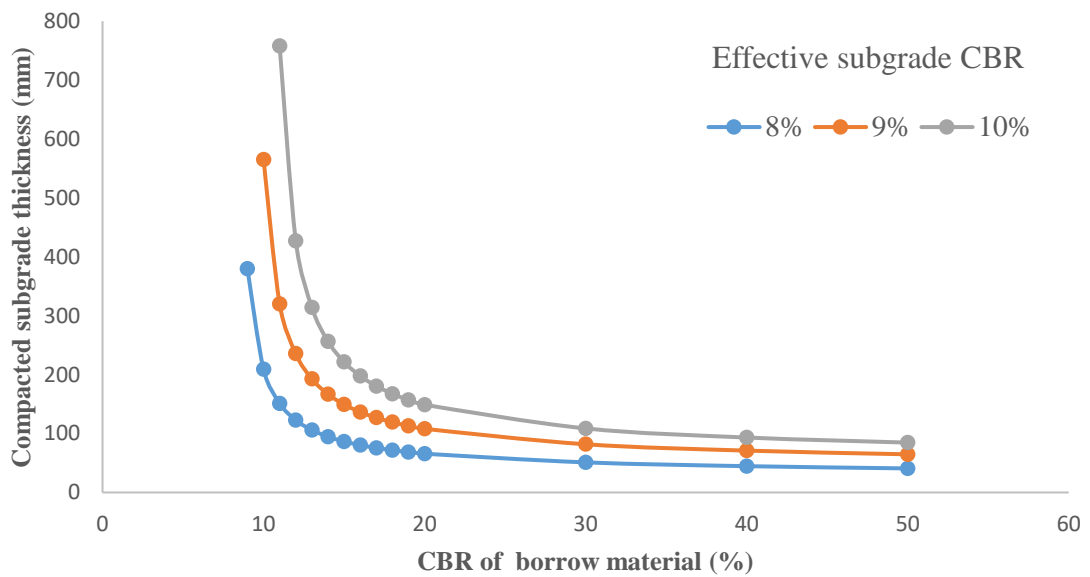
Figure 2.18: Variation of compacted subgrade thickness with change in CBR of borrow material for natural subgrade CBR of 7%
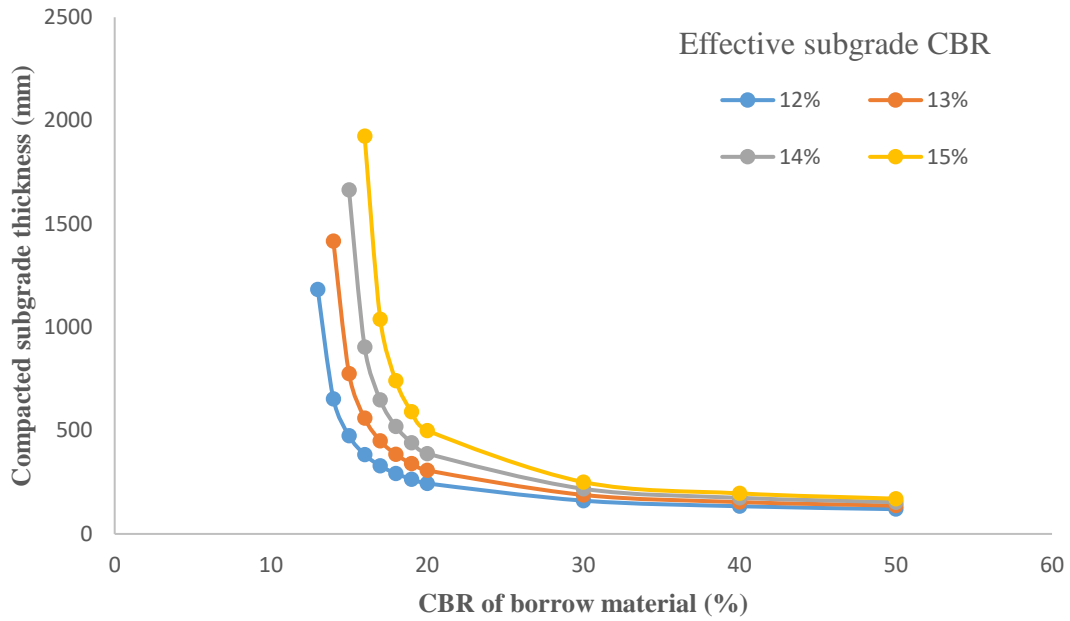
Figure 2.19: Variation of compacted subgrade thickness with change in CBR of borrow material for natural subgrade CBR of 7%

2.3.6   Validation of proposed model

For validation of test results, the analysis presented in IRC-37-2012 has been considered in the present study. The natural CBR of soil in the IRC-37-2012 [48] ranges between 1.5% to 7% whereas the CBR of borrowed soil has been considered from 7% to 50%. The effective CBR recommended in IRC: 37-2012 [48] has been estimated considering a thickness of 500 mm of compacted subgrade The effective CBR of subgrade in a two-layered system obtained using present method with similar variables of IRC: 37-2012 [48] corresponding to natural subgrade CBR between 1.5% to 7% have been presented in Figure 2.20 to Figure 2.21 and in Table 2.7 to Table 2.8 (Appendix 1A).It has been found that the effective CBR data obtained using present method matches closely with IRC-37-2012 [48] data. However, it is relevant to mention that the results obtained from IRC-37-2012 [48] are based on the output of ELAYER [145] computer program used by the researchers in IIT Kharagpur. The program is

based on Burmister's [37-41] analysis with a layered system having a rough interface. But, the present analysis is based on a linear elastic theory using the method of equivalent thickness. Therefore, convergence of output data in terms of effective CBR justifies the acceptability of the proposed methodology presented in this chapter.

However, in future, the effective CBRvalue may be estimated using strain and stress based approach where the vertical compressive strain and stress on top of the subgrade may be considered as design parameter. The strain and stress based method in such cases may include the number of standard axle load repetitions which the improved subgrade can withstand before it fails under rutting.
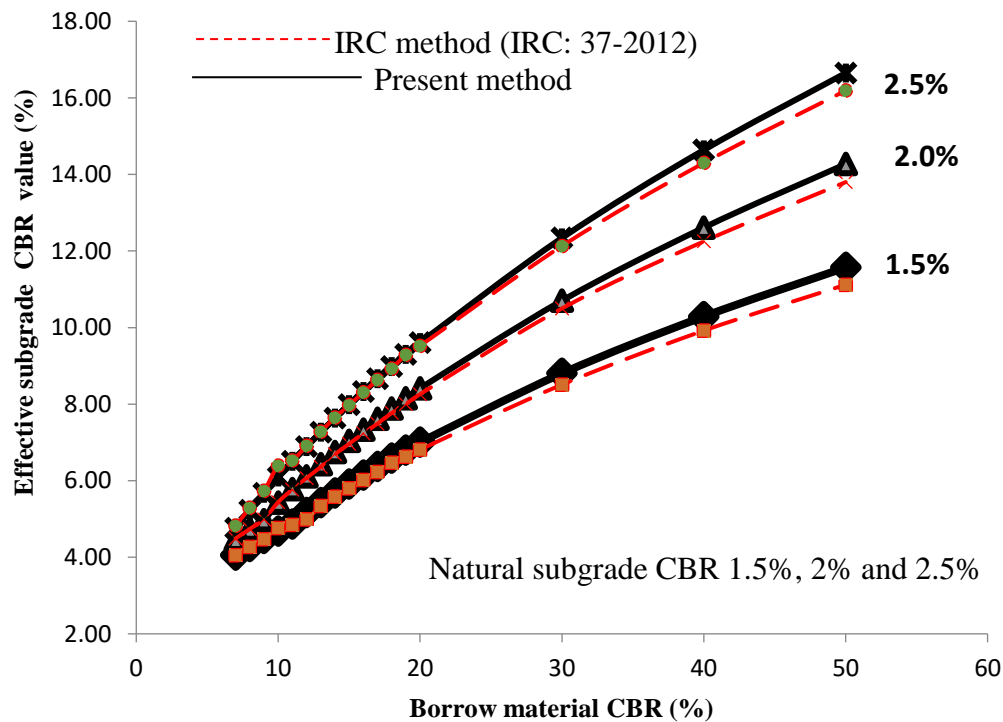
Figure 2.20: Comparison of Effective Subgrade CBR obtained using present method and IRC: 37-2012.
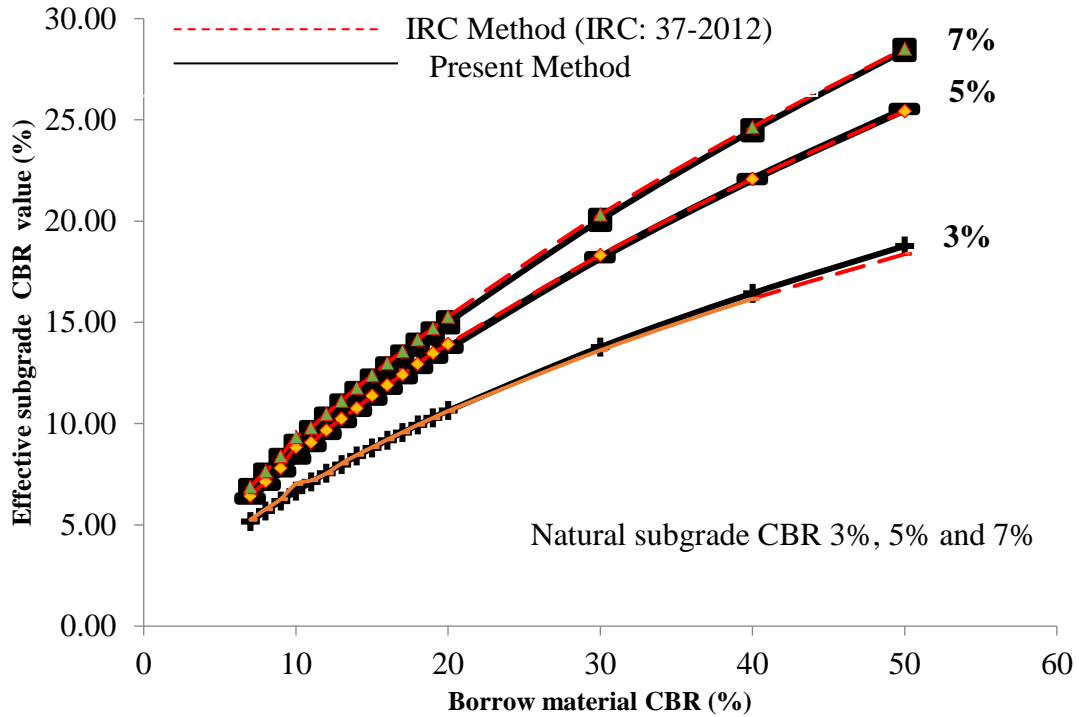
Figure 2.21: Comparison of effective subgrade CBR obtained using present method and IRC: 37-2012

2.3.7 Concluding remarks

Effective CBR can be estimated based on the fixed thickness of compacted borrow materials that are placed on the natural subgrade. However, the present method for estimation of compacted subgrade thickness may be used to achieve a required effective CBR of subgrade for the design of flexible road pavement. In this method, natural subgrade CBR, compacted soil subgrade CBR, and effective CBR are used as input variables while the compacted subgrade thickness becomes output. It is relevant to mention that when the natural subgrade CBR is less than 5%, the subgrade improvement becomes essential to make the pavement durable with a higher service life against rutting. It has been found from the present study that the thickness of compacted subgrade largely varies up to 20% CBR of borrowed soil , beyond which the variations are not significant In future, efforts are needed to estimate the effective subgrade CBR considering the service life of the pavement.

2.4 Determination of compacted subgrade thickness using vertical compressive strain as design parameter.

Often weak natural subgrade is strengthened by placing borrowed soil on top of it for formation of compacted subgrade. Strengthening of weak subgrade improves the service life of bituminous road pavement by reducing the probability of failure of pavement under rutting.

2.4.1 Objective

The objective of present study has been considered to formulate a Mechanistic - Empirical design approach for estimation of compacted subgrade thickness based on vertical compressive strain on top of natural subgrade.

2.4.2 Method of analysis

In order to estimate the allowable vertical stress on top of compacted subgrade, primarily the CBR – depth relationship of flexible pavement design as per ICAO method was considered. The method suggests an Equation 2.10 for determination of ACN value of an aircraft which has been considered in present analysis.

$$t = \sqrt{P \left[\frac{1}{8.1 CBR} - \frac{1}{p\pi} \right]} \tag{2.10}$$

Where P = Load of a single wheel in (lb)

p= Tyre pressure in (lb/in^2) and t = thickness of pavement (inches).
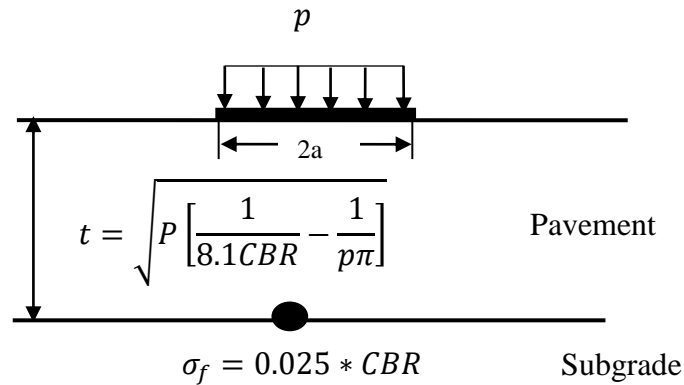
Figure 2.22: Two layer pavement with subgrade

Therefore the effect of wheel load on surface may be determined as vertical interface stress on top of subgrade, which has been determined in present analysis using Boussinesq's Equation. In Boussinesq's equation the vertical stress at depth (z) for a wheel load intensity (q) with a circular radius 'a' may be expressed in Equation 2.11.Therefore, the thickness of pavement determined from Equation 2.10 for a known subgrade CBR, wheel load and tyre pressure may be used in Boussinesq's Equation 2.11 for estimation of vertical stress on top of subgrade.

$$\sigma_z = q \left[1 - \frac{1}{\left\{ \sqrt{1+\left(\frac{a}{z}\right)^2} \right\}^3} \right] \tag{2.11}$$

The interface vertical stress on subgrade thus obtained has been considered as permissible stress on subgrade (σ_f) in present chapter. The correlation between permissible stress (σ_f) and subgrade CBR has been established from Equation 2.11 for a wheel load 12566 lb and tyre pressure 181 psi and contact radius of 4.7 inch , Which is shown in Equation 2.12.

$$\sigma_f = 0.025 \, CBR \tag{2.12}$$

Where σ_f = permissible stress on subgrade in MPa

In present analysis the permissible stress on subgrade has been estimated considering 10% CBR value for lower subgrade range. In such case the allowable load on compacted subgrade has been calculated using 0.25 MPa, using Equation 2.12. However where the compacted subgrade CBR is comparatively higher than allowable load intensity has been estimated considering a CBR of 15% using Equation 2.12, which results an allowable stress of 0.375 MPa for estimation of compacted subgrade thickness.

In present analysis lower compacted CBR includes subgrade with CBR less than 10% whereas the higher CBR group means when the compacted CBR of subgrade is increase 10%.

In the present study for the estimation of compacted subgrade thickness , the system has been considered as two layer system with , the top consists of

borrow material with higher subgrade CBR followed by natural subgrade with lower CBR and has been shown in Figure 2.23 . The elastic modulus of both natural and compacted subgrade may be estimated from the relationship developed by Powell et al [135] as given in Equation 2.8and2.9of the previous section
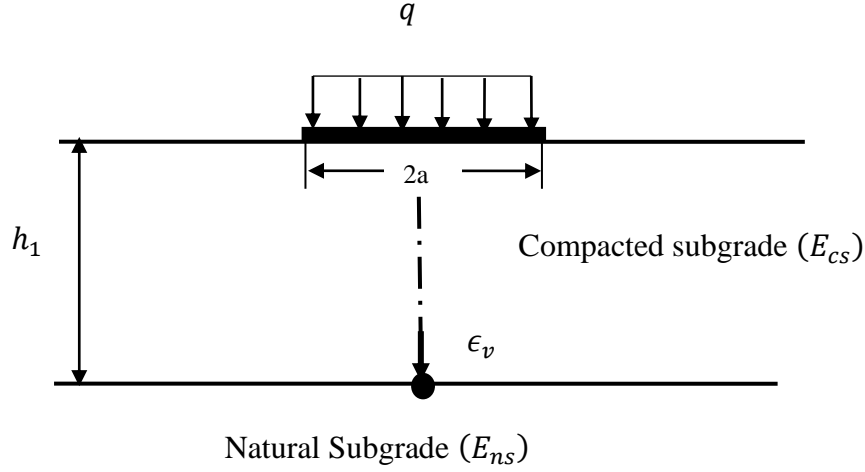
Figure 2.23: Two layered system with natural and compacted subgrade.
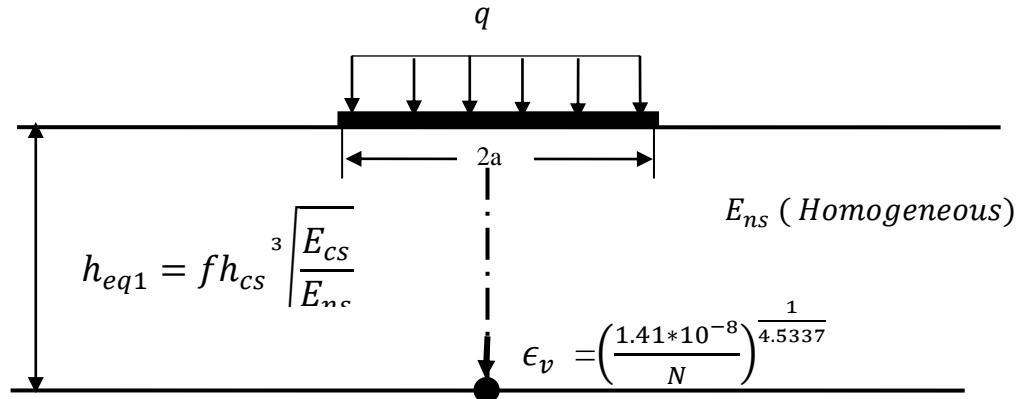
Figure 2.24: Transformation of two layered system into a homogeneous medium.

The permissible stress thus obtained from Equation.2.12 has been considered to act on the top of the compacted subgrade in the form of a circular flexible uniformly distributed load with same diameter as that of wheel load on surface . The vertical compressive strain (ϵ_v) on the top of the natural subgrade has been determined using theory of elasticity as proposed by Boussinesq's [34]

and is shown in Equation 2.13. It is known that the vertical compressive strain on top of subgrade relates the pavement failure under rutting. Therefore the vertical compressive strain which may likely to occur on top of natural subgrade should always be less than the permissible vertical strain corresponding to a specified axle load repetitions to be safe under rutting.

Therefore, to reduce the vertical compressive strain on weak natural subgrade with lower elastic modulus (E_{ns}), compacted subgrade with appropriate thickness would require with higher elastic modulus (E_{cs}) to limit the strain at layer interface, in a two layered system.

$$\epsilon_v = \frac{(1+v)q}{E} \left[\frac{\frac{z}{a}}{\left\{ \sqrt{1+\left(\frac{z}{a}\right)^2} \right\}^3} - (1-2v) \left\{ \frac{\frac{z}{a}}{\sqrt{1+\left(\frac{z}{a}\right)^2}} - 1 \right\} \right] \quad (2.13)$$

However, in present analysis the subgrade is a two layered system. Therefore, Odemarks method has been used in present section to transform the two layered system in to a homogeneous system. The equivalent thickness of the transformed section may be expressed as (h_{eq1}) and has been shown in Equation 2.14. The term h_{eq1} in place of 'z' has further been used in present analysis in Equation 2.13 with Ens (modulus of natural subgrade) and Ecs (modulus of compacted subgrade).

$$heq1 = 0.9\, h_{cs} \sqrt[3]{\frac{E_{cs}}{E_{ns}}} \quad (2.14)$$

However, the permissible vertical compressive strain on natural subgrade for specified standard axle load repetitions has been obtained from Equation 2.15 and has been used in Equation 2.13 to determine the required equivalent depth as shown in Equation 2.14.

$$N = 1.41 \times 10^{-8} \left(\frac{1}{\epsilon_v}\right)^{4.5337} \quad (2.15)$$

In the present analysis, the natural CBR of weak subgrade has been considered between 2% to 7.0%, whereas the compacted subgrade CBR has been considered from 8.0% to 15%. The flow diagram of the adopted methodology has been shown in Figure 2.25.
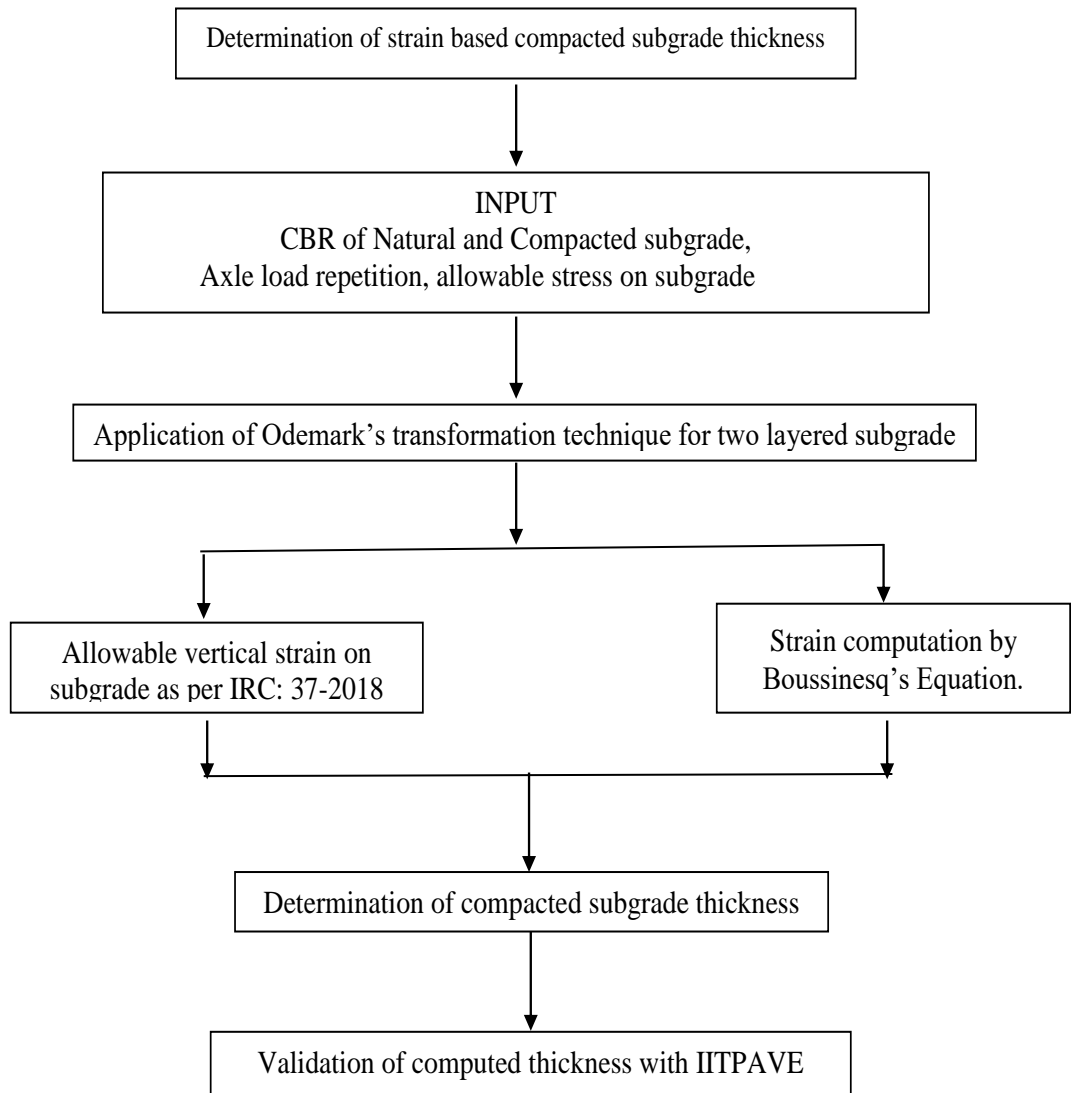
Figure 2.25: Flow diagram of adopted strain based methodology for estimation of compacted subgrade thickness

2.4.3   Results and Discussion

The methodology proposed in present study can be characterized as an analytical approach of soil improvement technique. The thickness of compacted subgrade has been so designed, can achieve the target CBR on the top of weak natural subgrade which rests below the granular subbase layer. The ranges of CBR of compacted subgrade chosen in the present analysis were between 8% to 15%. However, design load intensity on natural subgrade of 0.25 MPa and 0.375 MPa has been considered in the present analysis.

The thickness of compacted subgrade thus obtained corresponding to different natural subgrade and for different axle load repetitions are presented in Figure 2.26 to Figure 2.43 and Table 2.9 to Table 2.20 (Appendix 1B) considering load intensity of 0.25 Mpa and 0.375 MPa. It is relevant to note that, the failure of natural subgrade in terms of vertical strain changes with axle load repetitions on pavement. Therefore the design of compacted subgrade should also be based on expected axle load repetitions during the service life of pavement. In this context, analysis has been made in present study to establish correlation between thickness of compacted subgrade and axle load repetitions when placed over weak subgrade. The results obtained from present analysis show that the thickness of compacted subgrade reduces if the CBR of natural subgrade increases for a specific axle load repetition and vice versa. The reason of such result is obvious because the increased strength of natural CBR as foundation of the pavement would require less thickness of compacted subgrade if axle load repetition remains unchanged. It has been found from present analysis that the thickness of compacted subgrade increases with the increase in axle load repetitions where the CBR of both natural and compacted subgrade remains unaltered. It is relevant to note that the rate of change of thickness of compacted subgrade becomes significant up to a load repetition of 50 msa, beyond which the rate of such changes becomes less. It has been observed that, for weak subgrade with subgrade CBR of 2%, the compacted subgrade thickness increases 63% when the axle load repetition changes from 2msa to 150 msa. However such increase in thickness does not change much with the change in compacted subgrade CBR. Similarly for natural subgrade with higher CBR (7%) the increase of compacted subgrade thickness for 2 to 150 msa was found as

71%.In this backdrop, the effect of axle load repetitions on failure of compacted subgrade has to be understood in terms of failure under rutting. Ministry of Rural Development (MORD) specification for rural roads has defined the subgrade as top 300mm part of embankment just beneath the pavement crust. However, IRC:37-2018 [51], the guidelines for the design of flexible pavements in India recommends the thickness of compacted layer of subgrade as 500 mm immediately below the bottom of the pavement structure as a measure of subgrade improvement if the natural subgrade is weak in terms of its CBR. In this backdrop, the findings of the present study reveal that a finite thickness of compacted subgrade as recommended in IRC: 37-2018 [51] or in MORD specification may be under or over designed, resulting unsafe or uneconomic pavement.
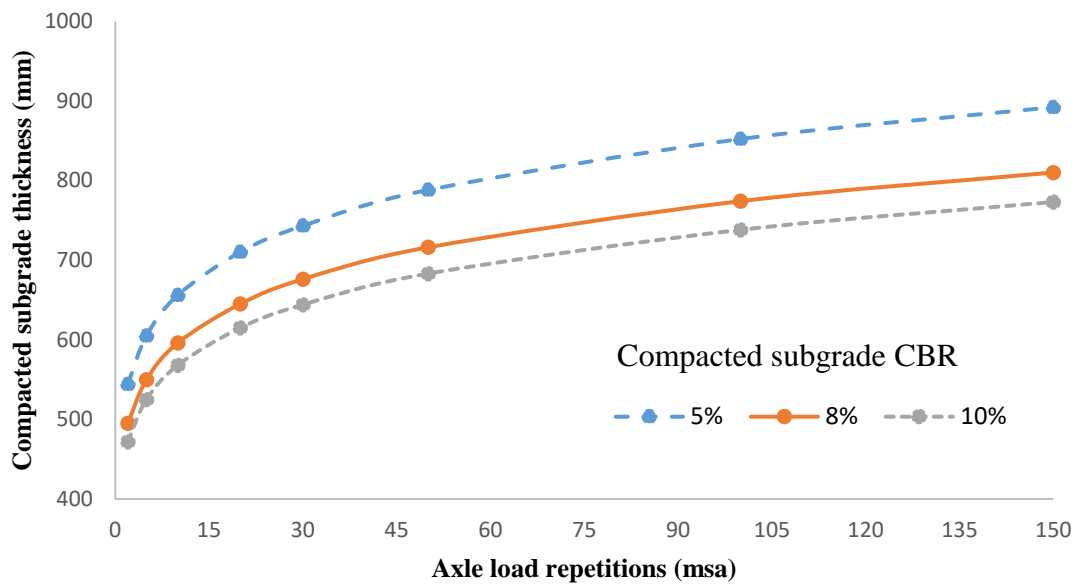
Figure 2.26: Variation of compacted subgrade thickness with axle load repetitions for 2% CBR of natural subgrade with 0.25 MPa contact pressure
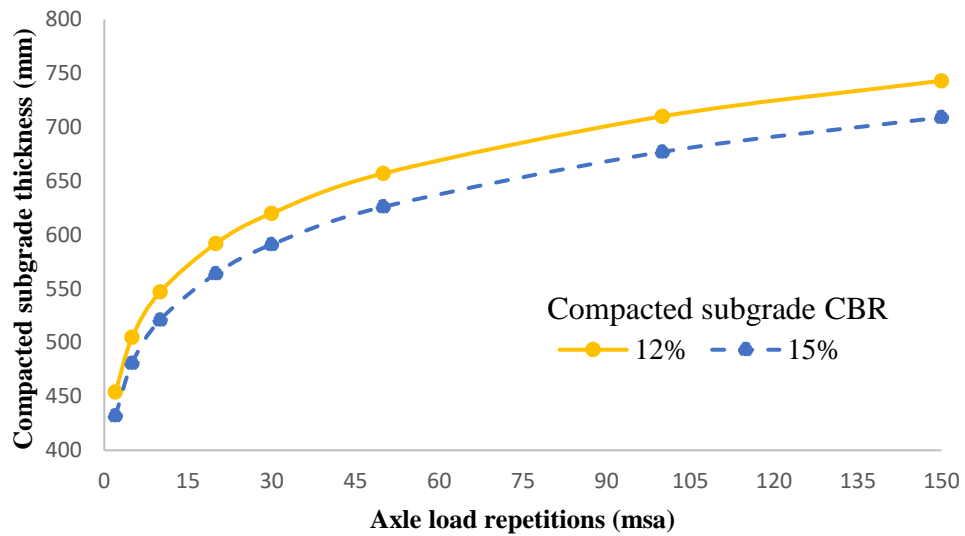
Figure 2.27: Variation of compacted subgrade thickness with axle load repetitions for 2% CBR of natural subgrade with 0.25 MPa contact pressure
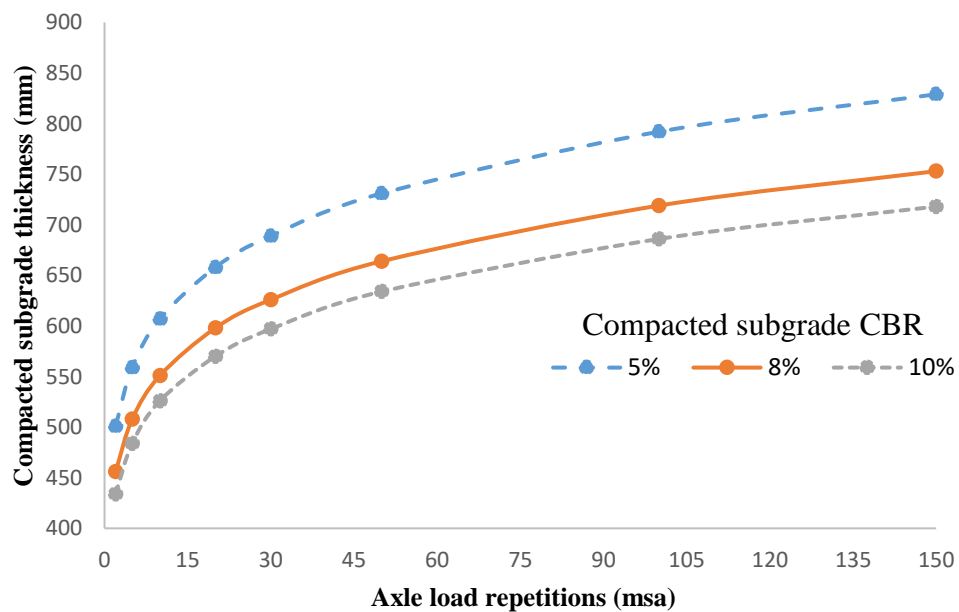
Figure 2.28: Variation of compacted subgrade thickness with axle load repetitions for 3% CBR of natural subgrade with 0.25 MPa contact pressure
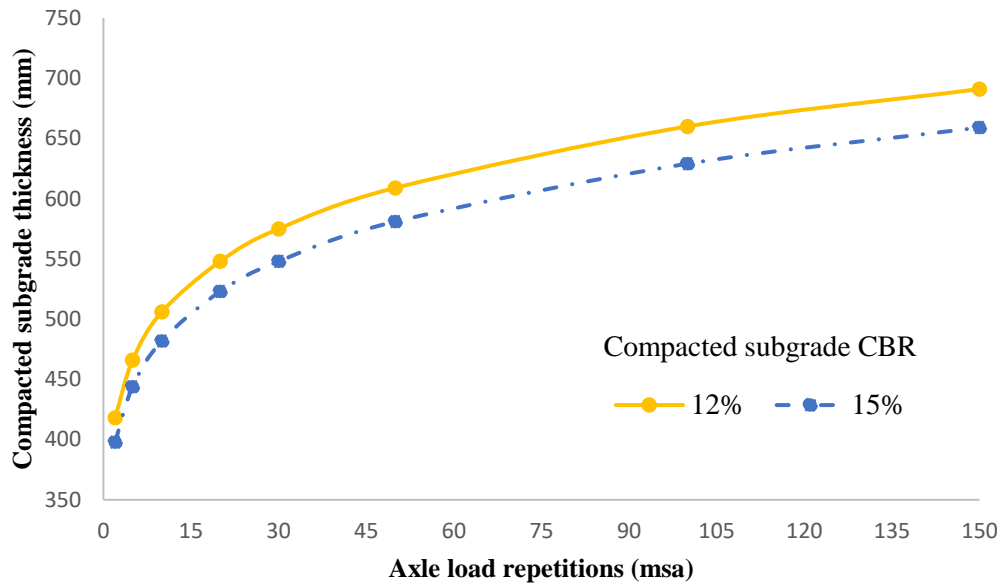
Figure 2.29: Variation of compacted subgrade thickness with axle load repetitions for 3% CBR of natural subgrade with 0.25 MPa contact pressure
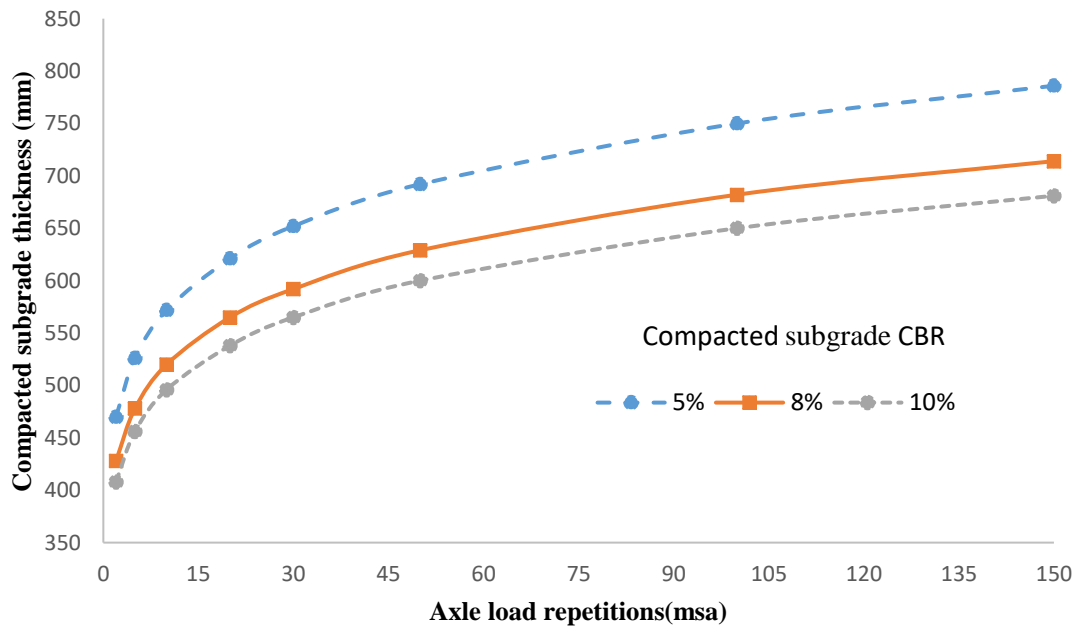
Figure 2.30: Variation of compacted subgrade thickness with axle load repetitions for 4% CBR of natural subgrade with 0.25 MPa contact pressure
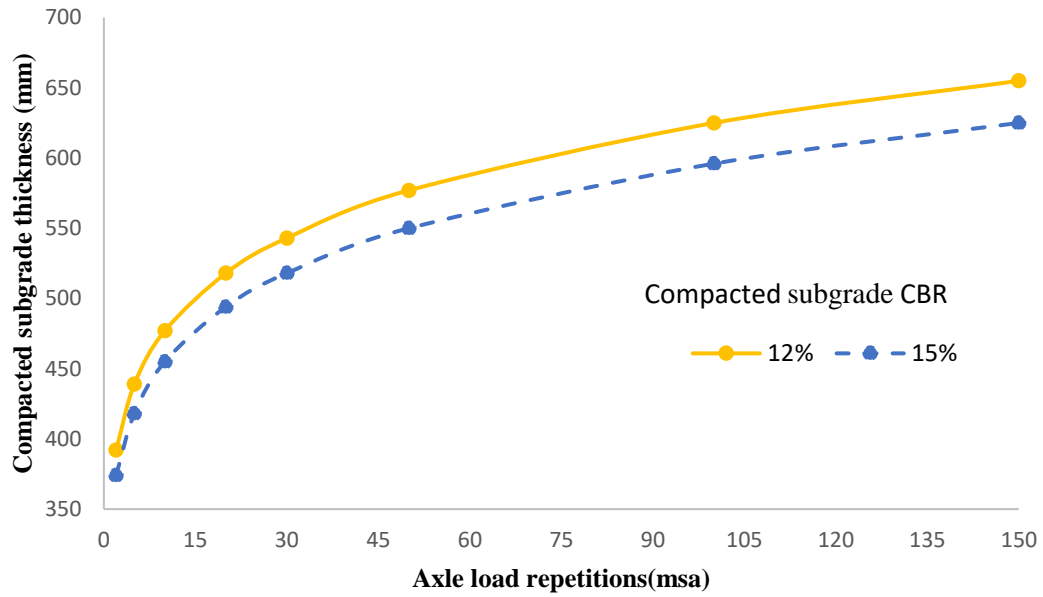
Figure 2.31: Variation of compacted subgrade thickness with axle load repetitions for 4% CBR of natural subgrade with 0.25 MPa contact pressure
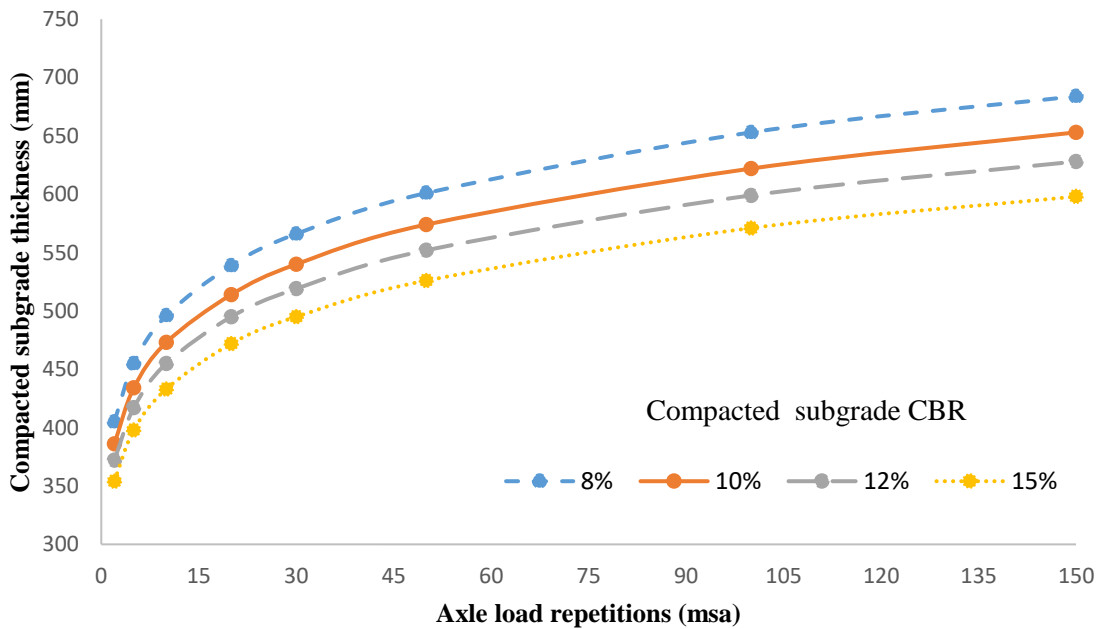
Figure 2.32: Variation of compacted subgrade thickness with axle load repetitions for 5% CBR of natural subgrade with 0.25 MPa contact pressure
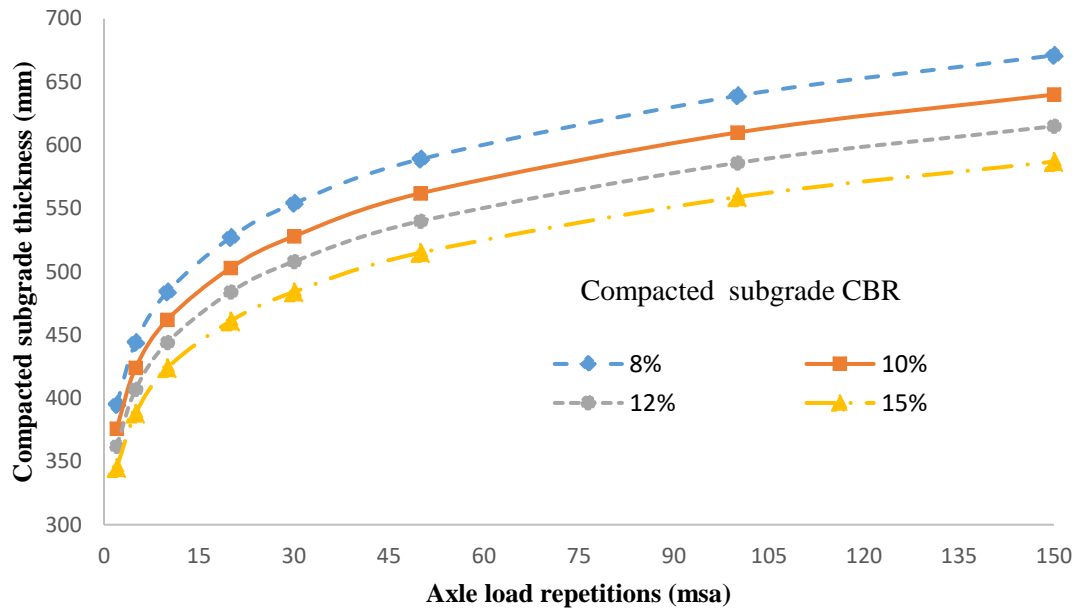
Figure 2.33: Variation of compacted subgrade thickness with axle load repetitions for 6% CBR of natural subgrade with 0.25 MPa contact pressure
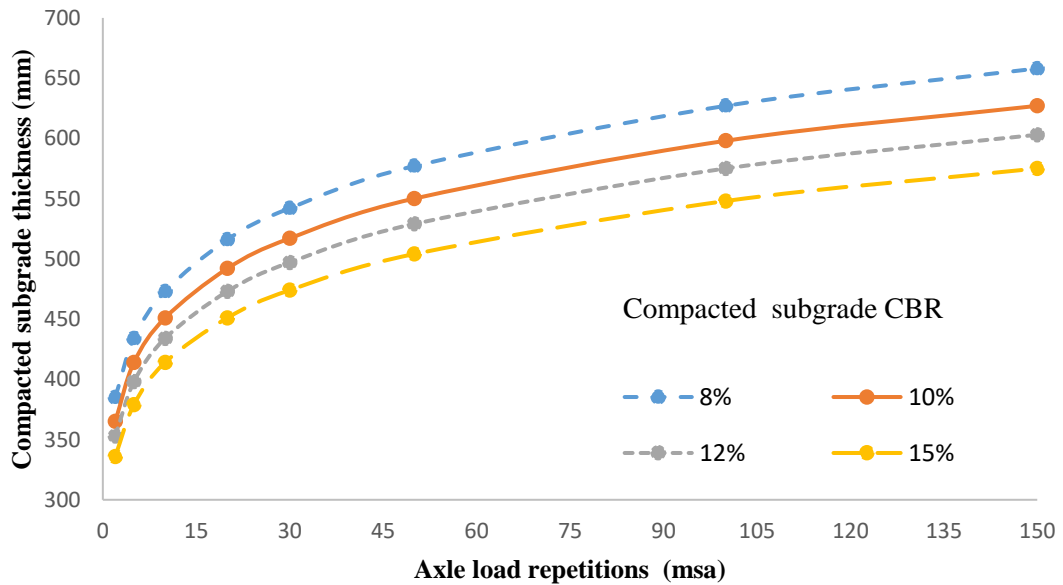
Figure 2.34: Variation of compacted subgrade thickness with axle load repetitions for 7% CBR of natural subgrade with 0.25 MPa contact pressure
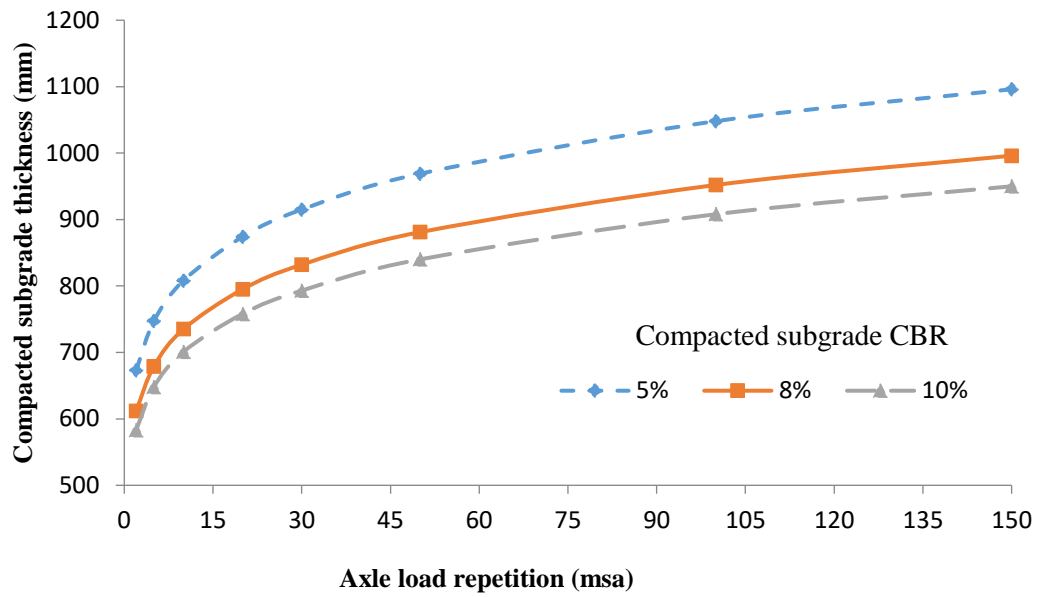
Figure 2.35: Variation of compacted subgrade thickness with axle load repetitions for 2% CBR of natural subgrade with 0.375 MPa contact pressure
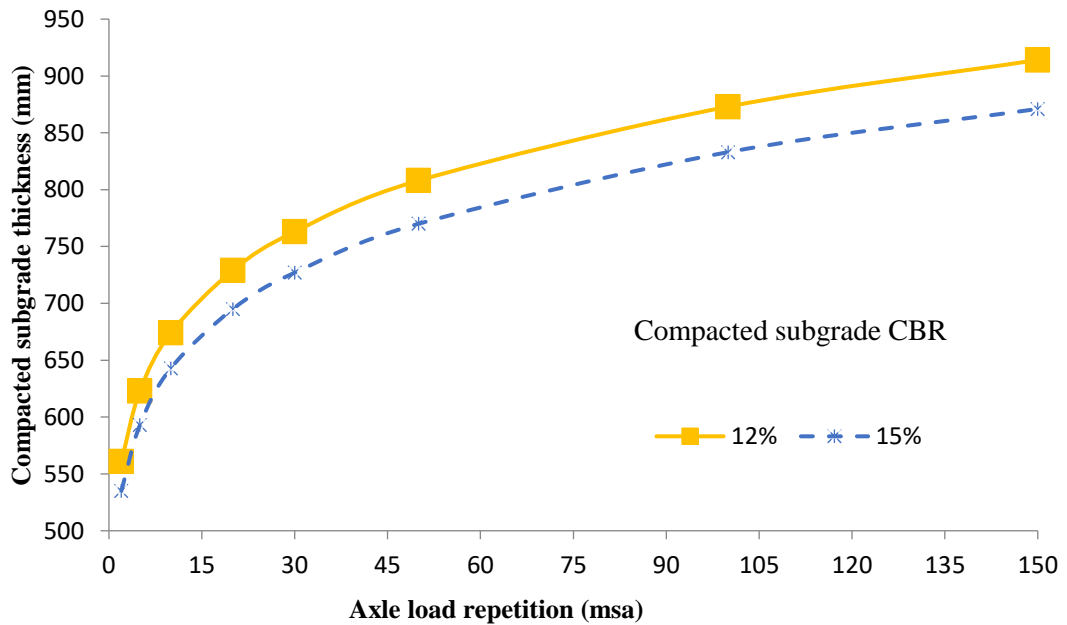
Figure 2.36: Variation of compacted subgrade thickness with axle load repetitions for 2% CBR of natural subgrade with 0.375 MPa contact pressure
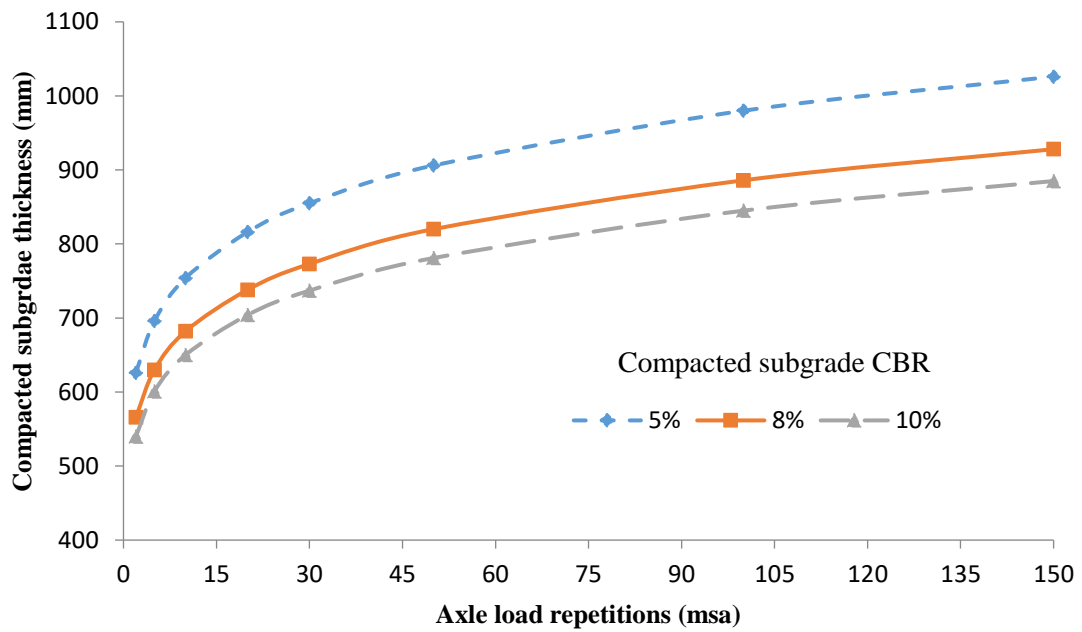
Figure 2.37: Variation of compacted subgrade thickness with axle load repetitions for 3% CBR of natural subgrade with 0.375 MPa contact pressure
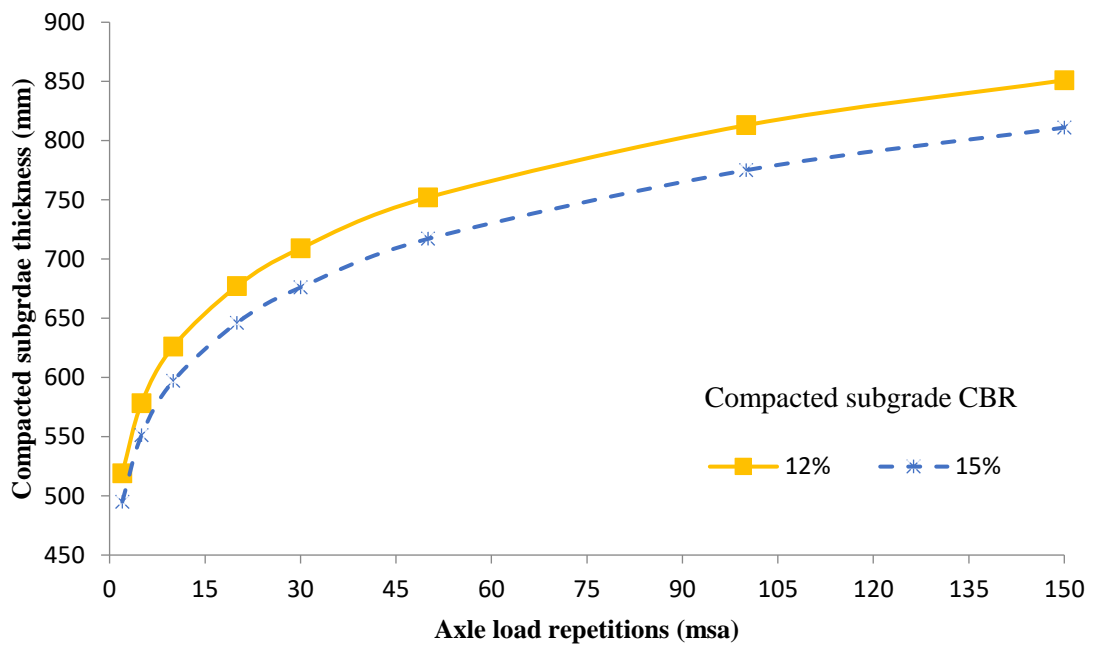
Figure 2.38 : Variation of compacted subgrade thickness with axle load repetitions for 3% CBR of natural subgrade with 0.375 MPa contact pressure

49
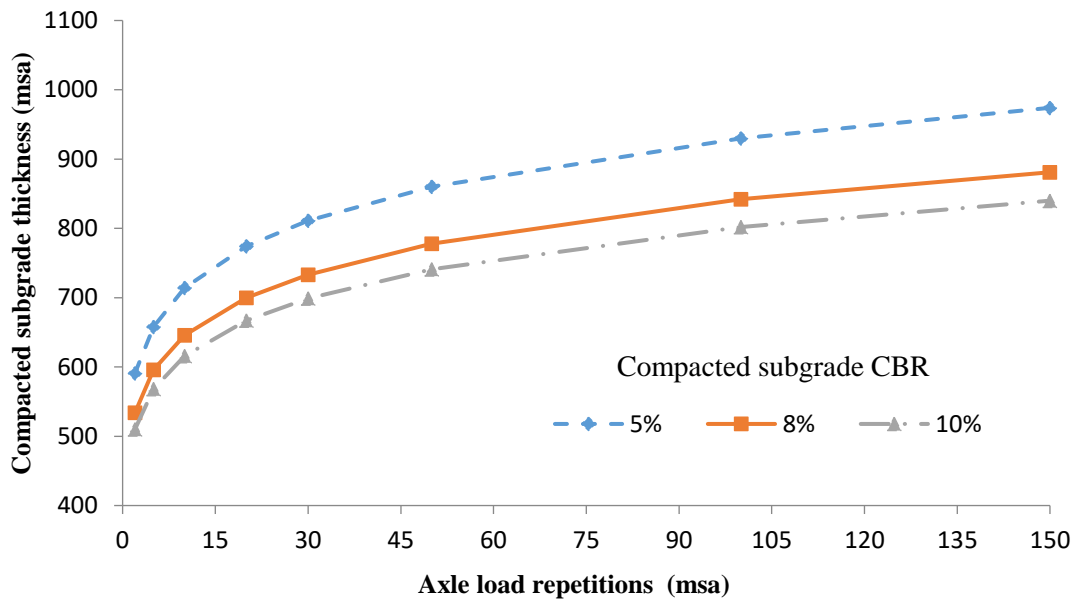
Figure 2.39: Variation of compacted subgrade thickness with axle load repetitions for 4% CBR of natural subgrade with 0.375 MPa contact pressure
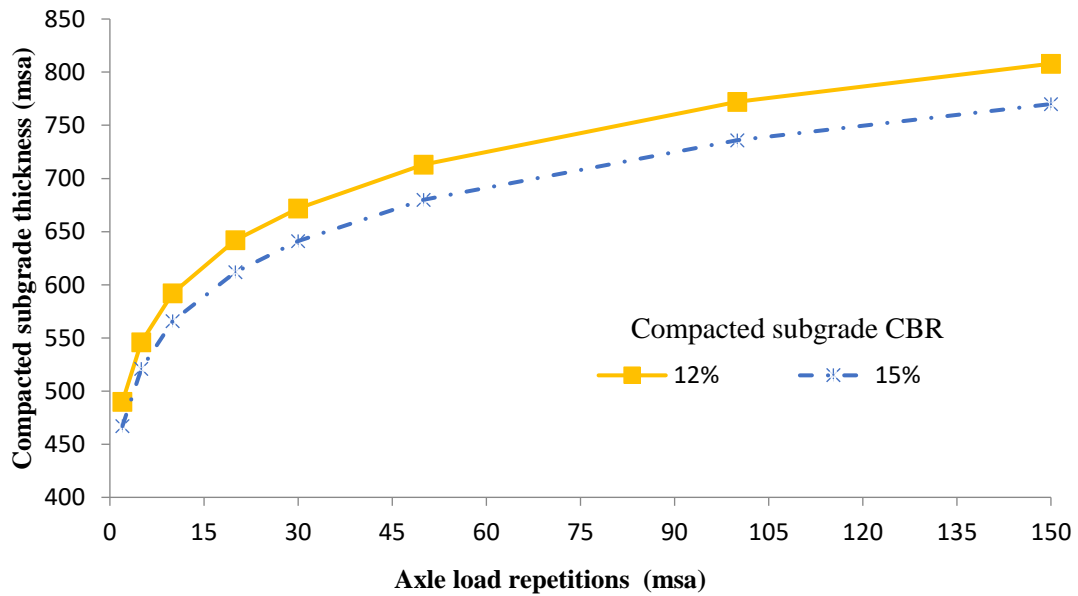
Figure 2.40: Variation of compacted subgrade thickness with axle load repetitions for 4% CBR of natural subgrade with 0.375 MPa contact pressure
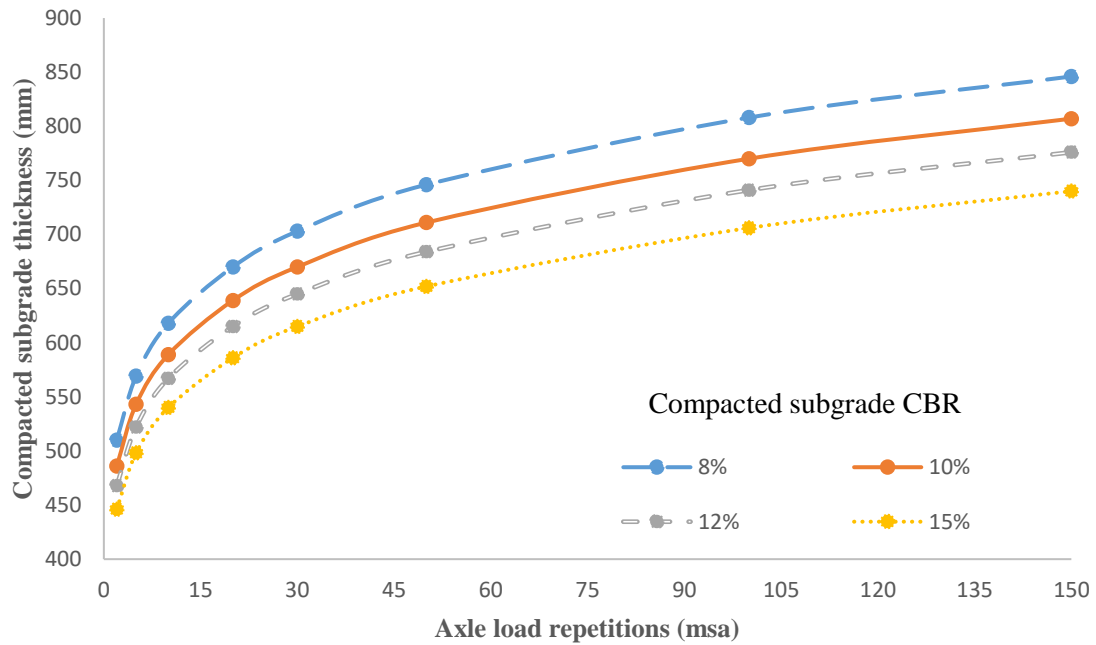
Figure 2.41: Variation of compacted subgrade thickness with axle load repetitions for 5% CBR of natural subgrade with 0.375 MPa contact pressure
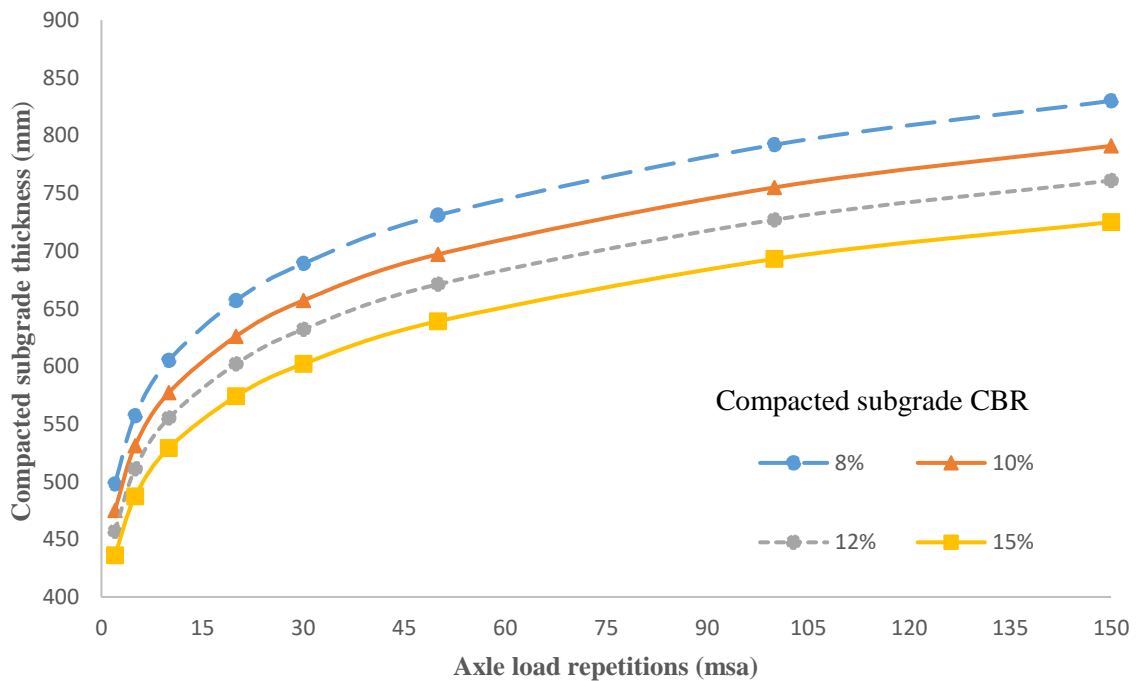
Figure 2.42: Variation of compacted subgrade thickness with axle load repetitions for 6% CBR of natural subgrade with 0.375 MPa contact pressure

51
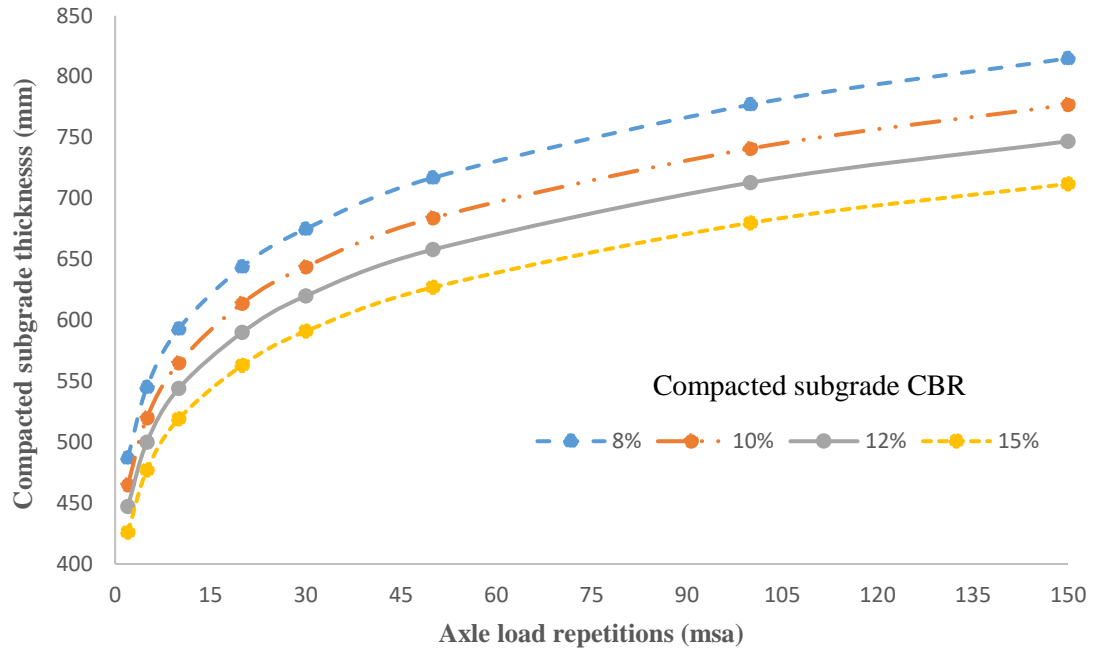
Figure 2.43: Variation of compacted subgrade thickness with axle load repetitions for 6% CBR of natural subgrade **with 0.375 MPa contact pressure**

2.4.4   Validation of Model: strain based approach

In this section attempts have also been made to compare the findings of present method with the thickness obtained using IITPAVE [51] software used for estimation of bituminous thickness in India. The thickness thus obtained has been presented in Figure 2.44 to Figure 2.55 and Table 2.21 to Table 2.26. It has been found from comparative study that the thickness obtained from present analysis are reasonably close to the results of IITPAVE [51] .In IITPAVE [51], the two layered subgrade with respective modulus of natural and compacted subgrade has been used as input parameters. The allowable vertical compressive strain on top of natural subgrade corresponding to a specified axle load repetition has been used for estimation of compacted subgrade thickness. The allowable vertical strain on top of natural subgrade has been considered from rutting criteria as laid in IRC: 37-2018[51].

The thickness of compacted subgrade thus obtained using IITPAVE [51] has been compared with the findings obtained using present methodology. However it is to be noted that IITPAVE [51] solution is based on elastic layer theory of pavement, where the present method uses method of equivalent thickness for estimation of layer thicknesses.
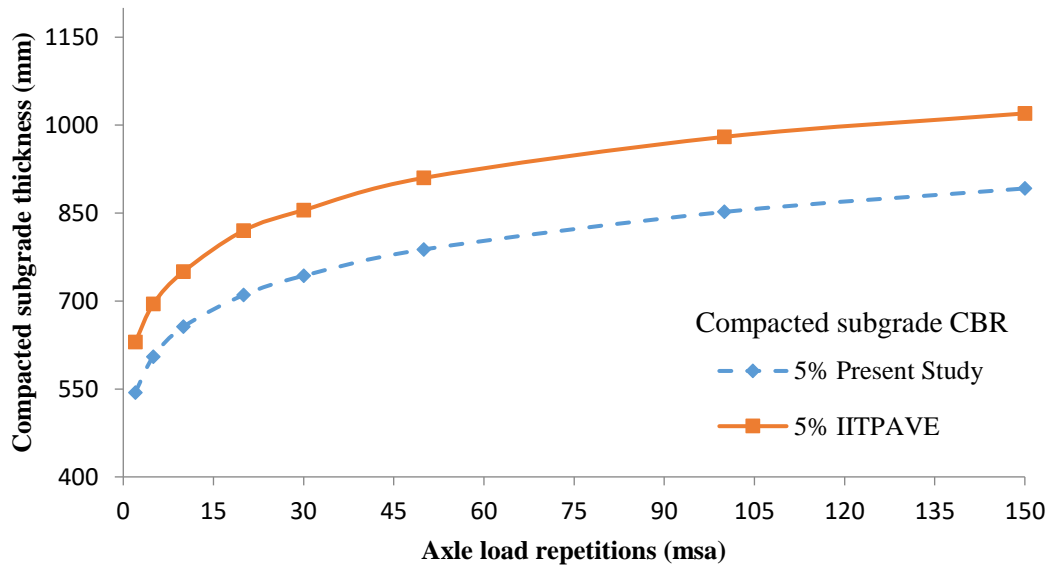
Figure 2.44: Comparison of variation of compacted subgrade thickness with axle load repetition for 2% CBR of natural subgrade with 0.25 MPa contact pressure
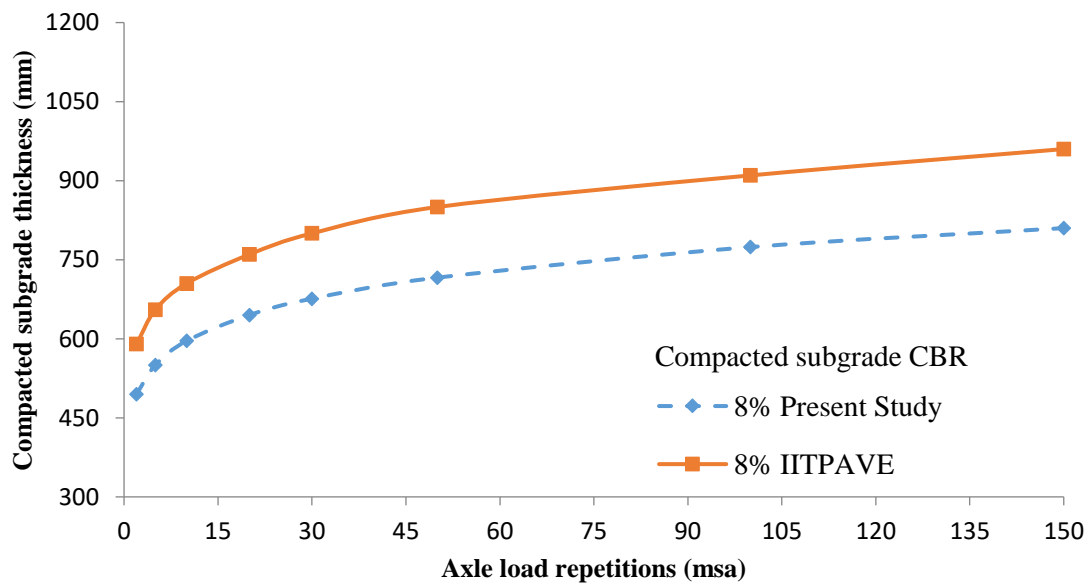
Figure 2.45: Comparison of variation of compacted subgrade thickness with axle load repetition for 2% CBR of natural subgrade with 0.25 MPa contact pressure
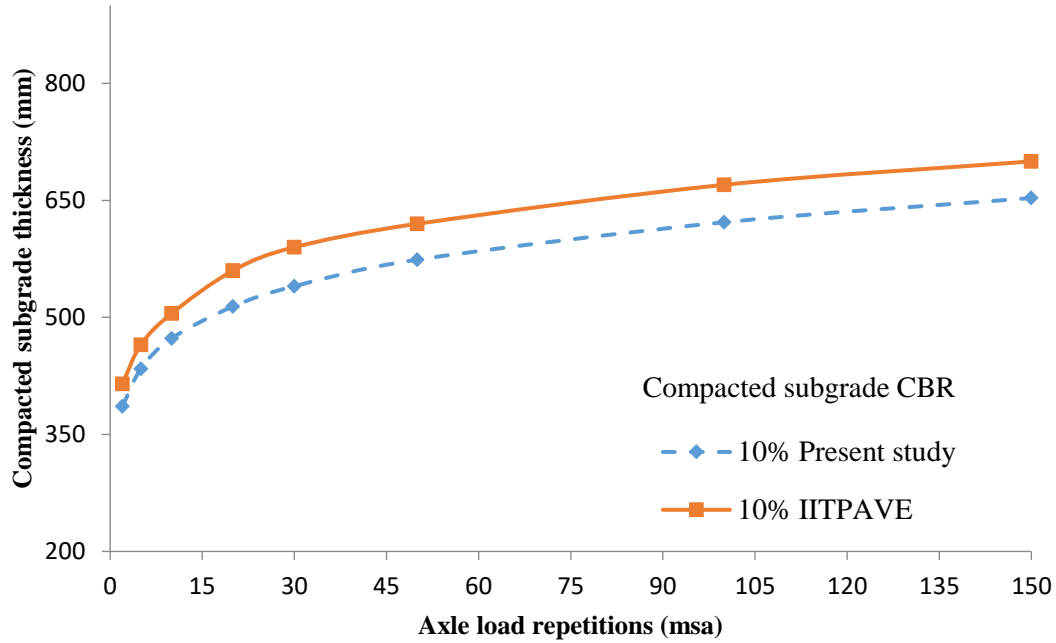
Figure 2.46: Comparison of variation of compacted subgrade thickness with axle load repetition for 5% CBR of natural subgrade with 0.25 MPa contact pressure
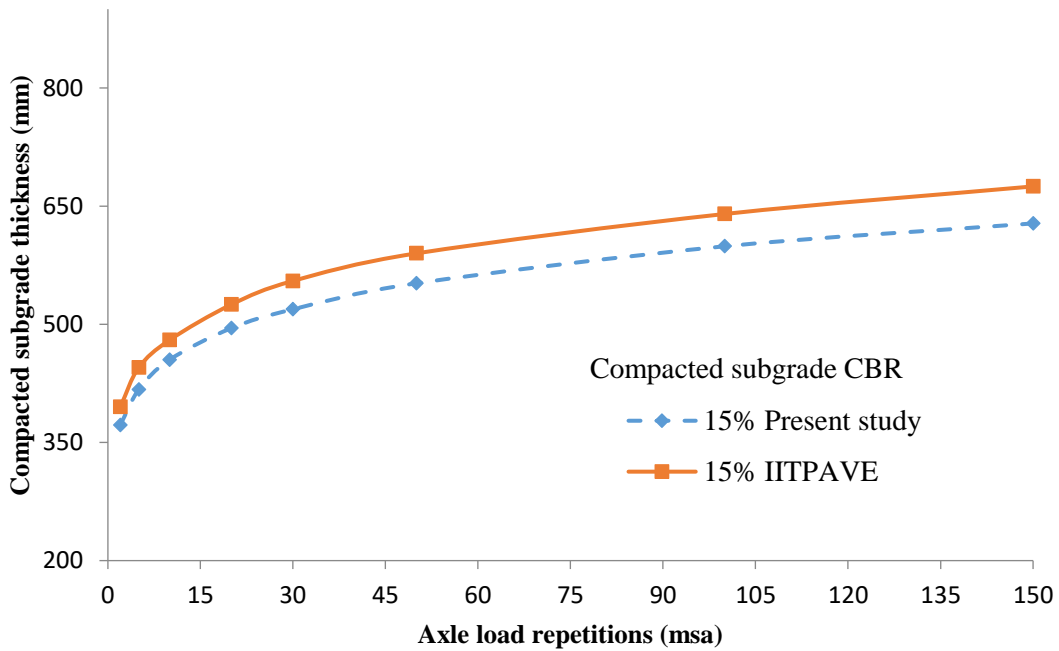
Figure 2.47 : Comparison of variation of compacted subgrade thickness with axle load repetition for 5% CBR of natural subgrade with 0.25 MPa contact pressure

54
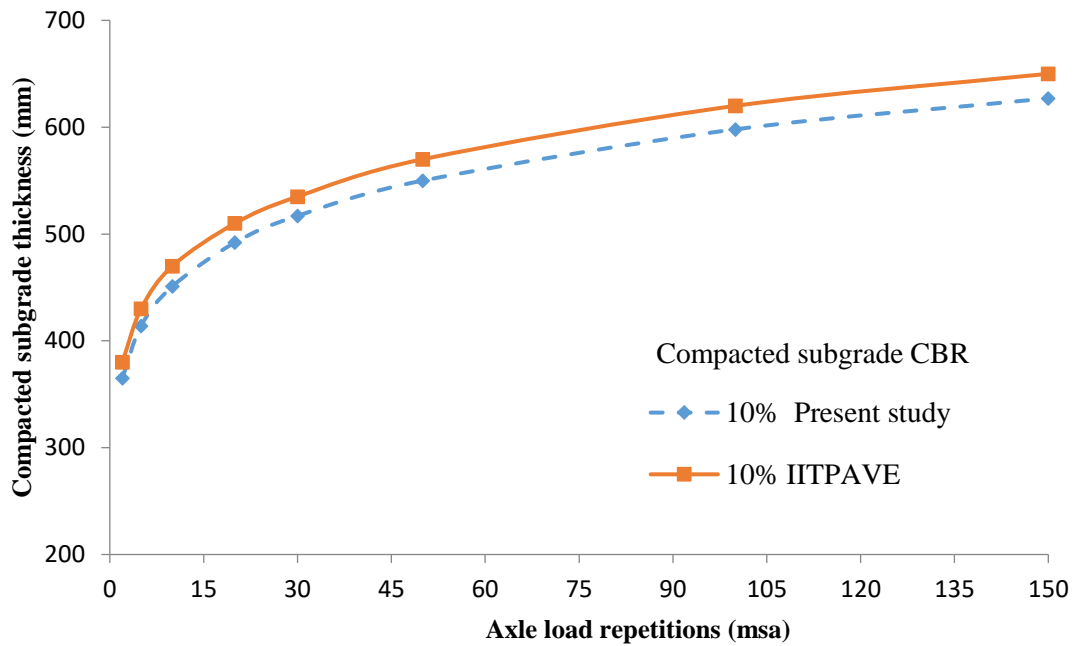
Figure 2.48: Comparison of variation of compacted subgrade thickness with axle load repetition for 7% CBR of natural subgrade with 0.25 MPa contact pressure
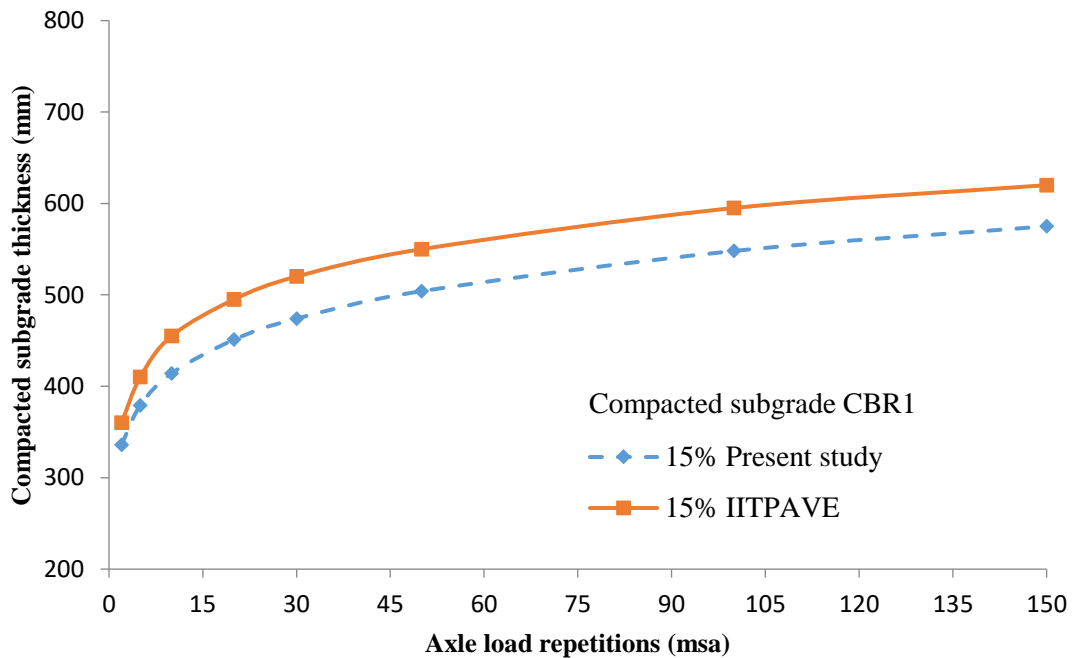
Figure 2.49 : Comparison of variation of compacted subgrade thickness with axle load repetition for 7% CBR of natural subgrade with 0.25 MPa contact pressure
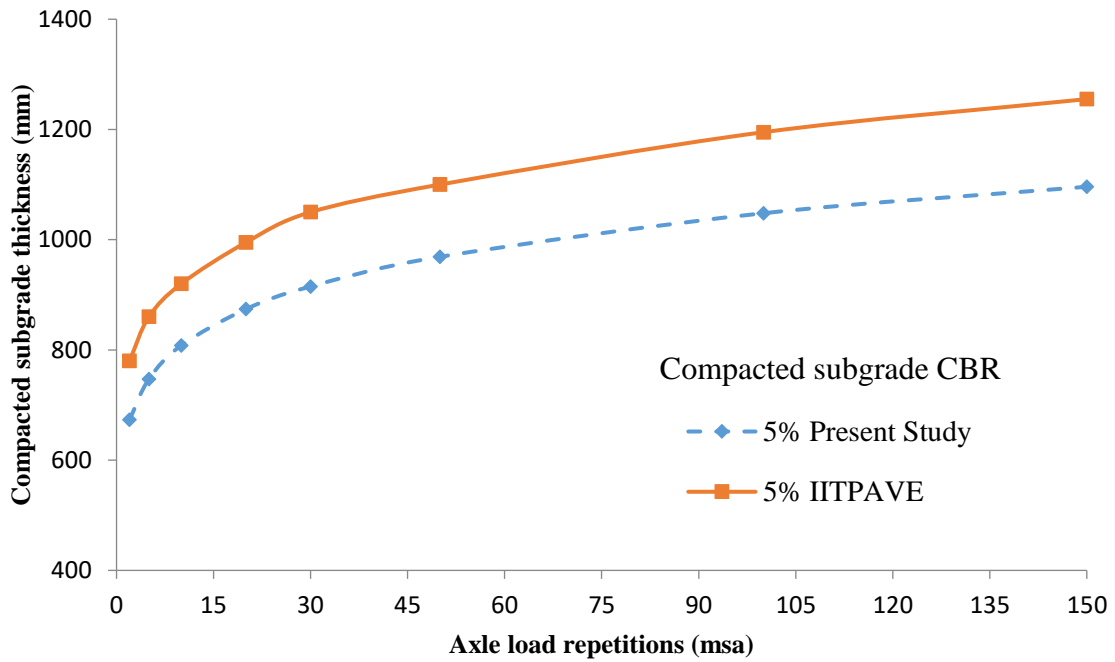
Figure 2.50: Comparison of variation of compacted subgrade thickness with axle load repetition for 2% CBR of natural subgrade with 0.375 MPa contact pressure
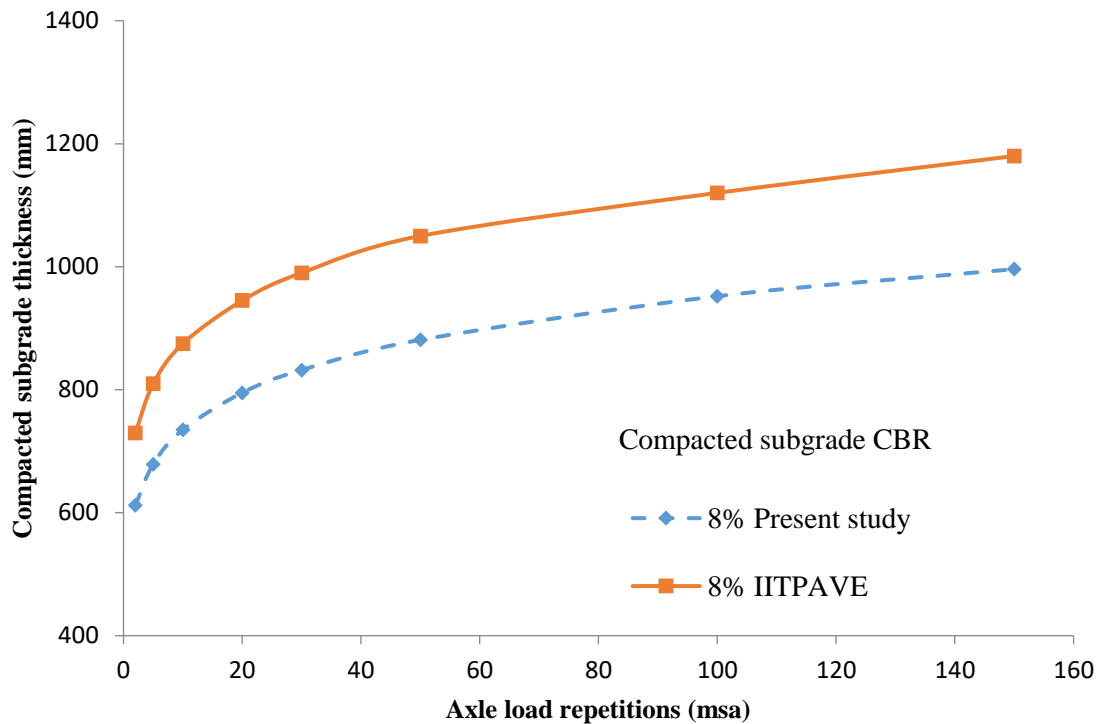
Figure 2.51: Comparison of Variation of compacted subgrade thickness with axle load repetition for 2% CBR of natural subgrade with 0.375 MPa contact pressure
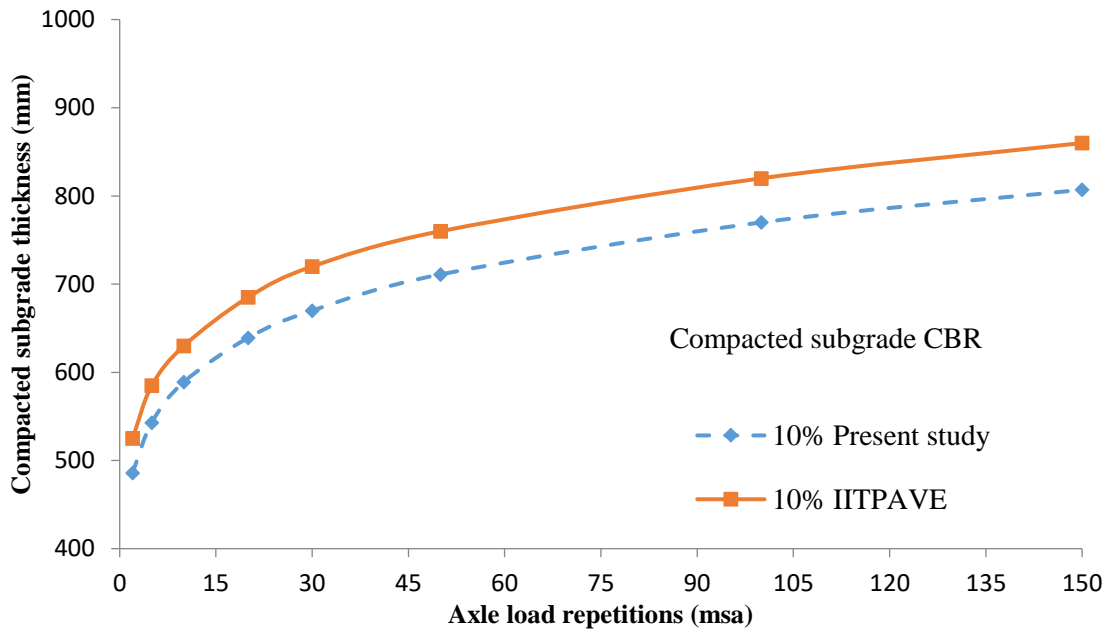
Figure 2.52: Comparison of variation of compacted subgrade thickness with axle load repetitions for 5% CBR of natural subgrade with 0.375 MPa contact pressure
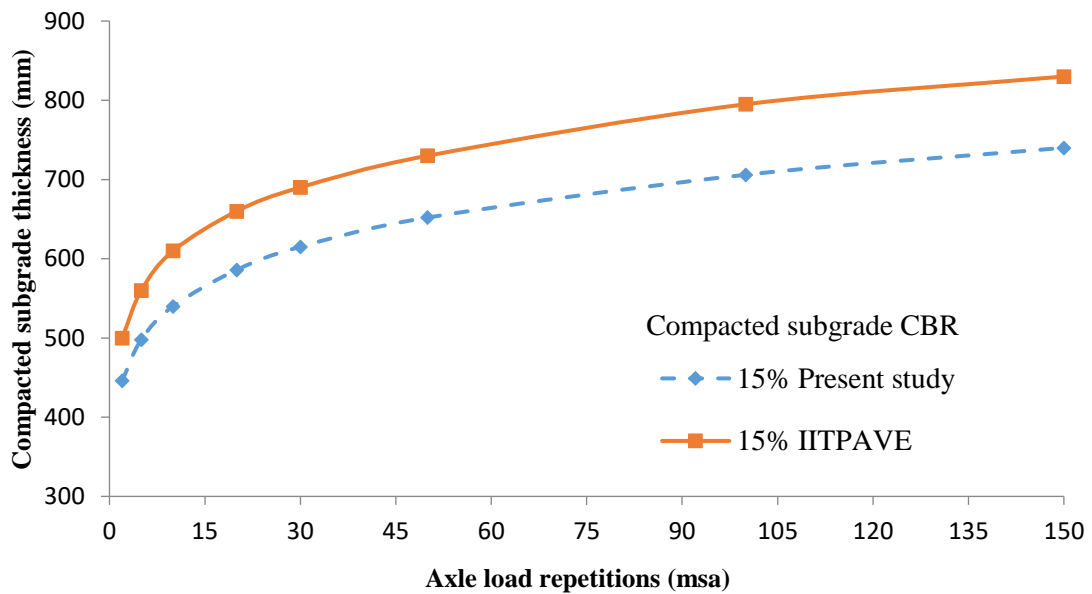
Figure 2.53 : Comparison of variation of compacted subgrade thickness with axle load repetitions for 5% CBR of natural subgrade with 0.375 MPa contact pressure
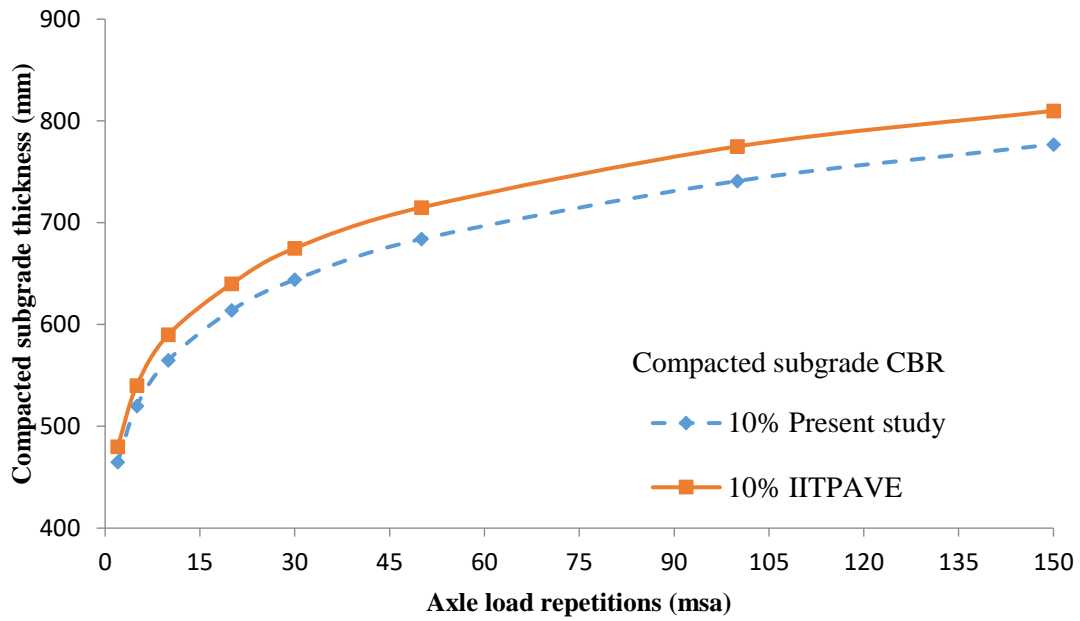
Figure 2.54: Comparison of variation of compacted subgrade thickness with axle load repetitions for 7% CBR of natural subgrade with 0.375 MPa contact pressure
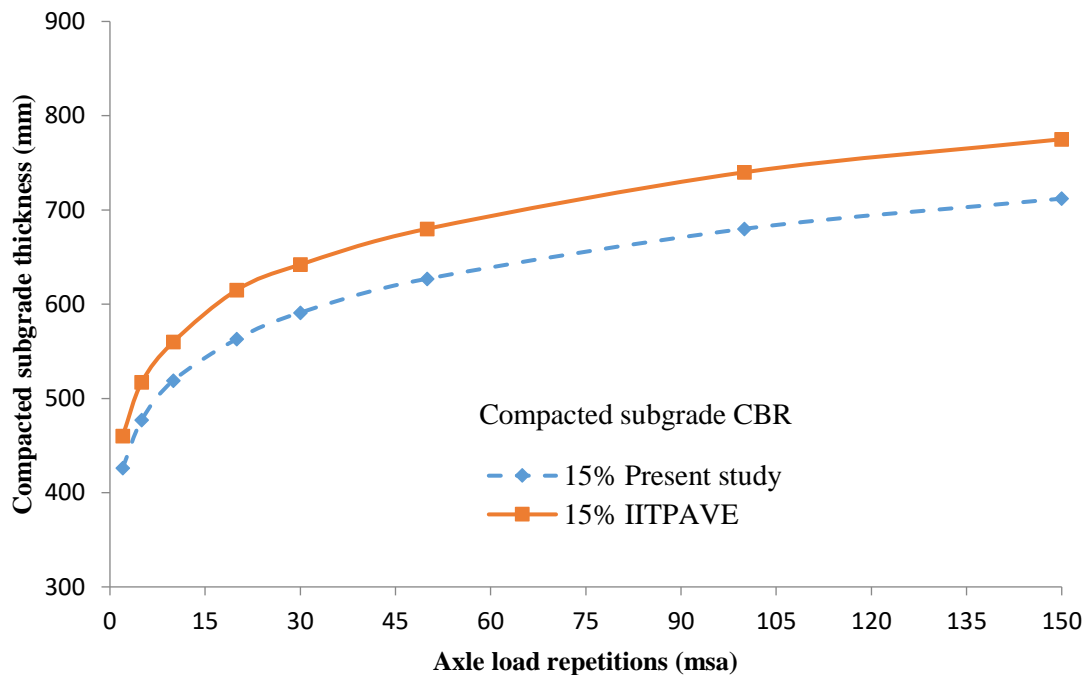
Figure 2.55: Comparison of variation of compacted subgrade thickness with axle load repetitions for 7% CBR of natural subgrade with 0.375 MPa contact pressure

2.4.5 Concluding remarks

The Mechanistic - Empirical approach used in present analytical study has been used to determine the compacted subgrade thickness on the top of a weak natural subgrade as a measure of ground improvement for specified axle load repetitions. It has been found that the thickness of compacted subgrade increases with the increase in axle load and decrease in strength of natural subgrade. If axle load varies from 2 msa to 150 msa for a specific natural subgrade CBR, percentage of variation in thickness remains almost unaltered though the CBR of compacted subgrade may vary from 5% to 15%. It has also been found that provision of considering 500 mm thickness of compacted subgrade as recommended in IRC: 37-2018 [51] or in MORD specification will result either an under designed or over designed section, causing unsafe or uneconomic pavement in terms of rutting failure. In this backdrop, present analytical approach may be used to estimate the thickness of compacted subgrade.

2.5 Determination of compacted subgrade thickness using stress based approach

Compacted subgrade over weak natural subgrade is placed as a measure of ground improvement. The stress due to wheel load on pavement surface gets distributed along the depth of pavement depending on the layer modulus of constituent layers in a pavement system. The failure of natural subgrade is characterized by the vertical compressive strain on the top of the subgrade corresponding to standard axle load repetitions. Therefore, thickness of the compacted subgrade should be selected with such an approach so that it can protect the failure of natural subgrade under rutting from anticipated axle load repetitions on pavement. In this context, attempts are made in this study to establish correlation between compacted layer thickness with strength of natural subgrade and anticipated axle load repetitions using Mechanistic - Empirical approach.

The compacted subgrade on top of natural subgrade is provided to reduce the effect of wheel load stress on pavement on natural subgrade so that the pavement does not fail under rutting.

2.5.1 Objective

The objective of present study has been considered to formulate a stress based Mechanistic-Empirical approach for determination of compacted subgrade thickness to withstand a specified number of standard axle load repetitions during its service life.

2.5.2 Proposed stress based model

In Present analysis compacted subgrade with higher CBR on the top of natural subgrade with lower CBR has been considered as a two layered system in the present analysis and shown in Figure 2.56.
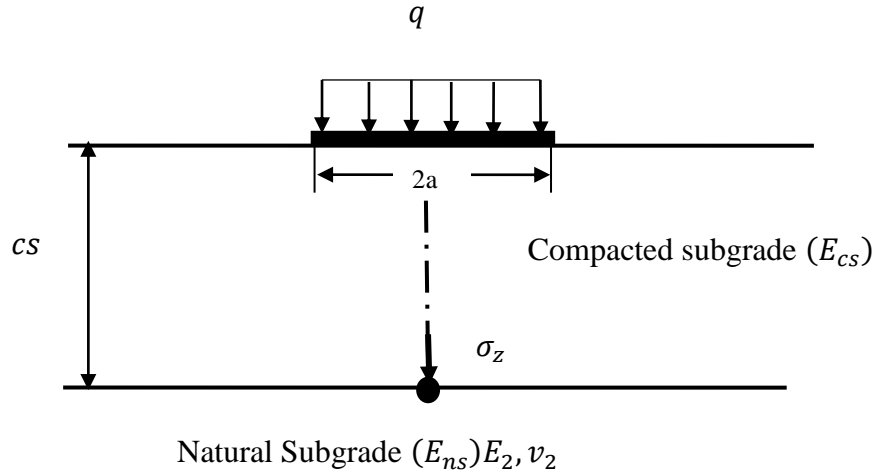
Figure 2.56: Two layered system with natural and compacted subgrade
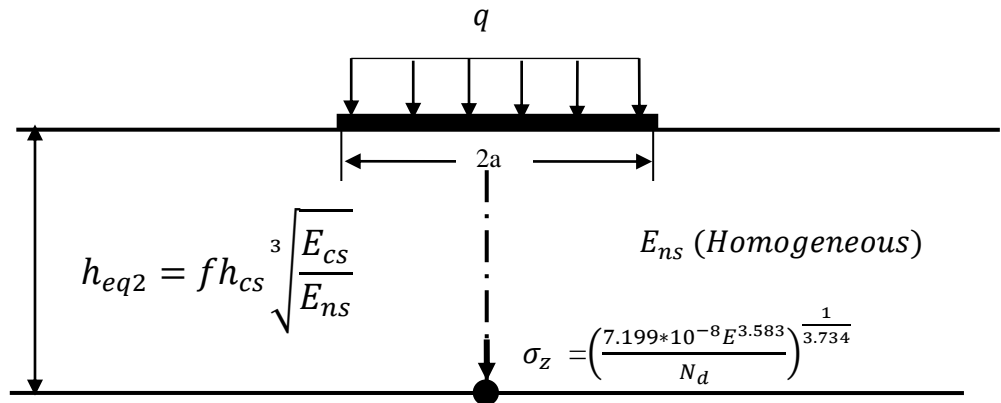
Figure 2.57: Transformation of two layered system into homogeneous system

The allowable vertical stress on top of natural subgrade may be determined by Huang [87-90] from AASTHO [1-4] equation and shell [164] design criteria and are as following

$$N_d = 7.199 \times 10^{-5} \times \sigma_z{}^{-3.734} \times E^{3.583} \tag{2.16}$$

Where N_d = Number of stress repetition to limit permanent deformation in natural subgrade

σ_z =   Vertical compressive stress on the surface of the subgrade (Kg/cm²).

E = Elastic Modulus of natural subgrade (Kg/cm²).

However the permissible stress on the top of compacted subgrade has been determined from the formulation of Yoder and Witczak [191-193] of CBR-depth relationship as shown in Equation 2.12.

Therefore, to reduce the vertical compressive stress on weak natural subgrade with lower elastic modulus (E_{ns}), compacted subgrade with appropriate thickness would require with higher elastic modulus (E_{cs}) to limit the stress up to layer interface, in a two layered system.However, in present analysis the subgrade is a two layered system. Therefore Odemarks method has also been used in present section to transform the two layered system in to a homogeneous system. The Boussinesq's equation for determination of vertical stress in a homogeneous medium as shown in Equation 2.11 has been used in present analysis.

The transformed thickness h_{eq2} may be obtained using the principle of Odemarks method which has been shown in Equation 2.17.

$$h_{eq2} = 0.9 \, h_{cs} \sqrt[3]{\frac{E_{cs}}{E_{ns}}} \tag{2.17}$$

The elastic moduli of compacted subgrade and natural subgrade have been determined using the empirical relationship expressed in Equation 2.8 and Equation 2.9.

The equivalent thickness of the transformed section of two layered subgrade system may be expressed as (h_{eq2}) as in Equation 2.17. The term h_{eq2} in place of 'z' in Boussinesq's [34] Equation 2.11 has been used in present analysis for estimation of vertical interface stress on top of natural subgrade which has been shown in Equation 2.18.

$$\sigma_z = q \left[1 - \frac{1}{\left\{ \sqrt{1+\left(\frac{a}{h_{eq2}}\right)^2} \right\}^3} \right] \tag{2.18}$$

Allowable stress on natural subgrade as shown in Equation 2.16 has been used in Equation 2.18 to get equivalent depth (h_{eq2}). The depth thus obtained from Equation 2.18 is the equivalent depth of soil mass corresponding to different modulus ratio. The depth of compacted subgrade thickness (h_{cs}) is back calculated using Equation 2.17. The thickness of compacted subgrade on top of natural subgrade thus obtained for various axle load repetitions. The flow diagram of the adopted methodology has also been shown in Figure 2.58.

2.5.3   Results and Discussion

The methodology proposed in this study can be considered as an analytical approach of soil improvement technique. The natural subgrade CBR has been considered in this analysis between 2% to 7%. The thickness of compacted subgrade has been determined to achieve the target CBR on the top of soft natural subgrade. The CBR of compacted subgrade considered in the present analysis ranged between 5% to 20%.

The thickness of compacted subgrade thus obtained for different natural subgrade and for different axle load repetitions are presented in Figure 2.59 to Figure 2.76. The limiting vertical stress on compacted subgrade against rutting depends on its elastic modulus and axle load repetitions. Therefore, the effect of load repetitions on performance of compacted subgrade in terms of its variation in thickness has also been shown in the Table 2.27 to Table 2.38 (Appendix 1C) for load intensity of 0.25 MPa and 0.375 MPa on top of subgrade. The results obtained from present analysis show that the thickness of compacted subgrade reduces if the CBR of natural subgrade increases for a specific axle load repetitions and vice versa. Moreover, the thickness of compacted subgrade was found to increase with the increase in axle load repetitions and vice versa. It is relevant to note that the rate of change of thickness becomes significant up to a load repetition of 50 msa. But such change in thickness becomes less significant between a load range of 50-150 msa.

```
┌────────────────────────────────────────────────────────────┐
│   Determination of stress based compacted subgrade thickness │
└────────────────────────────────────────────────────────────┘

┌────────────────────────────────────────────────────────────┐
│                           INPUT                              │
│   CBR of Natural and Compacted subgrade, Axle load repetition,│
│              permissible stress on subgrade                  │
└────────────────────────────────────────────────────────────┘

┌────────────────────────────────────────────────────────────┐
│       Application of Odemark's transformation technique      │
└────────────────────────────────────────────────────────────┘

┌──────────────────────────┐          ┌──────────────────────────────┐
│ Allowable vertical stress on│        │ Wheel load stress using Boussinesq's│
│ subgrade from Huang'     │          │ Equation and CBR-Depth relation from│
│ criteria                 │          │ Yoder and Witczak correlation │
└──────────────────────────┘          └──────────────────────────────┘

┌────────────────────────────────────────────────────────────┐
│        Determination of compacted subgrade thickness         │
└────────────────────────────────────────────────────────────┘

┌────────────────────────────────────────────────────────────┐
│        Validation of computed thickness with IITPAVE         │
└────────────────────────────────────────────────────────────┘
```

Figure 2.58 Flow diagram of adopted stress based methodology for estimation of compacted subgrade thickness

It has also been observed that for weak subgrade with natural subgrade CBR of 2%, the compacted subgrade thickness increases 84%, when the axle load repetitions changes from 2 to 150 msa. However such increase in thickness has not been found significant with the change in compacted subgrade CBR.

Similarly, for natural subgrade with higher CBR (7%), the increase of compacted subgrade thickness from 2 msa top 150 msa was found as 98%.

In present analysis, the compacted subgrade thickness was found to vary with axle load repetitions, CBR of natural subgrade and CBR of borrow materials. Therefore, consideration of a fixed compacted subgrade thickness irrespective of axle load repetitions is too approximate. Therefore, the recommendation of MORD for compacted subgrade thickness in rural road as 300mm and for other highways as 500mm requires revision. In this backdrop, present analysis may be considered as an effective approach for estimation of compacted subgrade thickness.

A comparative analysis has also been carried out between compacted subgrade thickness obtained from strain and stress based approach. The thickness of compacted subgrade obtained from two different models considered natural subgrade range between 2% to 7% and axle load repetitions between 2-150 msa which are presented in Figure 2.74 to Figure 2.91 & Table 2.39 to Table 2.46 (Appendix 1C) considering load intensity of 0.25 MPa and 0.375 MPa.

It has been observed from Table 2.27 to Table 2.52 (Appendix 1C) that the thickness of compacted subgrade increases with the increase in axle load repetitions. However, the rate of increase of compacted subgrade thickness is significant up to 50 msa beyond which the rate of increase becomes less significant.

The trend of increase in compacted subgrade thickness with axle load repetitions was found similar in both strain and stress based approach. Moreover, it has been observed that the thickness of compacted subgrade reduces when strength of borrow material increases for a specific axle load repetitions.

It has been observed that the thickness of compacted subgrade obtained from strain based criteria is more than the stress based criteria. In this analysis, for a load of 2 msa and an assumed contact pressure of 0.25 MPa, the average

increase in compacted subgrade thickness using strain based method was 36% for different natural subgrade and borrows materials. However, with the increase in axle load repetitions the difference in compacted subgrade thickness reduces considerably. It had been found that such differences in compact subgrade thickness reduce to 19% when the load repetions are 150 msa.

Similarly, for contact pressure of 0.375 MPa, for lower axle load repetitions (2msa) the average difference between stress and strain based subgrade thickness has been found as 34% whereas the same for 150 msa load has been found as 18%.
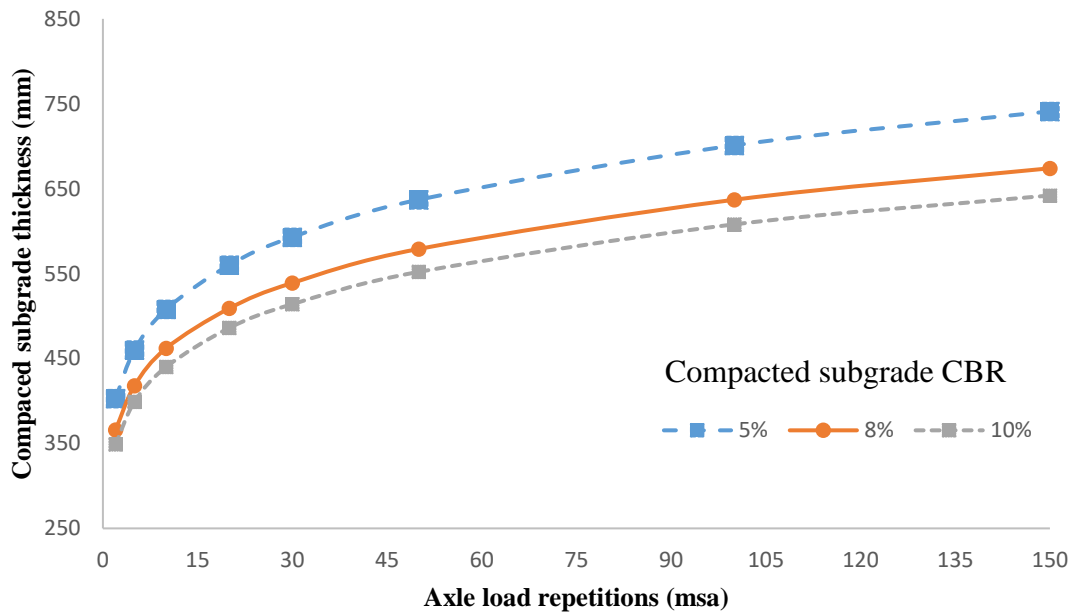
Figure 2.59: Variation of compacted subgrade thickness with axle load repetitions for 2% CBR of natural subgrade with 0.25 MPa contact pressure
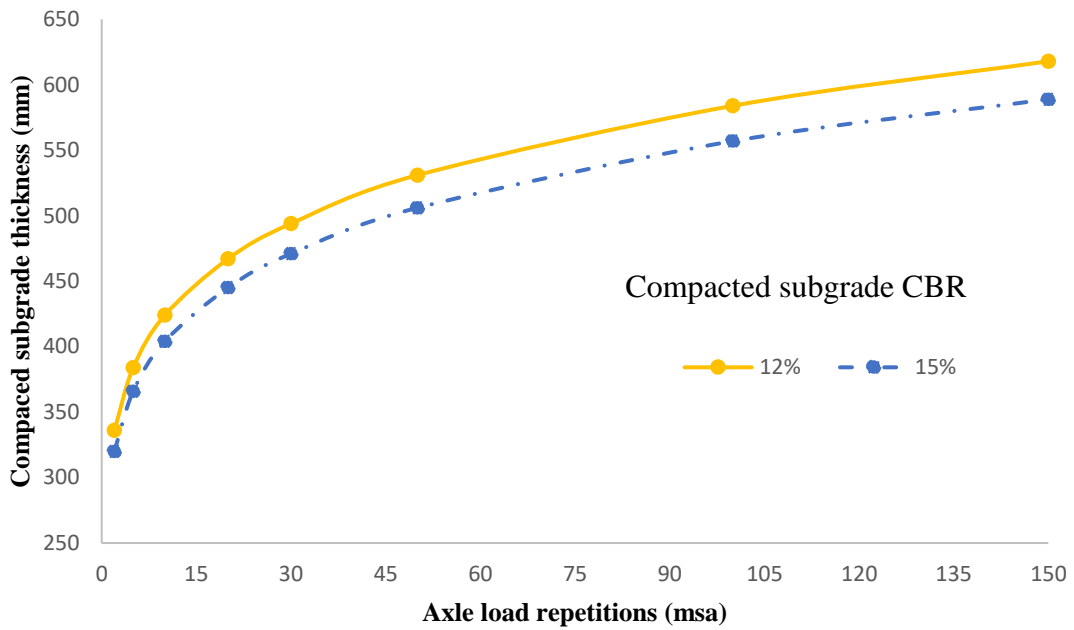
Figure 2.60: Variation of compacted subgrade thickness with axle load repetitions for 2% CBR of natural subgrade with 0.25 MPa contact pressure
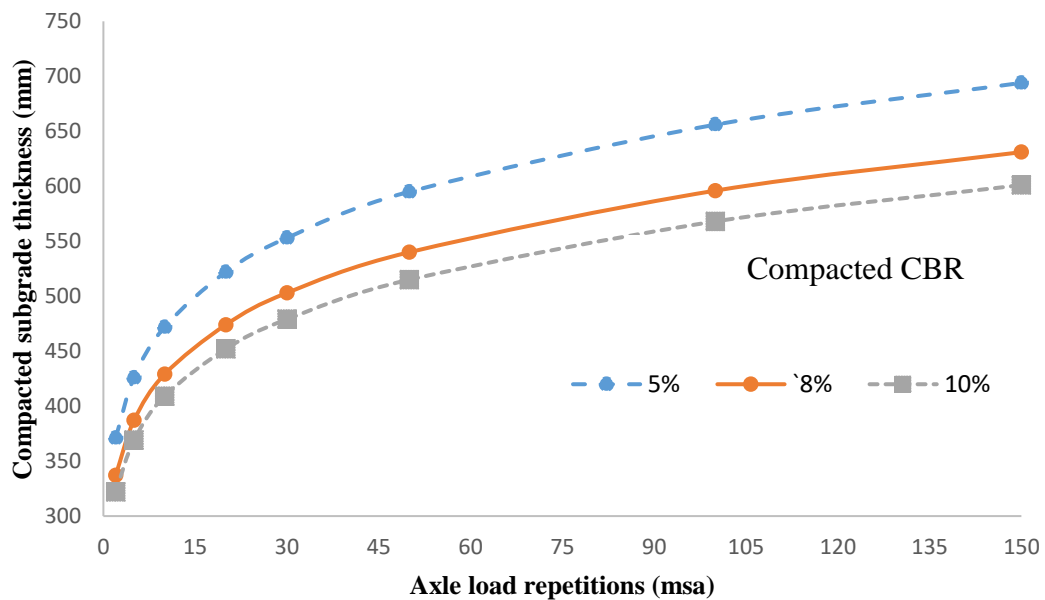
Figure 2.61: Variation of compacted subgrade thickness with axle load repetitions for 3% CBR of natural subgrade with 0.25 MPa contact pressure
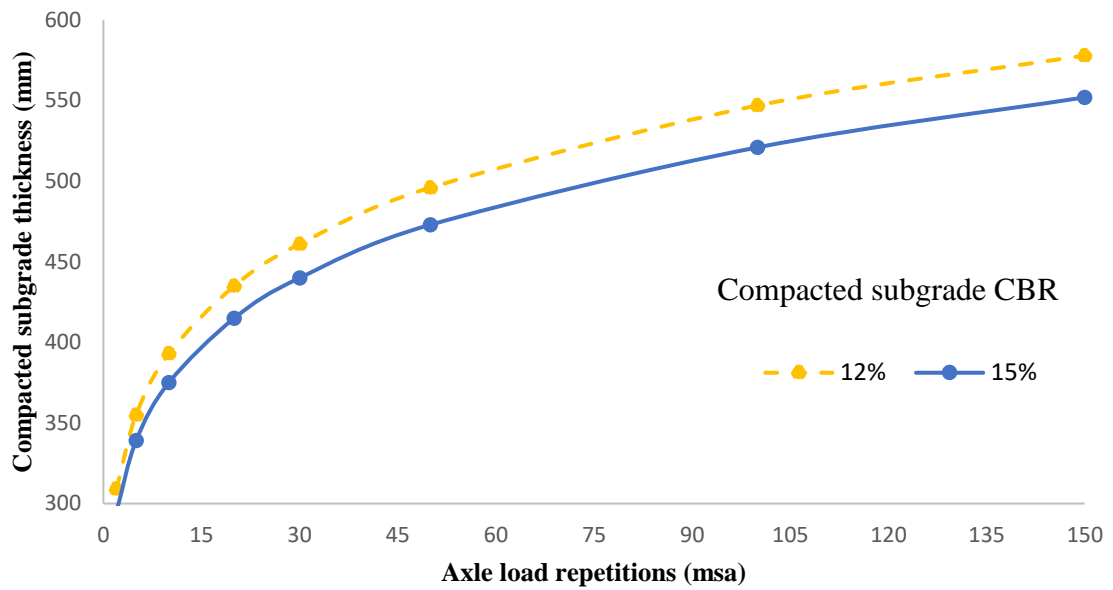
Figure 2.62: Variation of compacted subgrade thickness with axle load repetitions for 3% CBR of natural subgrade with 0.25 MPa contact pressure
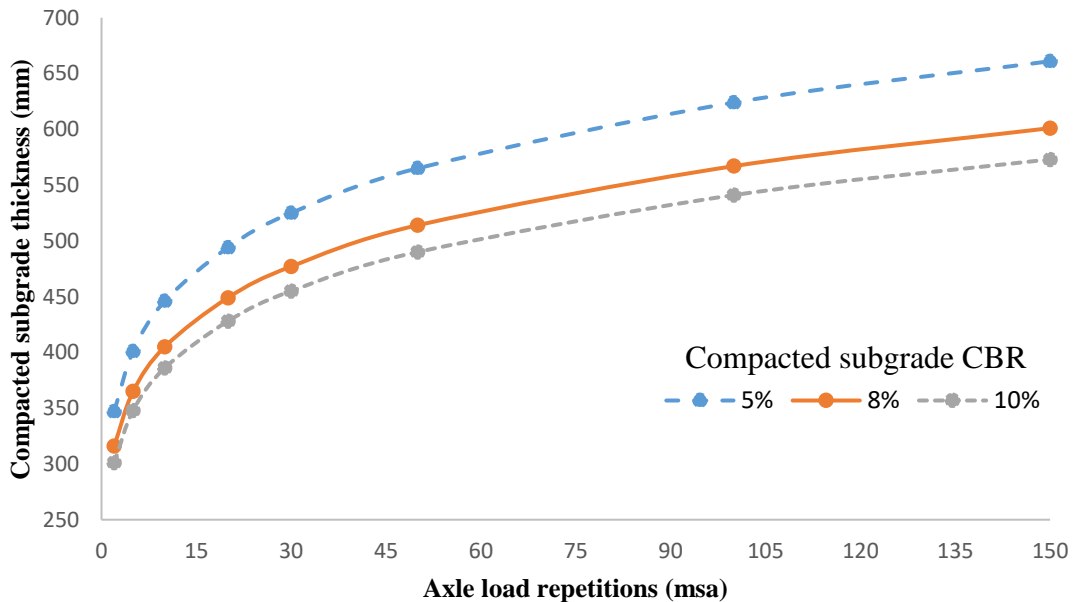
Figure 2.63: Variation of compacted subgrade thickness with axle load repetitions for 4% CBR of natural subgrade with 0.25 MPa contact pressure
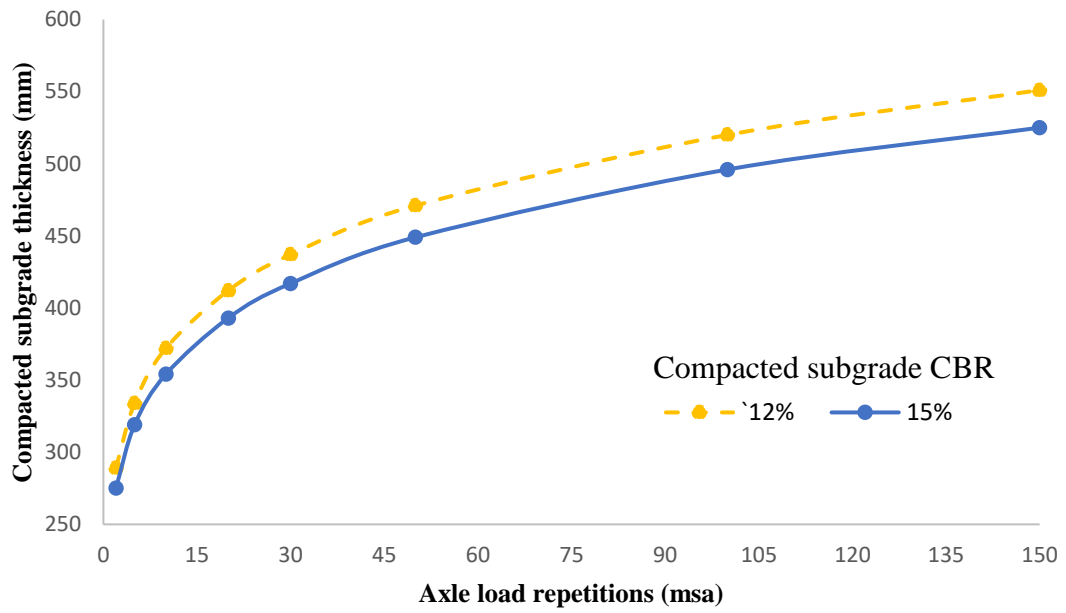
Figure 2.64: Variation of compacted subgrade thickness with axle load repetitions for 4% CBR of natural subgrade with 0.25 MPa contact pressure
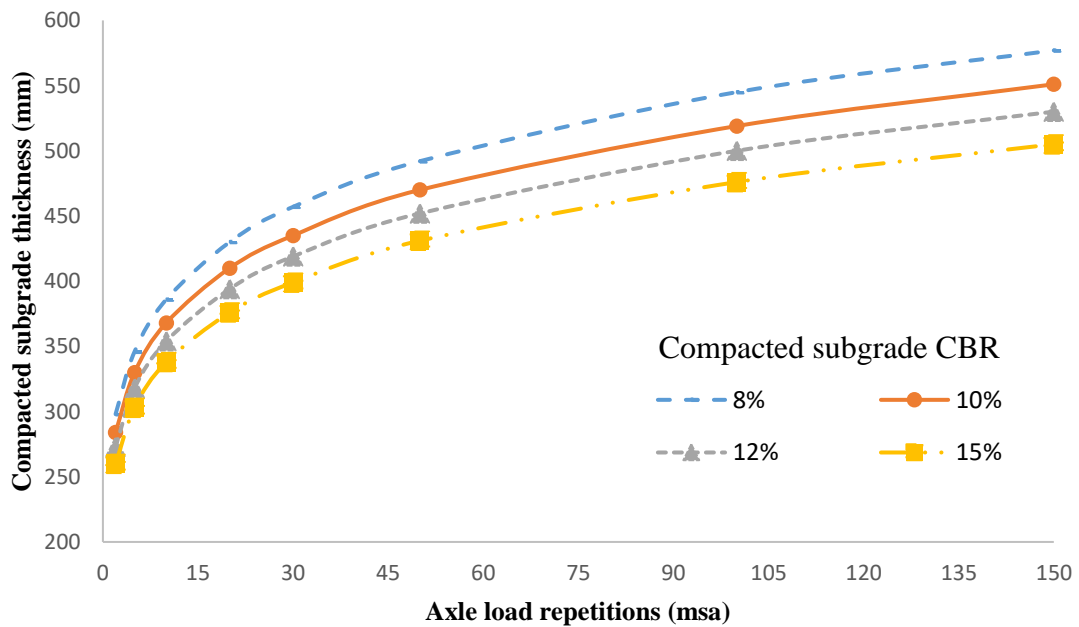
Figure 2.65: Variation of compacted subgrade thickness with axle load repetitions for 5% CBR of natural subgrade with 0.25 MPa contact pressure
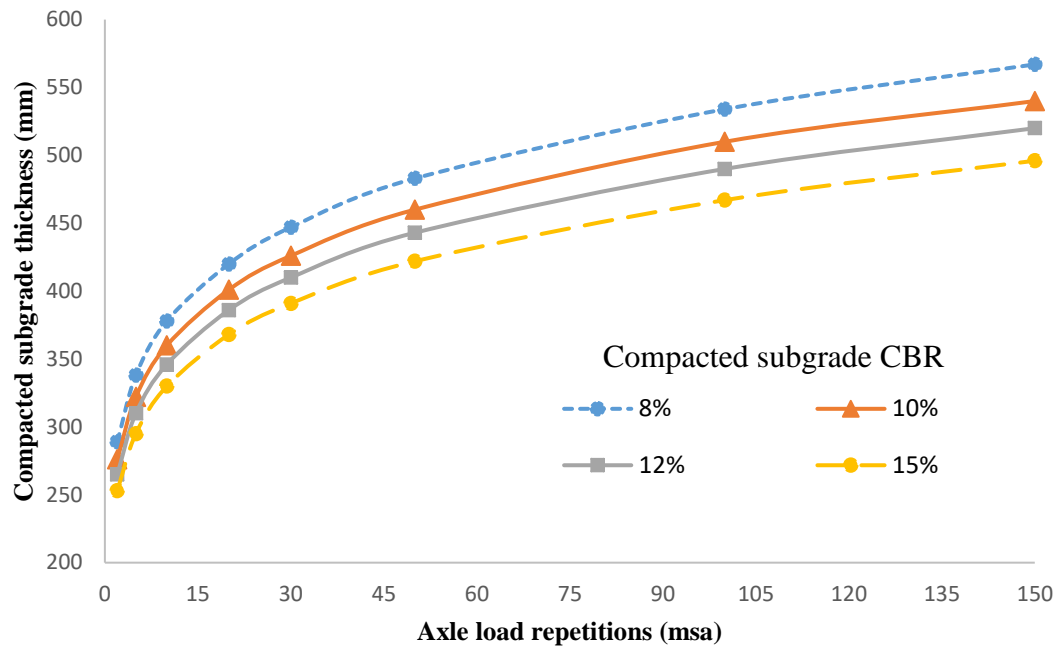
Figure 2.66: Variation of compacted subgrade thickness with axle load repetitions for 6% CBR of natural subgrade with 0.25 MPa contact pressure
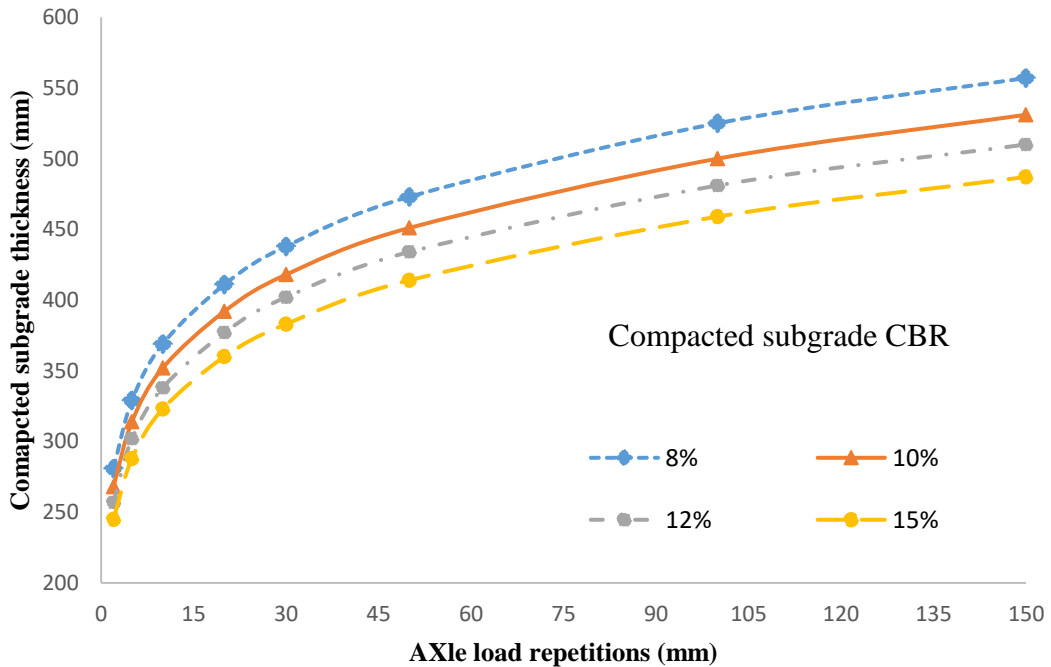
Figure 2.67: Variation of compacted subgrade thickness with axle load repetitions for 7% CBR of natural subgrade with 0.25 MPa contact pressure
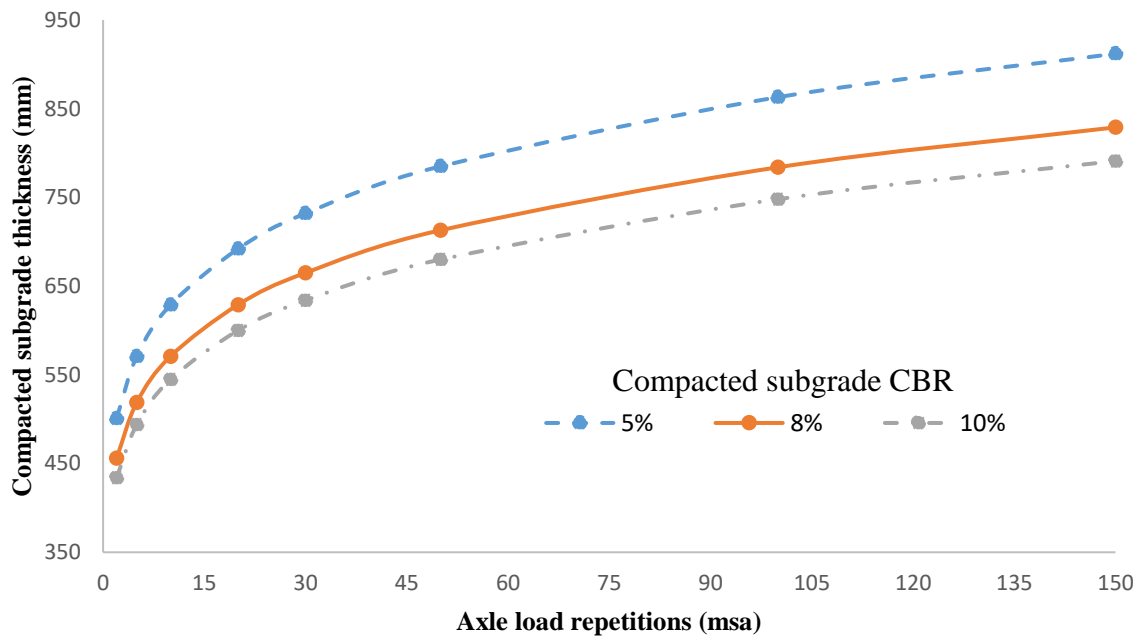
Figure 2.68: Variation of compacted subgrade thickness with axle load repetitions for 2% CBR of natural subgrade with 0.375 MPa contact pressure
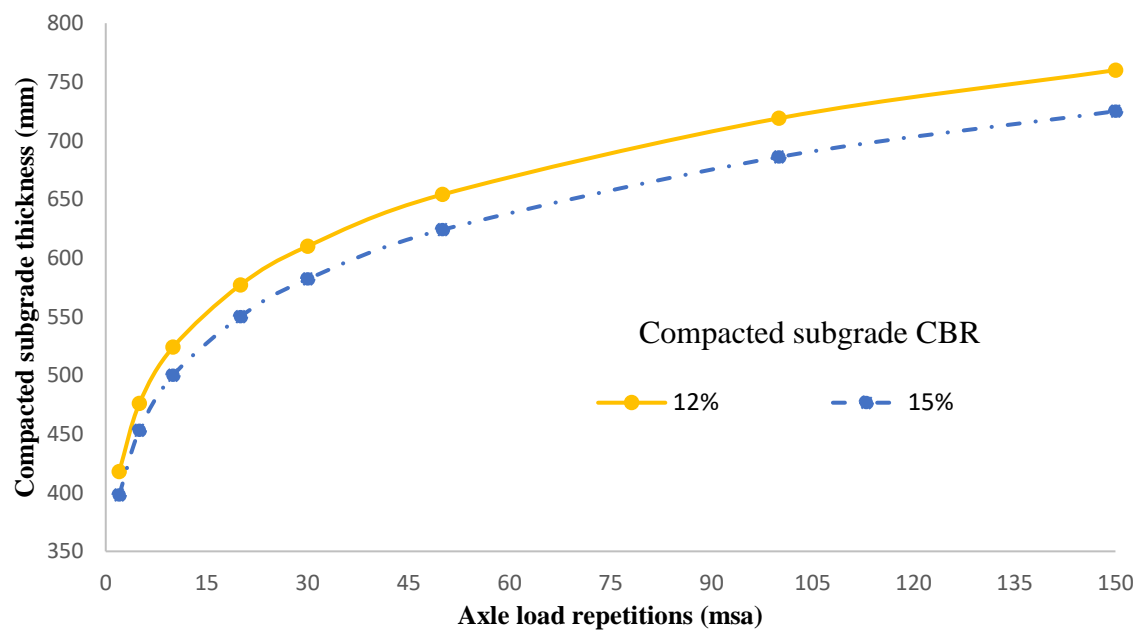
Figure 2.69: Variation of compacted subgrade thickness with axle load repetitions for 2% CBR of natural subgrade with 0.375 MPa contact pressure
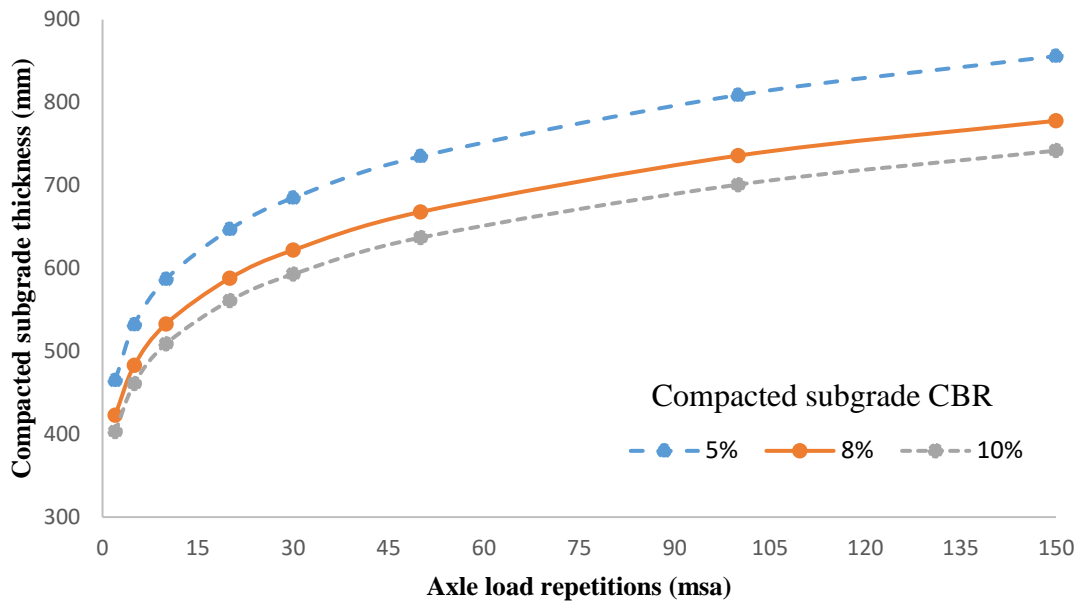
Figure 2.70: Variation of compacted subgrade thickness with axle load repetitions for 3% CBR of natural subgrade with 0.375 MPa contact pressure
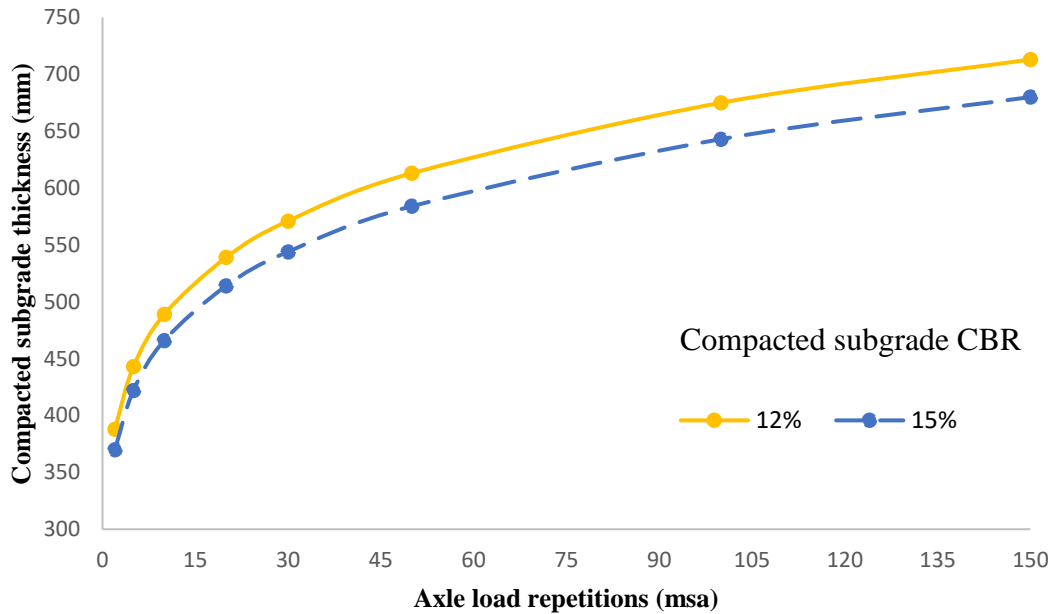
Figure 2.71: Variation of compacted subgrade thickness with axle load repetitions for 3% CBR of natural subgrade with 0.375 MPa contact pressure
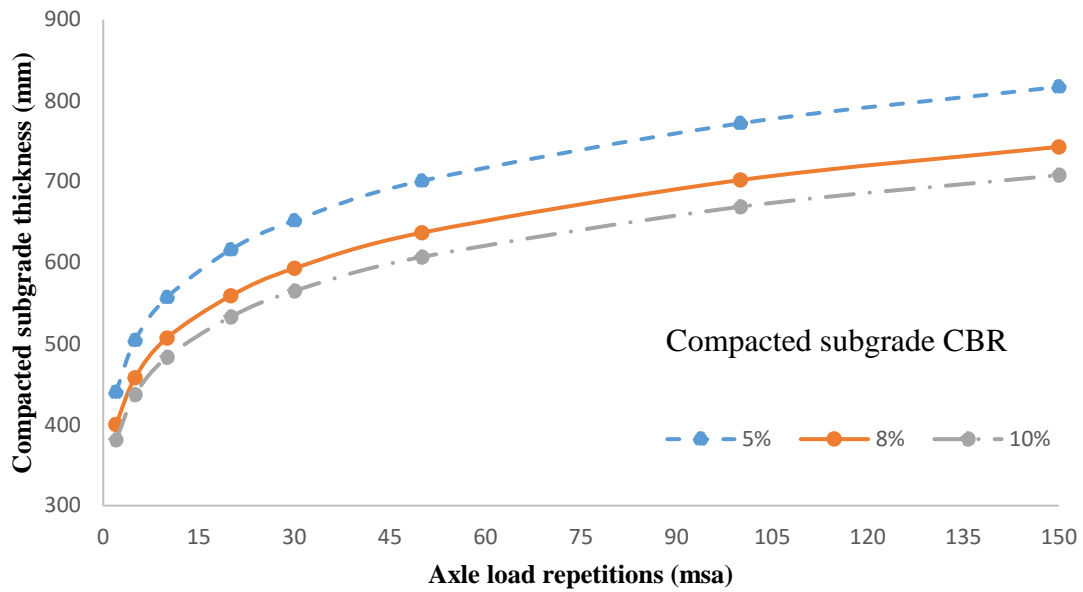
Figure2.72: Variation of compacted subgrade thickness with axle load repetitions for 4% CBR of natural subgrade with 0.375 MPa contact pressure
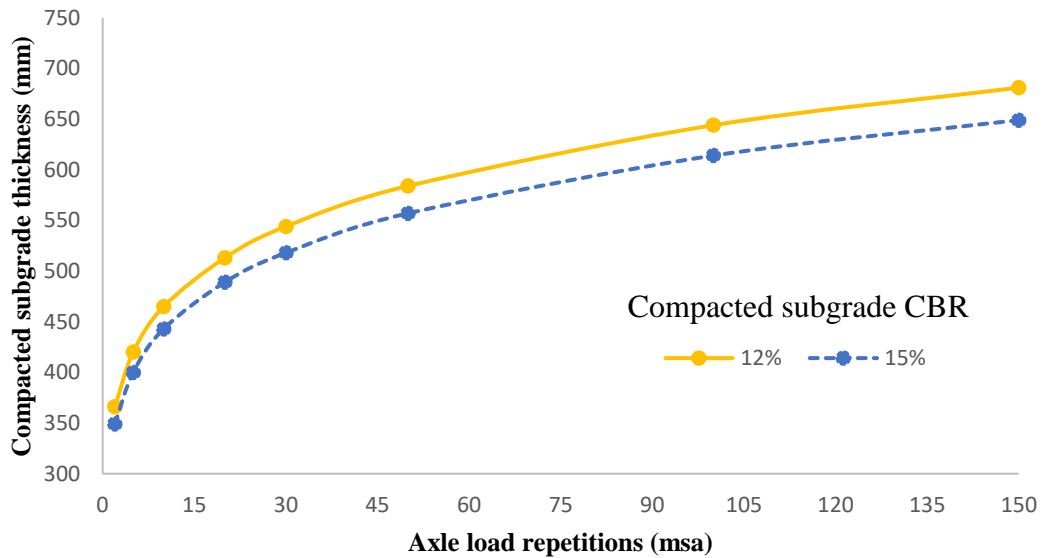
Figure 2.73: Variation of compacted subgrade thickness with axle load repetitions for 4% CBR of natural subgrade with 0.375 MPa contact pressure
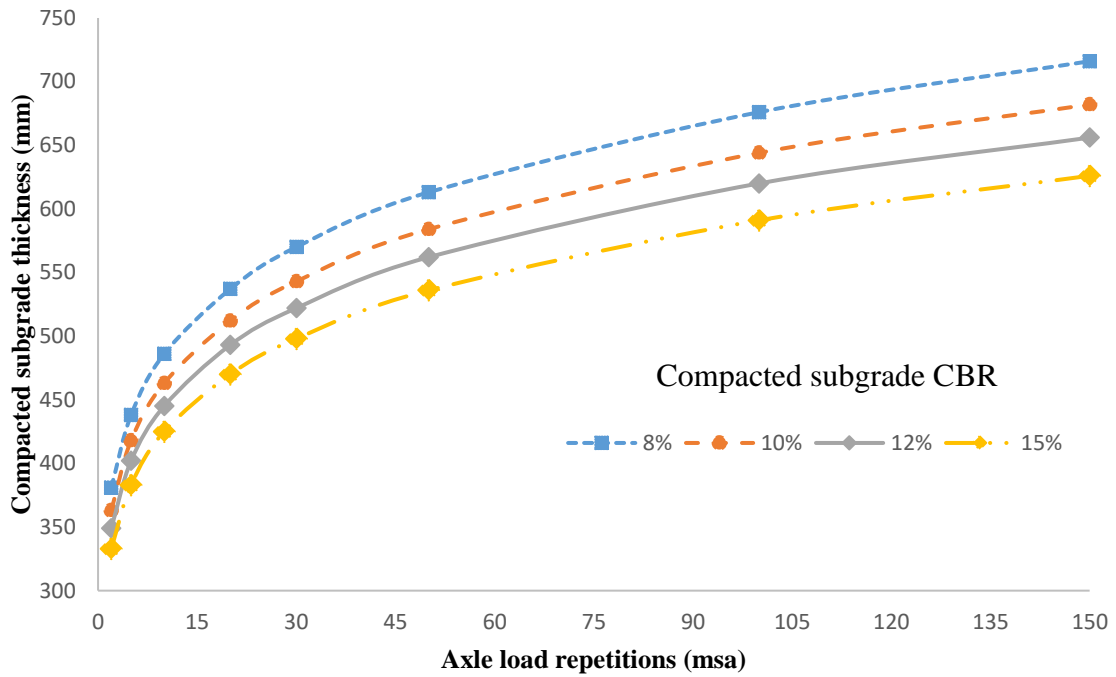
Figure 2.74: Variation of compacted subgrade thickness with axle load repetitions for 5% CBR of natural subgrade with 0.375 MPa contact pressure
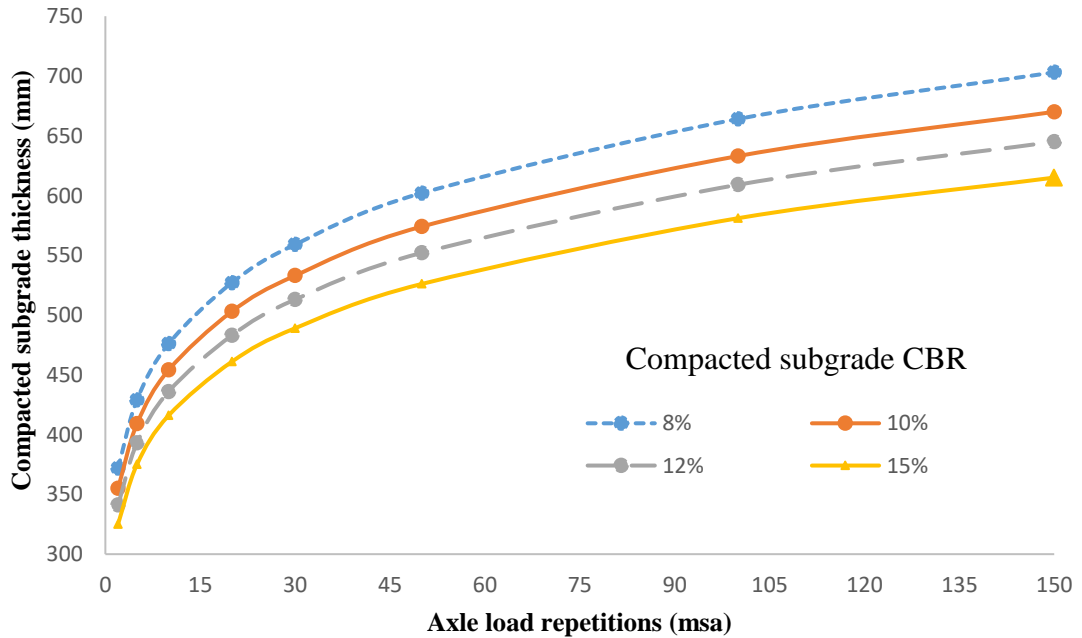
Figure 2.75: Variation of compacted subgrade thickness with axle load repetitions for 6% CBR of natural subgrade with 0.375 MPa contact pressure
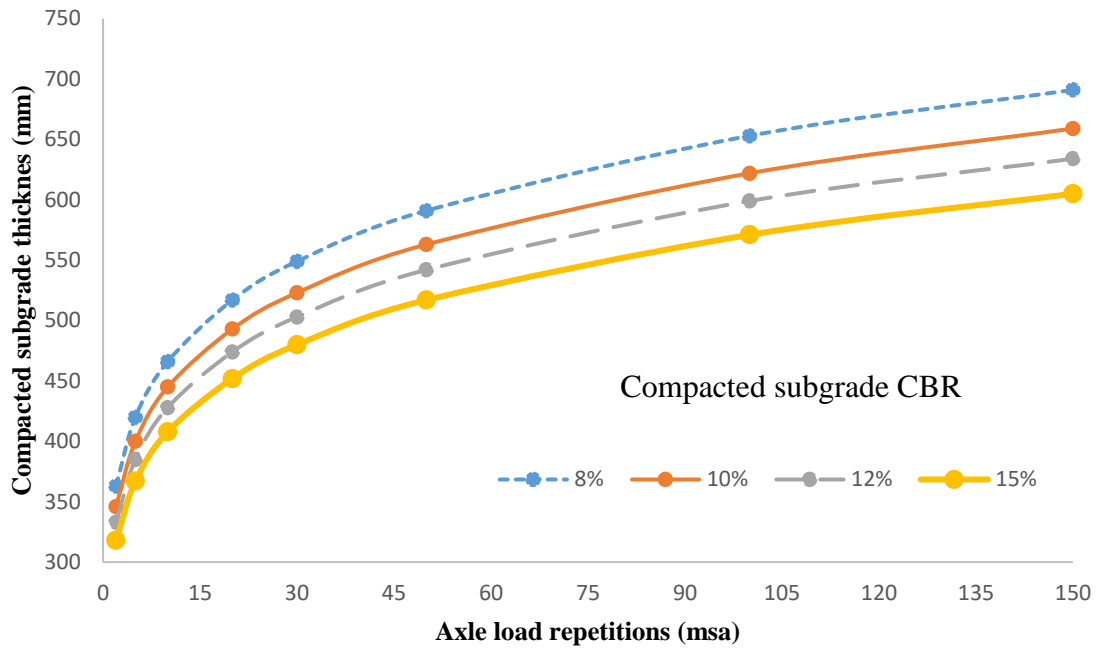
Figure 2.76: Variation of compacted subgrade thickness with axle load repetitions for 7% CBR of natural subgrade with 0.375 MPa contact pressure
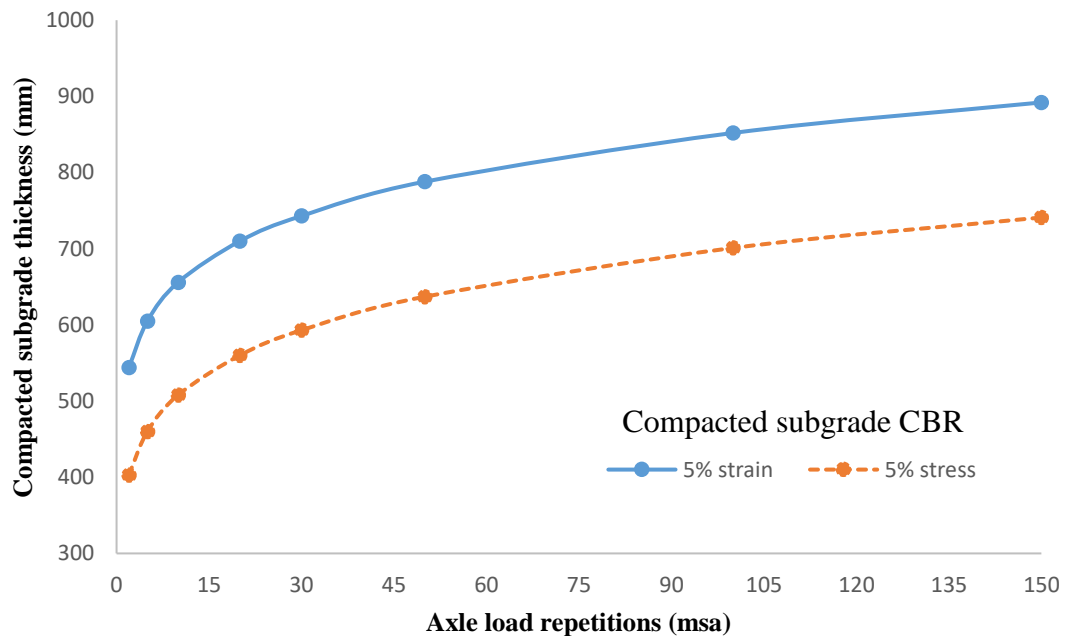
Figure 2.77: Variation of compacted subgrade thickness with axle load repetitions for 2% CBR of natural subgrade based on stress and strain based approach with 0.25 MPa contact pressure
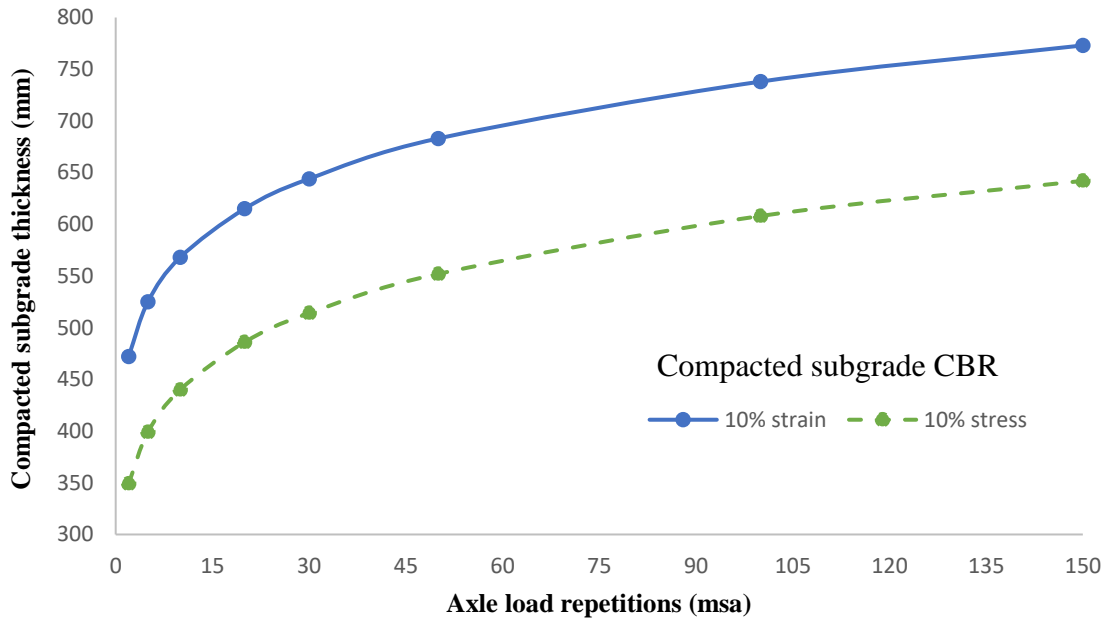
Figure 2.78: Variation of compacted subgrade thickness with axle load repetitions for 2% CBR of natural subgrade based on stress and strain based approach with 0.25 MPa contact pressure
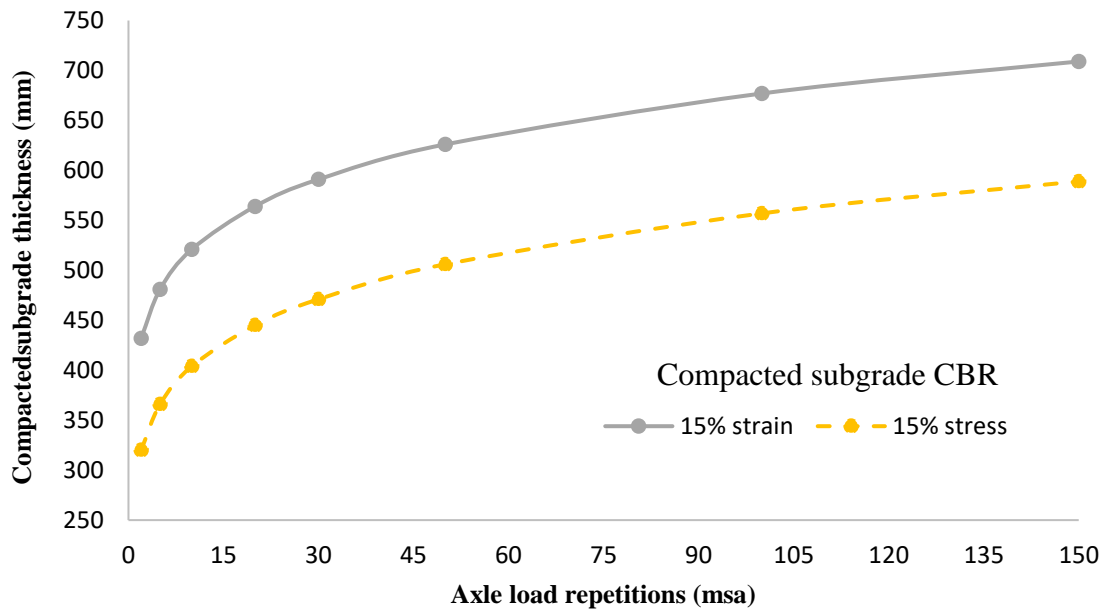
Figure 2.79: Variation of compacted subgrade thickness with axle load repetitions for 2% CBR of natural subgrade based on stress and strain based approach with 0.25 MPa contact pressure
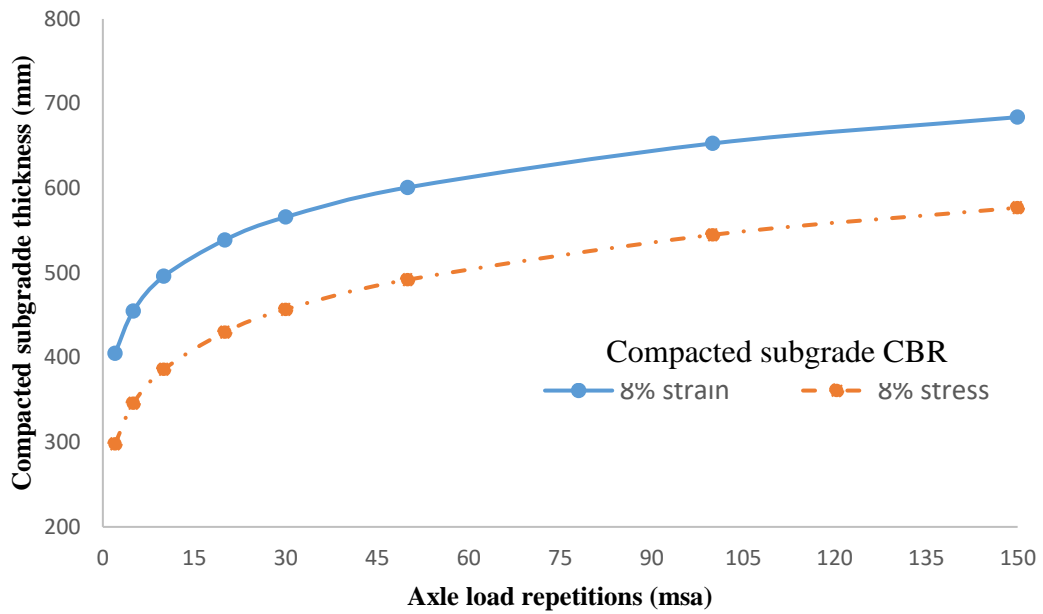
Figure 2.80: Variation of compacted subgrade thickness with axle load repetitions for 5% CBR of natural subgrade based on stress and strain based approach with 0.25 MPa contact pressure
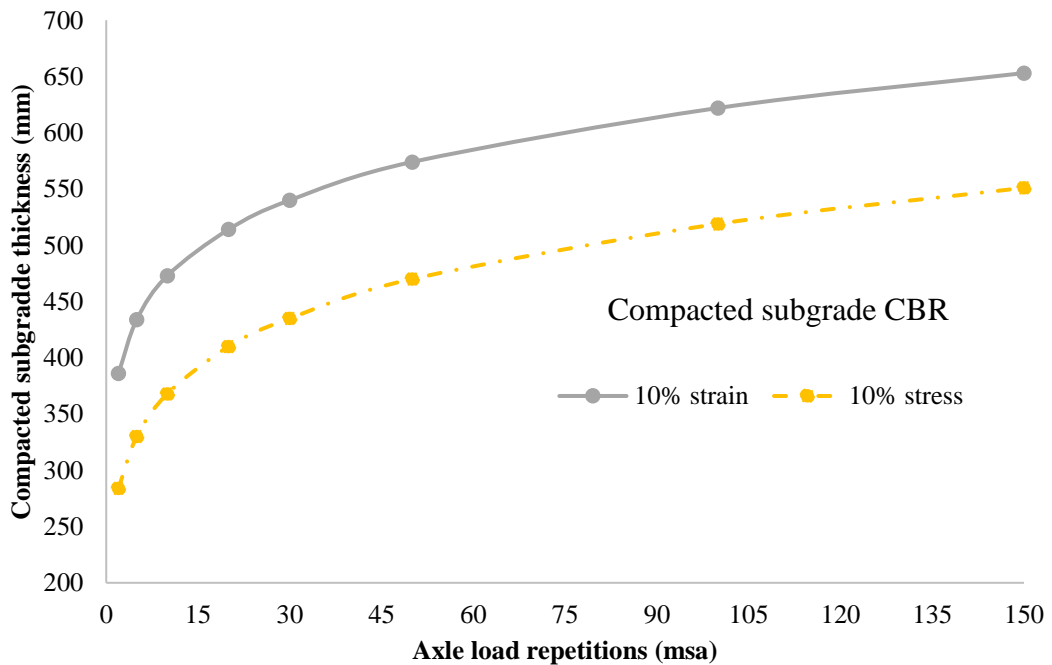
Figure 2.81: Variation of compacted subgrade thickness with axle load repetitions for 5% CBR of natural subgrade based on stress and strain based approach with 0.25 MPa contact pressure
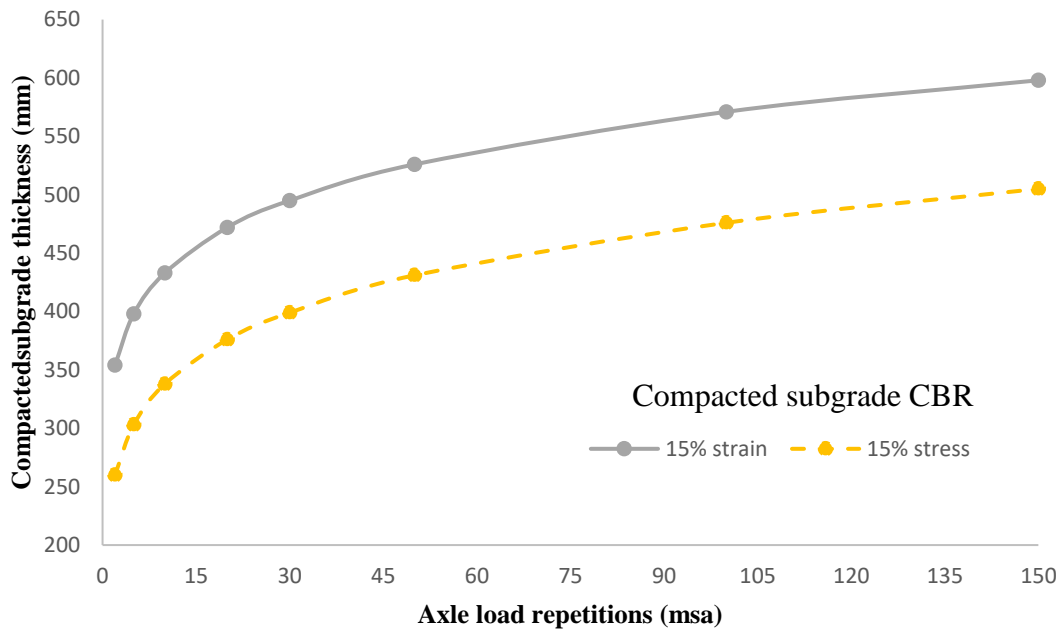
Figure 2.82: Variation of compacted subgrade thickness with axle load repetitions for 5% CBR of natural subgrade based on stress and strain based approach with 0.25 MPa contact pressure
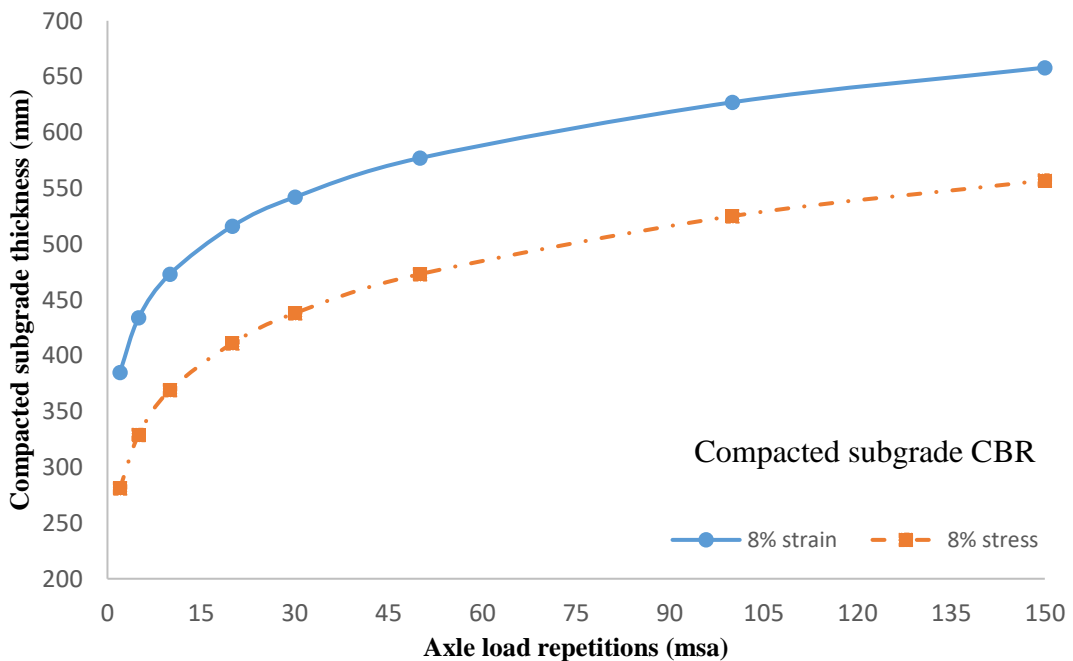
Figure 2.83: Variation of compacted subgrade thickness with axle load repetitions for 7% CBR of natural subgrade based on stress and strain based approach with 0.25 MPa contact pressure

77
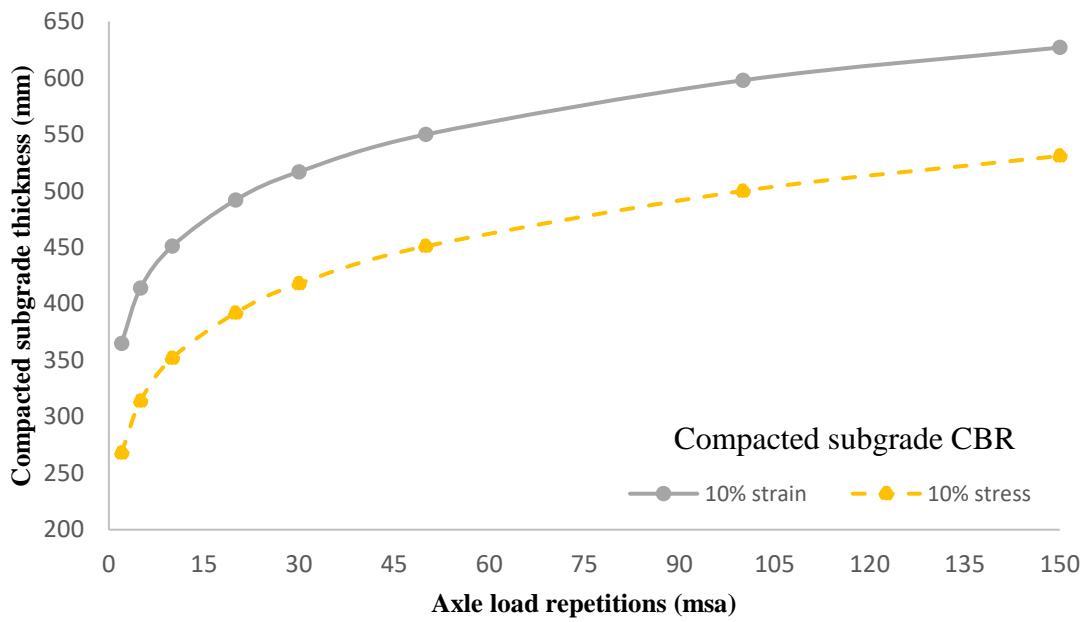
Figure 2.84: Variation of compacted subgrade thickness with axle load repetitions for 7% CBR of natural subgrade based on stress and strain based approach with 0.25 MPa contact pressure
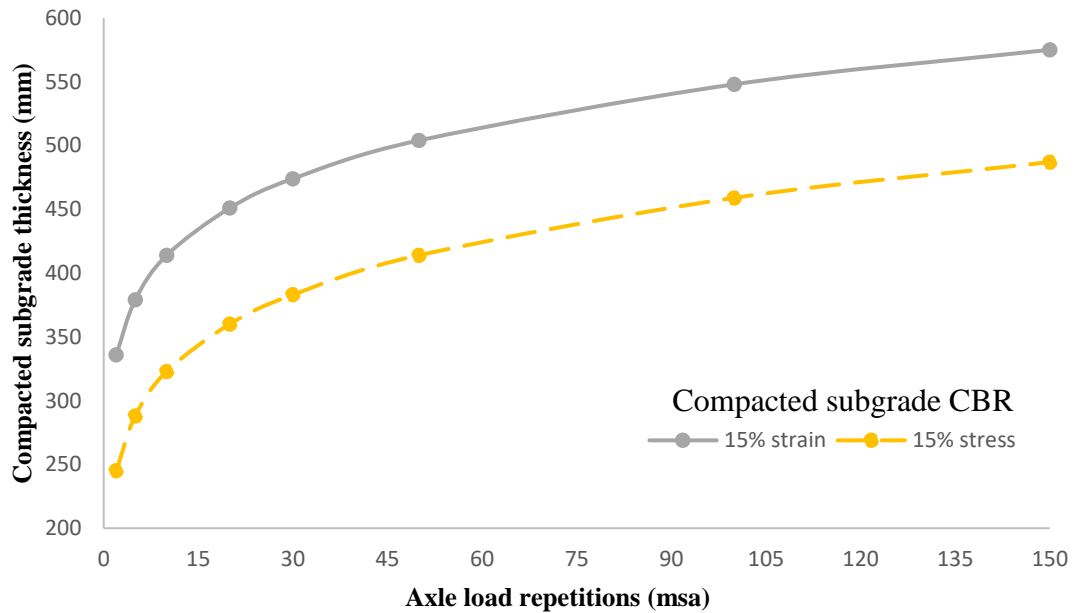
Figure 2.85: Variation of compacted subgrade thickness with axle load repetitions for 7% CBR of natural subgrade based on stress and strain based approach with 0.25 MPa contact pressure
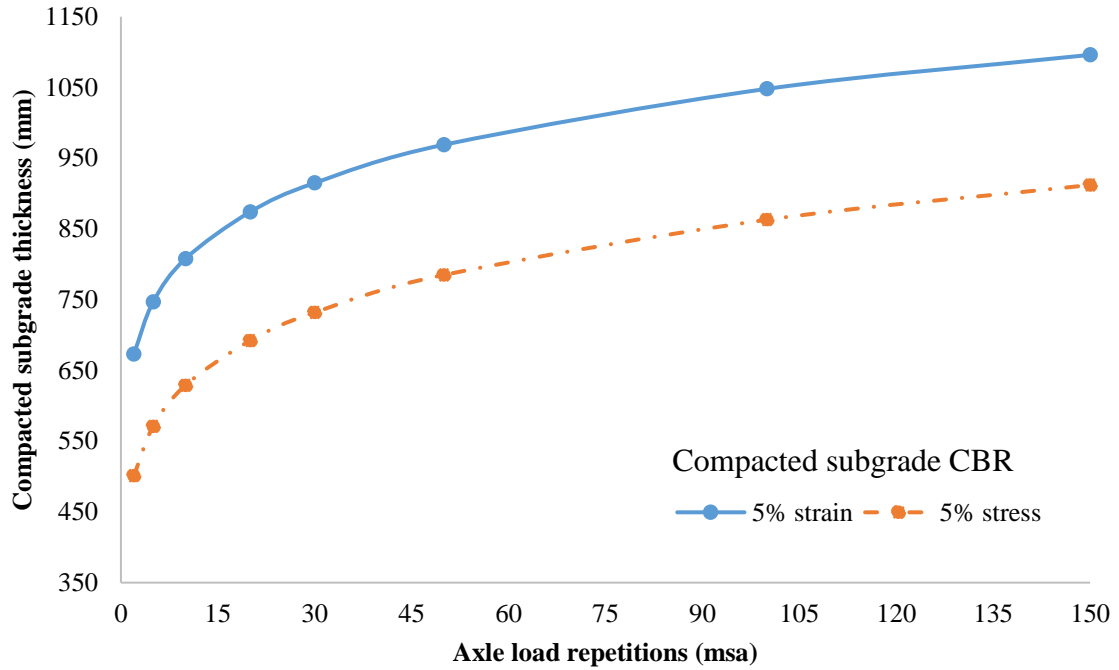
Figure 2.86: Variation of compacted subgrade thickness with axle load repetitions for 2% CBR of natural subgrade based on stress and strain based approach with 0.375 MPa contact pressure
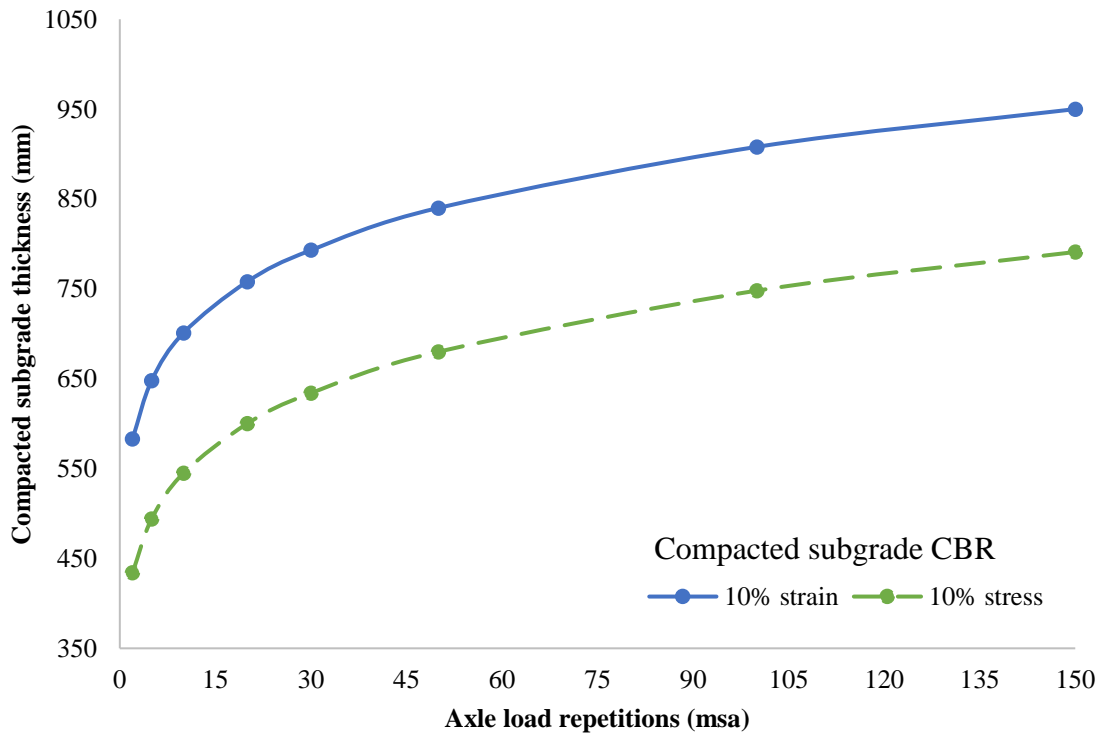
Figure 2.87: Variation of compacted subgrade thickness with axle load repetitions for 2% CBR of natural subgrade based on stress and strain based approach with 0.375 MPa contact pressure
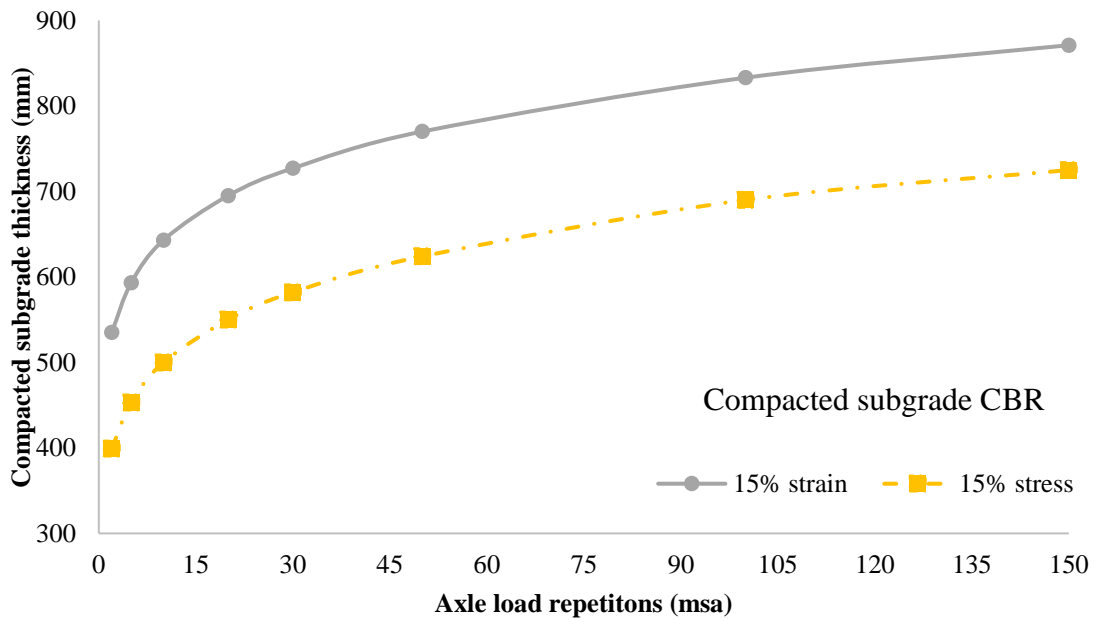
Figure 2.88: Variation of compacted subgrade thickness with axle load repetitions for 2% CBR of natural subgrade based on stress and strain based approach with 0.375 MPa contact pressure
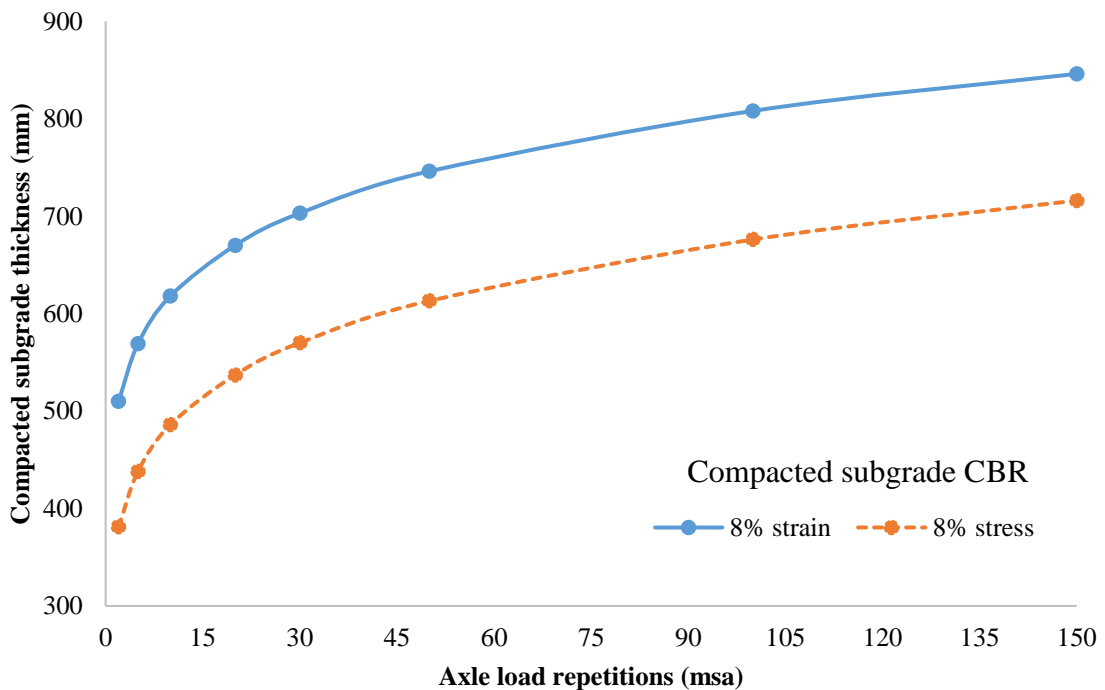
Figure 2.89: Variation of compacted subgrade thickness with axle load repetitions for 5% CBR of natural subgrade based on stress and strain based approach with 0.375 MPa contact pressure
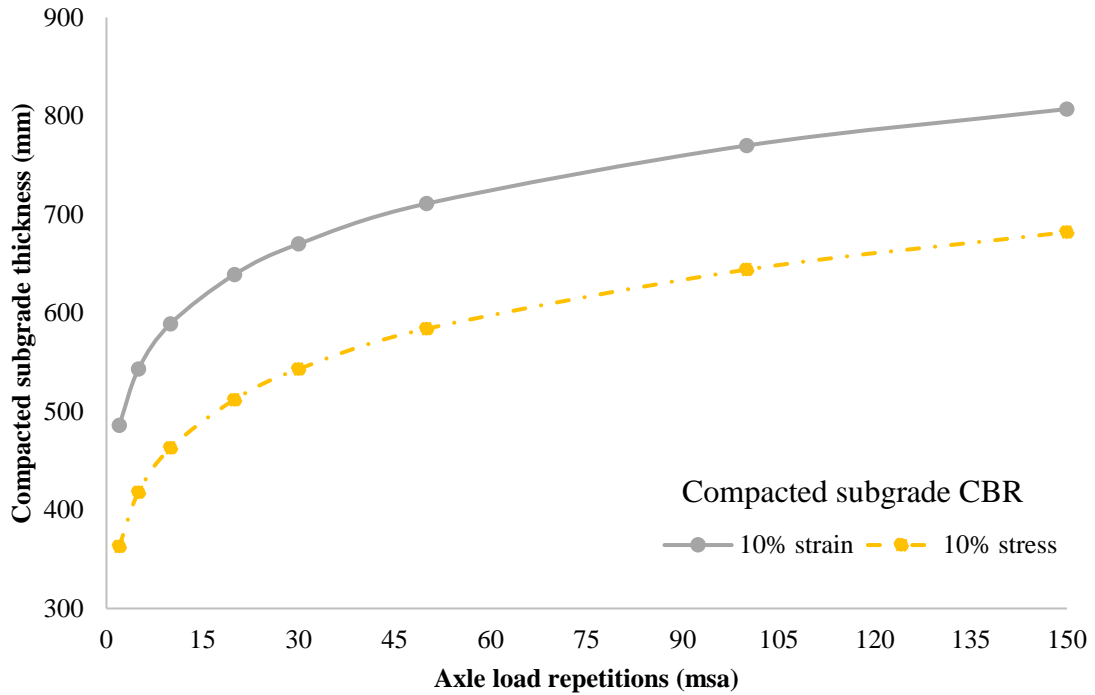
Figure 2.90: Variation of compacted subgrade thickness with axle load repetitions for 5% CBR of natural subgrade based on stress and strain based approach with 0.375 MPa contact pressure
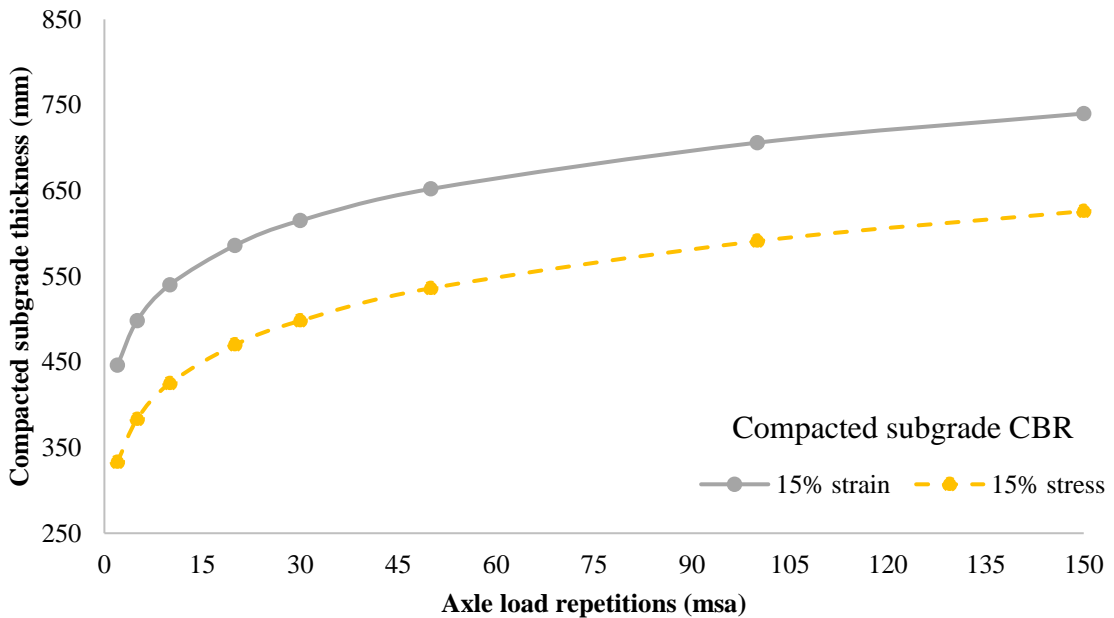
Figure 2.91: Variation of compacted subgrade thickness with axle load repetitions for 5% CBR of natural subgrade based on stress and strain based approach with 0.375 MPa contact pressure
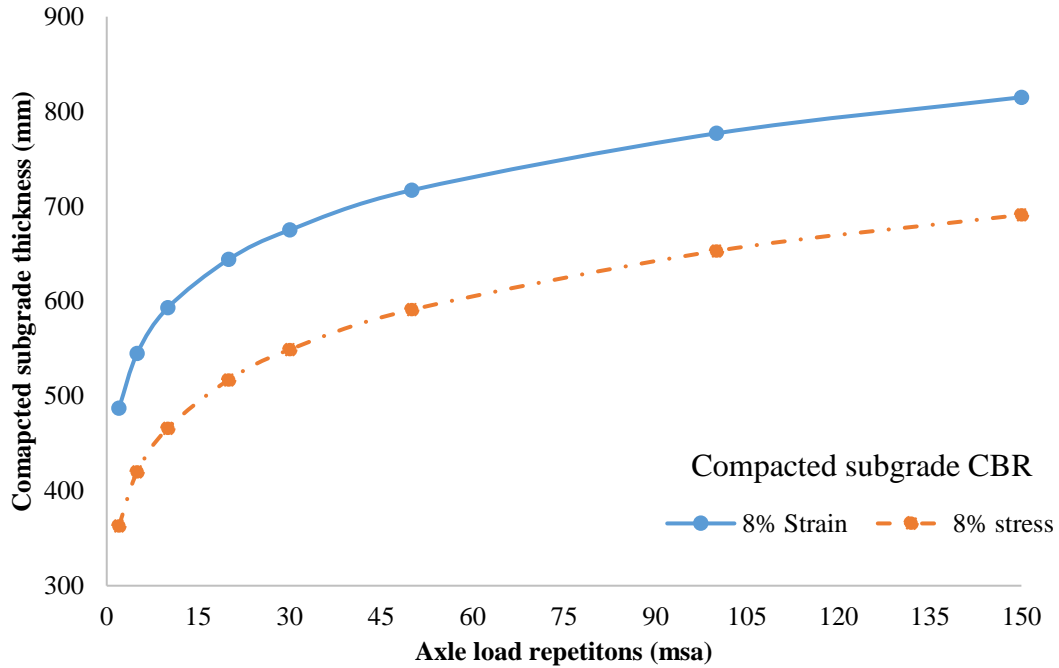
Figure 2.92: Variation of compacted subgrade thickness with axle load repetitions for 7% CBR of natural subgrade based on stress and strain based approach with 0.375 MPa contact pressure
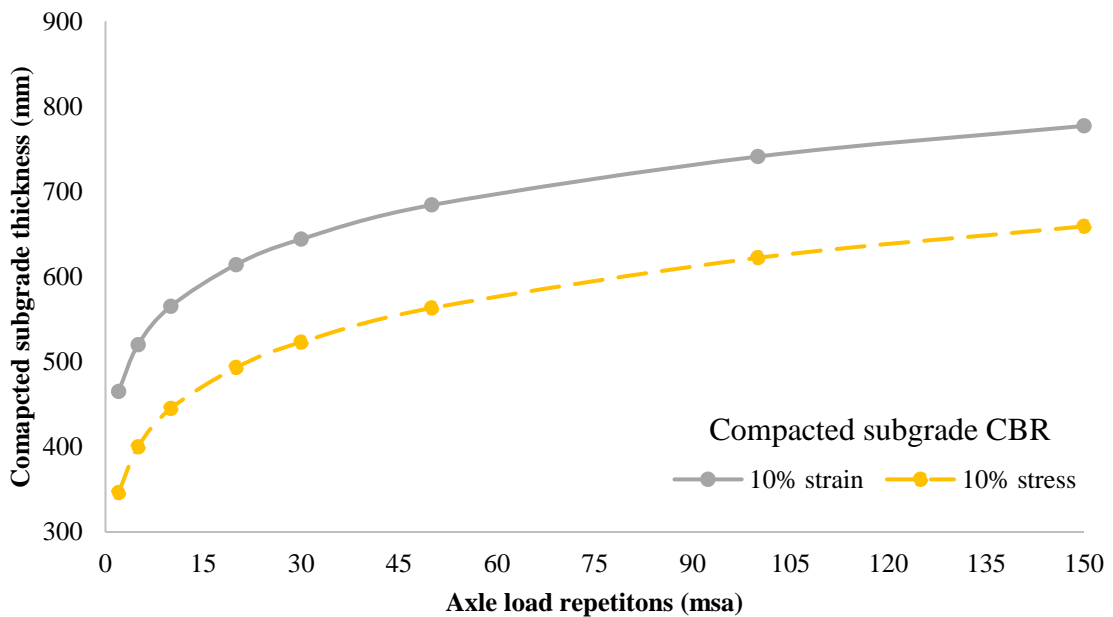
Figure 2.93: Variation of compacted subgrade thickness with axle load repetitions for 7% CBR of natural subgrade based on stress and strain based approach with 0.375 MPa contact pressure
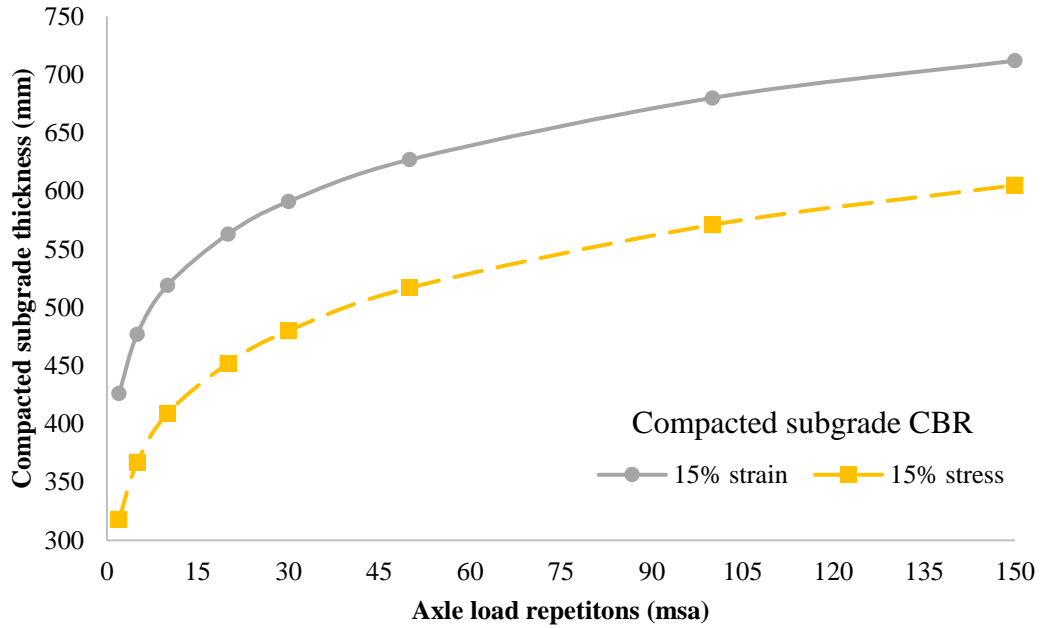
Figure 2.94: Variation of compacted subgrade thickness with axle load repetitions for 7% CBR of natural subgrade based on stress and strain based approach with 0.375 MPa contact pressure

2.5.4   Validation of Model: stress based approach

The comparison of test results obtained from the present analysis has been made with the results obtained using IITPAVE [51] and presented in Figure 2.96 to Figure 2.107 and Table 2.47 to 2.52 (Appendix 1C). The guideline of flexible pavement design IRC37:2018 [51] is based on IITPAVE [51] software which considers a Mechanistic-Empirical approach and linear behavior of paving materials. In IITPAVE [51], the two layered subgrade with respective modulus of natural and compacted subgrade has been used in present validation. The allowable vertical compressive stress on top of natural subgrade corresponding to a specified axle load repetition has been used for determination of compacted subgrade thickness. The allowable vertical stress on top of natural subgrade has been considered from Huang's correlation. The compacted subgrade thickness thus obtained from IITPAVE [51] and present stress based analysis was found reasonably close which in other way justifies the reliability of present method of analysis.
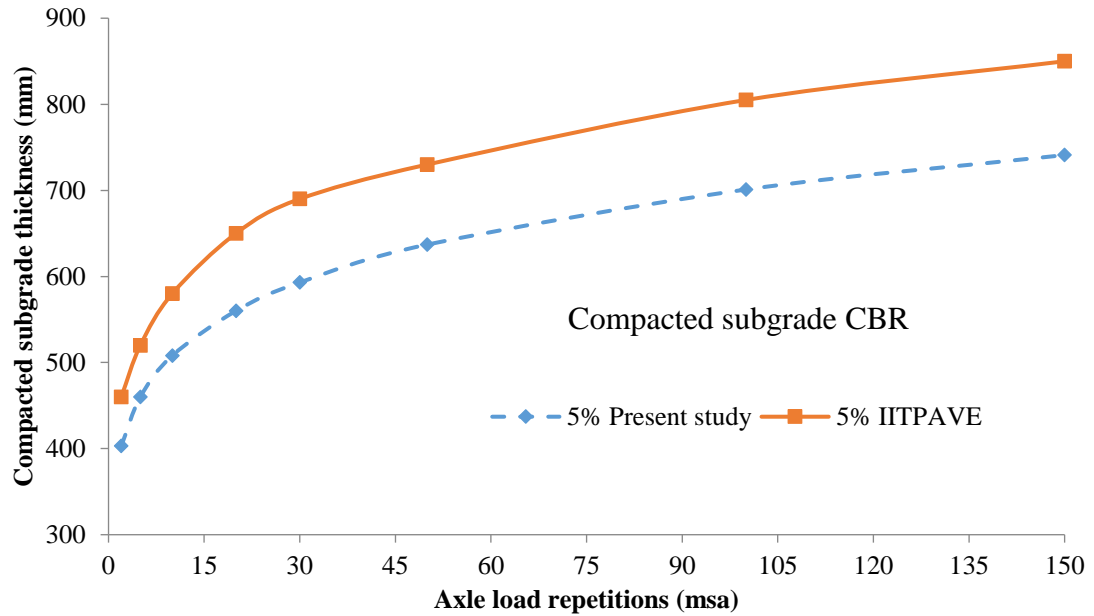
Figure 2.95: Comparison of variation of compacted subgrade thickness with axle load repetitions for 2% CBR of natural subgrade with 0.25 MPa contact pressure
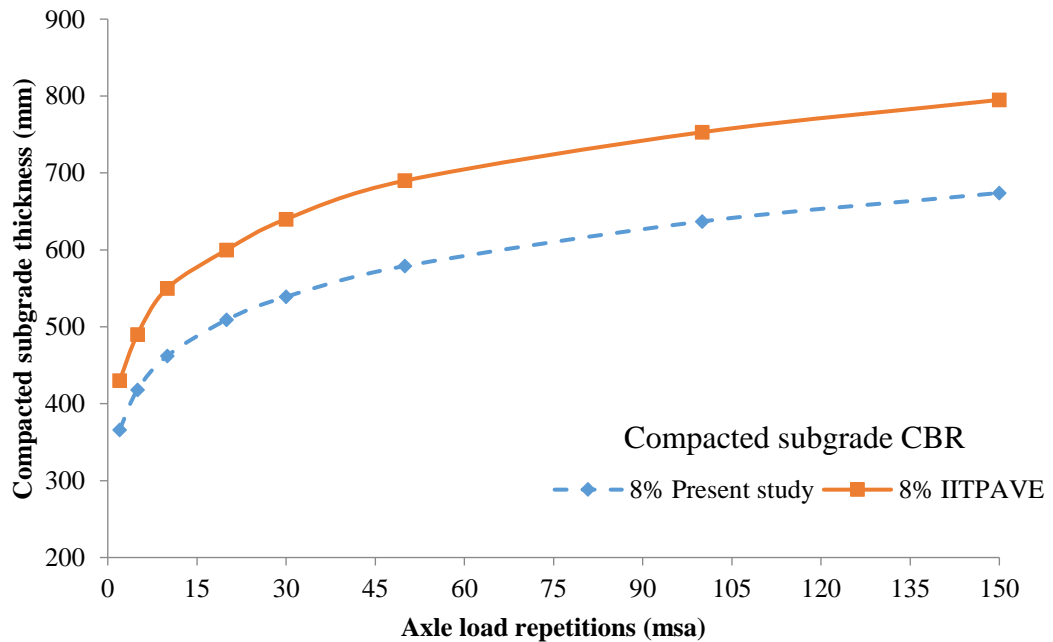
Figure 2.96: Comparison of variation of compacted subgrade thickness with axle load repetitions for 2% CBR of natural subgrade with 0.25 MPa contact pressure
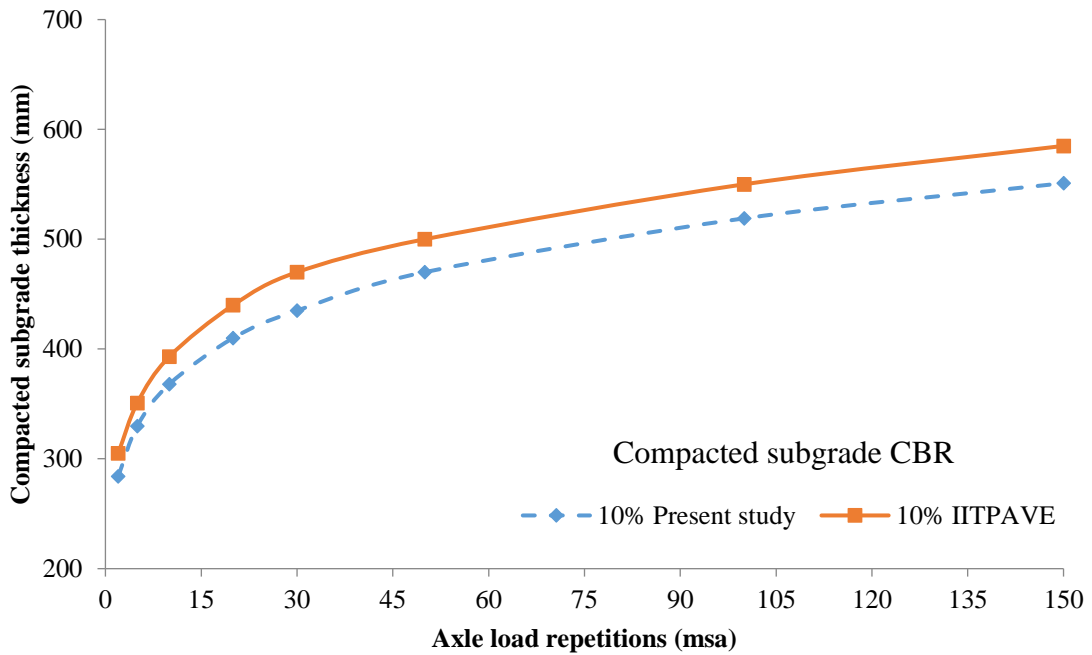
Figure 2.97: Comparison of variation of compacted subgrade thickness with axle load repetitions for 5% CBR of natural subgrade with 0.25 MPa contact pressure
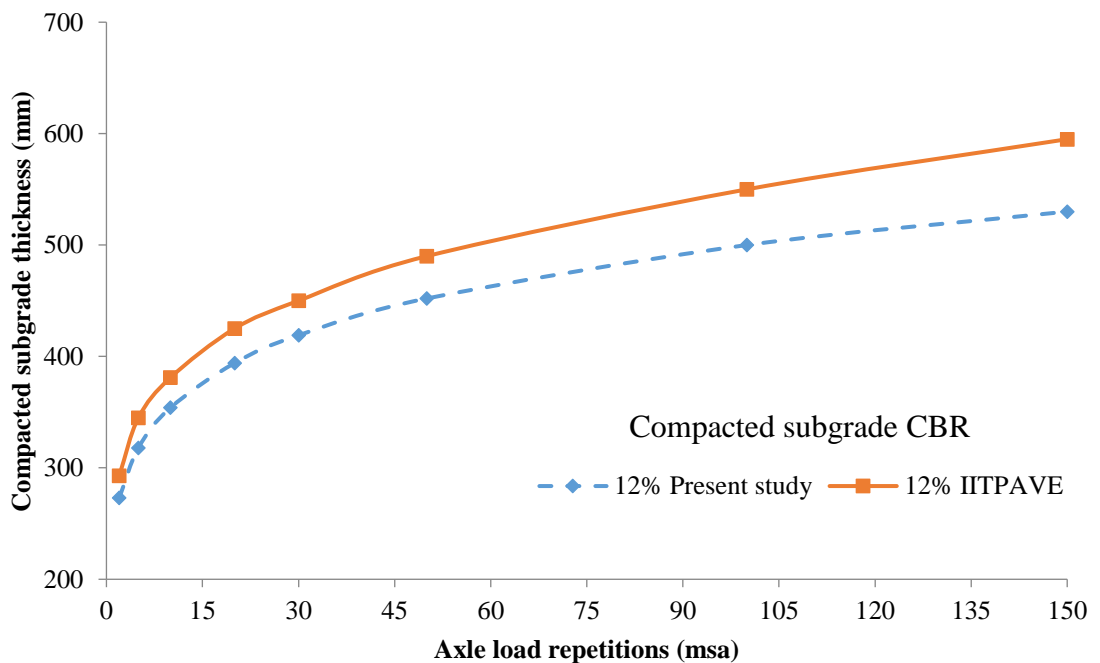
Figure 2.98: Comparison of variation of compacted subgrade thickness with axle load repetitions for 5% CBR of natural subgrade with 0.25 MPa contact pressure

85
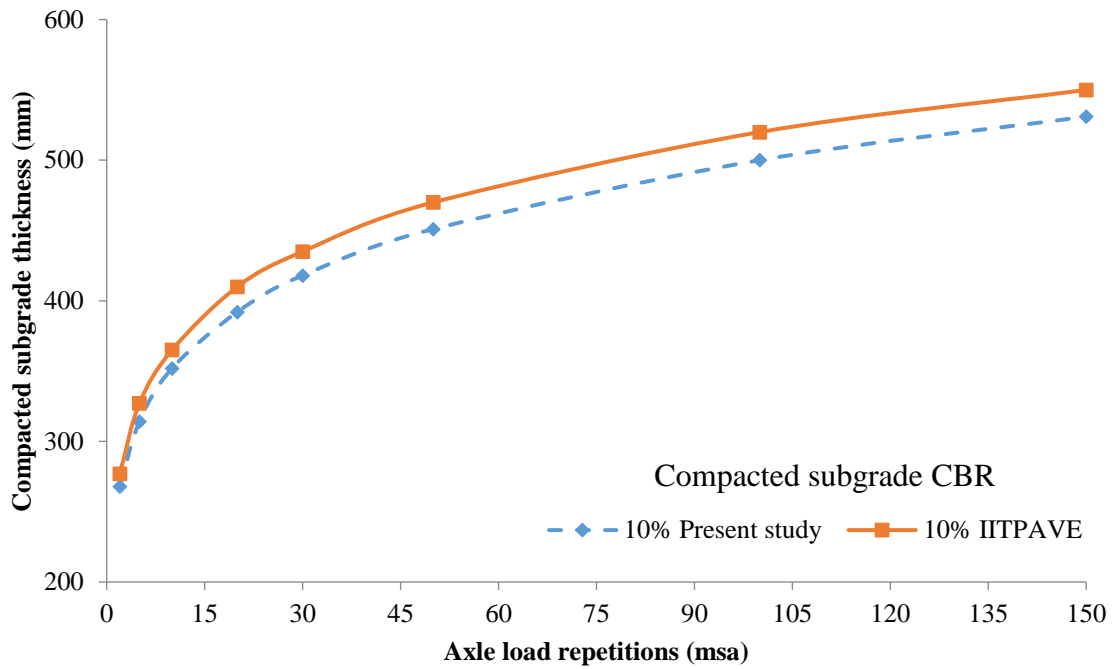
Figure 2.99: Comparison of variation of compacted subgrade thickness with axle load repetitions for 7% CBR of natural subgrade with 0.25 MPa contact pressure
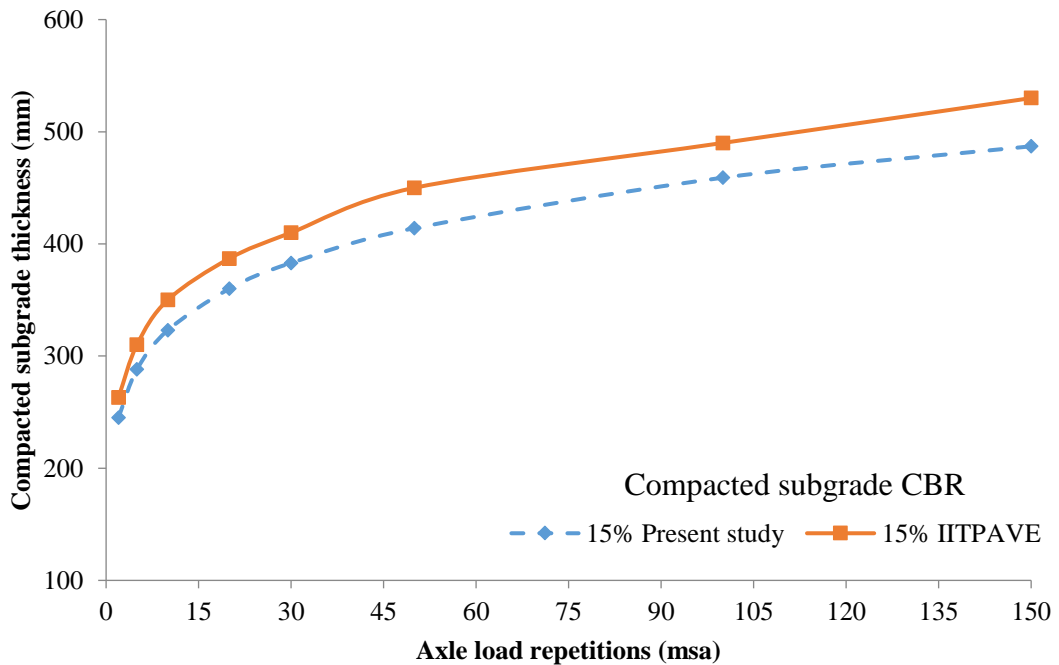
Figure 2.100: Comparison of variation of compacted subgrade thickness with axle load repetitions for 7% CBR of natural subgrade with 0.25 MPa contact pressure
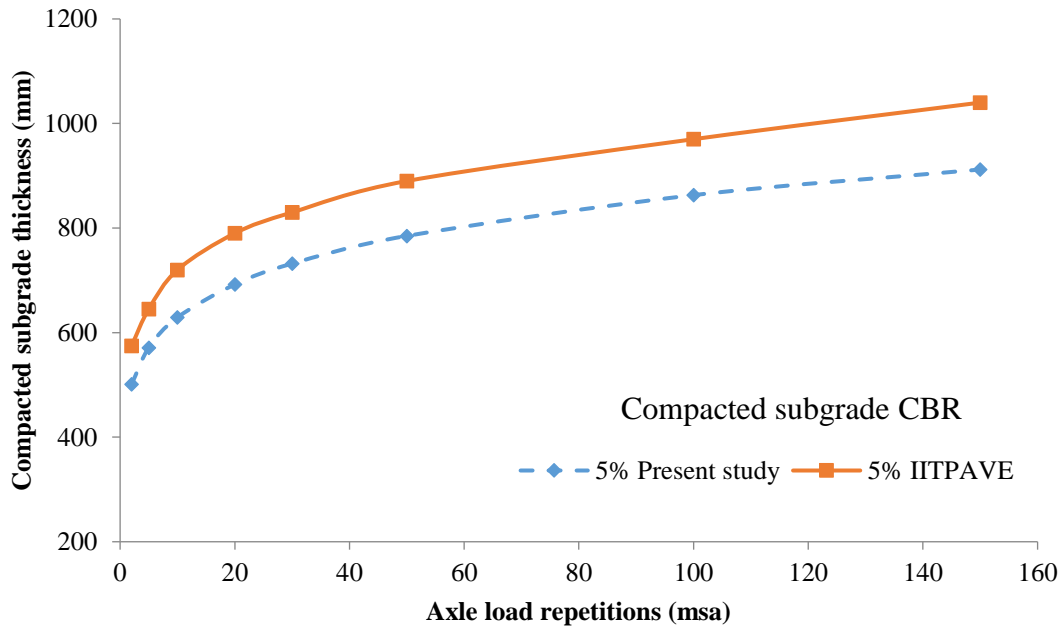
Figure 2.101: Comparison of variation of compacted subgrade thickness with axle load repetitions for 2% CBR of natural subgrade with 0.375 MPa contact pressure
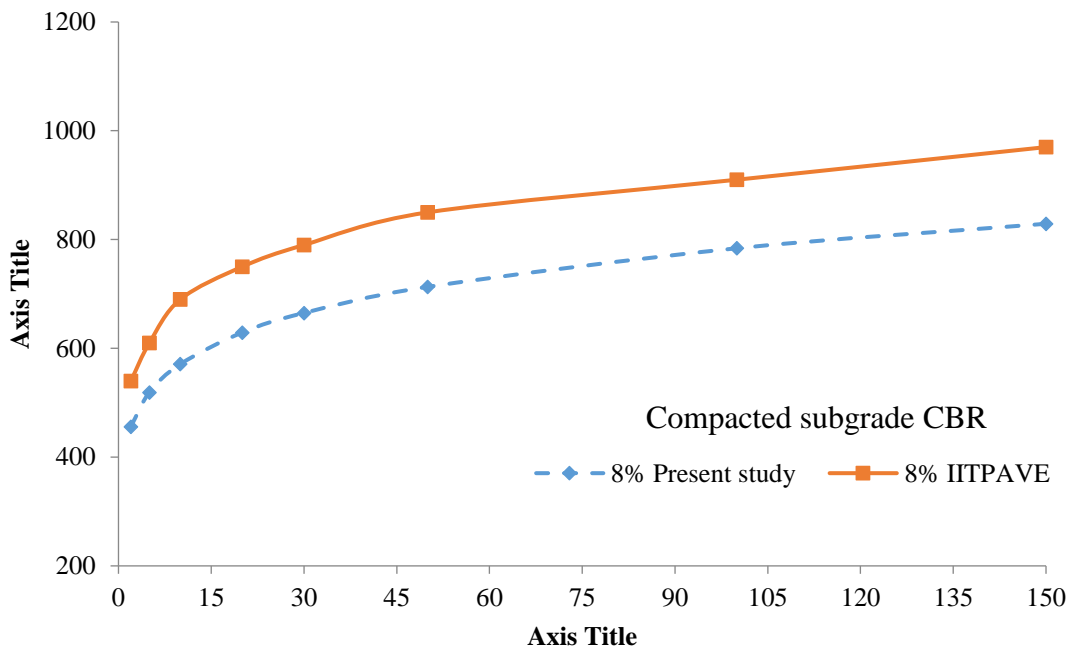
Figure 2.102:Comparison of variation of compacted subgrade thickness with axle load repetitions for 2% CBR of natural subgrade with 0.375 MPa contact pressure
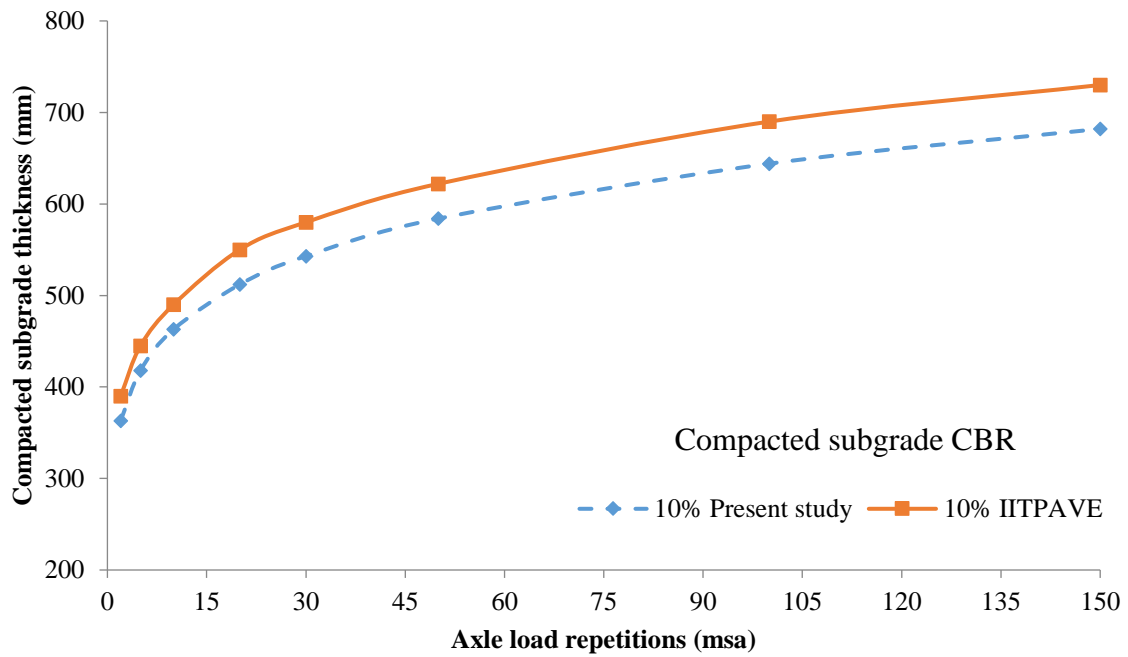
Figure 2.103: Comparison of variation of compacted subgrade thickness with axle load repetitions for 5% CBR of natural subgrade with 0.375 MPa contact pressure
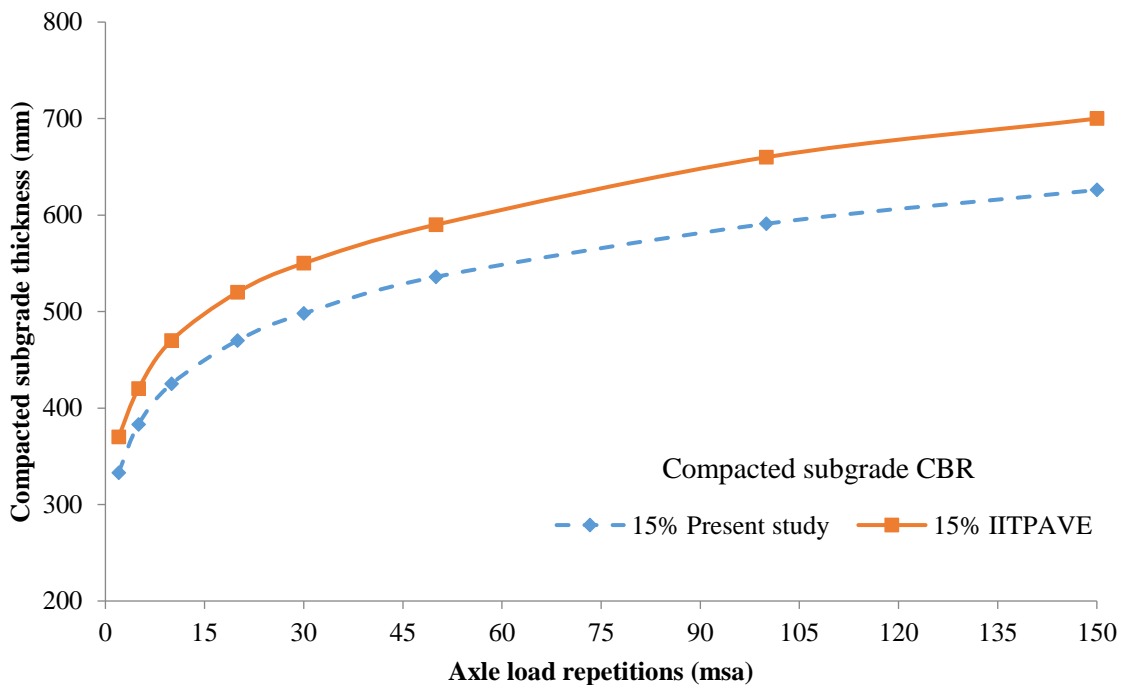
Figure 2.104: Comparison of variation of compacted subgrade thickness with axle load repetitions for 5% CBR of natural subgrade with 0.375 MPa contact pressure
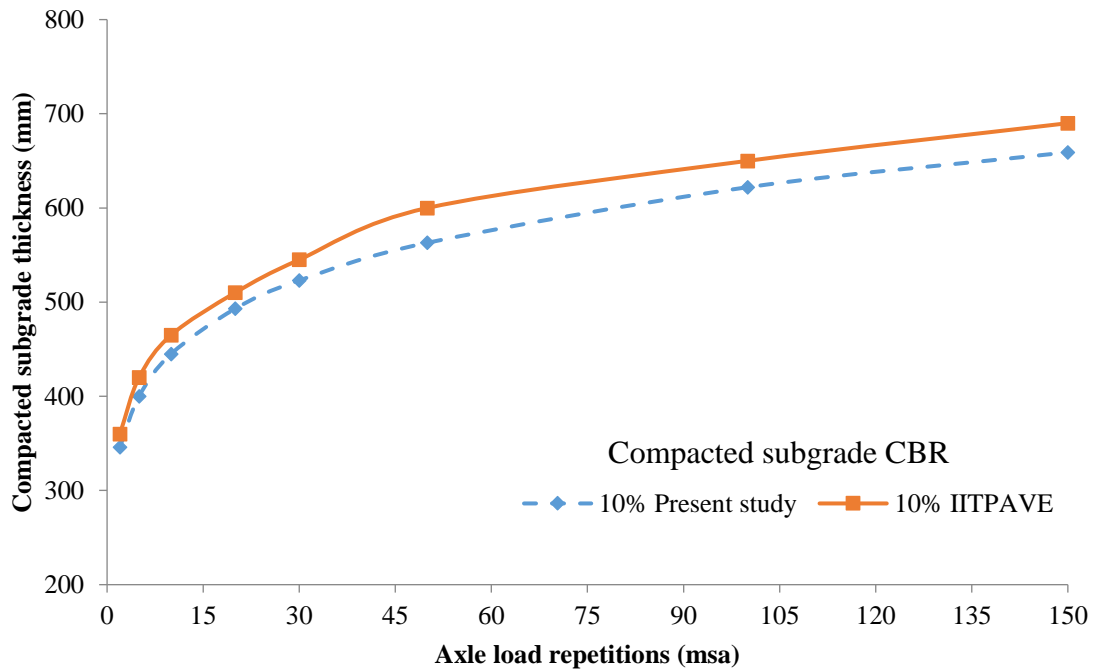
Figure 2.105: Comparison of variation of compacted subgrade thickness with axle load repetitions for 7% CBR of natural subgrade with 0.375 MPa contact pressure
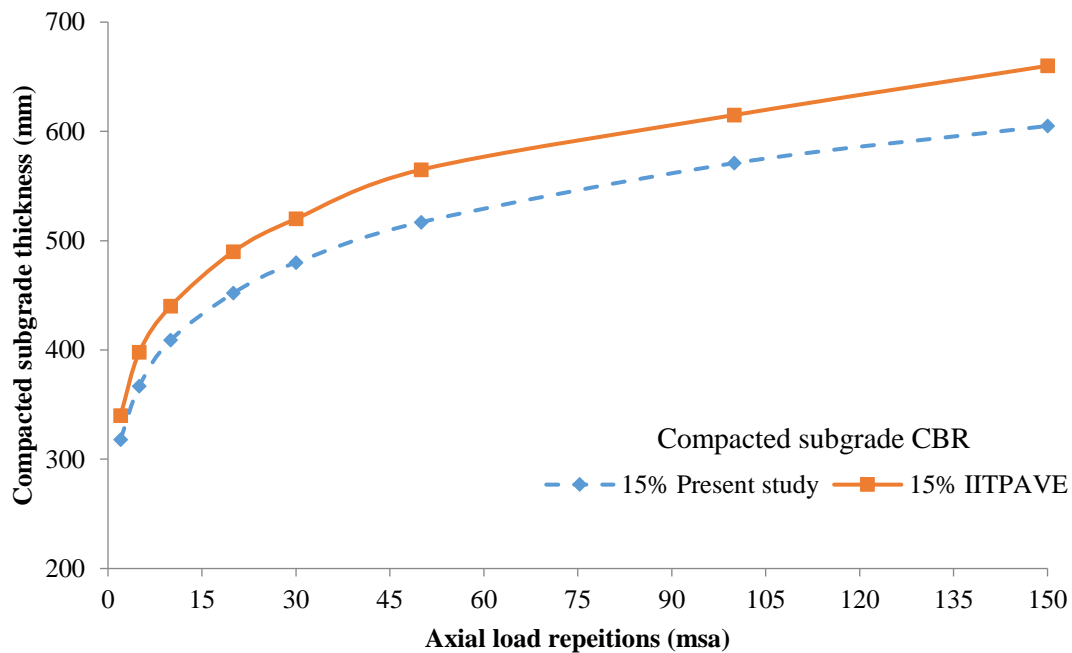
Figure 2.106: Comparison of variation of compacted subgrade thickness with axle load repetition for 7% CBR of natural subgrade with 0.375 MPa contact pressure

2.5.5   Concluding remarks

Effect of load repetitions on subgrade performance is important for estimation of service life of pavement against rutting. In this context, the thickness of compacted subgrade has been determined in this section using a Mechanistic-Empirical stress based approach which includes axle load repetition as an input variable. In present section, it has been found that the compacted subgrade thickness obtained from strain based criteria is more than the stress based approach. It has also been found that the increase of thickness of compacted subgrade is significant of upto 50 msa load repetitions beyond which it becomes less significant. In this context, recommendation for selection of a specified thickness of compacted subgrade by IRC/MORD may be revisited. Finally an effective Graphical user Interface (GUI) has been developed based on methodology as described in the respective sections of the chapter, using PYTHON and JAVA, to make it more convenient for practicing engineers.

CHAPTER 3
DESIGN OF LOW VOLUME RURAL ROAD PAVEMENT WITH UNBOUND MATERIALS

3.1   Introduction

India has emerged as one of the fastest growing economy in world in last decade. Presently, emphasis has been laid in its economic policy, to create better employment opportunity of direct and direct employment by enhancing its road network in order to reduce the gap of surface connectivity. India being one of the largest country with huge population, has adopted the plan of extensive rural road connection named as Pradhan Mantri Gram SadakYojna (PMGSY) with every village in the country by all weathered road. The length of such rural road network is about two third of India's total road length. However, most of the rural road section in India presently may be considered as low volume road which may further be upgraded to suitable level such as Other District road (ODR) or Major District Road (MDR) based on the actual traffic attracted in a given route during the service life of such roads. Low volume roads in India has been classified as the road sections which carry less than 450 commercial [49-50] vehicle per day or the road sections with design traffic during the service period as 2 msa or less [49-50].

Though in terms of gross road length, India ranks second in the global order but the riding quality on such road raises serious question about the durability of road pavement in India. Especially 33% of total road length in India is unsurfaced road which requires primary attention for repair and up gradation to make those functionally adequate and safe.

In order to achieve the path of sustainability in road construction, application of waste material and locally available resources has gained importance in recent times. Presently in India, annual solid production has reached 960 million ton generated as byproduct during industrial, mining, municipal, agricultural and other process. Out of this total waste nearly 30% consists of inorganic waste of industrial and mining sector, Blast furnace slag, construction and demolition material and mill tailing etc. which may be used as granular base or sub-base in road pavement section. Whereas Fly ash, Rice husks ash, Cement kilns dust; marble dust etc. may be used for soil stabilization or as filler in bituminous mix. Use of alternative materials in base and subbase including waste materials reduces the cost significantly in pavement construction with unbound granular base and sub-base.

Keeping this in view, application of alternative materials including waste in low volume rural road construction can be made with suitable design approach. In this context, efforts are to be made to develop suitable pavement design models of low volume road pavements without any use of bituminous binder base.

3.2   Literature review

Sahis et al. (2016) [27] formulated a method to optimize the construction cost of low volume road pavements through a Mechanistic-Empirical design approach, utilizing unbound granular materials. The study emphasized that enhancing the sub-grade and sub-base of road pavements can be achieved by incorporating a suitable mix of alluvial soil with appropriate admixtures. The pavement design methodology proposed here aims to restrict the vertical compressive stress at the interface of the granular unbound base and sub-base layers within a three-layer pavement structure. This formulation is based on the AASHO road test and involves reducing the Present Serviceability Index (PSI) by 2.0-2.5. The Odemark's approach is utilized to transform the multilayered system into a semi-infinite half space, enabling the use of Boussinesq's equation to determine stress and strains for determining the required pavement thickness. The results obtained through this approach are compared with relevant international studies, suggesting their potential for designing low volume rural roads using unbound granular materials with a higher degree of reliability.

El-Oshawa et al. (2020) [59] reported that road networks in Egypt mostly designed by AASHTO-1993 guidelines for flexible pavement system, where the resilient modulus (MR) of unbound materials like granular base/subbase and subgrade soils plays a crucial role. However, the California Bearing Ratio (CBR) test is primarily used in Egypt for quality control and material characterization due to its simplicity. The study conducted to assess various unbound materials used in Egyptian pavement projects, considering MR, CBR, and other material properties. The research also investigates the impact of aggregate gradation on MR and proposes a model to predict MR based on material properties. The study finally verifies the MR-CBR relationship in the

Egyptian Code of Practice and calibrates the model accordingly, providing rational MR estimates for local materials.

Chen et al. (2020)[44] studied the effect of permanent strain occurred in the granular layer of pavement system due to repetitive cyclic loading, which is a major concern for highway design throughout the globe. The study mentioned that two factors such as permanent strain and layer modulus are important design factor for the granular layer in road pavement and railway. Different models were generated to evaluate the permanent settlement of subgrade. Both static and cyclic stress within the subgrade were evaluated considering Boussinesq's (1885) strip loading on top of subgrade.

Shoos et al. (2020) [153] analyzed a two layered flexible pavement system for the design of low volume pavement. The study also defined low volume road as particular section of roads where a considerable depth of granular layer placed on top of natural soil with or without any bitumen binder on top. Among all the failures of pavement rutting was considered as a major mode of distress in this particular types of pavement. The study reveals that the effects of Poisson's ratio on unbound granular layers are very insignificant. The interface stresses and deflection are major pavement responses used in the design. This responses depends on the ratio of modulus of top layer with modulus of supporting layer. It was also observed that layer thickness and the ratio of layer modulus increases then interface stress decreases.

Al-Ameri et al. (2019) [96] formulated different models to evaluate the effect of permanent deformation on unbound granular layer. The models were generated applying empirical regression analysis and its validation has been done using repeated load tri-axial test for different load cycles.. The thicknesses and the quality of the granular layer plays a vital role to stop permanent deformation of the pavement. Stresses due to repetitive loading were used to determine the performance prediction model for permanent deformation of unbound granular layer.

Saride et al. (2019) [158] studied the performance of multilayer flexible pavement in terms of failure due to rutting and fatigue is mostly governed by the thickness of the respective layers and its resilient modulus. The study includes determination of strain related to fatigue and rutting, considering the pavement

as a multilayer elastic system. It was found that minimum subgrade CBR of 3% yields better pavement performance against rutting.

IRC: 37-2018 [51] focused on the design of flexible multi layered road pavement in India. The low volume pavement may be designed on the basis of rutting criteria as binder base is not usually applied on pavement crust, therefore low volume road pavement using vertical compressive strain based criteria with different level of reliability may be taken on the basis of recommendation under the respective code. Use of Locally available marginal/road building material/Industrial Waste/Municipal Solid Waste landfill for Road construction have been recommended. A minimum of 5% Effective CBR of subgrade has been adopted for Road pavement design Moreover, cement treated base and subbase to enhance the strength and SAAMI layer as crack relief layer has also been introduced in IRC:37-2018.

Gonzalez et al. (2018) [74] investigated strain data to characterize the unbound granular material to prove that as long as the vertical strain is in elastic zone, no permanent deformation can occur, but when the strain reaches the plastic zone, rutting failure of the pavement happened, that is why suitable thickness and suitable quality of unbound material is highly needed for low volume roads. Findings showed significant anisotropy in the horizontal plane of the road, with estimates of resilient modulus and Poisson's ratio derived from field strains differing from laboratory tests. This suggests the need for improved replication of real conditions in laboratory testing. A model was developed to estimate road material distress, indicating that using laboratory strains for calculations may overestimate material performance, potentially leading to unnecessary road overdesign. Overall, the study suggests that in-situ strain measurements in LVRs provide realistic data for material characterization, aiding in long-term structural design improvement, though further field research is warranted.

Zheng et al. (2018) [189] developed few models for evaluating stress path inside the unbound granular layer for multilayer flexible pavement system. This study focuses on understanding how unbound granular materials (UGMs) behave under repeated stress in pavement design. It presents results from laboratory tests where different stress paths were applied to two common UGMs, using both constant and changing confining pressures. The goal was to

examine how these materials deform under conditions similar to those experienced by moving wheel loads. The study derived a stable rate of plastic strain accumulation during the secondary stage of deformation, which is crucial for understanding long-term deformation behavior. Mechanistic models were developed based on these findings to predict how UGMs accumulate plastic strain over time, considering different stress paths. These insights can aid in accurately assessing the permanent deformation of UGMs under moving wheel loads, helping to evaluate their suitability for use in pavement foundations.

Erlingsson et al. (2017) [65] investigated the performance of thin asphalt layer thicknesses and properties of UGM (unbound granular layer) in stopping the failure phenomena of the pavement. The study focuses on two key properties of UGMs: resilient and permanent deformation. It discusses models to capture stress dependency, including the universal model and Bishop's effective stress approach for high fine content materials. The study shows that the compressive strain on the top of subgrade due to the vertical stress on the pavement and the shear stress on the vicinity of the wheels can cause severe failure in terms of rutting, which emphasizes the importance of proper characterization of those materials in term of strength.

Biswas et al. (2016) [30,31] proposed a study where suitable thickness of unbound granular layers such as base and subbase was designed using the vertical interface stress. The study considered the pavement as a three layer flexible unbound granular system with serviceability loss of 2.0-2.5. It was observed that the thickness of unbound granular sub base layer is more appropriate for subgrade CBR of 4% and the effective thickness of subbase is 150mm, above which it becomes insignificant.

Rahman et al. (2015) [143] Suggested that to reliably foresee how unbound granular materials (UGM) deform over time in pavement structures, it's crucial to assess the material properties of constitutive models through a multi-stage loading (MS) method. This study examined the forecast of permanent strain buildup in UGM using various existing models, expanded with a time-hardening approach, based on MS repeated load tri-axial tests (RLTTs). The study reported that only the underneath unbound granular layers such as base and sub-base, act as major load distributing layers. Permanent strain which is generated within these layers are very much crucial from rutting consideration of

pavement when large load repetitions are occurred. It was also mentioned that from design perspective both material quality and thickness of layers are important which provide strength and durability of pavement by enhancing its service life.

Pratibha et al. (2015) [133] mentioned that layer modulus is an important parameter for design of a flexible pavement system. Most of the wheel load that are coming on the pavement surface, majorly carrying by the underneath unbound granular layers, keeping that on mind the prediction of stress -strain behavior for that particular layer is very crucial . Both static and cyclic loading are used to evaluate the resilient property of the unbound granular material .and at the end it was concluded that permanent strain that accumulate into the unbound granular layers can predict its stress-strain response effectively.

IRC: SP: 72-2015 [49] provides a standard guideline to design a low volume pavement as per Indian scenario. IRC: SP: 72-2015 stands as a significant document within the corpus of IRC publications, addressing specific guidelines and standards for the design and construction of flexible pavements in India. This elaborate note aims to dissect and elucidate the key aspects of IRC: SP: 72-2015, highlighting its importance, contents, and implications in the realm of road engineering and infrastructure development. The document encompasses various facets of flexible pavement engineering, including material selection, structural design, construction techniques, quality control, and maintenance practices. IRC: SP: 72-2015 holds immense significance for various stakeholders involved in the planning, design, construction, and maintenance of road infrastructure in India. For engineers and consultants, it serves as a comprehensive reference document for ensuring the structural integrity, safety, and longevity of flexible pavements. Government agencies and regulatory bodies utilize the guidelines outlined in IRC: SP: 72-2015 to formulate standards, specifications, and contractual provisions for road projects. Contractors and construction firms adhere to these guidelines to deliver high-quality, resilient pavements that meet the expectations of clients and users. The thickness of gravel/aggregate-surface roads (unpaved roads) has been based on loss of serviceability criteria which is limited to 2.0 at terminal stage from 4..0, just at opening the traffic serviceability index indicating the requirement of rehabilitation. As per the Code, the reliability criteria of 50% have been

considered to design the pavement thickness. The CBR values of the corresponding layers such as natural subgrade, modified subgrade, subbase and base course has also been mentioned in this code. A readily available template can be used for validation purpose to develop any alternative method.

Gupta et al. (2014) [76] proposed a methodology for design of low volume road, based on permanent deformation that occurs within the underneath granular layer. Rutting is considered as a main mode of failure for this types of pavement system where very thin asphalt layer may be present may be not at the top most surface. To address this, the study advocates for an analytical rather than empirical approach. It involved conducting full-scale in situ tests on twenty LVR sections in West Uttar Pradesh and Uttarakhand over four years to account for weather and seasonal effects on rutting. The properties of the pavement material were then analyzed using the finite element method to calculate failure stresses and strains, forming the basis for a Mechanistic-Empirical design approach. Ultimately, the proposed method offers a simpler framework for LVR pavement design procedures. Charts were developed for the thickness of pavement layers and the optimum thickness of base is taken 150mm for subgrade modulus from (20-150) MPa.

Bagui et al. (2012) [19] proposed a study on low volume road network in India. Results are generated to visualize the points of accumulation of different strains within the pavement system. The study concluded that, among the generated strains only vertical compressive strain that acts on top of natural soil layer is important for determination of unbound granular layer thickness, which mostly affects the rutting failure of the pavement.

Gupta et al. (2011) [77] presented a methodology on pavement deterioration and maintenance model, where the study used ANN(artificial neural network) for the generation of pavement deterioration model, with input parameter such as traffic loading, pavement age, soil CBR, and output parameter such as deflection, riding quality and roughness. In Uttarakhand and Uttar Pradesh, India, 18 low volume pavement sections were monitored for two years, using statistical analysis and Artificial Neural Networks (ANN) to develop these models. The best fit model, determined by statistical performance indicators and logical relationships, utilizes polynomial equations. Validation via paired t-tests is performed. The study suggested a Maintenance Priority Index (MPI)

incorporating deflection, riding quality, and traffic which helps prioritize maintenance tasks.

Dawson et al. (2009)[54] mentioned a study where it was observed that the vertical compressive stress generated on top of natural soil layer was used to evaluate the stress-strain behavior of low volume road system. The proposed approach identifies the causes of rutting and suggests straightforward methods for assessing materials, suitable for local engineers with limited resources. The study also introduces an advanced testing and analytical method involving repeated load tri-axial testing and finite element analysis, which helps develop a stress-based design approach. This design method relies on simple stress analysis, aided by charts and computer-based computations, and utilizes easily accessible material evaluation techniques.

3.2.1 Design of low volume rural road pavement using Danish stress based approach

Presently low volume rural road (LVR) constitutes an integral component of the total road network in India. In this point of time, new construction and up gradation of such roads would require suitable design and construction approach with alternative materials for optimization of huge project cost. In this context, present section deals with determination of pavement thickness with unbound granular materials for low volumes rural roads based on AASHTO [1,2,3] recommendation using Odemark's [126] approach.

3.2.2 Objective

The objective of present study is to formulate a mechanistic- empirical design approach to estimate the thickness of constituent layers a three layered pavement by limiting vertical compressive stress on top of subgrade.

3.2.3 Proposed method of pavement design

In the present analysis, the pavement has been considered as three layer system as shown in Figure 3.1. The top layer consists of compacted granular base with elastic modulus (E_1). The intermediate layer is a granular sub-base with elastic modulus (E_2) resting on sub-grade soil with a modulus of (E_3).

q = 0.56MPa
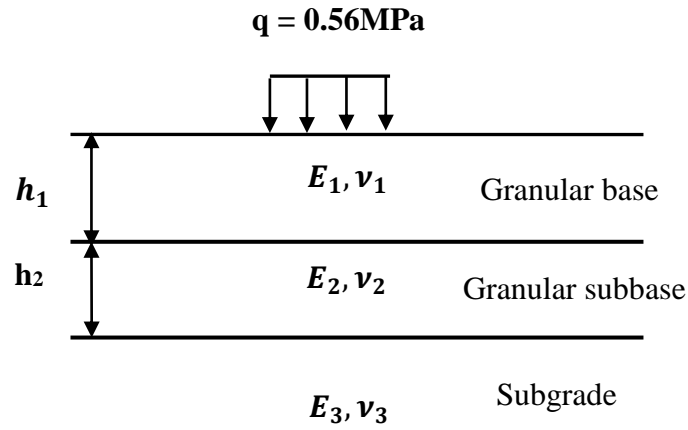
Figure 3.1: Typical structure of three layered flexible pavement section

Various research works [46-51] have been made for design of Flexible pavements which recommends the vertical compressive strain on the top of sub-grade or radial tensile strain at the bottom of bituminous layer as design criteria. Moreover, stress based or deflection based design criteria [87-90] have also been evolved. Each of these methods recommends limiting the stress, strain or deflection in different layer interface to determine the constituent layer thickness with required modulus in a pavement. Indian experience with gravel roads with different unbound materials are limited.

However, present method can be characterised as a stress based method which considers the permissible vertical compressive stress [139] on top of subgrade as a design parameter. The low volume road section in this analysis has been designed on the basis of rutting failure only because no bituminous binder base considered in present model. However, vertical compressive stress on subgrade can be estimated using Danish criteria [181] as shown in Equation 3.1which takes into account material properties, traffic and environment factors.

$$\sigma_{zper} = 0.164 \times \left(\frac{NR}{10^6}\right)^{\frac{-1}{3.26}} \times \left(\frac{E}{160}\right)^{\alpha} \qquad \text{(MPa)} \qquad (3.1)$$

Where, α = 1.16, if E < 160 MPa, else α = 1.0,

N is the number of standard axle load repetitions,

R is the regional factor which has been considered as 2.75 in Indian context and

E is the Modulus of subgrade material (MPa).

However, in order to determine the vertical stress on top of subgrade necessary layer transformations has been made using Odemark's [126] method. The depth from top of pavement to the top of subgrade has been determined using Odemark's [126] method in the following section.

3.2.4   Transformation of three layered system by Odemark's method

The basic principle of transformation of two layer system recommended by Denmark [126] can be used further for transformation of multilayer system in to a homogeneous medium by successive transformation. Such transformation of layers by Odemark's [126] method is necessary to use Boussinesq's [34] theory for determination of vertical stress at sub-base subgrade layer interface. In this section, transformation of three layer system has been explained in Figure.3.2   by successive transformation of pavement layers starting from granular base to subgrade. In present   analysis, the top two layers with respective elastic modulus of E_1 and E_2 has primarily been transformed by an equivalent thickness of h_{eq1} as shown in Figure 3(b) having an elastic modulus of E_2. Similarly, transformation of two layers with elastic modulus of E_2 and E_3 have been made further by an equivalent thickness of h_{eq2} with an elastic modulus of E_3, which characterizes a homogeneous system as shown in Figure 3(c).

Figure 3(a)   **Figure 3(b)**   **Figure 3(c)**
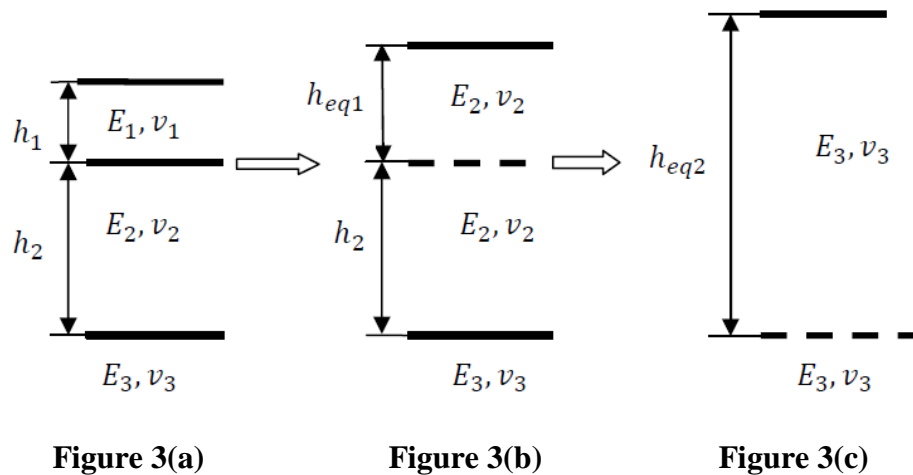
Figure 3.2: Successive transformation of a three layered system using Odemark's method

The equivalent thickness of h_{eq2} thus explained may be determined using Equation 3.2 below.

$$h_{eq2} = f_1 \left(f\, h_1 \sqrt[3]{\frac{E_1}{E_2}} + h_2 \right) \times \sqrt[3]{\frac{E_2}{E_3}} \tag{3.2}$$

Substituting $E_2 = 0.2\, h_2^{0.45}\, E_3$ (MPa) $\tag{3.3}$

Where h_2 = Thickness of granular sub-base (mm). Equation 3.2 can be expressed as

$$h_{eq2} = f_1 \left(f\, h_1 \sqrt[3]{\frac{E_1}{0.2 h_2^{0.45} E_3}} + h_2 \right) \times \sqrt[3]{\frac{0.2 h_2^{0.45} E_3}{E_3}} \tag{3.4}$$

Where f is Odemark's [126] correction factor for granular base- subbase interface and f_1 is the Odemark's [126] correction factor for granular subbase-subgrade interface. In present analysis, both f and f_1 have been considered as 0.80 as recommended by Sherif et al 2011[60]. Flow diagram of the adopted methodology for estimation of low volume pavement thickness using Danish stress based methodology has been shown in Figure 3.3.

3.2.5 Determination of vertical stress on top of subgrade

The vertical stress at a depth (z) under anuniformly distributed circular load with contact radius (a) can be determined using Boussinesq's [34] Equation 3.5.

$$\sigma_z = q \left[1 - \left(\frac{z}{\sqrt{a^2 + z^2}} \right)^3 \right] \tag{3.5}$$

So, the vertical stress on top of subgrade may be determined by using Boussinesq's [34] Equation where the term 'z' needs to be substituted by h_{eq2}.

Therefore by substituting h_{eq2} as 'z' in Equation 3.5, the following Equation 3.6 may be established

$$\sigma_z = q \left[1 - \left(\frac{h_{eq2}}{\sqrt{a^2 + h_{eq2}^2}} \right)^3 \right] \tag{3.6}$$

By solving Equation 3.6 and Equation 3.1, the thickness of pavement base (h_1), subbase (h_2) can be determined for specified axle load repetitions and subgrade strength. In present analysis, initially the thickness of subbase has been assumed and corresponding base thickness has been estimated using proposed

methodology. Pavement base thickness thus obtained using present method has been presented in Table 3.1 and Table 3.2 (Appendix 3A) with different input parameters as described below.

3.2.6 Input parameters

For determination of pavement thickness, the radius of the contact between the tyre and pavement has been considered as 150 mm, which carries an uniformly distributed load of 0.56 MPa [46-51] on the top of pavement surface and shown in Figure 3.1.

The minimum recommended elastic modulus (E_1) of unbound granular base layer has been considered as equivalent to 100% CBR. However, the elastic modulus of granular sub-base layer has been estimated in present analysis using the sub base thickness and subgrade CBR as input parameter as shown in Equation 3.3. Unbound Granular Subbase thickness of 100 mm and 150 mm has been considered in the present analysis. The elastic modulus of granular subbase (E_2) has been obtained using Equation 3.3.

The axle load repetitions has been considered in present section from 20000-10,00,000 ESAL.

However, for estimation of subgrade modulus the following equations have been used in present analysis.

$$E_3 = 10 \, CBR \qquad \text{(MPa) if CBR} \leq 5\% \tag{3.7}$$

$$= 17.6 \, (CBR)^{0.64} \;\; \text{(MPa) if CBR>5\%} \tag{3.8}$$

Where (E_3) is the Elastic Modulus of subgrade.

3.2.7 Results and Discussion

Rural roads designed for cumulative ESAL repetitions more than 1, 00,000 with unbound granular bases which comprise conventional Water Bound Macadam (WBM), Wet Mix Macadam (WMM) or Crusher run Macadam Base (CRMB) are used in India. For Rural roads for cumulative axle load repetitions less than 1, 00,000 ESAL, Gravel road is recommended except for a very poor subgrade. In this backdrop, design load as ESAL repetitions from 20000 to 1000000 has been considered in the present study. The result obtained using present approach has been compared with the results from other relevant guidelines. In present study, variation of sub-grade CBR from 2-10% has been considered for determination of granular base thickness.

```
┌─────────────────────────────────────────────┐
│  Design of Low Volume Rural Road Pavement    │
│  using Danish stress based approach          │
└─────────────────────────────────────────────┘

┌─────────────────────────────────────────────┐
│                 INPUT                         │
│  Subbase thickness, Elastic modulus of base,  │
│  subbase and subgrade, Tyre pressure,         │
│  Axle Load repetitions,                       │
└─────────────────────────────────────────────┘

                       ┌───────────────────────────┐
                       │ Application of Odemark's   │
                       │ transformation technique   │
                       └───────────────────────────┘

┌──────────────────────────┐      ┌──────────────────────────┐
│ Allowable vertical stress │      │ Determination of vertical │
│ on subgrade from Ullidtz  │      │ stress on subgrade using  │
│ criteria                  │      │ Boussinesq's theory.      │
└──────────────────────────┘      └──────────────────────────┘

┌─────────────────────────────────────────────┐
│ Determination of pavement base layer thickness│
└─────────────────────────────────────────────┘

┌─────────────────────────────────────────────┐
│ Validation of computed thickness with different│
│ standard practice                             │
└─────────────────────────────────────────────┘
```

Figure 3.3: Flow diagram of the adopted methodology for estimation of low volume pavement thickness using Danish stress based methodology.

Table 3.1 and Table 3.2 (Appendix 3A) show the comparison between pavement thickness determined by present analytical approach and the result of IRC: SP:72-2007 [49-50] , the guideline in India for design of low volume rural road pavement with gravel/aggregate surface and flexible pavements as paved road. The pavement design presented in IRC: SP: 72-2007 [49-50]   for both gravel and flexible pavements are performance based low volume road design as brought out in AASHTO [1, 2, 3] guide for design of pavement structures. The serviceability rating as per PMGSY [86] operation manual has been adopted in the guideline with a terminal serviceability index of 2.0. It is relevant to mention that the Equation 3.1 which has been used in the present analysis is also based on AASHTO [1,2,3] road test and relates a decrease of pavement serviceability index to 2.0 -2.5 as terminal value. In this backdrop, comparison of result using present approach and IRC: SP: 72 – 2007 [49-50] may be considered significant and meaningful. It is evident from the data that, the thickness obtained using present approach is reasonably close with recommended thickness in IRC:SP-72-2007 [49-50] up to 450000 ESAL. However, for higher loads, the required pavement thickness is less in present approach with respect to of IRC: SP:72-2007[49-50] . It is important to note that increase in sub-base thickness of 50mm may result decrease of total pavement thickness of 25mm, which has a direct impact on project cost. However, maximum thickness of granular sub-base having CBR between 20 -30% may be considered as 150mm for low volume roads.

3.2.8   Validation of test results

The thickness of pavement thus obtained has also been compared with Kentucky's [95] design curves for flexible pavement in Figure 3.4.   In Kentucky's [95]   empirical design approach, for conversion of wheel load from 5000 lb to 9000 lb, an equivalent load factor of 16 has been used to simulate the effect of 4100   kg wheel load. Figure 3.4 also compares results obtained fromIRC:37-2001 [95] , the Mechanistic – Empirical [26,27,135,149-151,44-47] strain based design guideline of flexible pavement in India and the results of stress based mechanistic analysis of Biswas (2005) [28] . It is relevant to mention that the results used in Figure 3.4 can be characterized as a mix of

results obtained from mechanistic, empirical and Mechanistic-Empirical approach. Comparison of those results shows that the finding of present study is in good agreement with other relevant findings in different ranges of soil subgrade strength.
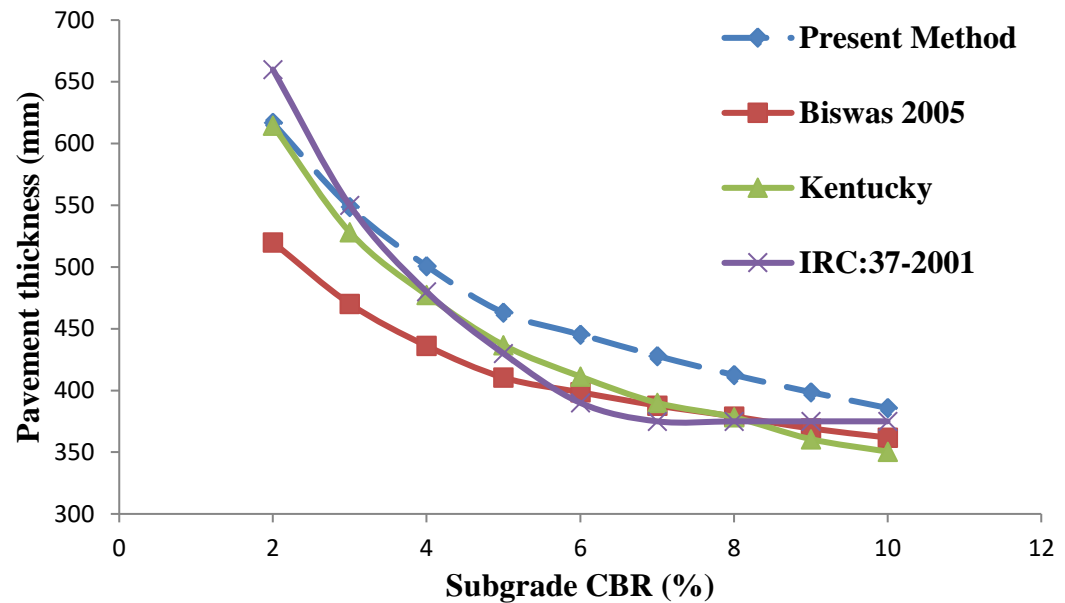
Figure 3.4: Comparison of pavement thickness obtained from different approaches

3.2.9   Concluding remarks

Proposed model of stress based pavement design shows comparable results with other relevant findings which include strain based design criteria. Convergence was found between the results obtained from Mechanistic; Empirical and Mechanistic-Empirical approach is a significant aspect of present study. It is also evident from this study, that the variation of pavement thickness on soft soil is more sensitive than hard soil. Thickness of pavement using alternative granular base with different elastic modulus may also be obtained using proposed method of pavement design.

3.3 Design of low volume flexible road pavement using concentration factor in a layered system

An appropriate design methodology needs to be developed to make in service and new road pavements more durable. The large volumes of unsurfaced road in India are primarily the rural roads with comparatively low volume traffic. Such pavement generally can be characterized as two layered system with unbound granular base and sub base course resting on subgrade soil. If the stresses in the subgrade, the half space, due to the wheel load are too high, a stiffer top layer is needed to reduce the stresses. Such a system with a stiffer layer on top on a softer half space, is characterized a two layer system Thin bituminous surfacing are often provided on the top of such road pavement to ensure a better riding quality but without having any function to withstand stress, strain or deflection due to wheel load. In view of these, present study is aimed to find out a design methodology for low volume rural road sections with unbound materials on virgin subgrade using Mechanistic-Empirical design approach.

3.3.1 Objective

The objective of present study is to formulate a Mechanistic - Empirical approach to determine the thickness of unbound granular low volume road pavement using concentration factor in Boussinesq's theory for estimation of vertical stress in a layered system.

3.3.2 Proposed method of pavement design

Design of low volume flexible pavement with unbound granular base can be made with stress based design approach. Vertical compressive stress on top subgrade has been considered as failure criteria in present method of flexible pavement design. In present study the pavement has been considered as a two layered system as shown in Figure 3.5.However, in present analysis failure of subgrade only under rutting has been considered as the design criteria for a two layered pavement with unbound granular materials. The allowable stress on top of the subgrade to limit rutting has been considered as design input from Huang's mechanistic- empirical design approach.

$$q = 0.56 \text{ MPa}$$
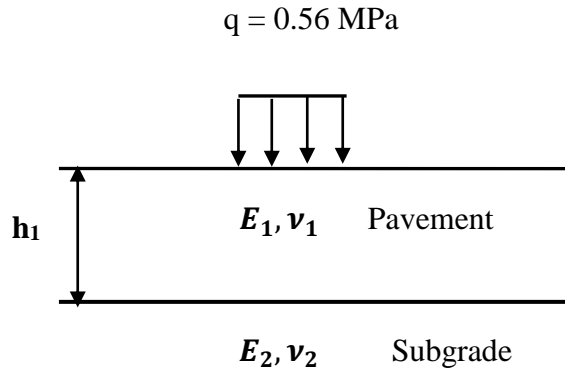
Figure 3.5: Typical structure of a two layered flexible pavement

3.3.2.1 Stress distribution in a layered System

Estimation of vertical stress by Boussinesq's [34] theory can be made if the medium is homogeneous. But in present section, the pavement has been modeled as two layered system. In this backdrop, determination of vertical stress in a two layered system has been done using the concept of concentration factor in Boussinesq's [34] equation. Therefore, in present analysis modified Boussinesq's [34] equation has been considered for estimation of vertical stress at a depth 'z' under a circular load as shown in Equation 3.9. In Equation 3.9 a new parameter (n), termed as concentration factor [191-193] has been used which depends on ratio of elastic modulus of pavement (E_1) and subgrade (E_2). The ratio thus used in present analysis has been termed as modulus ratio.

$$\sigma_z = q\left[1 - \left(\frac{z}{\sqrt{a^2 + z^2}}\right)^n\right] \tag{3.9}$$

Where 'a' is the contact radius between tire and pavement.

The Equation 3.9 may also be expressed in the following form for ease of analysis.

$$\sigma_z = q\left\{1 - \frac{1}{\left[1 + \left(\frac{a}{z}\right)^2\right]^{0.5n}}\right\} \tag{3.10}$$

107

The thickness of pavement in this work has been expressed in the form of a non-dimensional parameter (z/a). The modulus ratio for a two layered system may be determined in following manner.

Modulus ratio (MR) = $\frac{E_1}{E_2}$, Where E_1 = pavement modulus using unbound granular materials and E_2 = subgrade modulus.

In this study, the CBR of unbound granular material has been considered as 100% and corresponding elastic modulus has been estimated using Equation 3.8.

Therefore, E_1= 17.6 $(100)^{0.64}$ = 335.36 MPa

Similarly, the elastic modulus (E_2) may be estimated using Equation 3.7 and Equation 3.8 for different subgrade CBR.

The correlation between concentration factor and modulus ratio was developed by Biswas (2005 [28] and Purakayastha (2022) [138], which has been used in present analysis as shown in Equation 3.11.

$$n = 3.3394 \times (M_R)^{-0.5384} \tag{3.11}$$

The vertical stress using modified Boussinesq's [34] equation may be obtained using a known value of concentration factor which correlates the modulus ratio in a two layered system. Flow diagram of the adopted methodology based on stress based method using concentration factor has been shown in Figure 3.6.

3.3.2.2 Allowable vertical stress on subgrade

The allowable vertical stress on subgrade depends on the number of load repetitions and subgrade property. Based on the shell design-criteria [45,164] and ASSHTO (AASHTO, 1986, 1993) [1, 2, 3] equation, Huang et al. (1984a) [87-90] developed the following relationship.

$$N_S = 7.199 \text{ x } 10^{-5}\sigma_z^{-3.73}E_2^{3.583} \tag{3.12}$$

 E_2 = Elastic modulus of subgrade in (kg/cm^2),

σ_z = Vertical compressive stress on the top of the subgrade in (kg/cm^2).

N_S= Number of cumulative standard axle load repetitions

Now by solving Equation 3.10 and 3.12, the thickness of pavement (z/a) has been determined in present analysis for different subgrade strength (E_2) and wheel load repetitions (N_S).

3.3.3   Results and Discussion

Design of low volume pavement guidelines in India are performance based, as brought in the AASTHO [1, 2, 3] guideline for design of pavement structure. In this backdrop, design load range of 1-20 msa and the range of subgrade strength from 2-10% CBR have been considered in present study for estimation of pavement thickness and comparative analysis.

The modulus ratio has been determined as the ratio of modulus of elasticity of pavement and subgrade for different subgrade CBR. Values of modulus ratio thus obtained have been used to find out the values of concentration factor for different subgrade strengths. It has been found from present study that the pavement thickness increases with decrease in subgrade strength and increase in axle load repetitions, which is most logical in flexible pavement design.

The thickness of pavement expressed in this study is in a non-dimensional form (z/a) obtained by solving Equation. 3.10 and 3.12 for different axle load repetitions (N_S) with different subgrade CBR. The variation of pavement thickness (z/a) thus obtained for different axle load repetitions and subgrade strength have been presented in Figure.3.7 and Figure.3.8.

The thickness of pavement obtained in this study has been compared with Kentucky design curves for flexible pavements and has been presented in Table 3.3 (Appendix 3A). In order to transform the wheel load of 5000 lb to 9000 lb, an equivalent wheel load factor of 16 has been used in Kentucky's [95] correlation. Such conversion is important as the dual wheel load of 9000 lb or 4100 kg represents a 8200 kg standard axle load in the present analysis. Beside this, comparison of thickness of pavement obtained in this work has also been made with the results of Corps of Engineers (HRB, 1956 and U.S. Army Corps of Engineers, 1961) [183] corresponding to 9000 lb wheel load and presented in Table 3.4 (Appendix 3A).

```
┌─────────────────────────────────────────────────┐
│   Design of Low Volume Rural Road pavement with   │
│   unbound granular material using concentration   │
│   factor in Boussinesq's theory.                  │
└─────────────────────────────────────────────────┘
                         │
                         ▼
┌─────────────────────────────────────────────────┐
│                     INPUT                          │
│   Elastic modulus of unbound granular layer and   │
│   subgrade, tire pressure, wheel load, axle load  │
│   repetitions                                      │
└─────────────────────────────────────────────────┘
```

Allowable vertical stress on subgrade using Huang correlation

Determination of vertical stress using concentration factor in Boussinesq's equation

Determination of thickness (z/a) for different CBR and axle load repetitions

Determination of thickness of base layer

Validation of computed thickness with different standard practice

Figure 3.6: Flow diagram of the adopted methodology based on stress based method using concentration factor.

It is evident from comparative study that, with higher axle load repetitions and lower subgrade CBR, Kentucky result matches closely to the findings of present work. Similarly, with smaller load repetitions but with higher subgrade strength, Kentucky [95] results are comparable with present findings. Such nature of convergence of results indicate that, linear elastic failure may be a major trend in unbound paving materials, where failure in either way is controlled by subgrade strength or the magnitude of load repetitions.

It is relevant to mention that the findings from empirical approach have been found to be close with Mechanistic – Empirical design, where the linear elastic behavior of paving materials is considered. Moreover, the comparison of results of Corps of Engineers and Wyoming design chart [75,182,183] with the present work show, that the stress based model appears to be quite reasonable for design of low volume roads, with comparatively lower axle load repetitions. The thickness of pavement corresponding to CBR 4% to 5% shows reasonably good correlation obtained by different approaches.
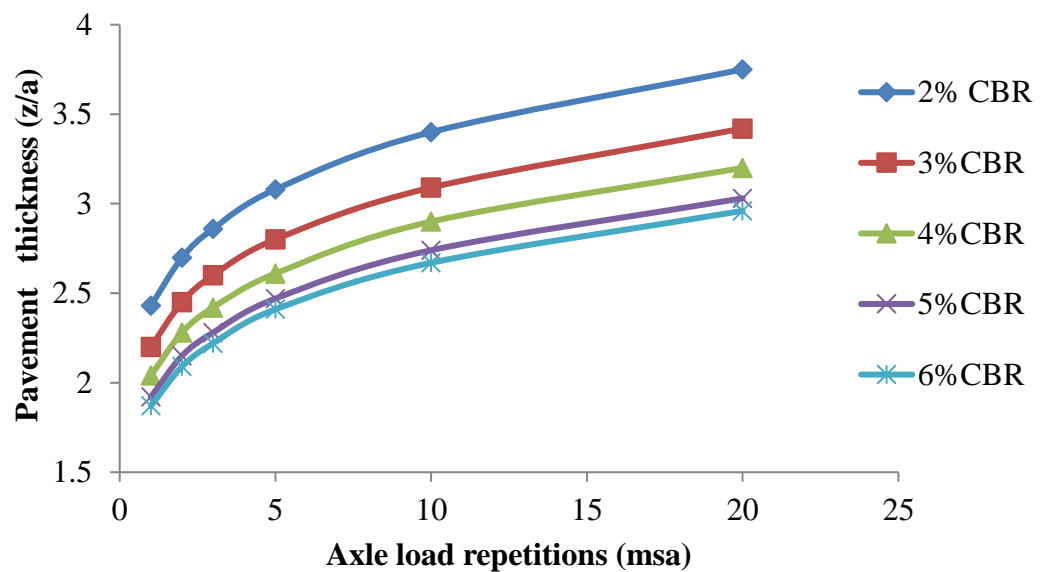
Figure 3.7: Variation of pavement thickness (z/a) with axle load repetitions for different subgrade CBR
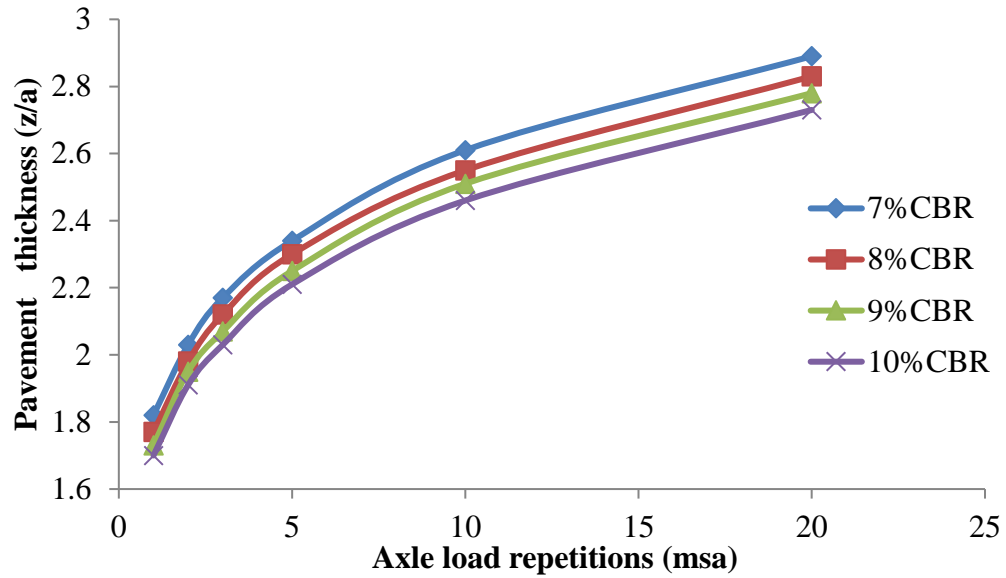
Figure 3.8: Variation of pavement thickness (z/a) with axle load repetitions for different subgrade CBR

The thickness of flexible pavement obtained from present analysis has been compared with the recommended thickness of pavement as laid down in IRC: SP 72-2007 [49-50]. The primary objective of this study is to develop a design methodology for low volume road pavement, therefore the pavement thickness for subgrade CBR ranging from 2-6% for 1 msa load has been considered in present section for comparative analysis and has been presented in Table 3.5 (Appendix 3A). It is evident from the analysis that the pavement thickness obtained using present method is comparable and marginally less than the thickness recommended in IRC: SP 72-2007 [49-50].

3.3.4 Concluding remarks

It can be concluded from present study that the Mechanistic- Empirical stress based design approach is reliable for estimation of pavement thickness for low volume flexible road pavements considering the pavement as a two layered system. Inclusion of allowable stress as failure parameter in present analysis makes the solution more realistic. Application of concentration factor for determination of vertical stress using modified Boussinesq's [34] equation is an useful tool not only in a two layered system but also in a multilayered system.

Pavement thickness obtained using present analytical approach is close to the thickness obtained by other researchers in the relevant field.   Therefore, thickness of pavement using alternative granular base with different elastic modulus may be obtained using proposed method of pavement design. The thickness of pavement between CBR 4% to 5% shows reasonably good correlation with results obtained from other empirical and Mechanistic - Empirical approaches.

CHAPTER 4

**OPTIMIZATION OF BITUMINOUS PAVEMENT THICKNESS
USING STRAIN BASED DESIGN CRITERIA**

4.1   Introduction

The approach of pavement design conceptually dynamic and is changing with the advancement of knowledge in construction material, methodology and equipment. Empirical approach of pavement design has been changed in association with mechanistic approach to evolve the Mechanistic – Empirical [2]approach, which is now being widely practiced worldwide. The basic mechanism of design of thickness is based on the concept of limiting the stress, strain and deflection of constituents paving layers. Such layers are arranged in order of decreasing magnitude of elastic modulus from top to bottom. Subgrade is the foundation of pavement structure and therefore durability of pavement structure largely depends on the performance of the foundation on which it is supposed to transfer the load to the soil.

Premature failure of bituminous road pavement is a major concern in developing country like India due to lack of connectivity with remotest part of the geographically large country. Most of the roads in India are flexible pavement which carry lion's share of cargo and passenger traffic. Therefore the durability of pavement becomes important to reduce the life cycle cost of the pavement. In this context, formulation of reliable method for estimation of crust thickness of multilayered bituminous road is of primary importance. The reliability of the method of pavement design is important to predict required thickness of constituent layers in a pavement which can protect it from the failure under rutting as well as cracking. However, it is relevant to mention that the bituminous layer as binder or wearing course can be replaced easily by putting overlay on top of an existing road but the inadequacy in terms of thickness and strength of granular layers cannot easily be corrected after the construction of full depth pavement during its service life . Keeping this in view, present analysis, deals with formulation of a methodology based on mechanistic-empirical approach to determine the thickness of bituminous and granular layers in a flexible road pavement .In this backdrop, present study deals with development of an optimization method of thickness design for a three-layered conventional flexible pavement using Odemark's [126] method often known as method of equivalent thickness (MET) [52,60].

4.2   Literature review

Ghanizadeh (2016) [71] proposed an optimization framework aimed at determining the ideal setup and thickness of various pavement layers, aligning with the Iran Highway Asphalt Paving Code Number 234 (IHAP Code 234). By employing this optimization model, the paper establishes the optimal thickness for pavement layers on secondary rural roads, major rural roads, and freeways, referencing pricing data from Iran's 2015 "Basic Price List for Road, Runway and Railway." Additionally, the study develops charts to guide the determination of optimal pavement layer thickness, accounting for road classification, design traffic, and subgrade resilience modulus. Notably, the analysis reveals that under the 2015 material price conditions, the utilization of asphalt-treated layers in pavement structures lacks cost-effectiveness. Furthermore, it indicates that as the subgrade soil strength increases, it becomes feasible to eliminate the subbase layer from the optimal pavement structure.

Saridee et al. (2019) [158] developed a RBDO framework to assess a four-layered flexible pavement system, emphasizing optimal design considering fatigue and rutting performance while accounting for variability in design variables. The study highlights the significance of bituminous layer thickness and resilient modulus in fatigue failure, contrasting with their lesser impact on rutting. It suggests adopting a 95% reliability against both fatigue and rutting failures for pavement systems. A comparison between conventional and reliability-based methods indicates an overestimation of reliability levels by 10% – 40% in the conventional approach due to neglecting variability in independent layer modulus.

Rajbongshi et al. (2005) [144] presented a typical asphalt pavement design method based on the mechanistic-empirical approach which recommends multiple design alternatives for a given set of input values. Proposed method emphasizes the cost as well as the reliability levels of different design alternatives are different. A simple methodology has been suggested in this study to assist a pavement designer in selecting an optimal pavement design thickness which is cost effective and higher degree of reliability of pavement design. Design charts have been developed to illustrate the superiority of proposed methodology as an improvement over the deterministic design.

Maji et al. (2008) [111] proposed a simulation and analytical based methodology on variability of pavement design input parameters with different reliability level for various failure definitions of a given pavement. The primary objective of the study was to find out the reliability for a given pavement design method as well as to design a pavement with a given reliability level. The study has considered all the possible variations in input parameters for comparison between simulation and FOSM (First Order Reliability Method) method. A sensitivity study has been carried out with different design parameters on pavement reliability which emphasizes the thickness of bituminous surface layer to influence mostly the reliability. Finally considering different reliability level pavement design charts have also been presented.

Xiao-yan LI et al. [189] reported that the sensitivity analysis of performance for flexible pavement is crucial for optimizing design and performance evaluation. This research analyzed traffic and material parameters using MEPDG method, using computer-aided engineering simulation techniques such as LHS and multiple regression analysis. The single factorial sensitivity analysis method was used to calculate sensitivity and validate the results. Traffic parameters, such as Two-way AADT, Dual tire spacing, and Vehicle operational speed, were found to be more significant. The largest effects on rutting were due to Air Void--2, Air Void--1, Poisson' Ratio--1, and Poisson' Ratio--2, while cracking was affected by Air Void--1, Poisson' Ratio--1, and Efficient Binder Content--1.

Peddinti et al.(2017) [130] examined the efficacy of reliability-based design optimization techniques in flexible pavement design, utilizing suitable probability density functions (PDFs) for design parameters. The goal was to optimize the reliability index. The study revealed that PDFs might not be universally applicable, especially when dealing with high variability in data, such as that arising from the use of different materials in a multilayered system. Traditional distribution patterns may not adequately analyze such variability. Furthermore, the research found that the choice of PDF significantly impacts the reliability indices for fatigue and rutting failure modes. Consequently, the study suggests selecting PDFs based on thorough statistical analysis.

Tsiknas, A. et al. (2018) [179] carried out a study to propose a cost optimal design method by comparing Asphalt Institute method, British method

and Egnatia Odos (EO) methods. The design parameters considered in this study include traffic volume, subgrade soil strength and air temperature. From the study, the AI method was found to offer the lowest-cost design solution whereas British design method shows cost effective solution for comparatively heavy traffic loads with a poor subgrade soil. However, road with heavy traffic and good-quality subgrade, the EO method produced the lowest cost.

Narasimha al. (2001) [120] developed an optimization technique was devised to identify the most efficient flexible pavement section, considering both structural integrity and cost-effectiveness. This was achieved through the utilization of elastic layered analysis principles, facilitated by the software FPAVE. Two methods, direct search and gradient, were employed to refine the pavement design. Computer codes were created to calculate the optimal combination of thickness, streamlining the process and rendering traditional methods, such as manual iterative search and pavement design charts, obsolete.

Paola DallaValle et al. (2018) [52] presented a sensitivity analysis comparing asphalt and subgrade strains from the method of equivalent thicknesses (MET) with those calculated using BISAR software. Prediction of the values of strain (as well as life) calculated with BISAR from those obtained with the MET methodology is done using linear regression analysis. The analysis showed acceptable predictions for subgrade strains, but significant differences greater than ±10% exist for asphalt strains. An alternative model is proposed to improve MET methodology results for 3-layer pavement structures, providing a simple and efficient method for practical purposes like Pavement Management Systems and pavement deterioration simulations.

Qadir et al (2018) [140] Investigated and compared the performance of polymer-modified asphalt (PMA), polypropylene (PP)-fiber-modified, and neat asphalt mixes, on their rutting behavior and life cycle costs [18]. The study suggested that although the initial cost of other mixes is higher than the conventional asphalt mix. But considering the life cycle cost, the PMA mixes can be a better choice to limit rutting on the pavement. Moreover, a linear regression model was developed to depict the rutting behavior with temperature and polymer type.

L. Mu-yu et al (2003) [117] proposed a model based on these factors is established, using genetic algorithms (GAs) as an intelligent method. This

research presents a new idea and technique for asphalt pavement structure optimization, analyzing rutting and cracking causes and control methods. The practical model is established, and case studies show that GAs have strong searching ability, good efficiency, and precision compared to other techniques like random test and complex search methods. Further studies on rutting prediction and cracking estimation are needed to meet the development of this research.

K. A. Abaza et al (2003) [8] developed a new approach for designing flexible pavements focusing on anticipated pavement performance and its life-cycle cost. The future pavement condition, initial construction cost and maintenance and added user costs is affected by pavement performance, defined using the initial and terminal serviceability indices. This approach is applied to the AASHTO design method, which considers pavement life-cycle disutility, the ratio of pavement life-cycle cost to pavement performance. The optimum design is associated with the minimum terminal serviceability index value, which replaces the general AASHTO design index recommendations of 2.0 and 2.5 for minor and major roads, respectively. The performance curve is generated using an incremental solution of the AASHTO basic design equation, indicating that pavements should be designed for higher terminal serviceability index values than currently recommended.

M. Sanchez-Silvaet al (2005) [156] presented a model for optimizing flexible asphalt pavement structures, considering fatigue damage and granular material degradation caused by repetitive loading cycles. Mechanical considerations are combined with construction and rehabilitation costs, as well as financial factors like discount rates. An illustrative example has been selected to demonstrates that reliability-based design optimization (RBDO) combined with a long-term maintenance policy produces appropriate integral designs.The proposed procedure offers advantages in predicting pavement deterioration and maintenance.

Sahis et al. (2021) [27] proposed a Mechanistic-Empirical method to determine the optimum thickness of bituminous and granular layer using Rutting and fatigue as model of failure for pavement. The study is focused on a three layered flexible pavement system. Vertical compressive strain and radial tensile strain in a three layered pavement system was considered for estimation of

optimum layer thicknesses. The study reveals that typical combination of bituminous and granular layer thickness is possible to safeguard the pavement against rutting and fatigue. The deflection of the pavement which predicts its performance was obtained by proposed method which shows good convergence against deflection from IITPAVE and KENPAVE.

Ghosh et al (2005) [73] developed a computational schemes for deterministic and probabilistic analyses of flexible pavement, including their FORTRAN codes. The deterministic analysis is based on the Mechanistic-Empirical (M-E) approach, as recommended in IRC: 37-2001. The developed computer program can check allowable fatigue and rutting strains for a given pavement section and develop a flexible pavement design chart for Subgrade, traffic, and Annual Average Pavement Temperature (AAPT) data. The probabilistic computation scheme uses the Mean-value First Order Second Moment (MFOSM) method of reliability analysis, while all basic system parameters are random variables. It has been observed that the design of a section based on deterministic basis could be quite misleading on applying program "FPAVE_REL" A sensitivity analysis was conducted to investigate the effects of variation of system parameters on the probability of failure for a given pavement section. The probability of failure is highly sensitive to the regression coefficients of the fatigue and rutting equations recommended in IRC: 37-2001.

Mansour Tohidi et al (2021) [177] developed an appropriate pavement thickness design with minimum possible cost is required since road pavements consume a significant portion of the financial resources of construction costs. This study compares the effectiveness of genetic algorithm and particle swarm optimization in determining the optimal pavement thickness design for road pavements. The software for implementing these algorithms and the simulation-optimization model were developed. Nine completed projects in Khuzestan, Southwestern Iran, were evaluated using the manual design approach of consulting engineers. The results showed that GA and PSO reduced design costs by 9-26.5% and 5-25%, respectively, compared to manual design. GA outperformed PSO by 1-5.5% in cost savings.

A. Pryke et al (2006) [136] analysed that as the existing methods do not explicitly include optimization processes, allowing for different criteria and objectives the study proposed a prototype system that optimizes an analytical

pavement design procedure using a genetic algorithm. This approach is flexible and can be used for any computerized pavement design method. The results are comparable to those from a well-known method, making it suitable for any type of road pavement and incorporating more complex optimization procedures.

Amakye et al (2022) [15] revealed that the thickness of road pavement and the depth of construction play pivotal roles in determining road construction expenses. To mitigate these costs, it is imperative to enhance the engineering properties of subgrades, such as the California bearing ratio (CBR). This investigation focused on optimizing road pavement thickness and construction depth based on CBR values. Incorporating expansive subgrades treated with 8% lime and 20% cement enhanced their engineering properties, rendering them suitable for road construction. The study scrutinized the characteristics, mineral structure, Atterberg limit, compaction, CBR, swell, and micro structural properties of expansive subgrades. The findings indicated a correlation between an increase in CBR value and a reduction in pavement thickness and construction depth. The treated samples exhibited CBR values exceeding 2%, thus rendering them viable for road construction. Moreover, a decrease in swell potential of up to 0.04% was observed for the treated expansive subgrade. In conclusion, augmenting subgrade materials and employing cement and lime as binders can effectively diminish pavement thickness and construction depth.

Deepthi et al (2023) [56] demonstrated that the reliability-based designs have gained acceptance in the pavement engineering community for sustainable and long-lasting structures. A reliability Based Design Optimization (RBDO) approach is formulated to design cost-effective flexible pavements in the presence of uncertainties. This study considers two meta-modeling approaches: the second-order adaptive Response Surface Model (RSM) and the adaptive Polynomial-Chaos based Kriging (PC-Kriging) meta-model. The study also highlights the need for adaptive meta-modeling techniques in reliability-based pavement structures, quantifying epistemic uncertainty. The model uncertainty was found to be around 1% for three-layer sections and below 2.5% for four-layer pavements. The SRBDO approach is also proposed to address the correlation between pavement failure modes and design the optimum combination of pavement layer thicknesses and moduli to meet target levels of reliability. The methodology integrates economic analysis of various pavement

design alternatives with the Mechanistic-Empirical procedure in a system reliability framework. Finally, the validation of the methodology is confirmed through crude Monte Carlo simulations to ensure that target system reliability levels align with established literature bounds.

4.3   Objective

In this backdrop , present study   deals with   development of   an optimization method for estimation of thickness in a three layer conventional flexible pavement using method of equivalent thickness (MET) [52,60].

4.3.1   Formulation of the present model
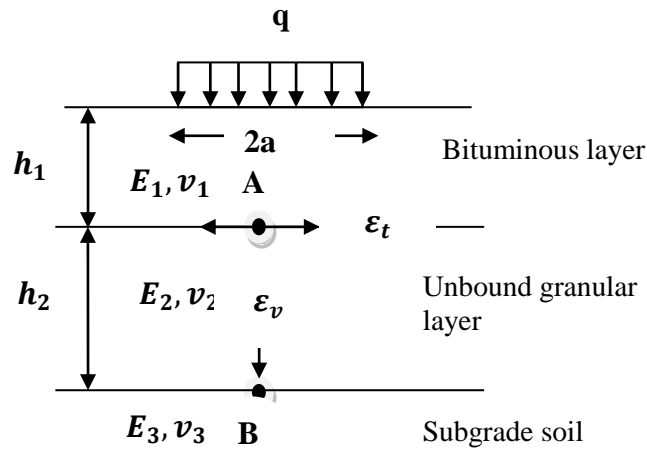
Figure 4.0 Typical flexible pavement section in a three-layer system.

In this study, the pavement system has been characterized as a three layered system. The top layer consist of bituminous layer with thickness h_1 and resilient modulus E_1, resting on a granular layer with thickness h_2 and elastic modulus of E_2, which has been shown in Figure 4.0. The pavement crust in the form of bituminous layer and the granular layer rest on a subgrade which is the foundation of the pavement, with an elastic modulus of E_3

In this section , the elastic modulus of granular layer (E_2) has been obtained using Equation 4.1 as recommended by Powell et al [131] whereas the elastic modulus (E_3) of subgrade soil has been estimated using   in Equation 4.2 and Equation 4.3 [131,154]

$E_2 = 0.2 \text{ x } (h_2)^{0.45}E_3 \text{ (MPa)}$ (4.1)

Where h_2 = thickness of granular layer in mm.

$E_3 = 10$ CBR (MPa) for CBR $\leq 5\%$. (4.2)

$E_3 = 17.6$ (CBR)$^{0.64}$ (MPa) if CBR $> 5\%$ (4.3)

Where, CBR is the California bearing ratio of subgrade.

In this study, a tyre pressure (q) of 0.56 MPa has been assumed to act on circular area of diameter (2a) as 310 mm for a dual wheel load of 40 kN.

The thickness of bituminous layer against cracking in a bituminous pavement is determined on the basis of radial tensile strain which occurs at the bottom of bituminous layer at point A in Figure 4.0. The thickness of bituminous layer with its required elastic modulus, limits the radial tensile strain at the interface of bituminous layer and granular base. The strain based design criterion has been recommended in IRC -37:2012 [48] to consider the failure of pavement under cracking as in Equation 4.4.

$$N_f = 2.21 \times 10^{-04} \times \left[\frac{1}{\epsilon_t}\right]^{3.89} \times \left[\frac{1}{M_R}\right]^{0.854} \quad (4.4)$$

N_f = Fatigue life in number of cumulative standard axles.

ϵ_t = Maximum tensile strain at the bottom of bituminous layer.

M_R = Resilient modulus of the bituminous layer (MPa)

Similarly, the total thickness of bituminous layer, and granular layer against rutting has been determined on the basis of vertical compressive strain, which occurs on the top of subgrade at point B in Figure 4.0.The increase in pavement crust thickness with higher elastic modulus reduces the vertical compressive strain at the interface of granular layer and soil subgrade. However, due to the aging of pavement, the reduced elastic modulus of constituent layers increases the vertical compressive strain on top of subgrade thereby reducing the remaining life of the pavement under rutting. The correlation between vertical compressive strain and anticipated wheel load repetitions before failure of pavement in terms of rutting has been considered in Equation 4.5 as recommended in IRC -37:2012 [48] .

$$N = 1.41 \times 10^{-08} \times (\epsilon_v)^{-4.5337} \quad (4.5)$$

Where, N = Number of cumulative standard axle repetitions before rutting failure.

ϵ_v = Maximum vertical compressive strain on the top of subgrade.

4.3.2 Odemark's Transformation

In the present work, the three layer system has been transformed into a homogeneous system by application of Odemark's [126] method [181] as described earlier in Chapter 3 and Chapter 4.

In the present analysis, if the Poisson's ratio of the pavement layers are considered equal i.e. $v_2 = v_1$ the equivalent layer thickness of first layer may be expressed as shown in Equation 4.6.

$$h_{eq1} = f\,h_1\sqrt[3]{\frac{E_1}{E_2}} \tag{4.6}$$

However, using the value of E_2 as explained in Equation 4.1 and considering the value of f, the Odemark's [126] correction factor for bituminous base–granular base interface as 0.9 with Poisson's ratio as 0.35, Equation 4.6may further be simplified as in Equation 4.7.

$$z_1 = h_{eq1} = 0.9 \times h_1\sqrt[3]{\frac{E_1}{0.2\,h_2{}^{0.45}E_3}} \tag{4.7}$$

where, $z_1 = h_{eq1}$ = Equivalent depth of layer –I with modulus E_2 in the pavement

The basic principle of transformation of two layer system as recommended by Odemark [126] can be used to transform multilayered system in to a homogeneous one by successive transformation.

In such case, the equivalent thickness of h_{eq2}, which represents equivalent section of layer- I and II with modulus E_3,   may be determined using Equation 4.8 below.

$$h_{eq2} = z_2 = f_1\left(f\,h_1\sqrt[3]{\frac{E_1}{0.2h_2{}^{0.45}E_3}} + h_2\right) \times \sqrt[3]{\frac{0.2h_2{}^{0.45}E_3}{E_3}} \tag{4.8}$$

Where f_1 is the Odemark's correction factor for subgrade – base interface, which has been considered as 0.8 as recommended by Sherif, M et al[60].

4.3.3 Model based on fatigue failure

The Boussinesq's equation for uniformly distributed load has been used in this analysis to determine the fatigue strain (ε_t) and rutting strain(ε_v) in different points in a multi layered system by appropriate transformation of layers in to a homogeneous system using Odemark's approach. According to

Boussinesq's theory, the radial strain at a depth (z) in a homogenous, elastic and isotropic medium due to an uniform circular load acting at surface with contact radius (a) and load intensity (q) may be obtained using Equation 4.9. However , in Equation 4.9 the value of (z) has been considered as the equivalent depth (h_{eq1}) with an elastic modulus of (E_2) for the transformed section for determination of radial strain.

$$\epsilon_t = \frac{(1+\upsilon)q}{2E_2}\left[\frac{-\frac{z}{a}}{\left\{\sqrt{1+\left(\frac{z}{a}\right)^2}\right\}^3} - (1-2\upsilon) \times \left\{\frac{\frac{z}{a}}{\sqrt{1+\left(\frac{z}{a}\right)^2}} - 1\right\}\right] \qquad (4.9)$$

It is to be noted that Odemark's method of equivalent layer thickness (MET) [52,60] has also been widely used for pavement response analyses (Ullidtz 1987 [181]) and FWD back calculation. Ullidtz (1987) [181] reported pavement responses in terms of stress, strain and deflection calculated by the method of equivalent thickness using Boussinesq's [34] equation   are in good agreement with those calculated for the same pavement section with the CHEVRON (Elsym5) [181] computer program. The results obtained with MET [52,60] method were reported to vary between 89% and 92% of the values obtained from the theory of elasticity based analysis [52,60]. Zhang and Macdonald (2000) [194] concluded that for the horizontal strains at the bottom of the asphalt layer, the calculated values with all three methods namely Odemark's method (MET) [52,60], the linear elastic method [87,88] (LET) and the Finite element method (FEM) could be seen to match the measured values. Despite of its simplification, the MET used in this analysis has been found efficient enough to predict the strains and stresses in pavement layers.

In this context, the analytical solution of Equation 4.4, Equation 4.7 and Equation 4.9 has been made in this analysis to develop correlation between bituminous layer thickness (h_1) and granular layer thickness (h_2) with respect to failure under cracking . The results obtained from proposed analysis have been presented   through Figure 4.2 to Figure 4.49 and Table 4.1 to Table 4.8 (Appendix 3A)   for a variation of axle load from 5 msa to 50 msa considering effective subgrade CBR range between 5% to 15%. The resilient modulus of bituminous mix (E_1) has been considered in this analysis as 3000 MPa as recommended in IRC:37-2018 [51] for use of Bituminous Concrete (BC) and

Dense Bituminous Macadam (DBM) as binder course with VG40 bitumen at 35°C.

4.3.4   Model based on rutting failure

In order to determine the vertical compressive strain at point B as shown in Figure 4.0, the top two layers of the pavement with thickness (h_1) and (h_2) in a three layer system has been suitably transformed as in Equation 4.8. The vertical compressive strain at point B , at a depth (z) due to an uniform circular load acting at surface with contact radius (a) and load intensity (q) in an elastic homogeneous medium can be determined using Boussinesq's corelation as given in Equation 4.10. However , in Equation 4.10 the value of (z) has been considered as the equivalent depth $\left(h_{eq2}\right)$ with an elastic modulus of (E_3) for determination of vertical strain on top of subgrade .

$$\epsilon_v = \frac{(1+\upsilon)q}{E_3}\left[\frac{\frac{z}{a}}{\left\{\sqrt{1+\left(\frac{z}{a}\right)^2}\right\}^3} - (1-2\upsilon) \times \left\{\frac{\frac{z}{a}}{\sqrt{1+\left(\frac{z}{a}\right)^2}} - 1\right\}\right] \quad (4.10)$$

The analytical solution of Equation 4.5, Equation 4.8 and Equation 4.10 has been used in this study to develop correlations between bituminous layer thickness (h1) and granular layer thickness (h_2) against rutting which has been presented through Figure 4.2 to Figure 4.49 and Table 4.1 to Table 4.8 (Appendix 3A).   In present analysis, axle load range between 5 msa to 50 msa and the effective subgrade CBR between   5% to 15% were considered. In this study, the range of trial bituminous layer thicknesses (h_1) has been considered from 50 mm to 320 mm as indicative value. The values of trial bituminous layer thickness (h_1) has been used to determine the thickness of unbound granular layer (h_2) using present analytical approach.

The curves shown in Figure 4.2 to Figure 4.49 show the variation of bituminous layer thickness (h_1) and granular layer thickness (h_2) with respect to failure of pavement under cracking as well as rutting, with a point of intersection. Therefore, the coordinates of such intersection point will be the optimum thickness of bituminous (h_1) and granular layer (h_2) satisfying both rutting and cracking criteria for specified axle load repetitions on different subgrade. The thickness obtained using the present approach has been termed in

this paper as optimized pavement thickness. Flow diagram of adopted methodology for optimization of pavement thickness based on MET has been shown in Figure 4.1
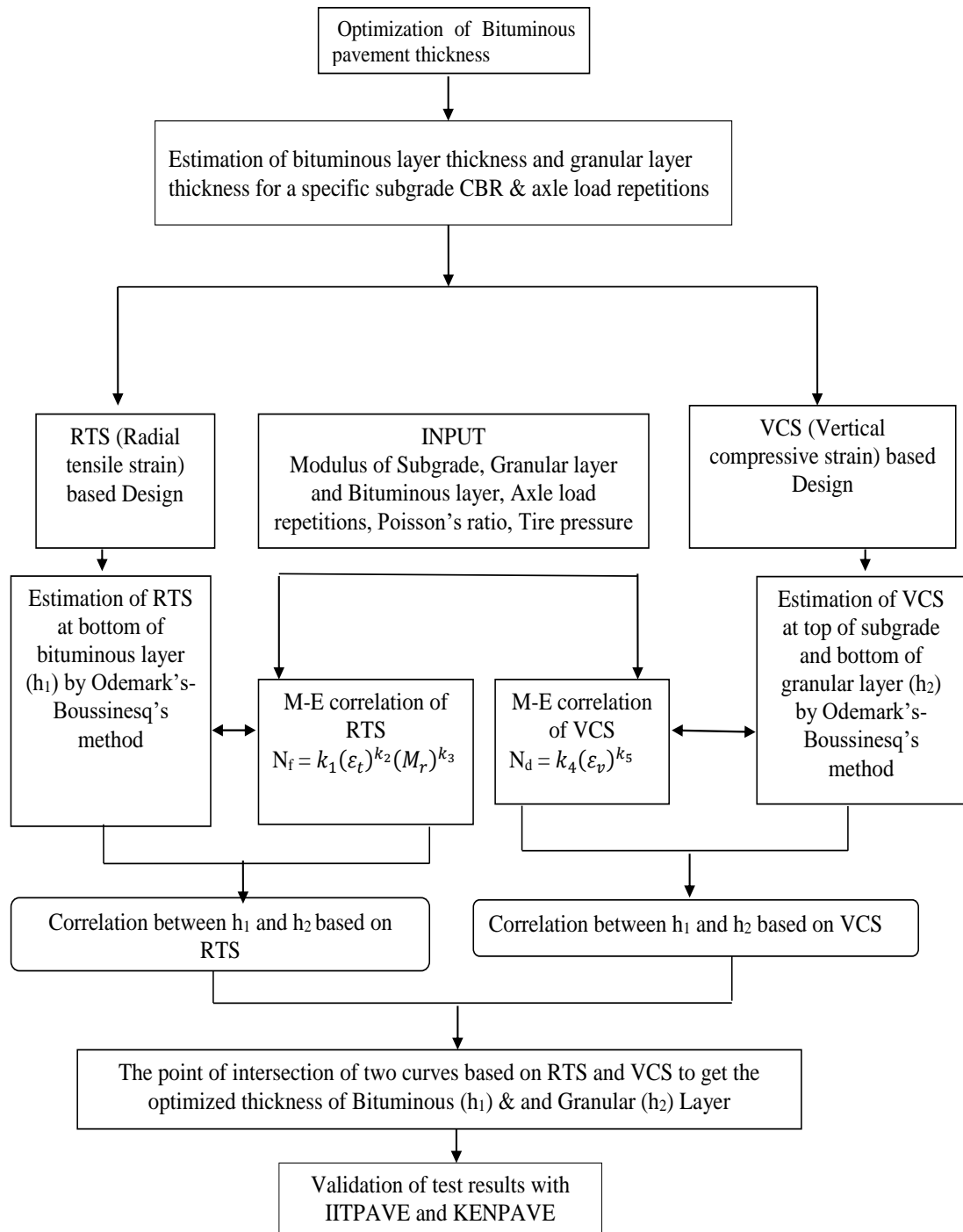
Figure 4.1: Flow diagram of adopted methodology for optimization of pavement thickness based on MET

4.4   Results and Discussion

It has been found from present analytical study that the thickness of granular layer increases with decrease in bituminous layer thickness and vice versa for a specified axle load repetition against rutting as well as fatigue failure. However, it is relevant to note that the gradient of the curve showing the variation for thickness of bituminous and granular layer under rutting is significantly higher than that of cracking. But the correlation between bituminous and granular layer under cracking show that the change in required bituminous layer thickness becomes insignificant after the granular layer thickness of 150 mm or more. The trend of variation of thickness in the curve obtained for fatigue thus indicates the reason of variation of granular layer thickness as more sensitive under rutting. In this backdrop, the optimized thickness of bituminous and granular layer has been obtained from the coordinates of the intersection point of the curves under rutting and cracking as shown in Figure 4.2 to Figure 4.49. The thickness of optimum pavement section thus obtained is safe both under rutting and cracking for a specified axle load repetitions for a given soil subgrade. It can be observed that the rate of change of bituminous layer thickness remains almost constant with the variation of granular layer thickness irrespective of change in effective CBR and load repetitions.   Whereas rate of change in granular layer thickness becomes constant beyond 150 mm of bituminous layer thickness corresponding to 5% effective CBR and load repetitions of 5 msa. Similar trend has also been observed for 15% effective CBR and 50 msa load repetitions. In this case , the rate of change of granular layer becomes insignificant beyond 120mm of bituminous layer thickness. In present analysis, MATHEMATICA programming language has been used solve all equations.
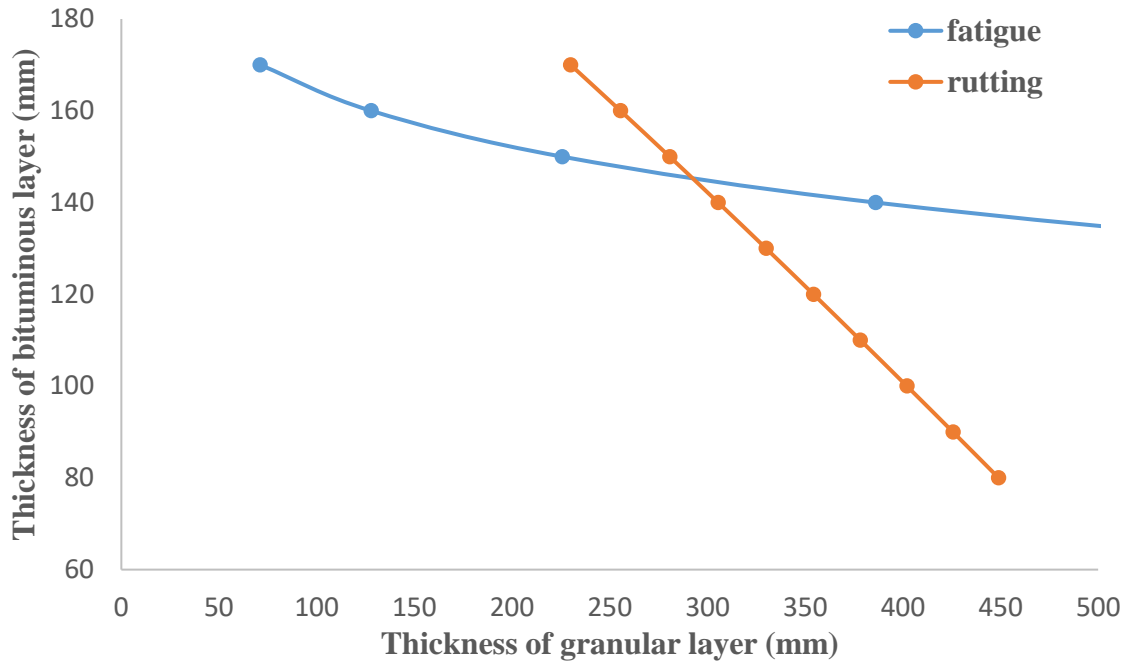
Figure 4.2 : Variation of bituminous layer and granular layer thickness under fatigue and rutting for 5 % subgrade CBR with 5 msa axle load repetitions
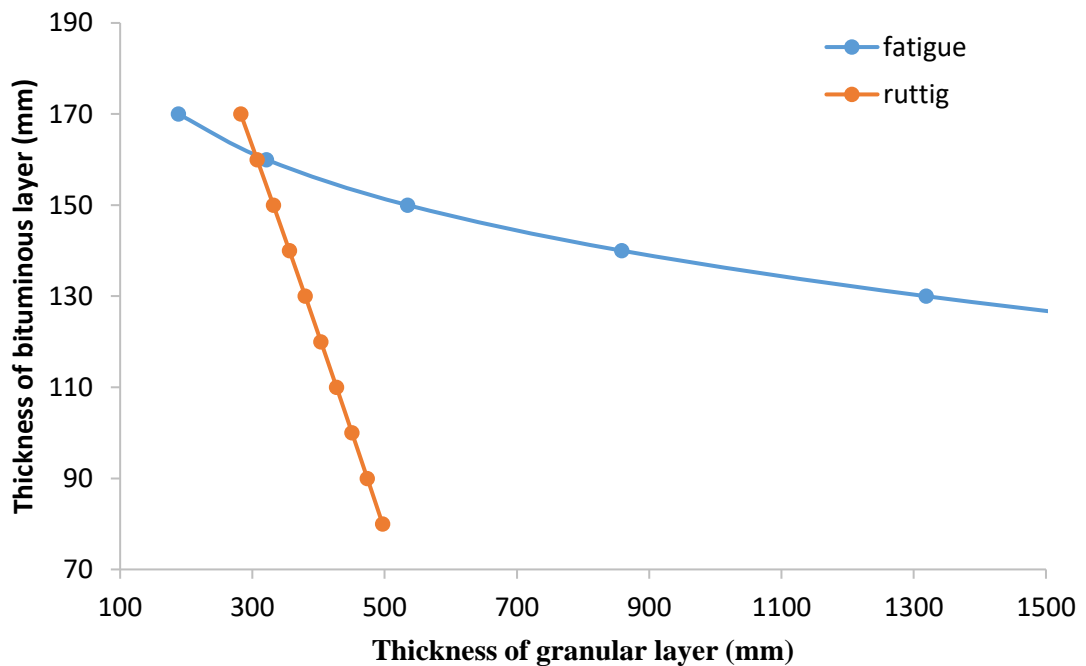
Figure 4.3 : Variation of bituminous layer and granular layer thickness under fatigue and rutting for 5 % subgrade CBR and 10 msa axle load repetitions
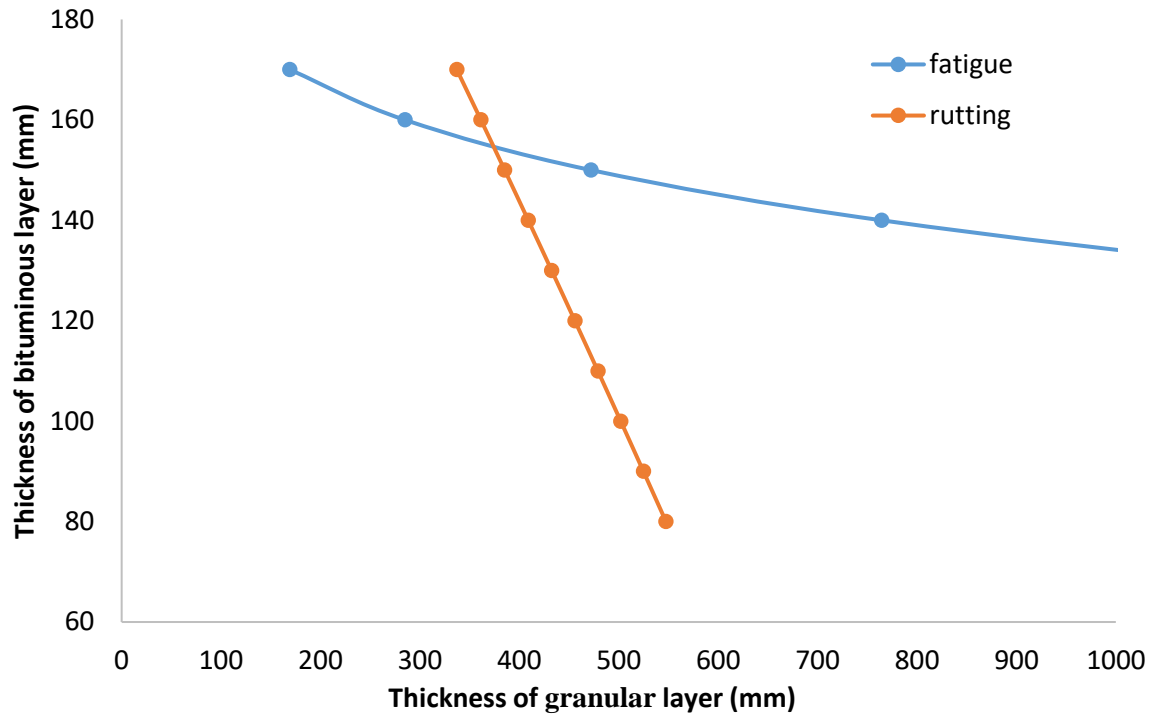
Figure 4.4 : Variation of bituminous layer and granular layer thickness under fatigue and rutting for 5 % subgrade CBR and 20 msa axle load repetitions
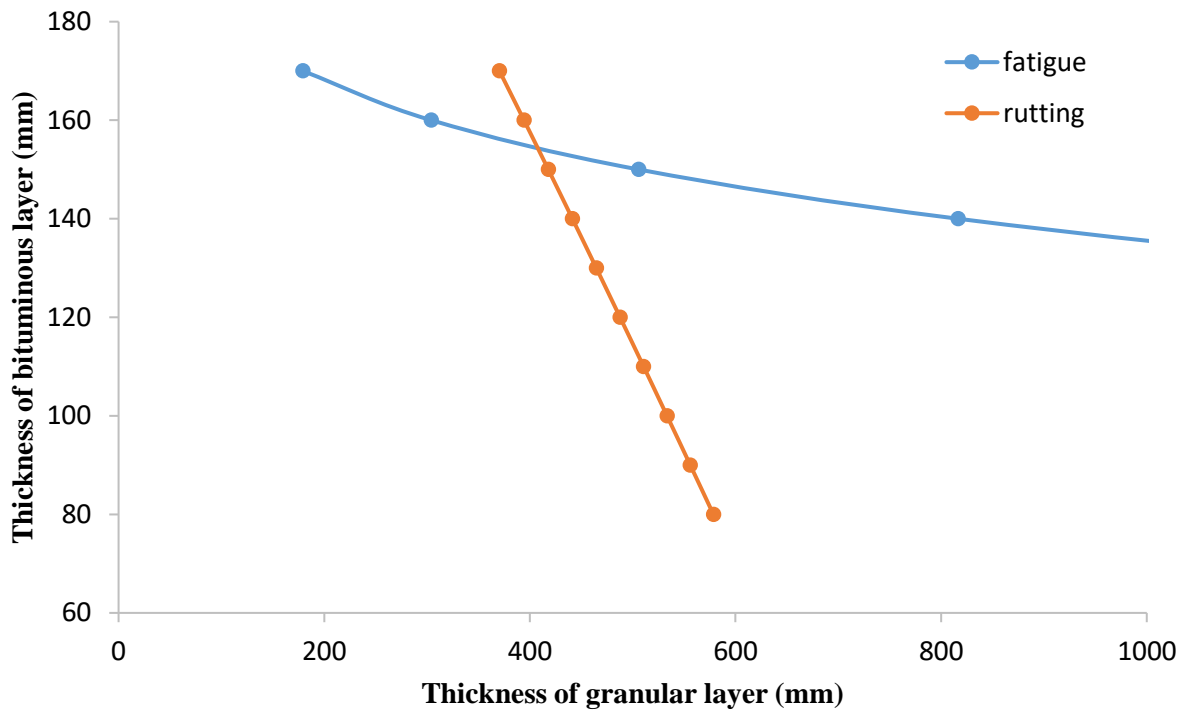
Figure 4.5: Variation of bituminous layer and granular layer thickness under fatigue and rutting for 5 % subgrade CBR and 30 msa axle load repetitions

130
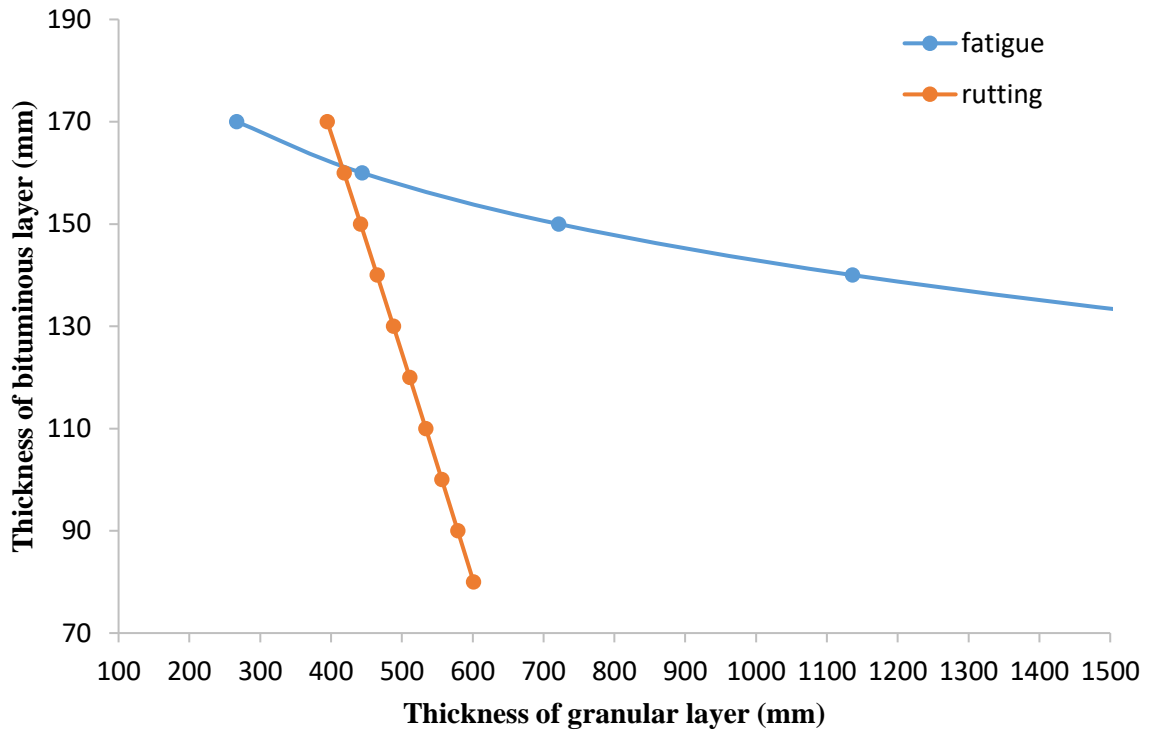
Figure 4.6 : Variation of bituminous layer and granular layer thickness under fatigue and rutting for 5 % subgrade CBR and 40 msa axle load repetitions
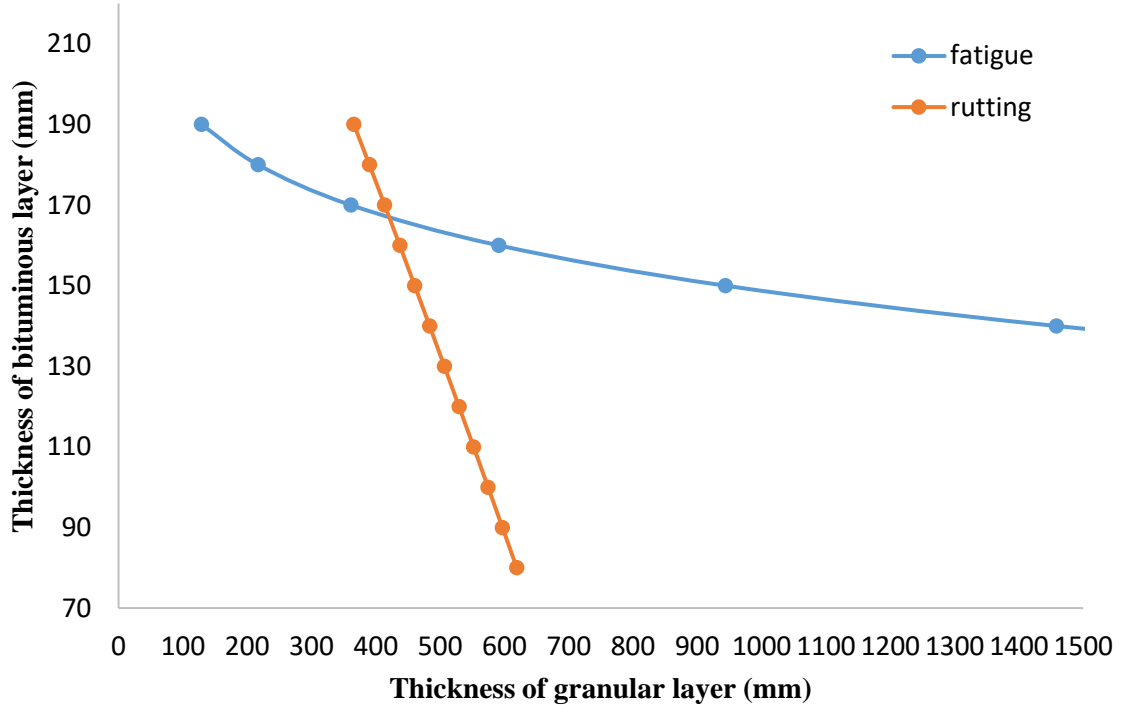
Figure 4.7 : Variation of bituminous layer and granular layer thickness under fatigue and rutting for 5 % subgrade CBR and 50 msa axle load repetitions
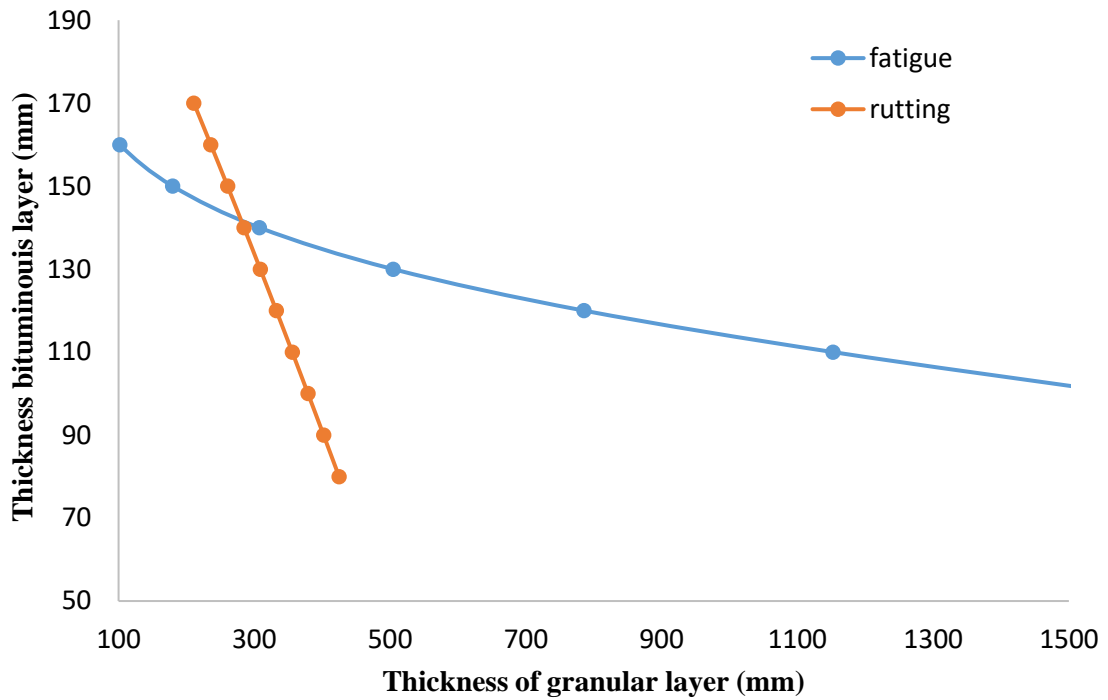
Figure 4.8 : Variation of bituminous layer and granular layer thickness under fatigue and rutting for 6 % subgrade CBR and 5 msa axle load repetitions
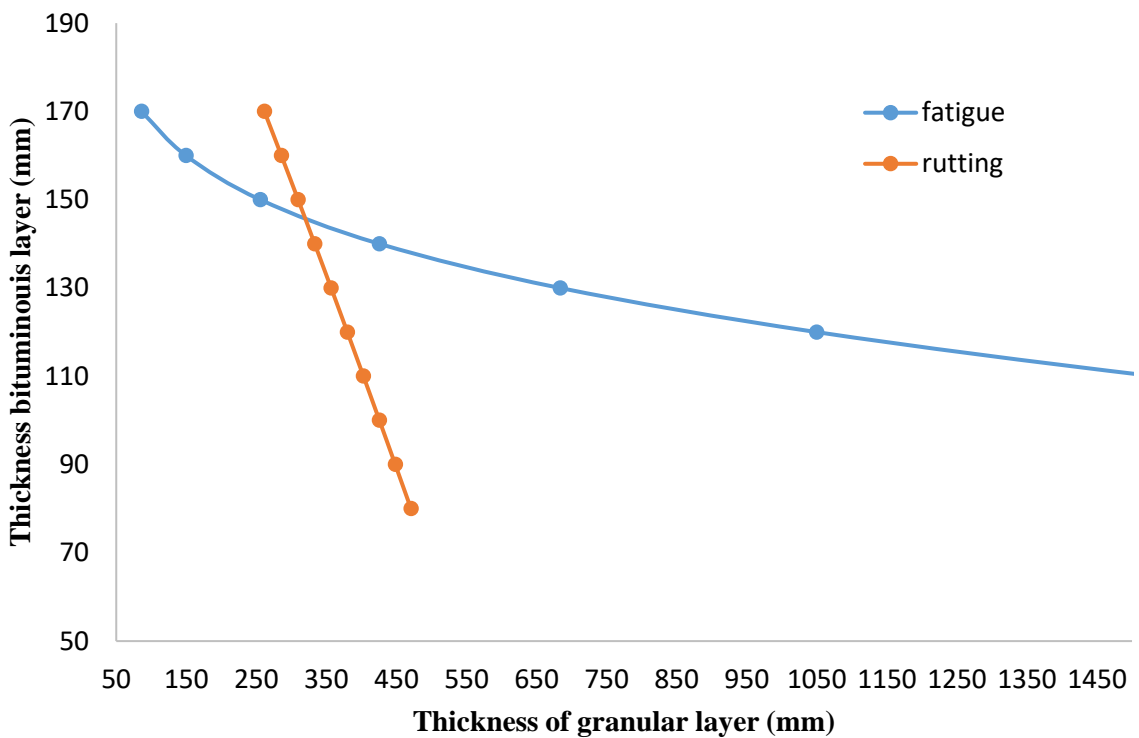
Figure 4.9 : Variation of bituminous layer and granular layer thickness under fatigue and rutting for 6 % subgrade CBR and 10 msa axle load repetitions

132
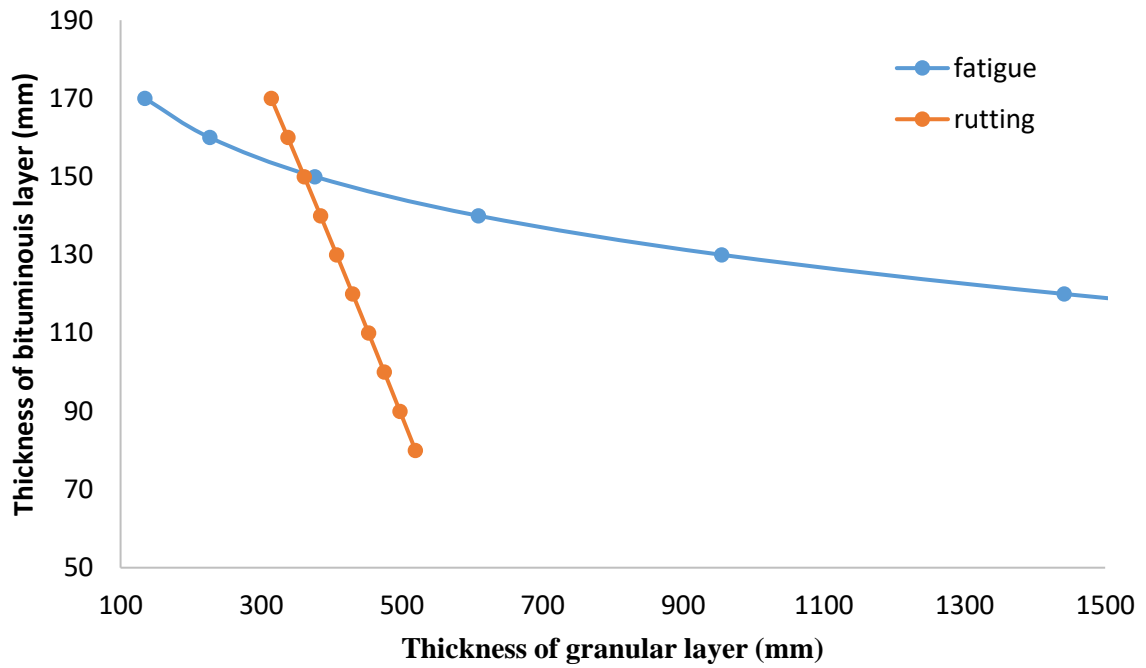
Figure 4.10 : Variation of bituminous layer and granular layer thickness under fatigue and rutting for 6 % subgrade CBR and 20 msa axle load repetitions
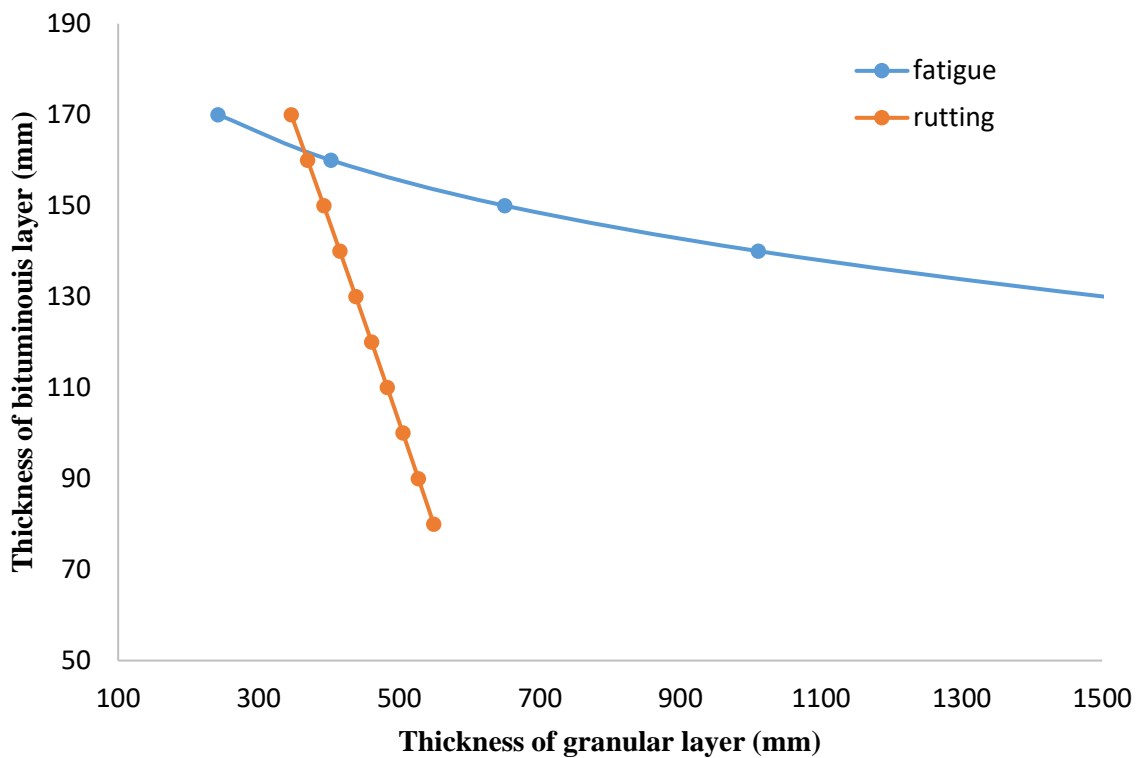
Figure 4.11 : Variation of bituminous layer and granular layer thickness under fatigue and rutting for 6 % subgrade CBR and 30 msa axle load repetitions
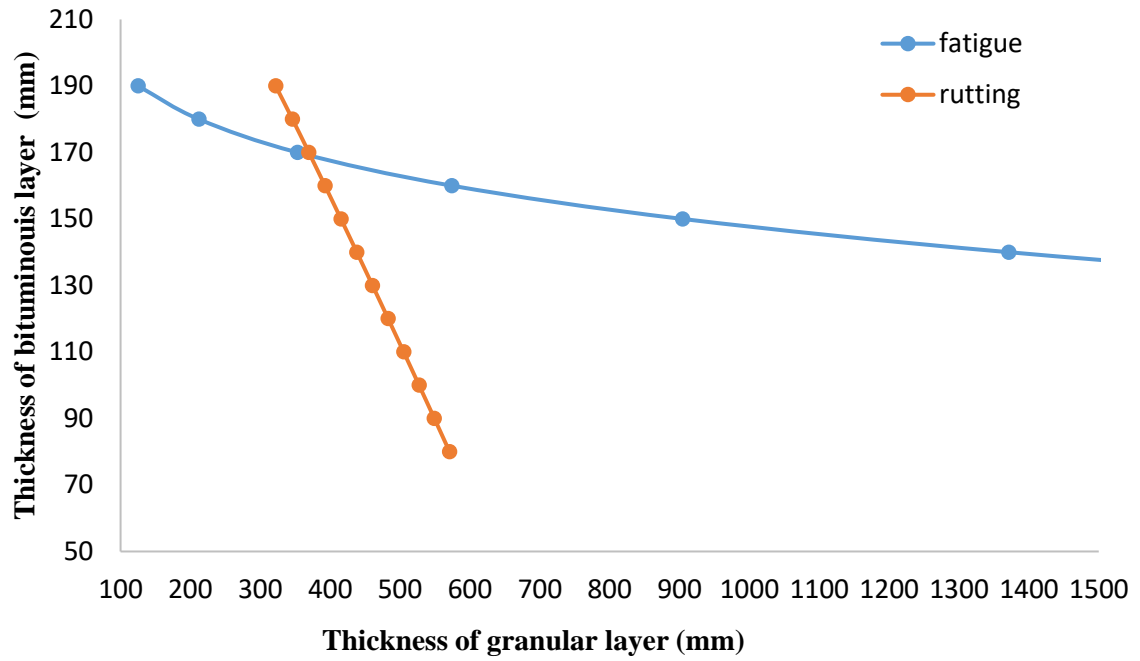
Figure 4.12 : Variation of bituminous layer and granular layer thickness under fatigue and rutting for 6 % subgrade CBR and 40 msa axle load repetitions
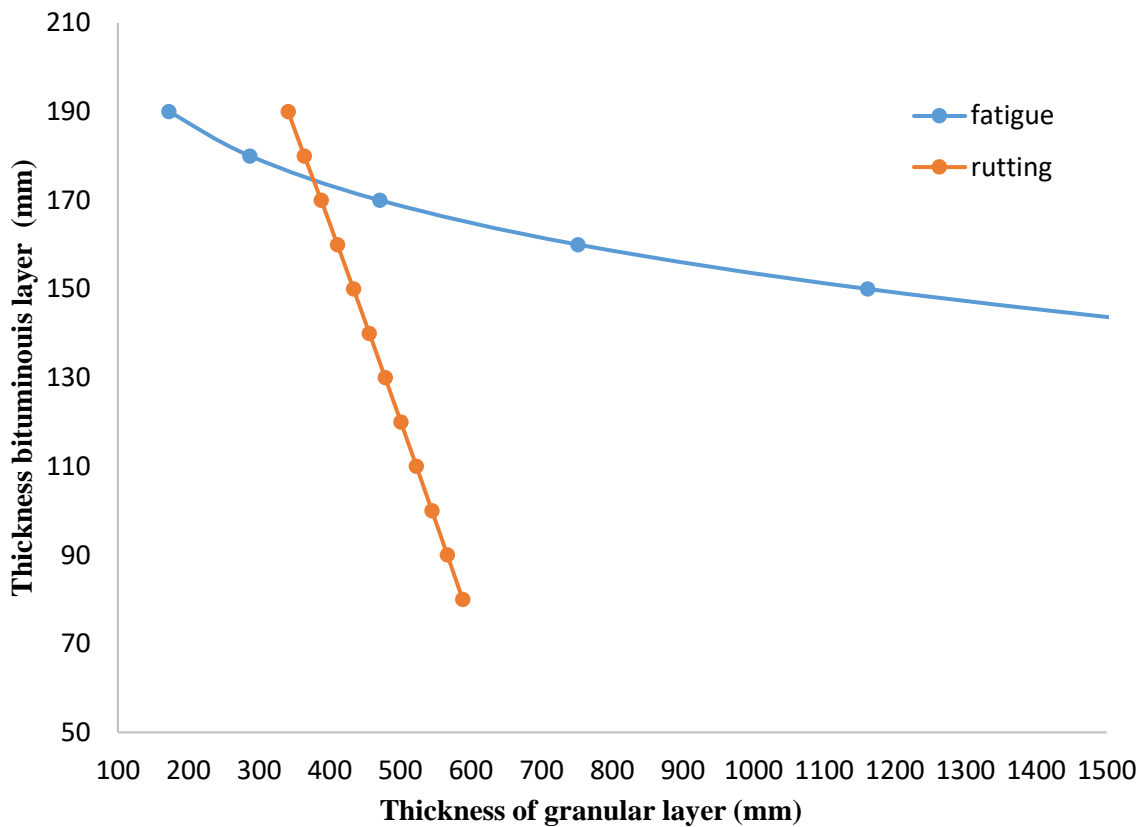
Figure 4.13 : Variation of bituminous layer and granular layer thickness under fatigue and rutting for 6 % subgrade CBR and 50 msa axle load repetitions
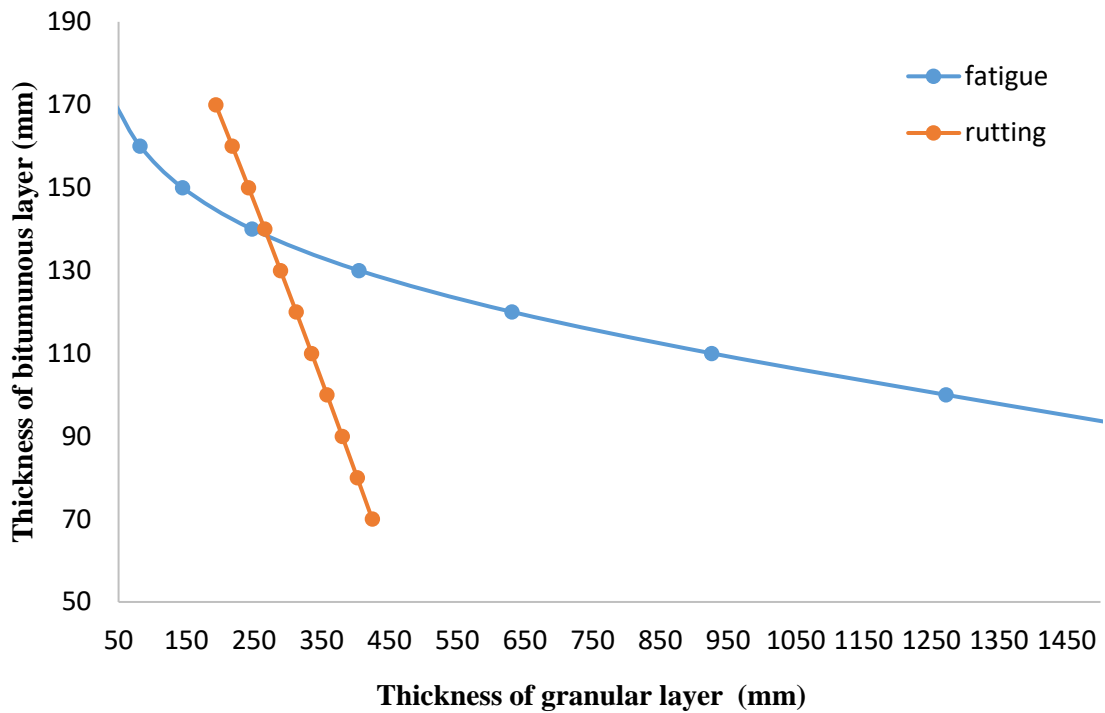
Figure 4.14: Variation of bituminous layer and granular layer thickness under fatigue and rutting for 7 % subgrade CBR and 5 msa axle load repetitions
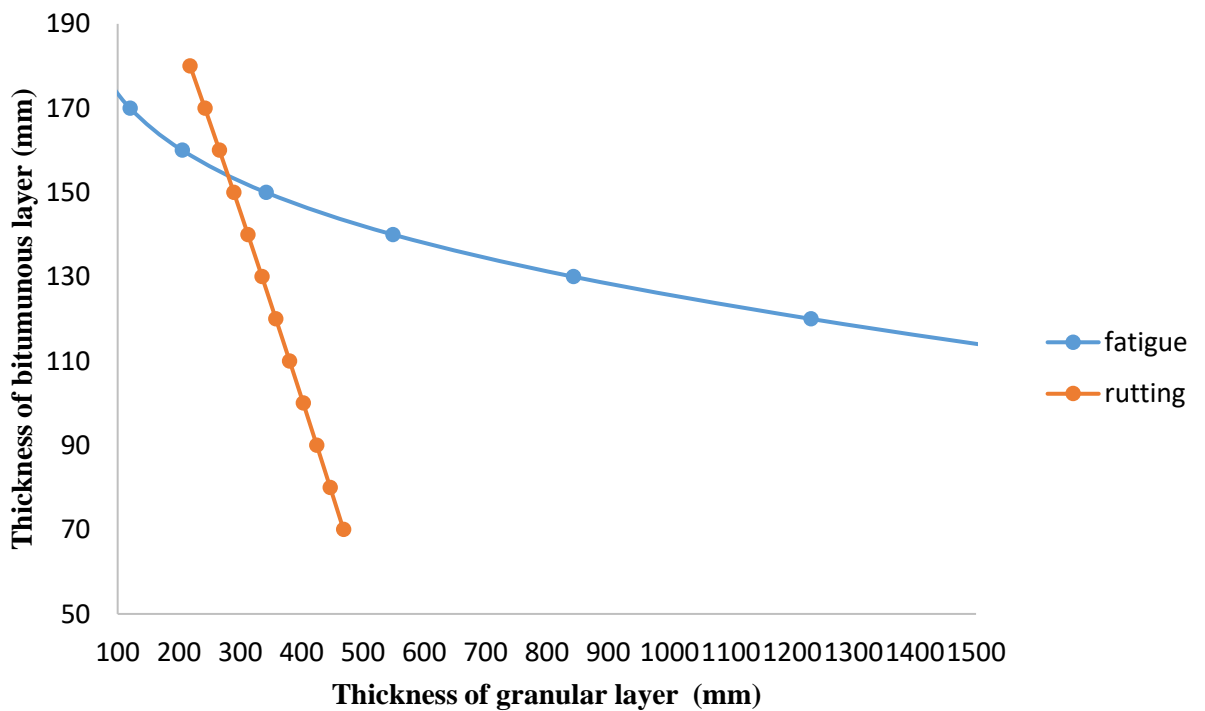
Figure 4.15: Variation of bituminous layer and granular layer thickness under fatigue and rutting for 7 % subgrade CBR and 10 msa axle load repetitions

135
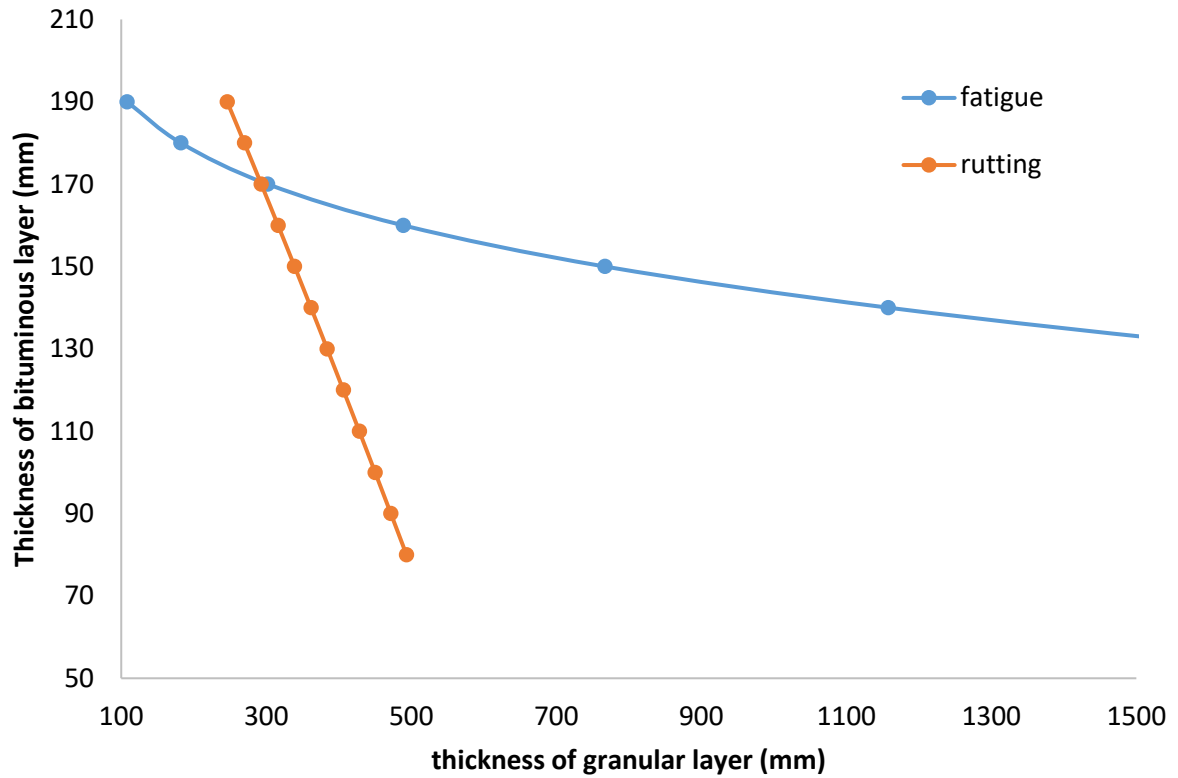
Figure 4.16: Variation of bituminous layer and granular layer thickness under fatigue and rutting for 7 % subgrade CBR and 20 msa axle load repetitions
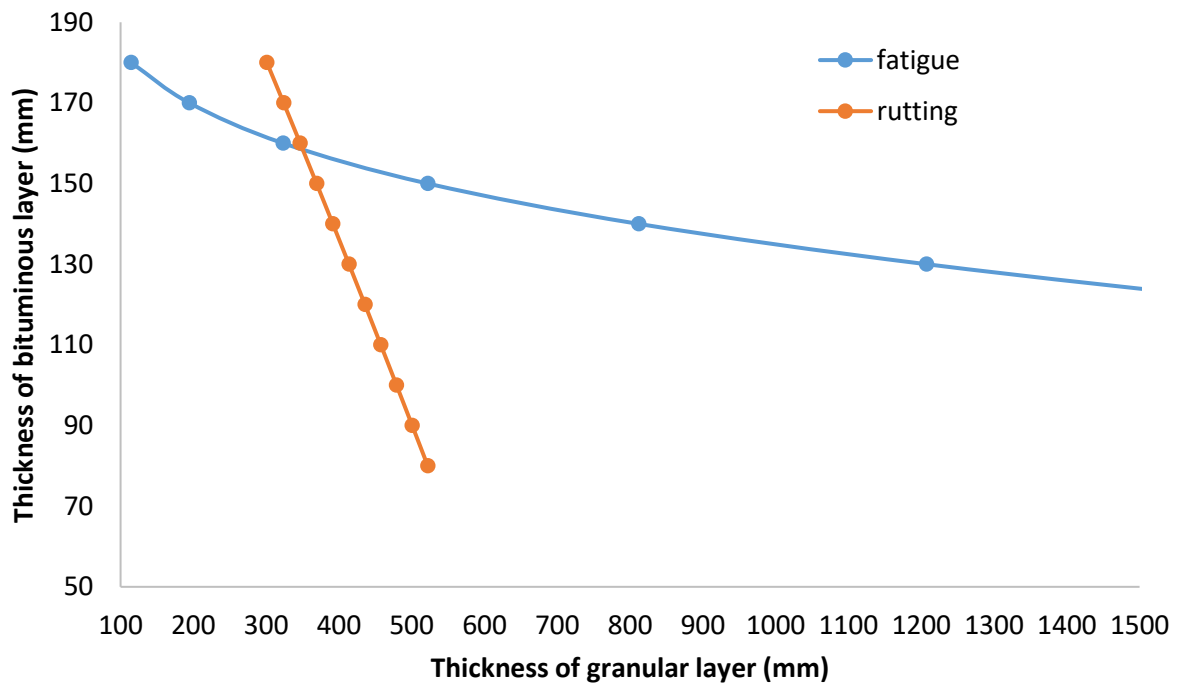
Figure 4.17: Variation of bituminous layer and granular layer thickness under fatigue and rutting for 7 % subgrade CBR and 30 msa axle load repetitions
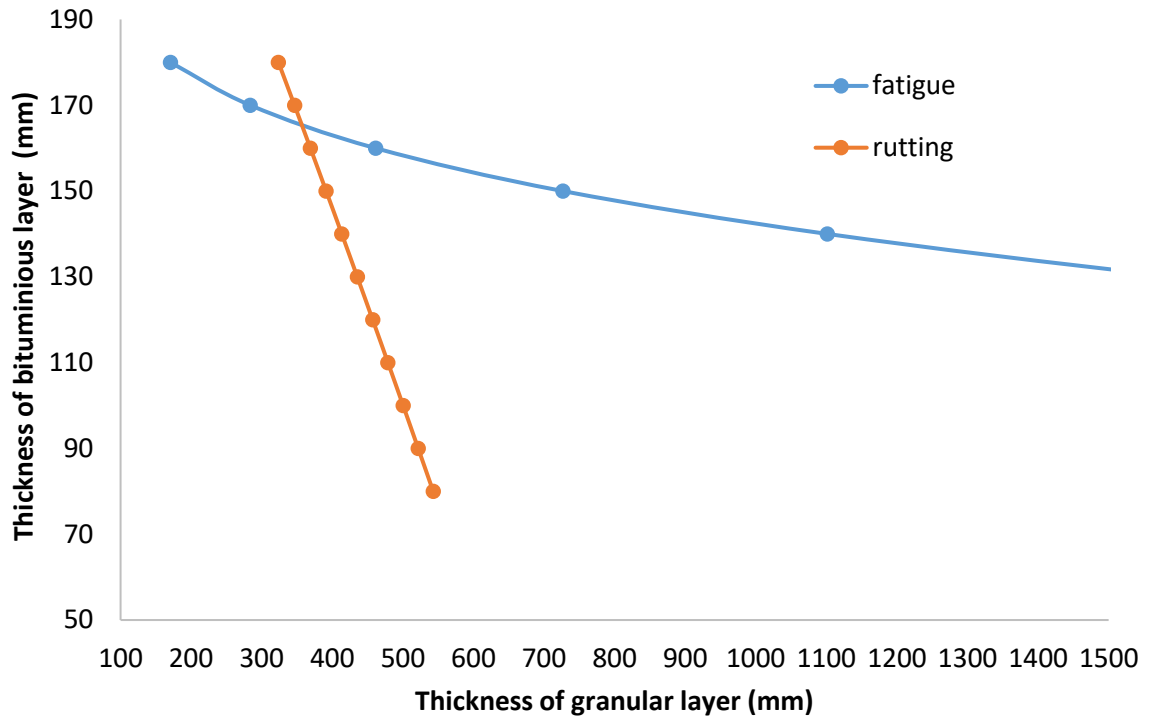
Figure 4.18 : Variation of bituminous layer and granular layer thickness under fatigue and rutting for 7 % subgrade CBR and 40 msa axle load repetitions
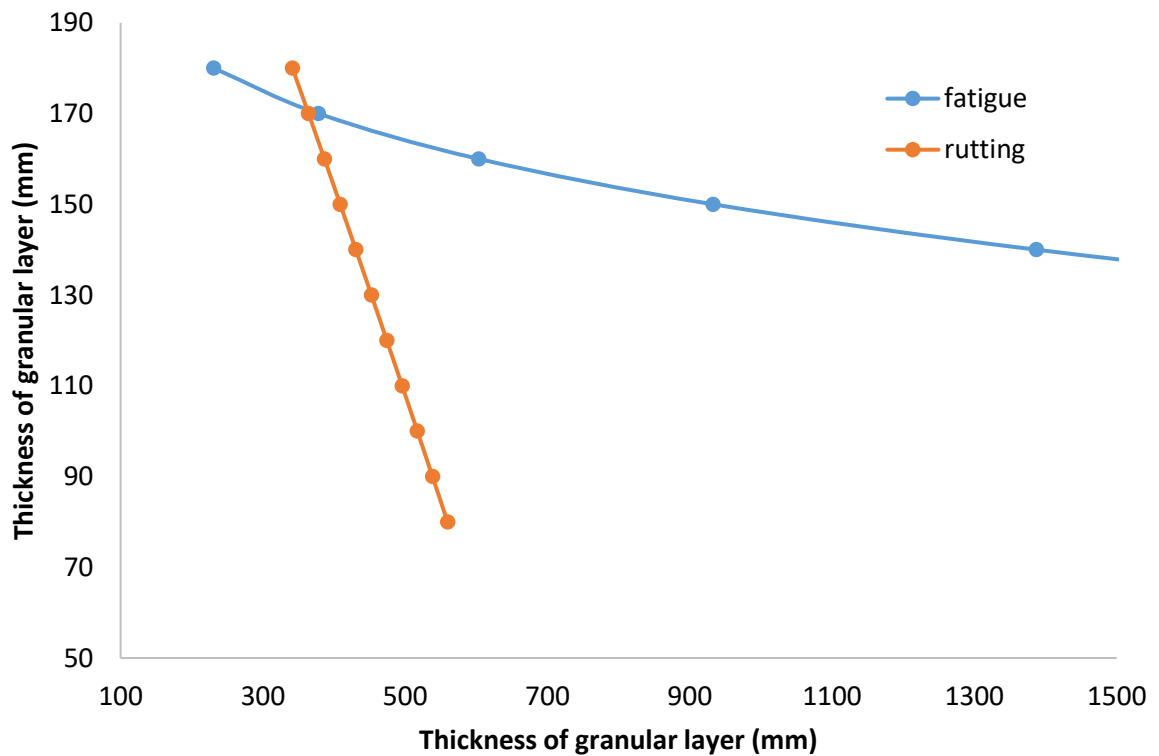
Figure 4.19 : Variation of bituminous layer and granular layer thickness under fatigue and rutting for 7 % subgrade CBR and 50 msa axle load repetitions
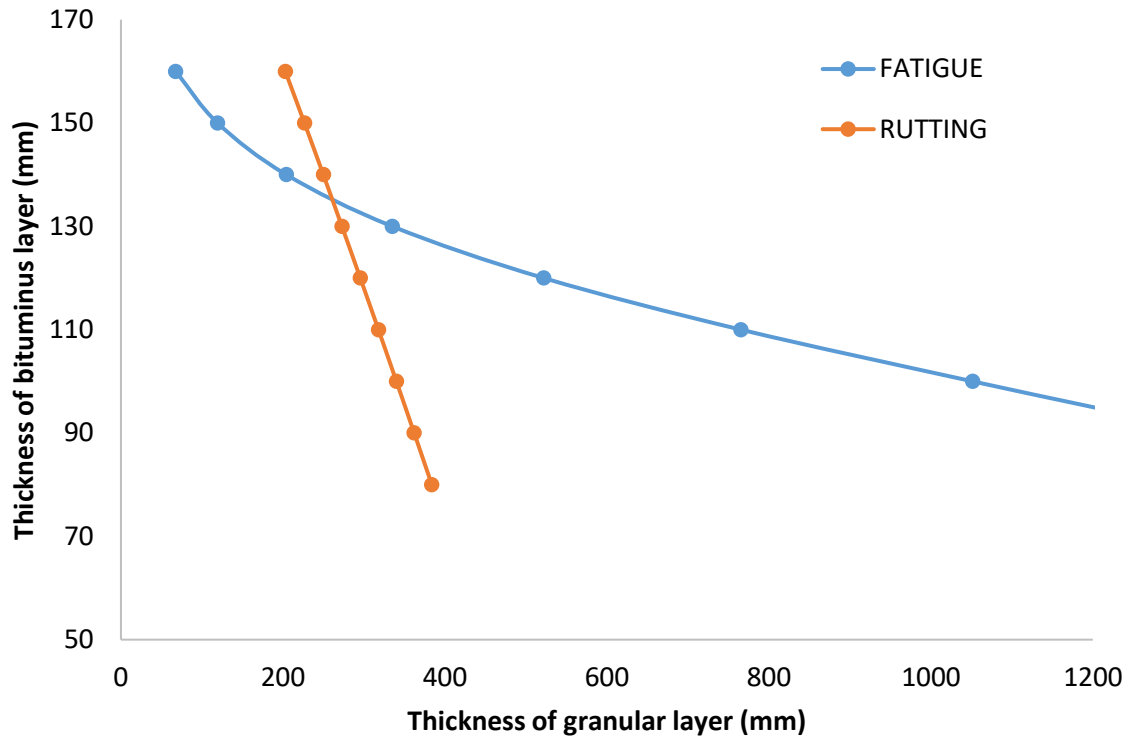
Figure 4.20: Variation of bituminous layer and granular layer thickness under fatigue and rutting for 8 % subgrade CBR and 5 msa axle load repetitions
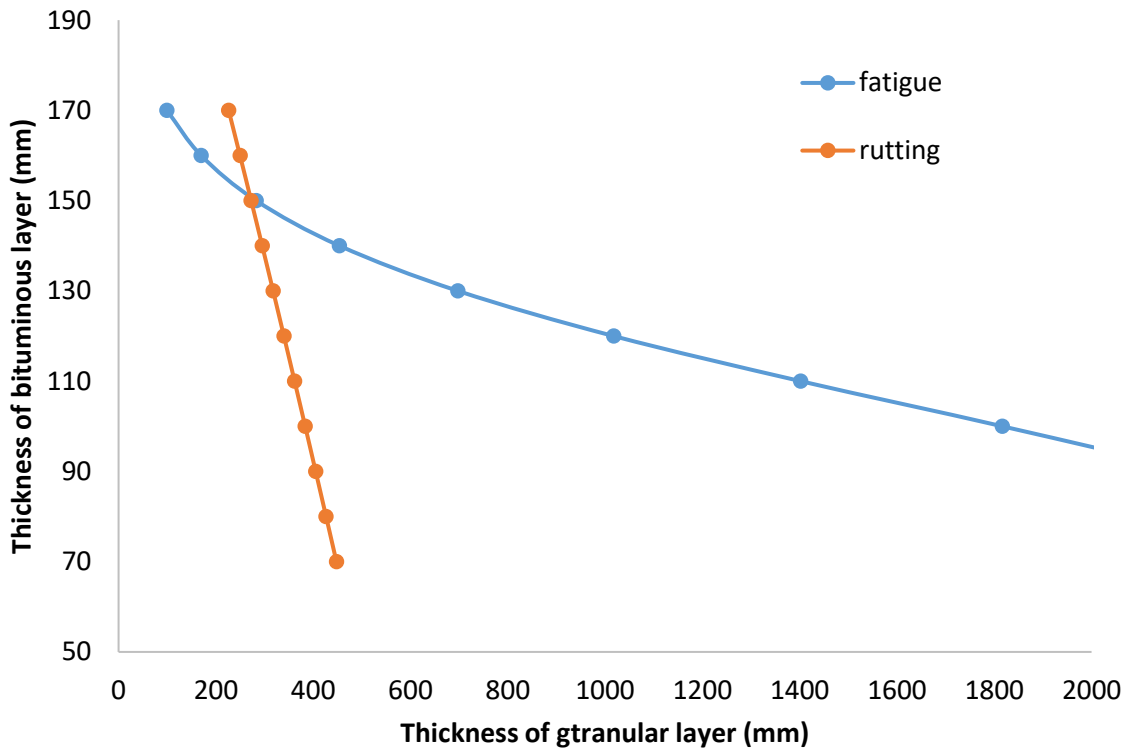
Figure 4.21: Variation of bituminous layer and granular layer thickness under fatigue and rutting for 8 % subgrade CBR and 10 msa axle load repetitions
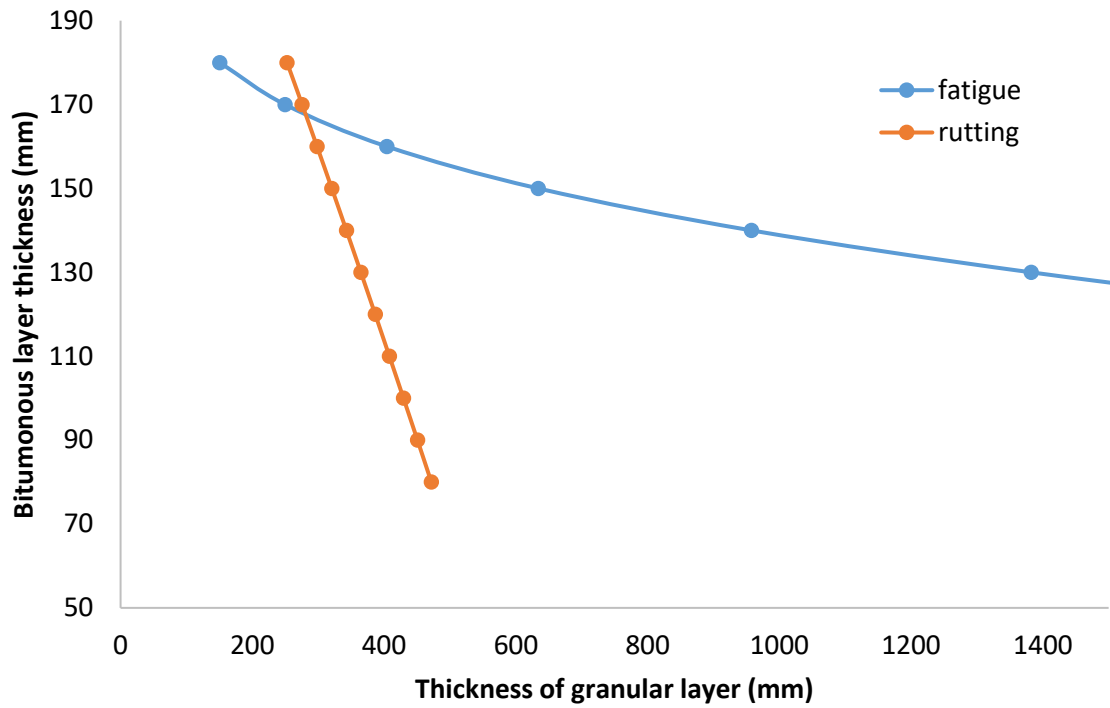
Figure 4.22: Variation of bituminous layer and granular layer thickness under fatigue and rutting for 8 % subgrade CBR and 20 msa axle load repetitions
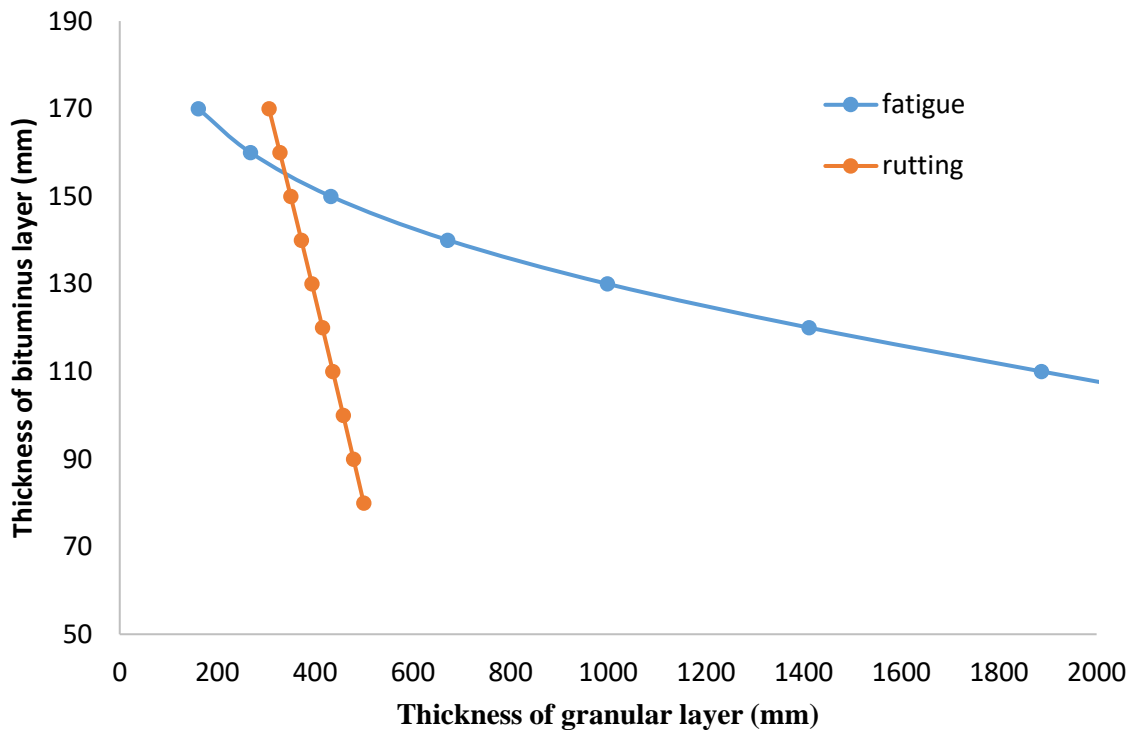
Figure 4.23: Variation of bituminous layer and granular layer thickness under fatigue and rutting for 8 % subgrade CBR and 30 msa axle load repetitions
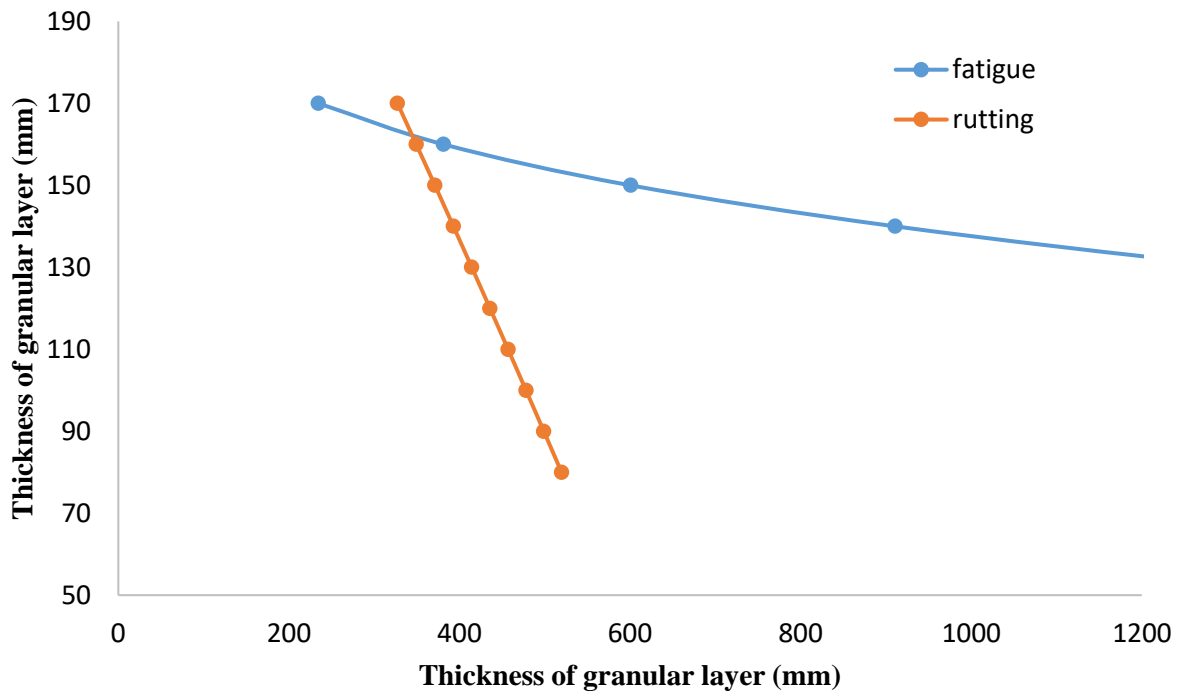
Figure 4.24 : Variation of bituminous layer and granular layer thickness under fatigue and rutting for 8 % subgrade CBR and 40 msa axle load repetitions
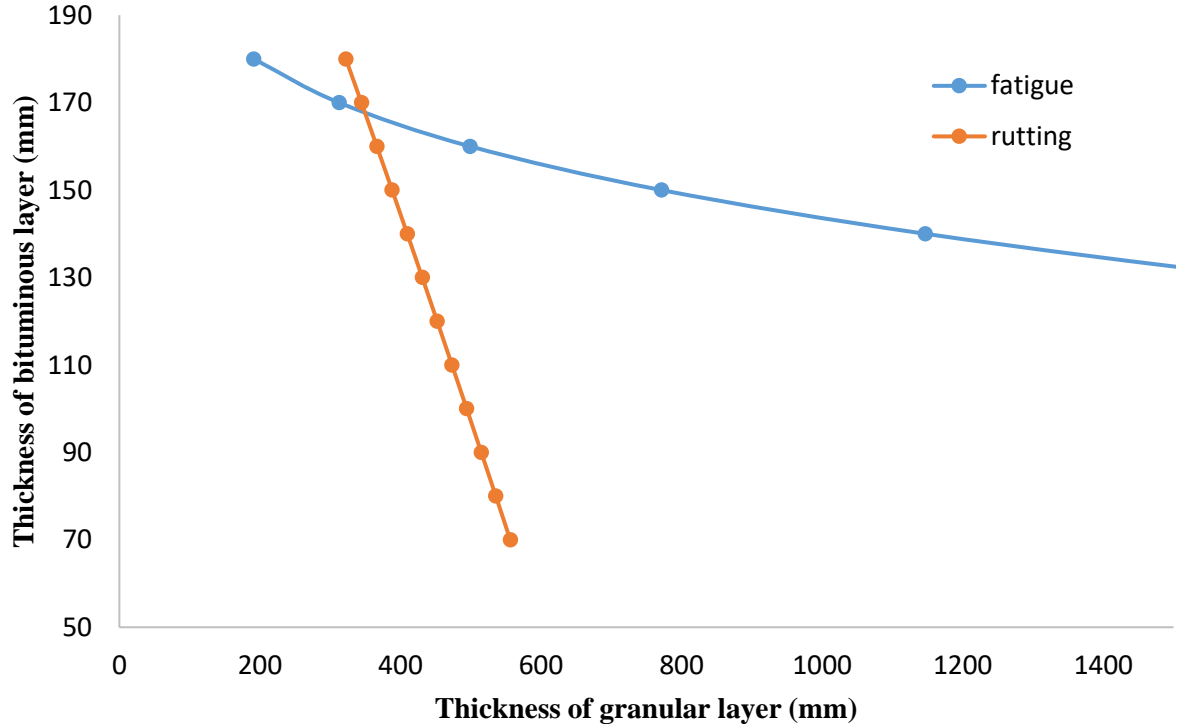
Figure 4.25 : Variation of bituminous layer and granular layer thickness under fatigue and rutting for 8 % subgrade CBR and 50 msa axle load repetitions
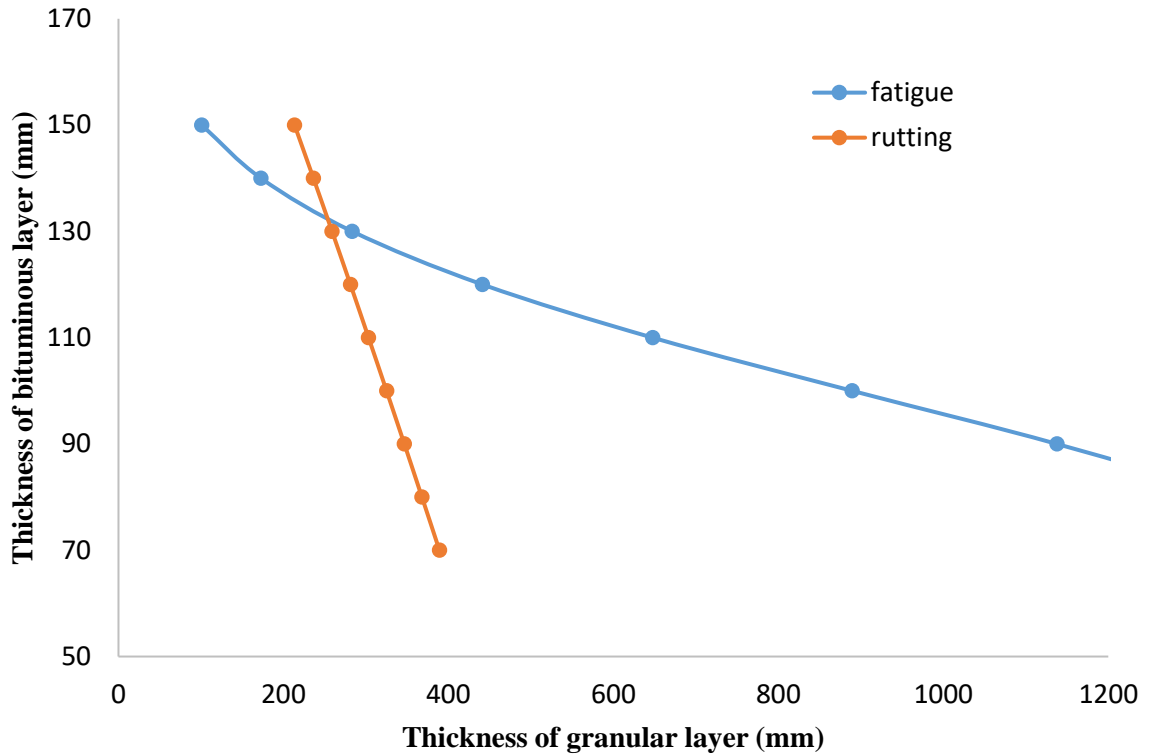
Figure 4.26 : Variation of bituminous layer and granular layer thickness under fatigue and rutting for 9 % subgrade CBR and 5 msa axle load repetitions
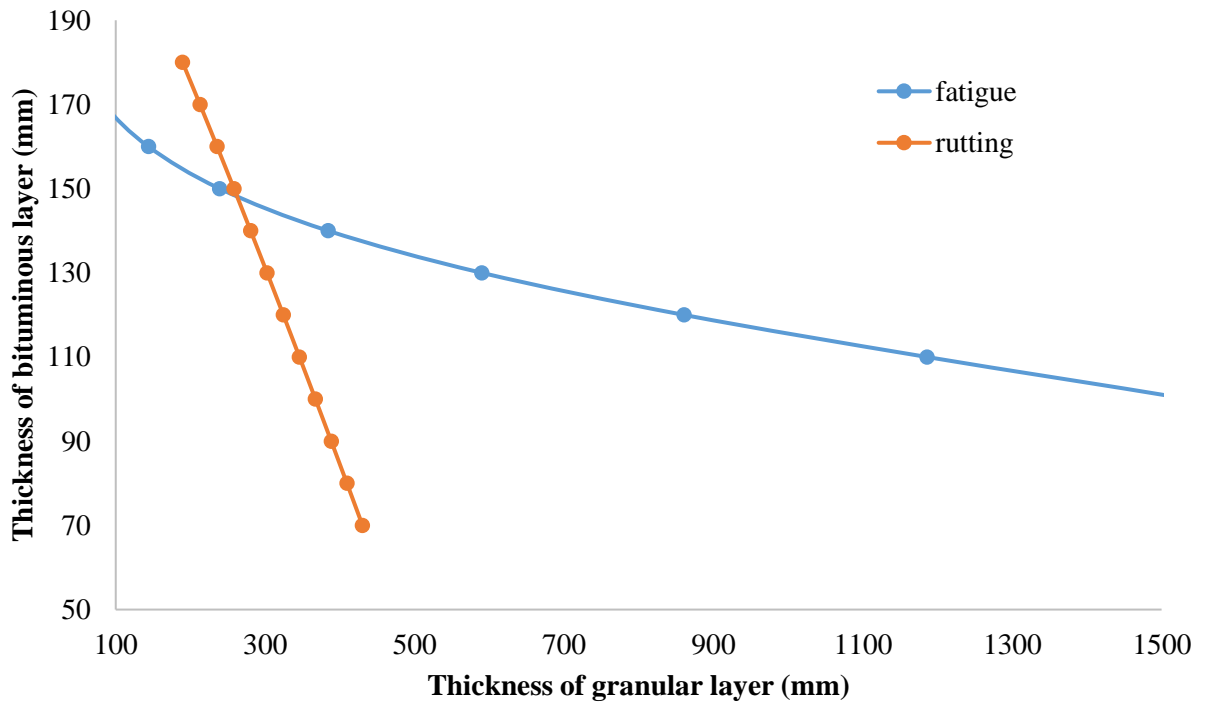
Figure 4.27 : Variation of bituminous layer and granular layer thickness under fatigue and rutting for 9 % subgrade CBR and 10 msa axle load repetitions
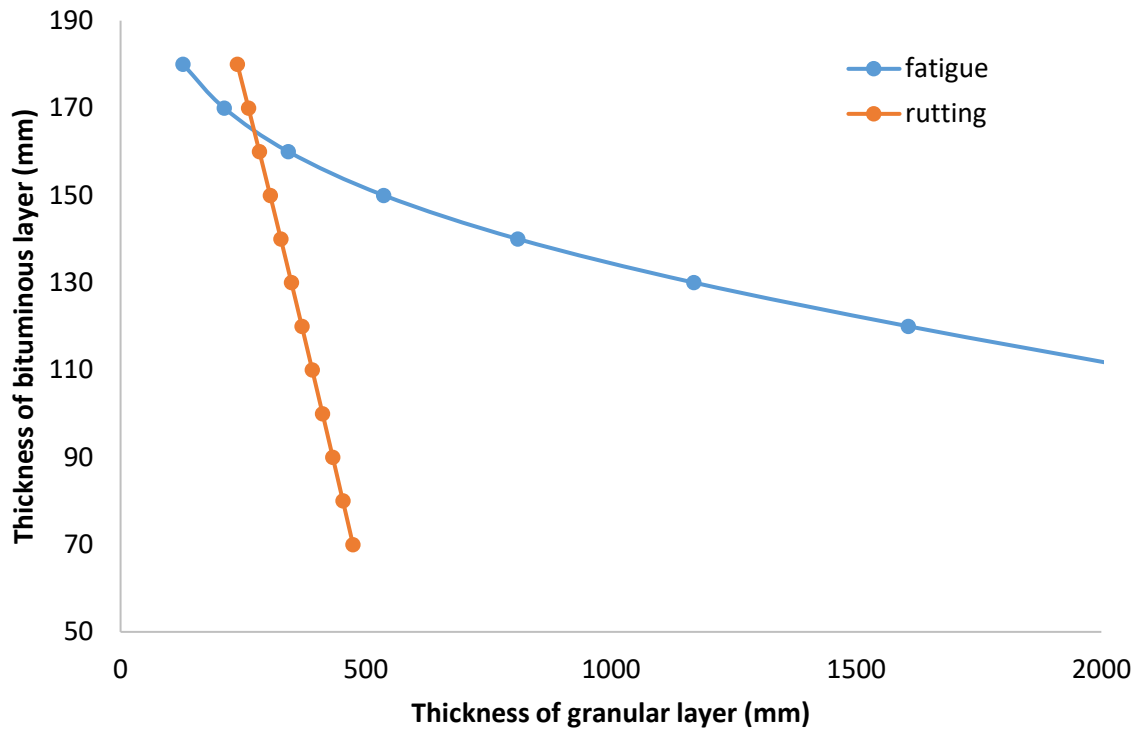
Figure 4.28: Variation of bituminous layer and granular layer thickness under fatigue and rutting for 9 % subgrade CBR and 20 msa axle load repetitions
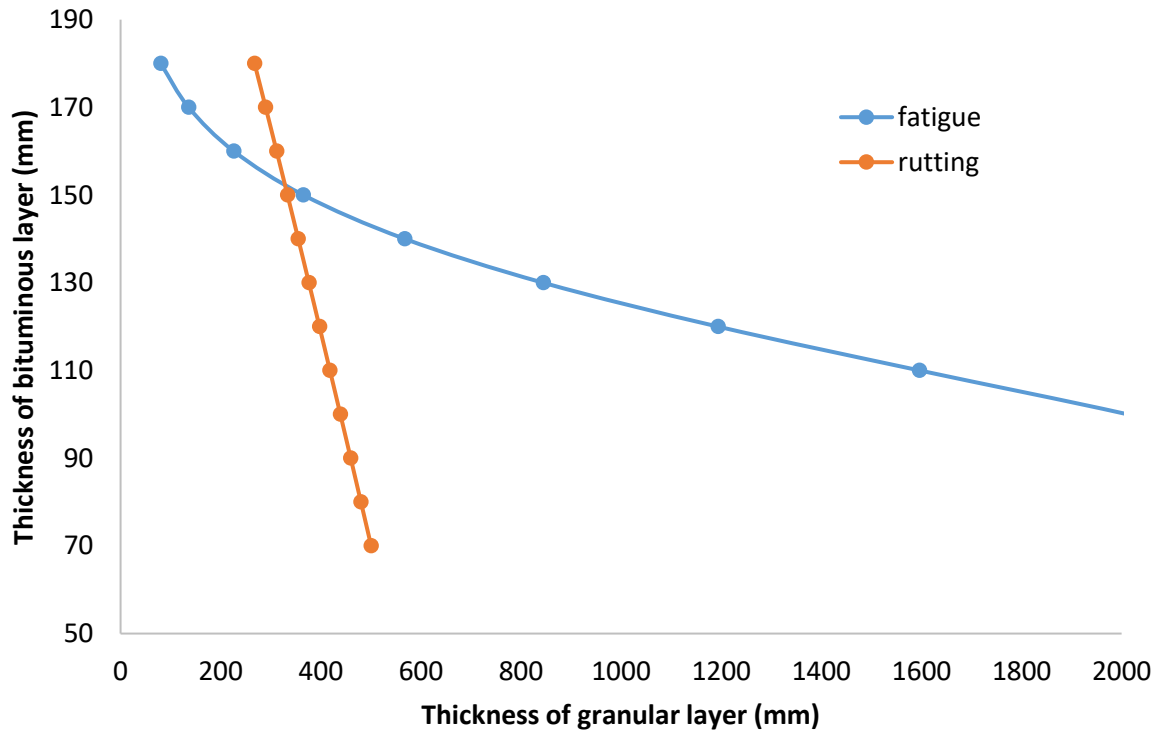
Figure 4.29: Variation of bituminous layer and granular layer thickness under fatigue and rutting for 9 % subgrade CBR and 30 msa axle load repetitions
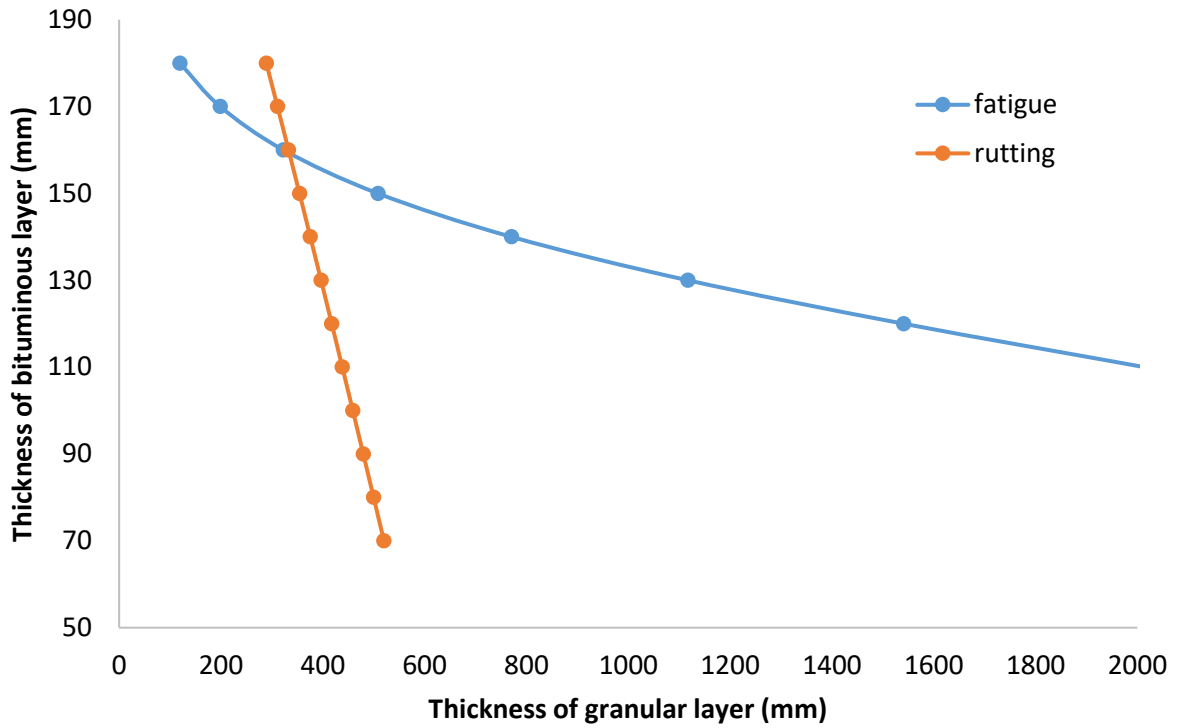
Figure 4.30: Variation of bituminous layer and granular layer thickness under fatigue and rutting for 9 % subgrade CBR and 40 msa axle load repetitions
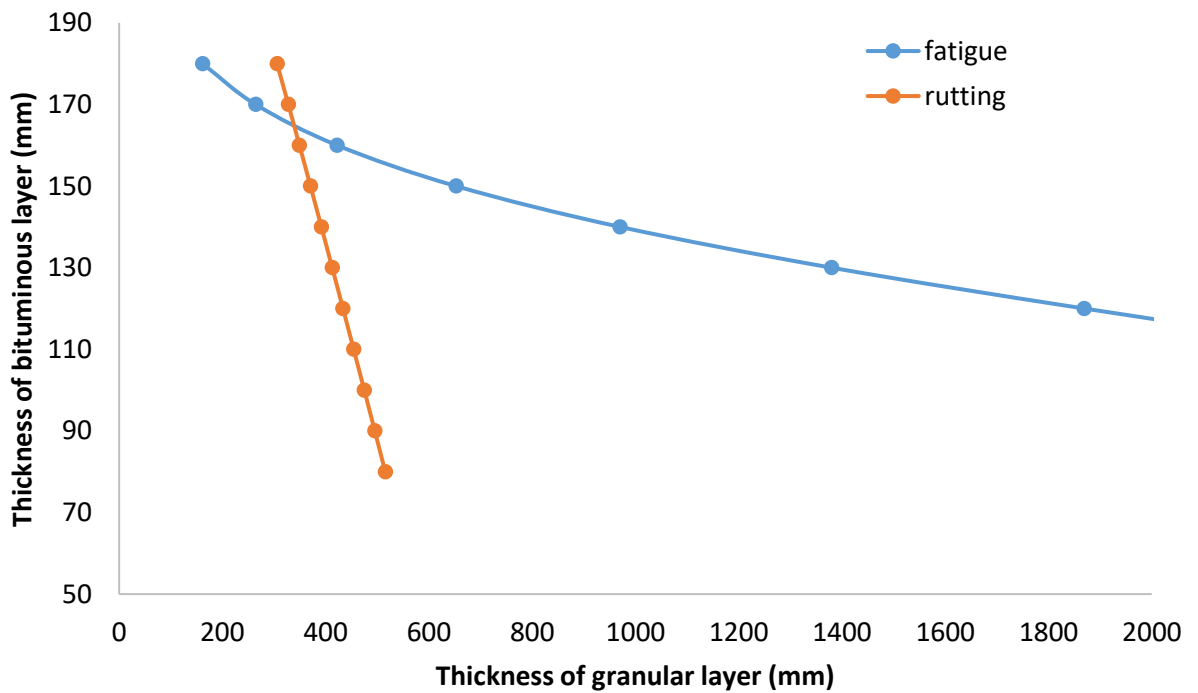
Figure 4.31: Variation of bituminous layer and granular layer thickness under fatigue and rutting for 9 % subgrade CBR and 50 msa axle load repetitions
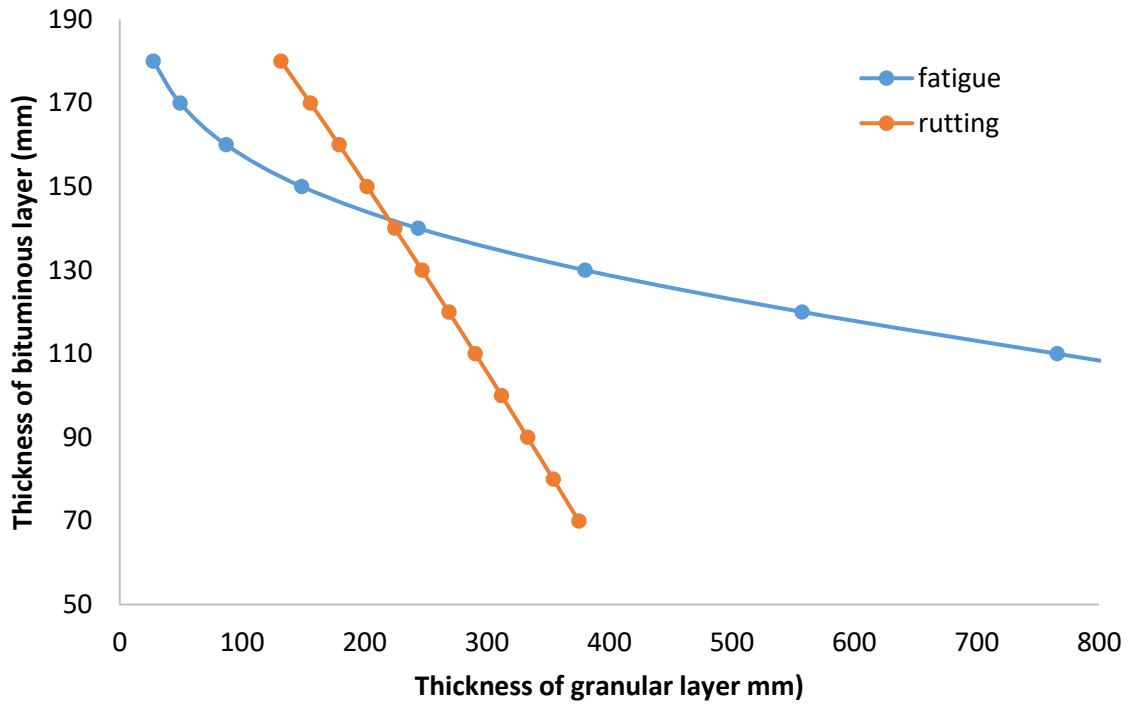
Figure 4.32 : Variation of bituminous layer and granular layer thickness under fatigue and rutting for 10 % subgrade CBR and 5 msa axle load repetitions
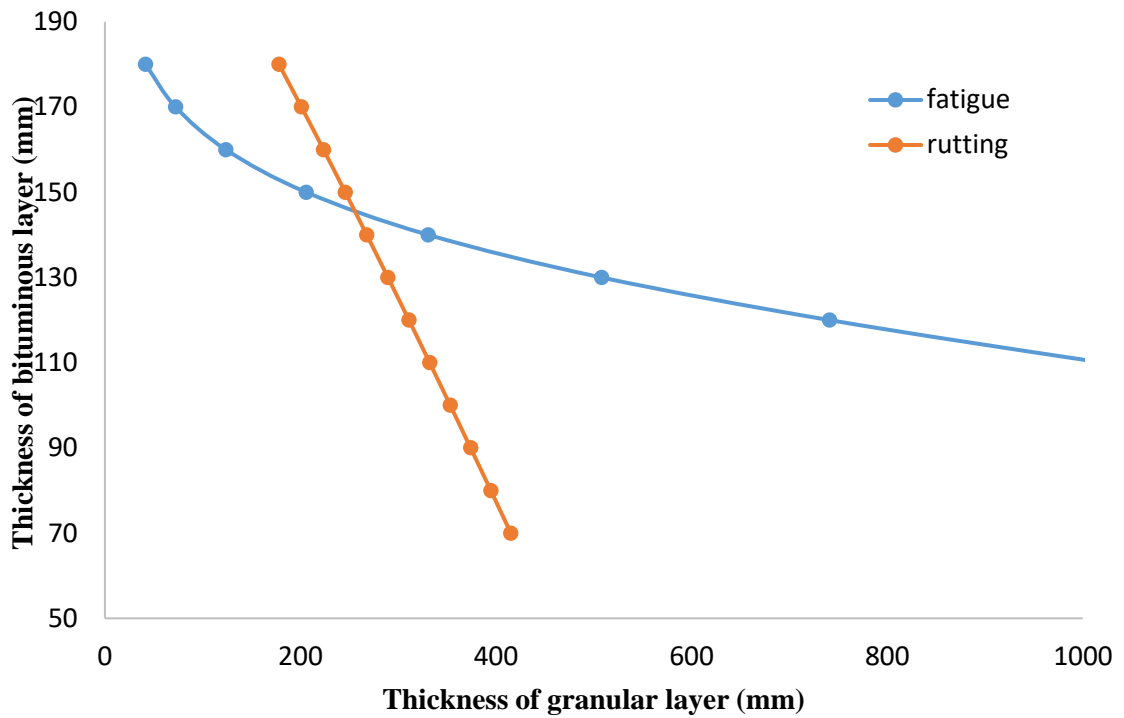
Figure 4.33: Variation of bituminous layer and granular layer thickness under fatigue and rutting for 10 % subgrade CBR and 10 msa axle load repetitions
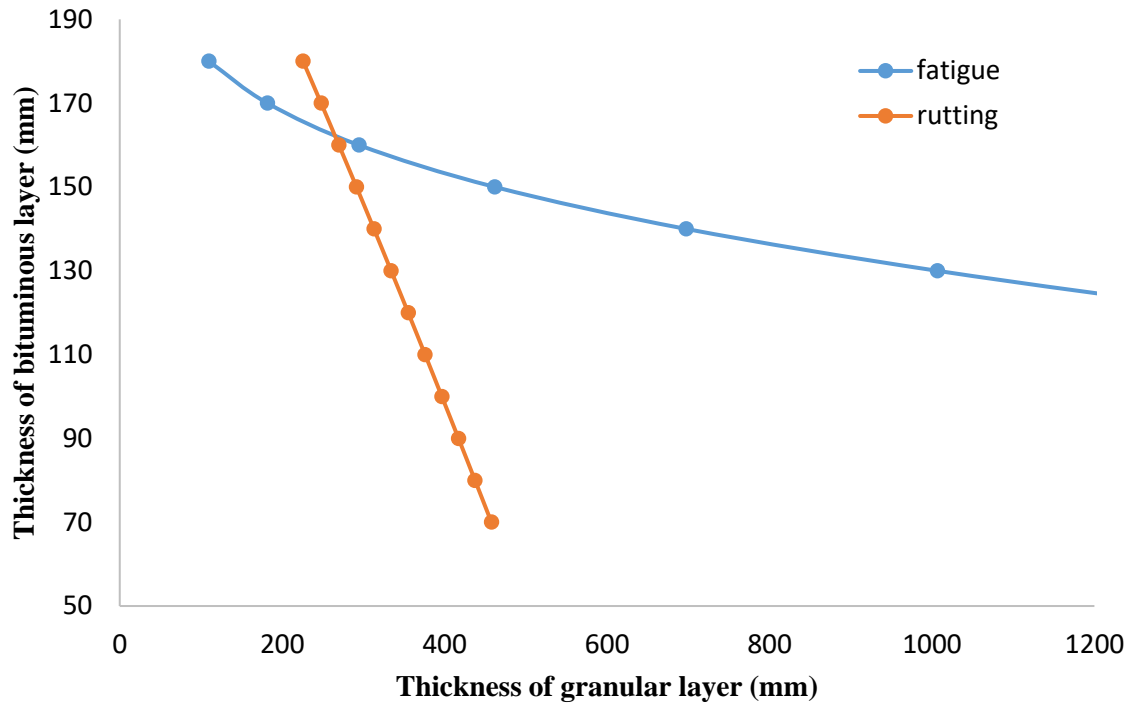
Figure 4.34: Variation of bituminous layer and granular layer thickness under fatigue and rutting for 10 % subgrade CBR and 20 msa axle load repetitions
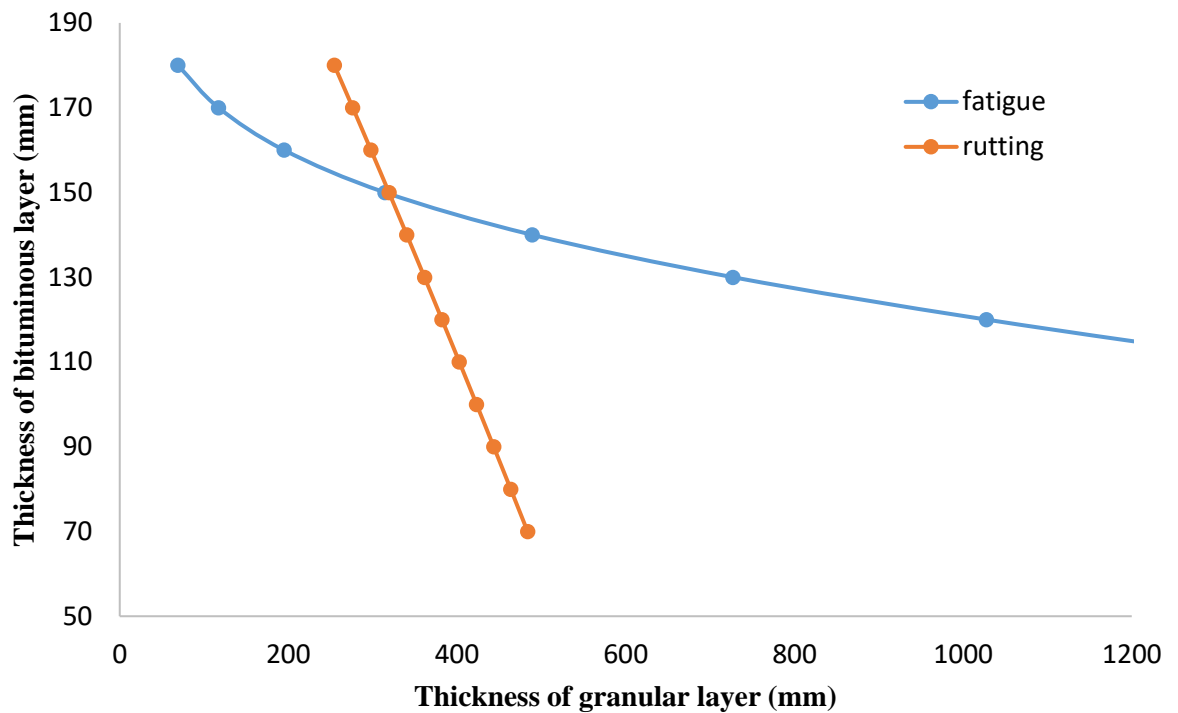
Figure 4.35 : Variation of bituminous layer and granular layer thickness under fatigue and rutting for 10 % subgrade CBR and 30 msa axle load repetitions

145
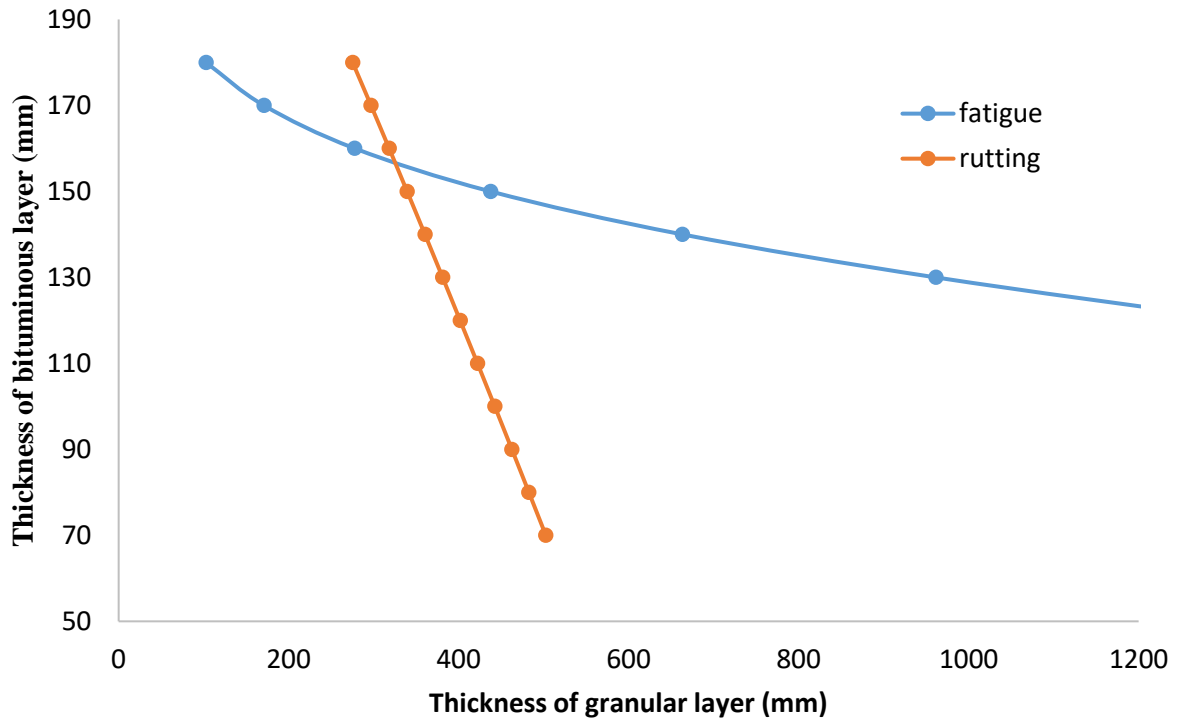
Figure 4.36 : Variation of bituminous layer and granular layer thickness under fatigue and rutting for 10 % subgrade CBR and 40 msa axle load repetitions
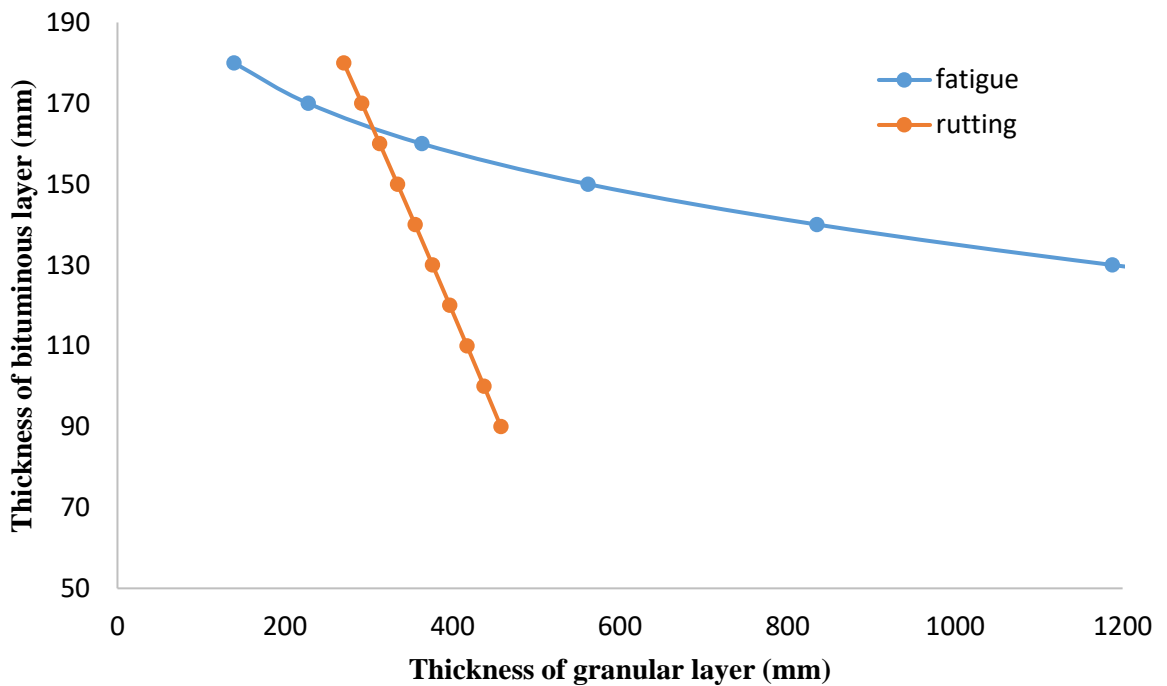
Figure 4.37: Variation of bituminous layer and granular layer thickness under fatigue and rutting for 10 % subgrade CBR and 50 msa axle load repetitions
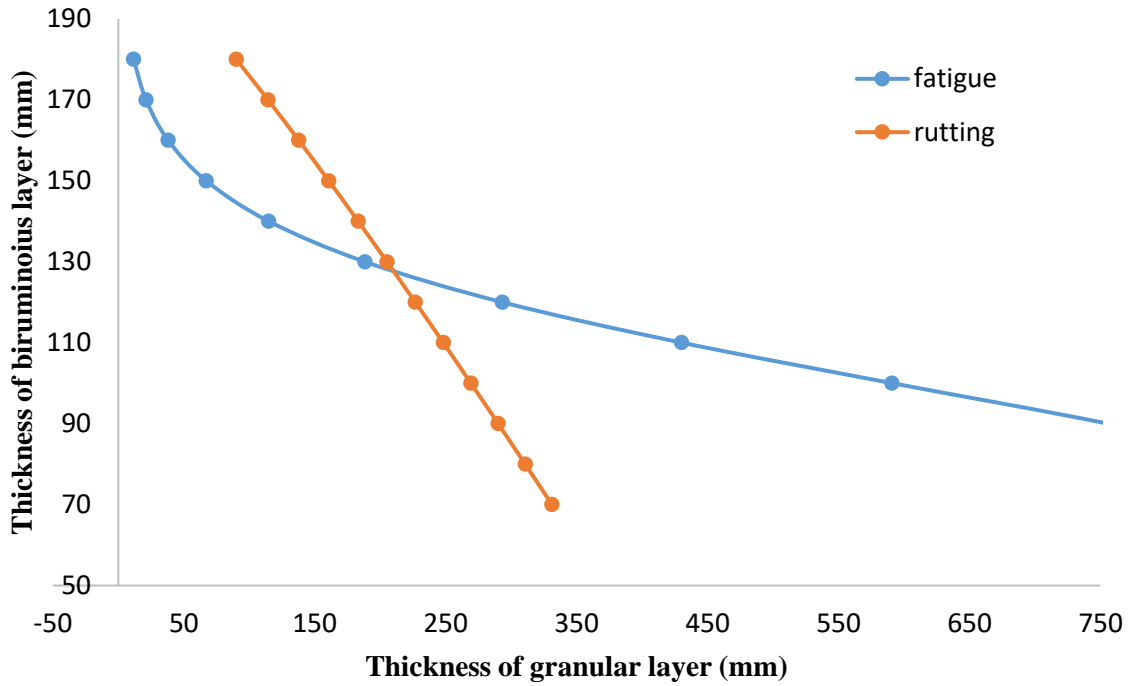
Figure 4.38 : Variation of bituminous layer and granular layer thickness under fatigue and rutting for 12 % subgrade CBR and 5 msa axle load repetitions
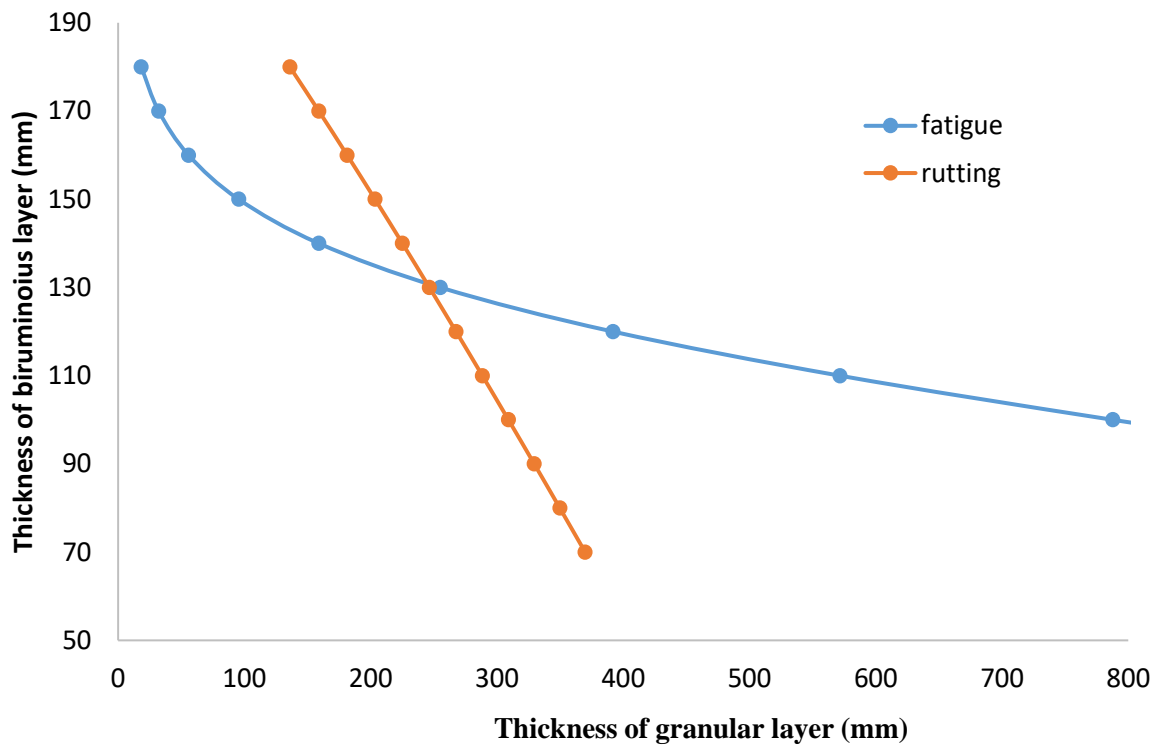
Figure 4.39: Variation of bituminous layer and granular layer thickness under fatigue and rutting for 12 % subgrade CBR and 10 msa axle load repetitions
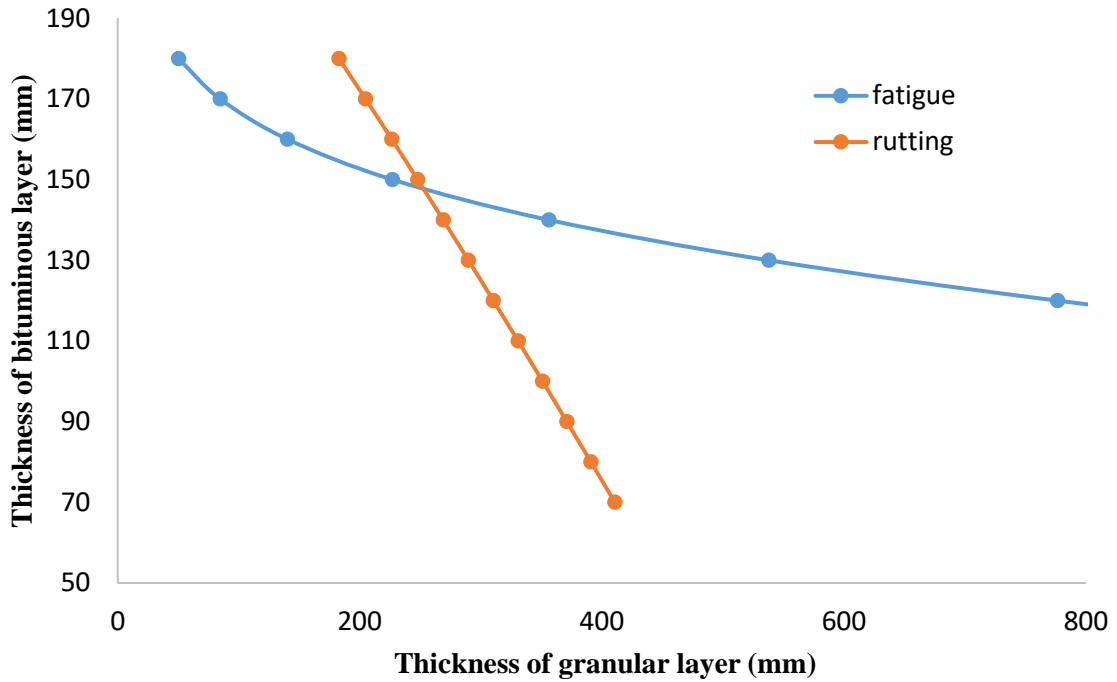
Figure 4.40: Variation of bituminous layer and granular layer thickness under fatigue and rutting for 12 % subgrade CBR and 20 msa axle load repetitions
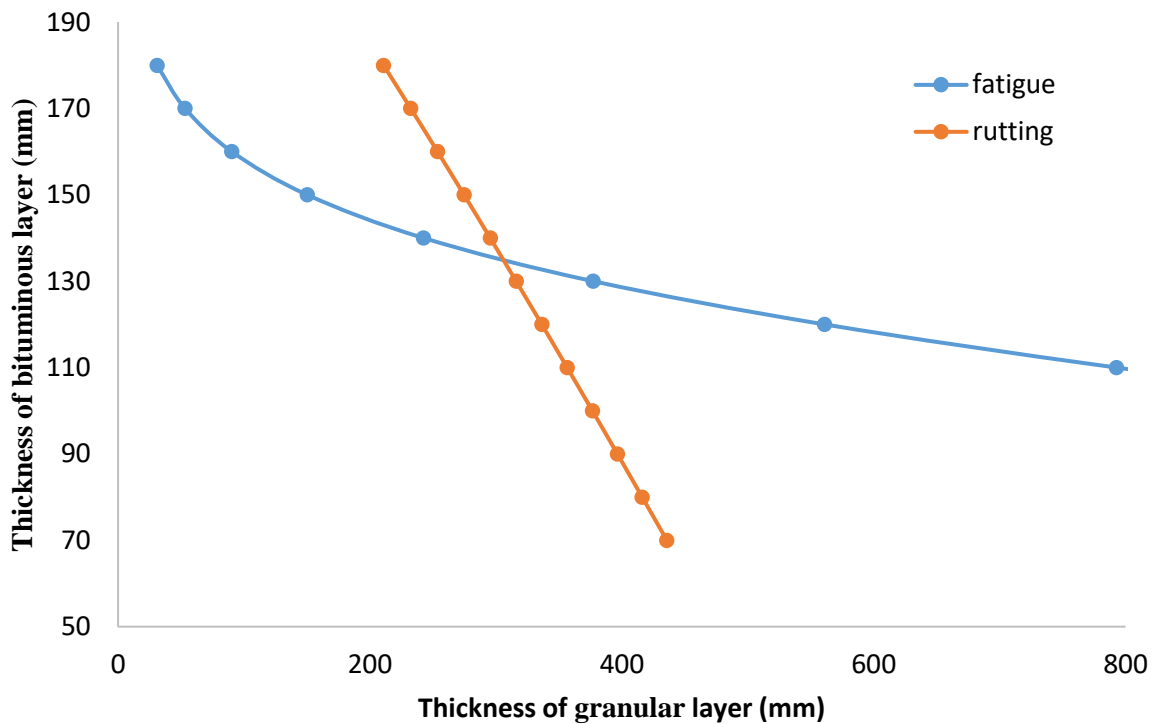
Figure 4.41: Variation of bituminous layer and granular layer thickness under fatigue and rutting for 12 % subgrade CBR and 30 msa axle load repetitions
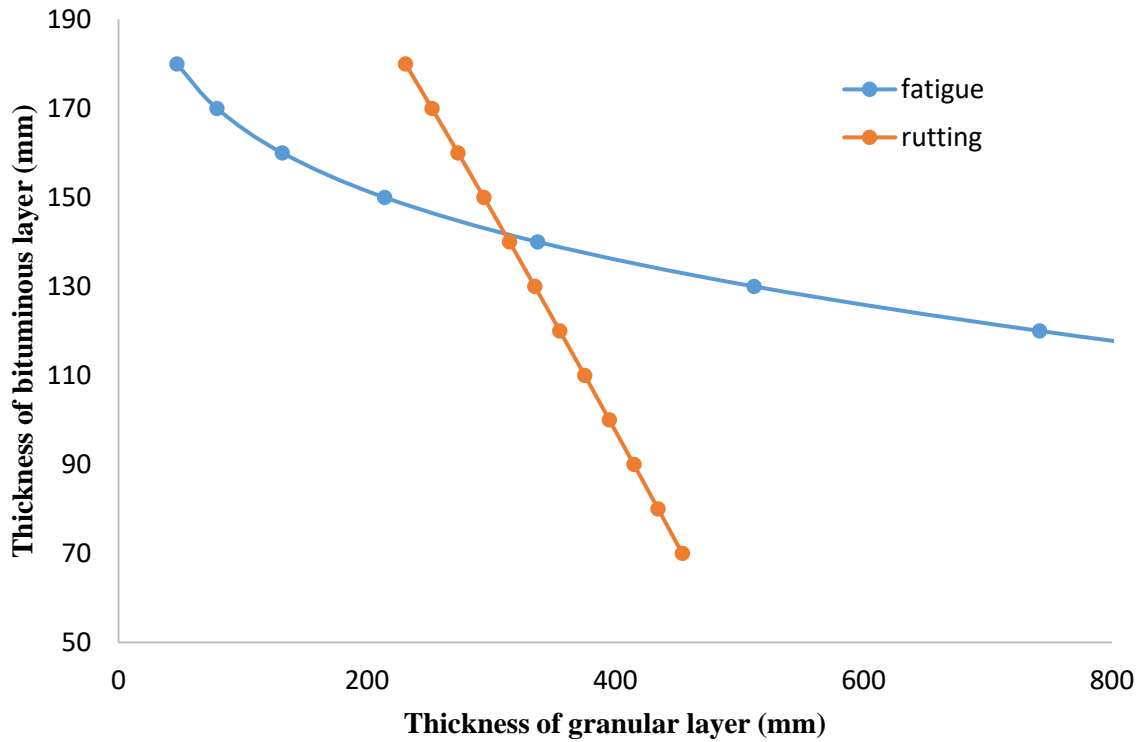
Figure 4.42 : Variation of bituminous layer and granular layer thickness under fatigue and rutting for 12 % subgrade CBR and 40 msa axle load repetitions
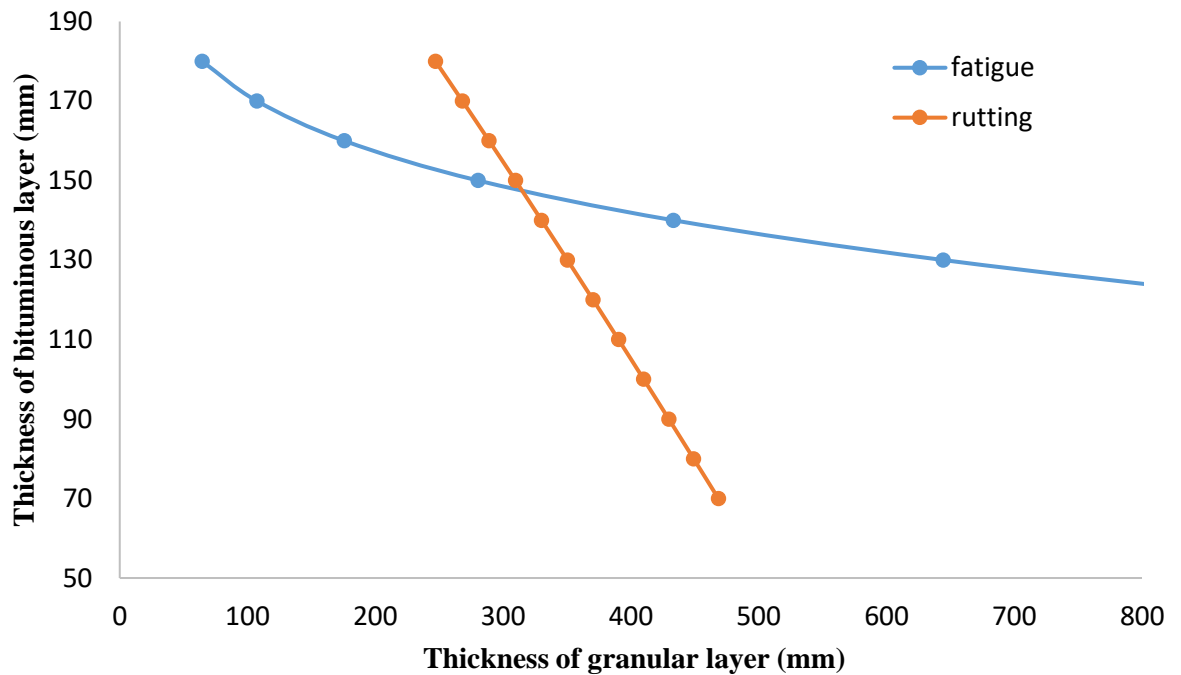
Figure 4.43 : Variation of bituminous layer and granular layer thickness under fatigue and rutting for 12 % subgrade CBR and 50 msa axle load repetitions
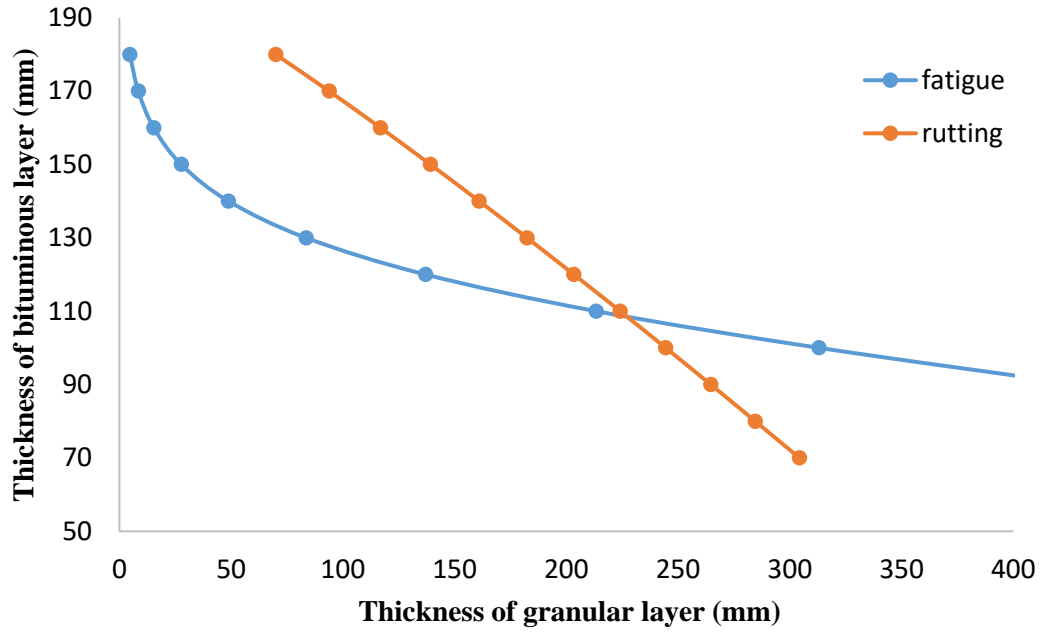
Figure 4.44: Variation of bituminous layer and granular layer thickness under fatigue and rutting for 15 % subgrade CBR and 5 msa axle load repetitions
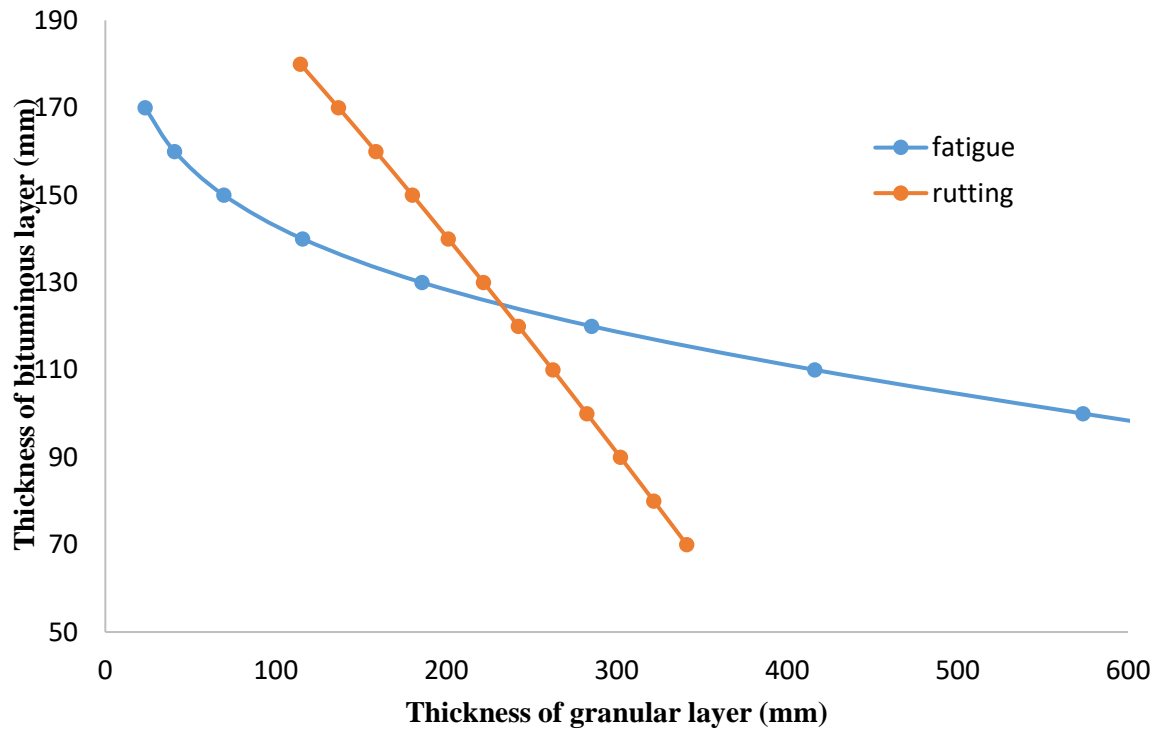
Figure 4.45 : Variation of bituminous layer and granular layer thickness under fatigue and rutting for 15 % subgrade CBR and 10 msa axle load repetitions
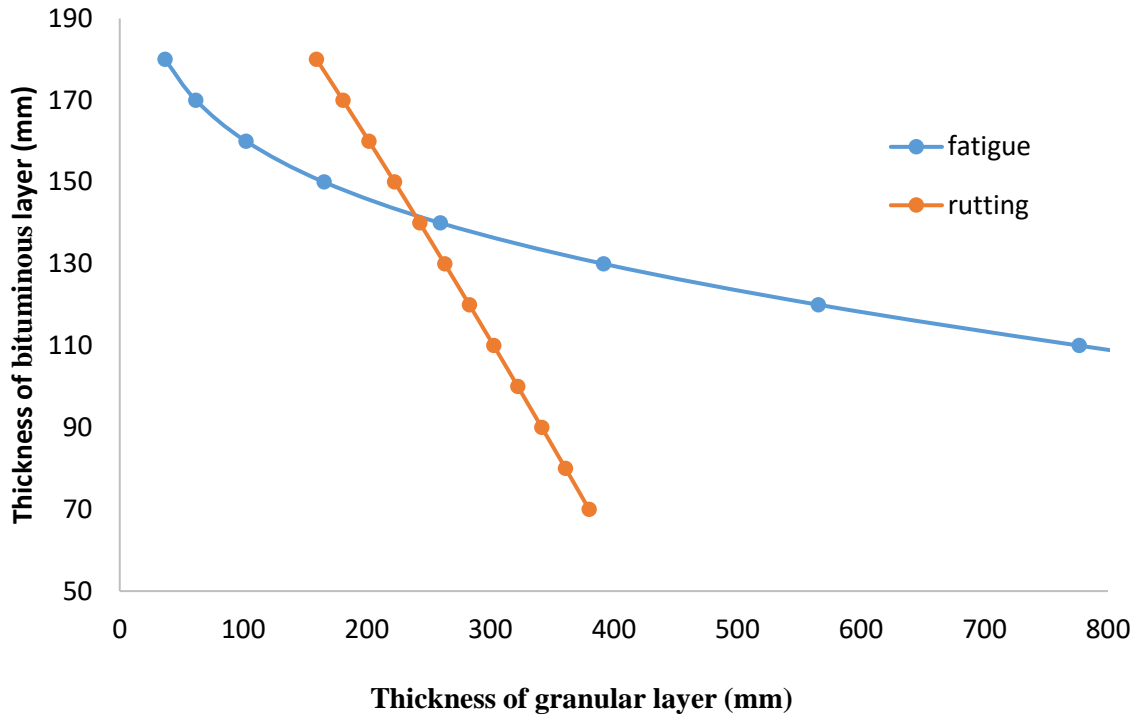
Figure 4.46 : Variation of bituminous layer and granular layer thickness under fatigue and rutting for 15 % subgrade CBR and 20 msa axle load repetitions
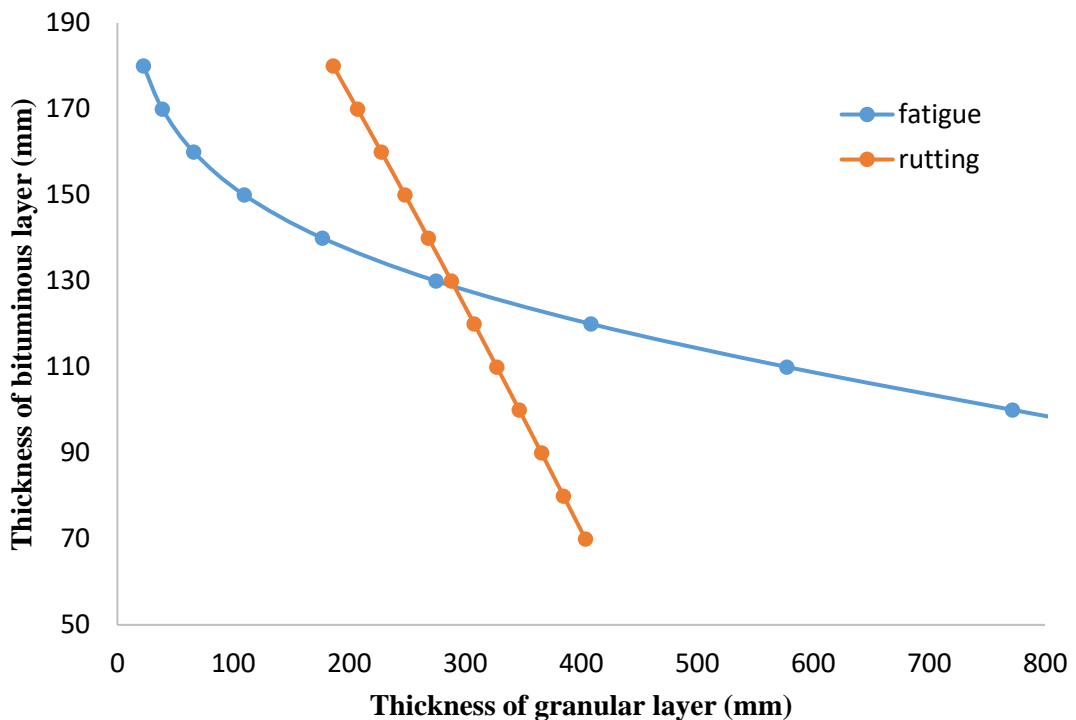
Figure 4.47 : Variation of bituminous layer and granular layer thickness under fatigue and rutting for 15 % subgrade CBR and 30 msa axle load repetitions
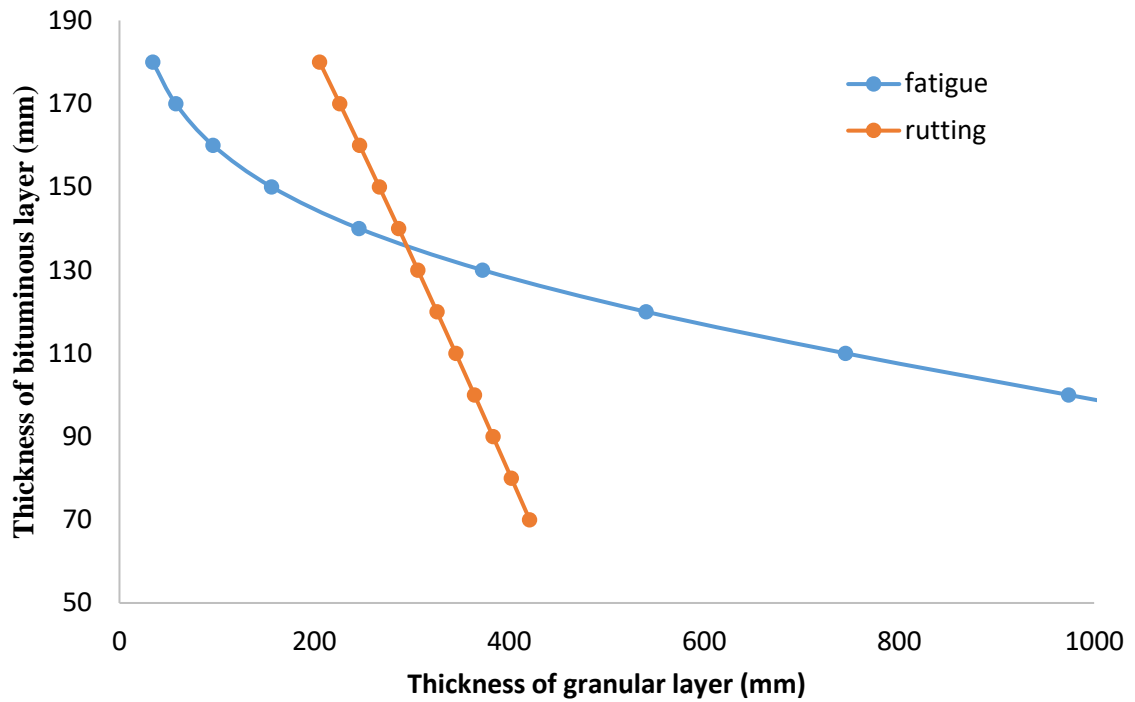
Figure 4.48: Variation of bituminous layer and granular layer thickness under fatigue and rutting for 15 % subgrade CBR and 40 msa axle load repetitions
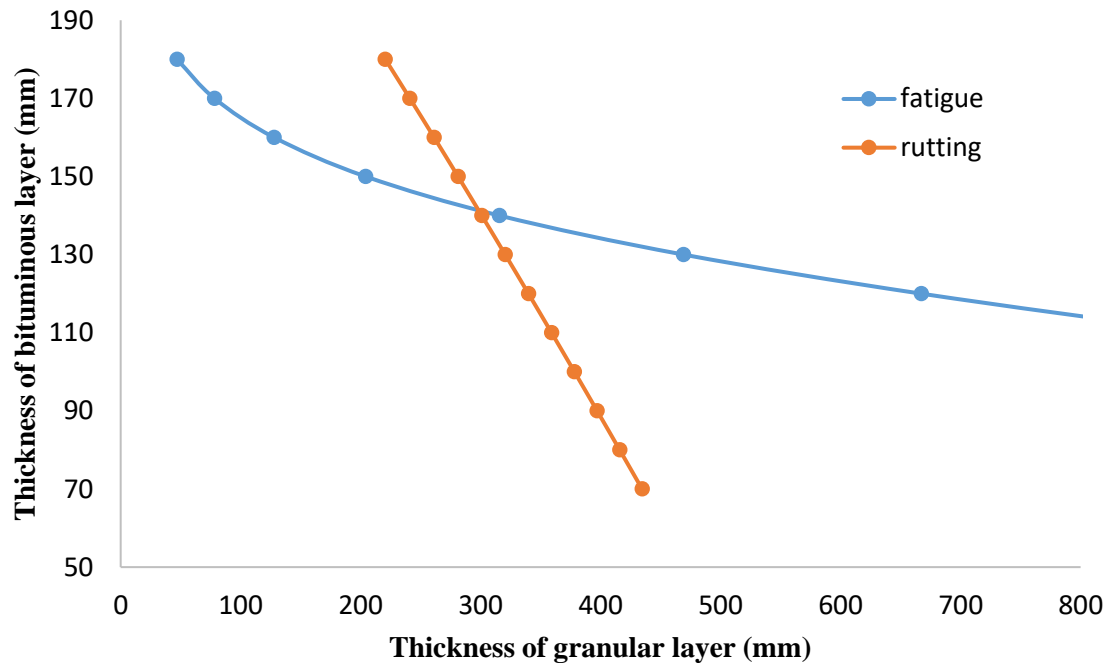
Figure 4.49: Variation of bituminous layer and granular layer thickness under fatigue and rutting for 15 % subgrade CBR and 50 msa axle load repetitions

4.5   Validation of the present model

Pavement deflection is often considered as the indicator of pavement performance. Therefore, attempts are made in this study to validate the thickness of pavement obtained from present analytical method with other comparable formulations using deflection data. The deflection in all the layers of the pavement have been determined by the theory of elasticity after transformation of respective layers in to a homogeneous section by application of Boussinesq's - Odemark's [34,126] method as explained earlier. Summation of deflections in all the constituent layers in a pavement thus obtained may be considered as total pavement deflection. A dual wheel load of 40 kN and a tyre pressure of 0.56 MPa have been considered in present analysis for determination of pavement deflection.   The deflection thus obtained for the optimized pavement section using present approach has been compared with the results obtained from IITPAVE [51] and KENPAVE [87] software and are presented in Table 4.9 to Table 4.11(Appendix 3A). Convergence of pavement deflection data obtained using present method and other software with different boundary conditions for different CBR and axle load were evident in Table 4.9 to Table 4.11 (Appendix 3A), which justifies the validity of present method for estimation of pavement thickness with reasonable degree of accuracy. Moreover, in order to validate the results obtained from present method, comparison between findings by Narasimham, K.V. et al (2001) [120] and I. Ghosh (2005) [73] have also been made in Table 4.12 (Appendix 3A) ,which further exhibits moderately good convergence .

Present method considers that the elastic modulus of all the constituent layers in a pavement remain unchanged till the elastic failure of pavement. Moreover, the material behavior in present model has been considered as linear elastic in nature. But the changes in the modulus of pavement during its service life need to be considered in future for more accurate estimation of pavement thickness.

4.6   Concluding remarks

Present methodology is based on mechanistic-empirical approach to determine required thickness of bituminous layer and granular layer against rutting and fatigue in a flexible road pavement. It has been found in this study that the variation of granular layer thickness is more sensitive than the bituminous layer thickness on pavement performance in terms of rutting. The methodology proposed in this section to determine optimum thickness of pavement satisfies terminal fatigue and rutting criteria. The performance of pavement section in terms of deflection has been found good in comparison with other international findings. In this context, the proposed method may be considered as an acceptable approach in pavement design. However, the effect of variation of modulus of pavement layers on pavement thickness need to be considered in future to increase the reliability of the method. In present analysis, a Graphical User Interface (GUI) has been developed by using PYTHON and JAVA, so that the developed algorithm may be used more conveniently.

CHAPTER 5

MECHANISTIC-EMPIRICAL DESIGN OF PERPETUAL FLEXIBLE ROAD PAVEMENT USING STRAIN BASED DESIGN APPROACH

5.1 Introduction

It can be noted that the unbridled increment of traffic volumes and unexpected axle loads along with the gradual demands for freight corridor has impelled to conceptualize the perpetual pavement. Presently, flexible pavement is generally designed considering the structure of the pavement as a multilayered system. The basic method of flexible pavement design started with an assumption of a two-layered system and gradually evolved into a multi-layered system of pavement design. The design of pavement primarily depends on the methodology adopted and the boundary conditions assumed in course of design. The main concept of perpetual pavements is that the asphalt pavement should be constructed with an impermeable, rut- and wear-resistant top layer placed on a rut-resistant and durable intermediate layer with a fatigue-resistant and durable base layer. Limiting strain distribution and maximum fatigue ratios to resist bottom-up FC (fatigue cracking) is sometimes used to design a perpetual pavement [42, 62]. Although various endurance limits of perpetual pavement have been proposed, none have been determined and field validated for efficient design [42, 62, 63, and 92,100,102,103,106]. The National Center for Asphalt Technology (NCAT) suggested the FEL (Fatigue Endurance Limit) [112,124,125,134,147,149,152] value for most perpetual pavement are designed in the range of 70 to 100 $\mu\varepsilon$. This concept was first proposed by Monismith and Mc Clean in (1972) [67-68] based on the laboratory test [67-68]. However, based on the results of different in-service pavement sections, some researchers suggested the Fatigue Resistance Layer (FRL) [154,161,162,165] can withstand up to 150 $\mu\varepsilon$ depending on the type of bituminous mixture used [,171,172,174,187,190] for the layer. In this backdrop present section has been aimed to develop a Mechanistic – Empirical flexible pavement design method based on MET [52,181] as it provides direct close-form solution.

5.2 Literature review

Shuvo Islama et al. (2018) [92] studied the validity of the assumptions related to the design of perpetual pavement sections using Per Road and AASHTOWare Pavement M-E Design software. Moreover, by using the

bottom-up cracking and FWD deflection data, fatigue life and layer moduli were estimated. The comparative results as derived from Per Road showed a higher value than AASHTOWare Pavement ME design values. The study also recommended that the rich bituminous mix if used in the base layer can be useful as the most successful perpetual pavement.

Scheer Matthew J. (2013) [161] evaluated the performance of perpetual pavement structures through the installation of several sensors in a different layer in a pavement. Pavement response thus obtained as fatigue strain at a critical location in pavement section was compared with expected strain to assess the durability of pavement. The influence of axle configuration, speed, and tire pressure, were analyzed to understand its effects on pavement responses. **Timm et al. (2015)** [110] proposed a design procedure (Per Road) based on principles of perpetual pavement. Moreover, the study also focused on developing a Monte Carlo simulation-based reliability approach to minimize the risk of structural failure. A field-based limiting strain threshold was also developed to adopt these values from cumulative distributions of field-measured tensile strains in the 2003 and 2006 research cycles. Per Road, a stochastic perpetual pavement design programme was used to predict strains for the same 2006 sections. A comparison study was also carried out to observe differences in predicted and measured strains. The study concluded that the limiting strain distribution and maximum fatigue ratios may be included for designing the perpetual pavements to resist bottom-up FC.

Mazumder et al. (2016) [112] reviewed the importance of perpetual pavement in future road networks and also mentioned the mechanistic-empirical design principles and differences with conventional pavement. Definition of perpetual pavement including its mechanistic-empirical design principles and difference with conventional pavement are discussed with specific layer purposes and distresses are provided. Recommendations have been given for future research in order to obtain an optimum asphalt perpetual pavement design.

John Liao et al. (2010) [106] presented a three-dimensional linear visco-elastic finite element model to simulate the behavior of a perpetual pavement structure subjected to traffic loading at different temperatures and vehicular speeds. The study considers HMA as pure elastic solids. The developed model

relatively accurately predicted not only the stress and strain responses but also the deflection response concurrently. The results of this research may be effective to use viscoelastic analysis of perpetual pavements in comparison with the conventional elastic models.

Lee, S. I., et al. (2020) [103] reported the cost-effective PP (perpetual pavement) design alternatives to improve design optimization, material quality, and constructability. The structural and economic validations indicated that the design alternatives analytically meet expected performance limits, which last for the 50-year design life without significant structural failures, with a total agency cost saving of up to 19% compared with the current design procedure.

Das (2015) [120] presented review on various pavement design guidelines on the structural design of asphalt pavements with reference to the design principles employed. The focus was primarily kept on the mechanistic-empirical pavement design approach. The discussion covers a few specific aspects of asphalt pavement design.

Kollaros et al. (2017) [100] proposed a methodology to reduce the maintenance cost of perpetual asphalt pavements by reduction of damage per million equivalent single axle loads and increase in expected service-life has been achieved with the increase of moduli values and thicknesses of different layers in the pavement structure. Layered pavements have been analyzed under specific loading conditions and the effect of the variability of these conditions on pavement's longevity has also been studied in order to understand the technical behavior of structures with a high strength surface layer considering different software by varying input parameters.

Tarefder RA et al. (2012) [172] proposed an optimal perpetual pavement by combinations of layer, stiffness, and thickness for implementation on New Mexico State highways. The Mechanistic-Empirical Pavement Design Guide (MEPDG) trial designs are analyzed for a 50-year design life of perpetual pavements. The required thickness ranges from 10 to 15 inches for moderate to high truck traffic roads. The study finds low bottom-up fatigue cracking and little or no top-down cracking at the end of 50 years, and low rutting in the intermediate layer at the end of the 10-year maintenance cycle. Resurfacing plans are recommended to remove rutting every 10 years. The study also examines perpetual pavements with and without rich-binder layers (RBLs), with

recommendations for using a non-RBL pavement based on life-cycle cost analysis. Debonding of hot mix asphalt (HMA) layers is also investigated, with 88% of perpetual pavements failing by top-down cracking and bottom-up cracking increasing significantly in a debonded environment.

El-Hakim et al. (2012) [62] presented a case study to examine how perpetual pavement design is a feasible solution for sustainable roads by explaining and analyzing the construction of a test section on Highway 401 in Woodstock, Ontario, Canada. The study considered construction of three sections, representing conventional pavement design, perpetual design without rich bottom mix, and perpetual design with rich bottom mix next to each other for a comparison of their performance with different sensors. The study suggested that sustainability in road construction is crucial for the environment, economy, and social development and that perpetual pavement design, despite higher construction costs, requires less maintenance and rehabilitation. The use of recycled asphalt pavement in all pavement layers in the project undertaken led to the conclusion that the use of recycled materials enhanced the pavement mechanical characteristics and maximized the efficient use of resources.

Von Quintus HL (2001)[185] studied an approach for designing the thickness of hot-mix asphalt (HMA) layers to enhance the longevity of bituminous pavements. The performance of HMA pavement relies on how pavement responses interact with the strength and modulus of various layers. Wheel loads generate stresses and strains in each layer, causing damage to both bound and unbound materials. Structural degradation typically manifests as cracking and rutting. The methodology outlines a process for designing durable HMA pavement structures for heavily trafficked roads, with a focus on limiting tensile strain at the bottom and VCS at the top. It employs the cumulative damage concept to anticipate fatigue and subgrade distortion, accounting for seasonal variations and material properties using the "equivalent modulus" approach. Two criteria are utilized for mechanistic-empirical thickness design assessments: restricting maximum surface deflection under the design load and controlling the modulus ratio between adjacent unbound pavement layers. The methodology tackles three key issues concerning fatigue cracking in HMA layers: defining an "endurance limit," determining the location of load-induced cracks, and understanding the fatigue properties of HMA layers. Long-Term

Pavement Performance data is leveraged to substantiate the criteria and methodology.

Willis JR. (2009) [187] evaluated field-based strain thresholds for flexible perpetual pavement design. The study considered recent efforts to design roadways that can withstand 50 years of traffic without structural fatigue damage. The study indicated that perpetual pavements, designed using mechanistic-empirical methodologies, limit strain at the bottom of the bituminous layer to a specific value, avoiding bottom-up fatigue damage. The study established field-based strain thresholds for perpetual pavement design and formulated a relationship between laboratory fatigue thresholds and field-measured strain. The main objective of the study was to improve efficiency in perpetual pavement design.

Islam S. et al. (2020) [92] proposed mechanistic-empirical design of perpetual pavement for four perpetual pavement sections which are scheduled for rehabilitation for top-down surface cracking. The study revealed that perpetual pavements use durable asphalt layers to create a safe, smooth, and long-lasting road. The bottom layer resists tensile strain from traffic, preventing cracks from forming. A study revisited the design of perpetual pavement sections using PerRoad and AASHTOWare Pavement ME Design software to verify design assumptions and fatigue lives. Results showed predicted strain values were lower than tensile strains computed using FWD deflection data. PerRoad required a higher asphalt thickness than AASHTOWare Pavement ME Design software over a 50-year design period. The results of the study indicated that the most successful perpetual pavement design was the one with a rich bituminous mix in the base layer.

M. Robbins M. et al. (2015) [110] modified and validated stochastic limiting strain distribution and fatigue ratio principles for eternal pavement design. The study reveals that traditional perpetual pavement thickness design focuses on controlling strain levels at the bottom of the asphalt concrete layer to prevent bottom-up fatigue cracking (FC). A field-based limiting strain threshold and fatigue ratio was developed to understand the limiting strain needed to control FC. The study suggests necessity to adapt the thresholds to strains predicted by perpetual pavement design tools. PerRoad, a stochastic perpetual pavement design program, was used to predict strains for 2006 sections, and the

updated limiting strain distribution and maximum fatigue ratios were validated for designing perpetual pavements to resist bottom-up FC.

Guo Z et al. (2016) [171] evaluated life cycle costs of Chinese perpetual and traditional semi-rigid pavements using operational pavement management systems and examine their suitability for more economical and durable flexible pavements. The study illustrates that pavement design and management aim to build sustainable structures with minimal costs throughout their life. However, uncertainties like future traffic estimation, material behavior, vehicle weights, and funding availability make it crucial to apply pavement stage construction techniques. In China, perpetual asphalt pavement (PP) technology has been applied since 2000, with the semi-rigid base being a typical component of high-class highways. The study suggests that the stage construction of asphalt layers in PP over semi-rigid pavement foundations creates more sustainable and trusted structures, despite a 2-5% increase in total cost.

5.3   Objective

The objective of present analytical study to develop a strain-based model of perpetual bituminous pavement design based on a method of equivalent thickness (MET) using fatigue and rutting as design criteria.

5.4   Perpetual pavement design model based on fatigue and rutting criteria

In this study, the pavement system has been characterized as a three-layer system as shown in Figure 5.1. The top layer consists of a bituminous binder base with thickness h_1 and resilient modulus E_1. The middle layer consists of unbound granular materials with thickness h_2 and composite elastic modulus of E_2 which ultimately rests on soil subgrade with an elastic modulus of E_3. The subgrade layer in a three-layered system has been considered as the foundation of pavement crust. In this study, the elastic modulus of the unbound granular layer has been estimated using Equation 5.1 as recommended by Powell et al (1984) [131]**.**

$$E_2 = 0.2\,(h_2)^{0.45} E_3 \; (MPa) \tag{5.1}$$

Where h_2 = thickness of the unbound granular layer, which is the summation of granular base and sub-base thickness (mm)
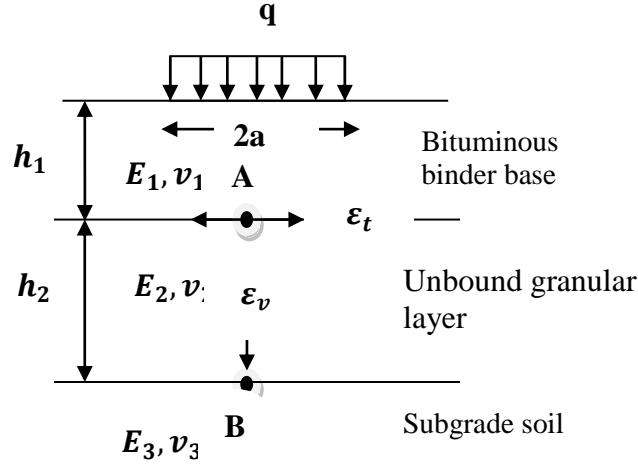
Figure 5.1: Typical flexible pavement section in a three-layered system

Moreover, the modulus of E_2 and E_3 may be determined by Equation 5.2 and Equation 5.3.

$$E_3 = 10 \; CBR \; (MPa) \; for \; CBR \le \; 5\% \tag{5.2}$$

$$E_3 = 17.6\,(CBR)^{0.64} \quad (MPa) \; for \; CBR > \; 5\% \tag{5.3}$$

Where CBR is the California Bearing Ratio of subgrade.

The thickness of the bituminous binder base in a bituminous pavement may be determined on the basis of radial tensile strain (RTS) occurring at the bottom of the bituminous binder base at point A or the vertical compressive strain (VCS) on the top of subgrade at point B in Figure 5.1. In bituminous road pavement, RTS at the bottom of the bituminous base relates to the pavement performance under fatigue whereas VCS on the top of the subgrade relates to the pavement performance under rutting. In the present study, the unbound granular layer thickness in a three-layered system has been considered constant for the estimation of binder base thickness. In order to estimate the VCS on subgrade or RTS in asphalt layer due to wheel load using Boussinesq's theory [34], the three-layered pavement system has been transformed into a homogeneous system by Odemark's [126] approach.

5.4.1 Transformation of multi-layered pavement system to homogeneous system by Odemark's method

In the present analysis, based on Odemark's [126] principle as described in Chapter 2 and Chapter 3, the equivalent thickness of bituminous binder base (h_1) may be expressed by Equation 5.4.

$$h_{eq1} = z = f h_1 \sqrt[3]{\frac{E_1}{E_2}} \tag{5.4}$$

However, substituting E_2 from Equation 5.1 in Equation 5.4, the following equation may be established

$$h_{eq1} = z = f_1 h_1 \sqrt[3]{\frac{E_1}{0.2\, h_2^{0.45} E_3}} \tag{5.5}$$

Similarly, the transformation of granular and soil layer with an elastic modulus of E_2 and E_3 respectively, has been made in present analysis with an equivalent thickness of h_{eq2}. The transformed layer h_{eq2} thus obtained will have an elastic modulus of E_3 .

$$\text{Therefore, } h_{eq2} = z_1 = f_2\left(h_{eq1} + h_2\right) \sqrt[3]{\frac{E_1}{E_3}} \tag{5.6}$$

However, substituting E_2 from Equation 5.1 and h_{eq1} from Equation 5.5 in Equation 5.6, the following Equation 5.7 has been established

$$h_{eq2} = z_1 = f_2 \left(f_1 h_1 \sqrt[3]{\frac{E_1}{0.2\, h_2^{0.45} E_3}} + h_2 \right) \sqrt[3]{\frac{0.2\, h_2^{0.45} E_3}{E_3}} \tag{57}$$

5.4.2 Design of perpetual pavement

In this analytical study, the concept of perpetual pavement design has been based on IRC-37-2018 [51. In IRC-37-2018, [51] the pavement with an axle load of 300 msa or more has been defined as perpetual pavement which has a minimum age of fifty years. Moreover, according to the guideline, the thickness of the bituminous base in a three-layered perpetual pavement may be determined on the basis of an allowable RTS of 80 µε at the bottom of a bituminous binder base. Furthermore, the thickness of a bituminous binder base may also be obtained by limiting the VCS on the top of the subgrade to 200 µε as recommended in IRC: 37-2018 [51]. The higher value of the bituminous binder base thus obtained from RTS and VCS criteria has been recommended in

this study as design thickness for perpetual road pavement. In present analysis, RTS at the bottom of the bitumen base has been termed as fatigue strain and similarly the VCS on top of subgrade as rutting strain.

5.4.3 Determination of bituminous binder base thickness based on radial tensile strain (RTS)

According to Boussinesq's [34] theory, in a homogeneous, elastic and isotropic medium with an elastic modulus of (E_2), the RTS (ϵ_t) at a depth (z) due to an uniformly distributed circular load intensity (q) with a contact radius (a) may be expressed as shown in Equation 5.8 and Figure 5.2.

$$\epsilon_t = \frac{(1+v)q}{2E_2}\left[\frac{-\frac{z}{a}}{\left\{\sqrt{1+\left(\frac{z}{a}\right)^2}\right\}^3} - (1-2v)\left\{\frac{\frac{z}{a}}{\sqrt{1+\left(\frac{z}{a}\right)^2}} - 1\right\}\right] \tag{5.8}$$
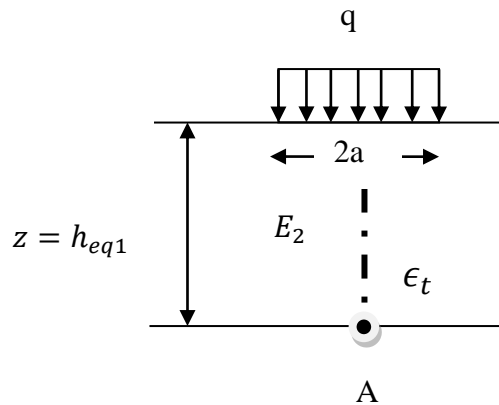
Figure 5.2: Transformed section up to bottom of bituminous binder base

In the present analysis a combined base and sub base thickness of 450 mm (h_2) has been considered as input parameter for most of the road sections with relatively higher axle loads as recommended in IRC-37-2018 [51].

In order to determine the RTS below the bottom of the bituminous base in pavement, the top two layers in a three-layered system may be transformed as explained earlier with the equivalent thickness h_{eq1} as shown in Figure 5.2. The Equation 5.8 is a generalized equation applicable in a homogeneous system, which has been used in the present analysis by substitution of the term 'z' by transformed depth h_{eq1} as explained in Equation 5.5 Assuming (z/a) = M, and

considering f = 0.9 for the layer interface of binder base and unbound granular layer Equation 5.8 may further be modified as shown in Equation 5.9.

$$\epsilon_t = \frac{(1+v)q}{2\times0.2\, h_2{}^{0.45}E_3}\left[\frac{-M}{\left\{\sqrt{1+(M)^2}\right\}^3} - (1 - 2*v)\left\{\frac{M}{\sqrt{1+(M)^2}} - 1\right\}\right] \qquad (5.9)$$

Therefore, the thickness of the binder base (h_1) in a perpetual pavement may be estimated by limiting the RTS (ε_t) at the bottom of bituminous binder base. In present analysis, the allowable fatigue strain of 80 μɛ has been used in Equation 5.9 to estimate the binder base thickness for different subgrade CBR ranging from 5% -15%.

5.4.4 Determination of bituminous binder base thickness based on vertical compressive strain (VCS)

To determine the VCS (ϵ_v) at point B as shown in Figure 5.1, the top two layers of the pavement with thickness h_1 and h_2 in a three-layer system may be transformed using Odemark's [126] method as shown in the Figure 5.3. The VCS at point B in an elastic homogeneous medium with an elastic modulus (E_3) at a depth z_1 under an uniformly distributed circular load intensity(q) with a contact radius (a) can be obtained using Boussinesq's [34] theory as expressed in Equation 5.10.

$$\epsilon_v = \frac{(1+v)q}{E3}\left[\frac{\frac{z_1}{a}}{\left\{\sqrt{1+\left(\frac{z_1}{a}\right)^2}\right\}^3} - (1 - 2v)\left\{\frac{\frac{z_1}{a}}{\sqrt{1+\left(\frac{z_1}{a}\right)^2}} - 1\right\}\right] \qquad (5.10)$$

To determine the VCS (ϵ_v)at the top of subgrade as shown in Figure 5.1, in a three-layered system, the depth $\left(h_{eq2}\right)$ up to top of subgrade has been determined in Equation 5.7. However, considering $M_2 = z_1/a$ and $f_2 = 0.9$ for the interface of subgrade and unbound granular layer Equation 5.10 may further be modified as Equation 5.11.
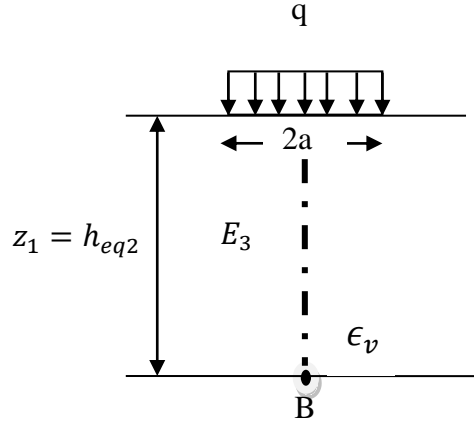
Figure 5.3: Transformed section up to top of subgrade

$$\epsilon_v = \frac{(1+v)q}{E_3}\left[\frac{M_2}{\left\{\sqrt{1+(M_2)^2}\right\}^3} - (1-2v)\left\{\frac{M_2}{\sqrt{1+(M_2)^2}}1\right\}\right]$$
(5.11)

Therefore, the thickness of the binder base (h₁) in a perpetual pavement may be estimated by limiting the VCS (ε_v) on the top of the subgrade layer. In present analysis, the allowable strain of 200 µε has been used in Equation 5.11 to estimate the binder base thickness for different subgrade CBR ranging from 5% -15%. The higher value of the thickness of binder base obtained from RTS or from VCS has been considered as design thickness.

5.4.5 Design of bituminous binder base thickness based on axle load criteria

An alternative approach for the design of perpetual pavement has been explored in the present study considering the load-carrying capacity of the pavement as 300 msa as recommended in IRC: 37-2018. [51] The allowable RTS at the bottom of the bituminous base corresponding to 300 msa load repetitions has been determined from the mechanistic-empirical correlations recommended in IRC: 37-2018 [51] and shown in Equation 5.12 and 5.13 for different reliability levels. The allowable strain thus obtained corresponding to 300 msa with 90% reliability level has been used in Equation 5.9 for estimation of binder base thickness for different subgrade CBR ranging from 5% to 15%. The allowable fatigue strain in the present analysis for 300 msa load repetitions was obtained as 112 µε considering 90% reliability.

$$N_f = 1.6064 \text{ xC x}10^{-04}\text{x} \left[\frac{1}{\epsilon_t}\right]^{3.89} \text{x} \left[\frac{1}{M_R}\right]^{0.854} \quad \text{For 80\% reliability} \quad (5.12)$$

$$N_f = 0.5161\text{x C x}10^{-04} \text{ x} \left[\frac{1}{\epsilon_t}\right]^{3.89} \text{x} \left[\frac{1}{M_R}\right]^{0.854} \text{For 90\% reliability} \quad (5.13)$$

Where $C = 10^M$ and $M = 4.84 \text{ x} \left(\frac{V_{be}}{V_a+V_{be}} - 0.69\right)$

N_f= Fatigue life in the number of cumulative standard axles.

ϵ_t = Maximum tensile strain at the bottom of the bituminous base, and

M_R= Resilient modulus of the bituminous base (MPa).

V_{be} = Percent of the volume of effective bitumen in bituminous mix

V_a = Percent of the volume of air voids in bituminous mix

The allowable VCS on top of the subgrade has also been determined from the Mechanistic-Empirical correlations recommended in IRC: 37-2018 [51]. The correlation between VCS and anticipated wheel load repetitions before failure of the pavement under rutting has been shown in Equation 5.14 and Equation 5.15 for different reliability levels.

$$N = 4.1656 \text{ x}10^{-08}\text{x} \left[\frac{1}{\epsilon_v}\right]^{4.5337} \text{For 80 \% reliability} \tag{5.14}$$

$$N = 1.41\text{x } 10^{-08}\text{x} \left[\frac{1}{\epsilon_v}\right]^{4.5337} \qquad \text{For 90 \% reliability} \tag{5.15}$$

N = Number of cumulative standard axles before failure in rutting

ϵ_v = Maximum VCS on the top of subgrade layer

The allowable VCS on the top of the subgrade layer corresponding to 300 msa load repetitions has been estimated as 250µε for 300 msa load with 90% reliability level using Equation 5.15.The allowable VCS thus obtained has been used in Equation 5.11 for estimation of binder base thickness for different subgrade CBR ranging from 5% to 15%. It is to be noted that the binder base thickness has its influence both on radial strain at the bottom of the binder base at the first interface and also on VCS on top of subgrade at the second layer interface, in a three-layered system. Against this backdrop, the design of perpetual pavement in the present study has been made based on both fatigue and rutting as failure criteria. Flow diagram of adopted methodology for perpetual pavement design has been shown in Figure 5.4
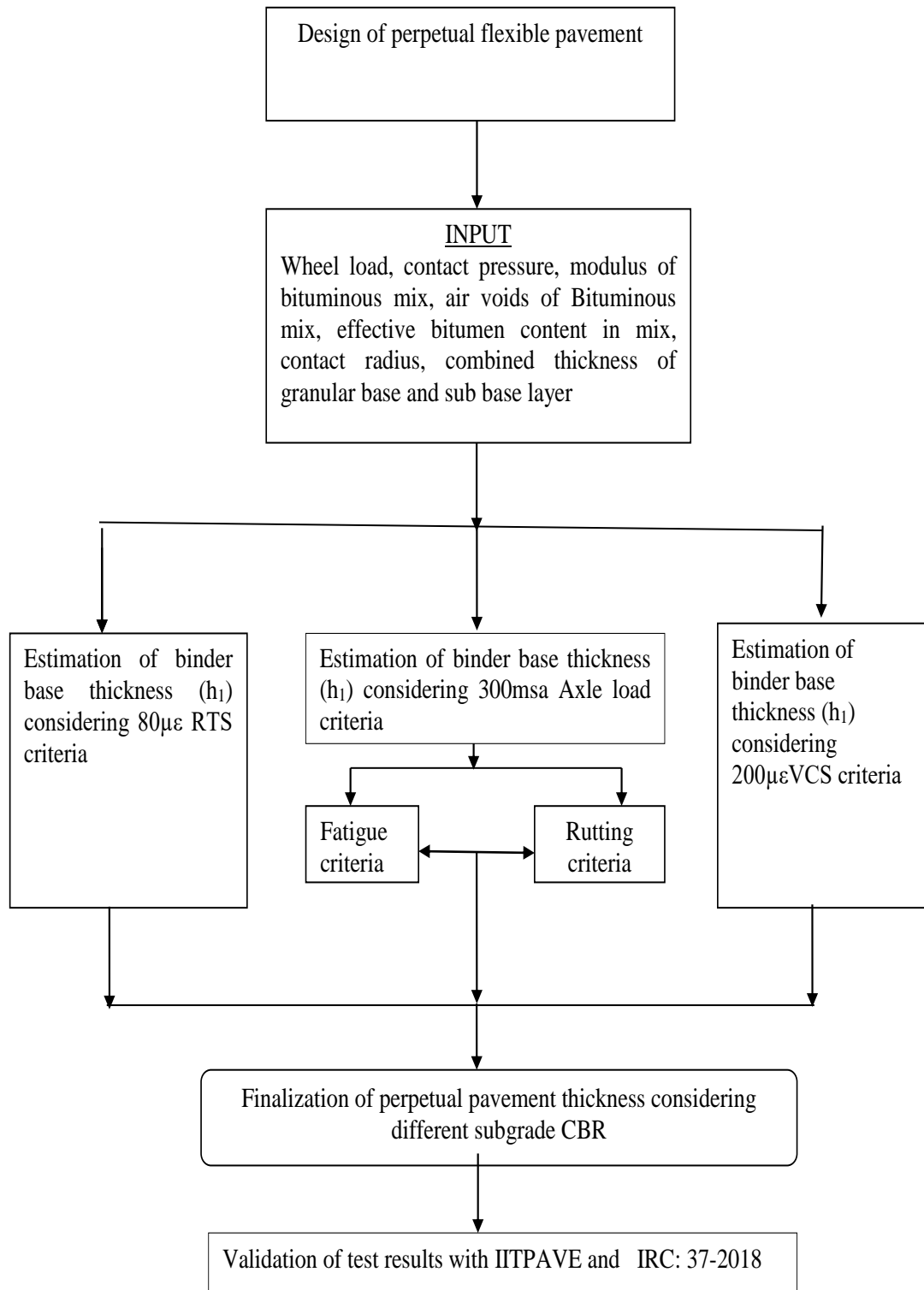
Figure 5.4: Flow diagram of adopted methodology for perpetual pavement design

5.4.6   Input parameters used in pavement design

The input parameters used in the estimation of bituminous binder base thickness are as follows

Wheel load = 40 kN

Contact pressure of wheel on pavement surface = 0.56 MPa

Resilient modulus of Bituminous mix = 3000 MPa

Air voids in bituminous mix = 3.5%

Volume of effective bitumen in bituminous mix = 11.5%

Contact radius between tire and pavement = 151 mm

The combined thickness of unbound granular layer = 450 mm

5.5   Results and discussion

The thickness of binder base estimated using present methodology on the basis of allowable fatigue strain of 80 με and an allowable rutting strain of 200 με have been presented in Table 5.1 to Table 5.2 (Appendix 4A) and Figure 5.5 to Figure 5.6.It has been observed that the thickness of the binder base reduces with the increase in subgrade CBR both under fatigue and rutting failure. The thickness of binder base under fatigue was found to vary between 307mm to 264 mm for change in subgrade CBR from 5% to 15% and the same under rutting was found to range between 308 mm to 203 mm. It is evident that the rate of change of binder base thickness is higher under rutting than fatigue. It has also been observed from present analysis that the thickness of the bituminous binder required to withstand fatigue is generally more than that required to withstand rutting under specified axle load repetitions. Therefore, the recommended thickness of bituminous binder base has been considered as the thickness obtained against fatigue criteria. Hence, it can be concluded that the performance of perpetual pavement is generally governed by its failure under fatigue.

Definition of perpetual road pavement includes the load-carrying capacity of road pavement in Indian conditions as 300 msa which may sustain up to 50 years without major distress. In this backdrop, the bituminous binder base thickness for perpetual pavement has also been estimated considering 90%

reliability level of fatigue and rutting criteria as recommended in IRC-37-2018 [51].Therefore, the allowable strain values for perpetual pavement design against rutting as well as fatigue have been determined from Equation 5.13 and Equation 5.15 corresponding to 300 msa load repetitions. The allowable RTS and VCS were estimated as 112 $\mu\varepsilon$ and 250 $\mu\varepsilon$ respectively, which have been used for the design of binder base using the present methodology. The thicknesses of the binder base thus obtained have been presented in Table 5.3 and Table 5.4 (Appendix 4A) and Figure 5.7 and Figure 5.8.It has been observed from the data in Table 5.3 and Table 5.4 (Appendix 4A) that, the binder base thickness obtained from fatigue criteria using present method is higher in comparison with the thickness obtained from rutting criteria. Therefore, the recommended thickness of the binder base shall be governed by the fatigue strain. The thickness thus obtained based on fatigue strain has been found safe both from cracking and rutting. The thickness of binder base under fatigue was found to vary between 255 mm to 215 mm for change in subgrade CBR from 5% to 15% and the same under rutting was found to vary between 254 mm to 155 mm. It is relevant to mention that the thickness of the binder base of a perpetual road pavement thus obtained considering 300 msa load appears to be less in comparison to the thickness obtained using 80$\mu\varepsilon$ finite fatigue strain and 200$\mu\varepsilon$ finite rutting strain. The reason for such reduction in binder base thickness is due to an increase in allowable fatigue strain corresponding to 300 msa load repetitions. The thicknesses obtained from finite strain and finite load based approaches have been presented in Table 5.5 (Appendix 4A) and Figure 5.9 to get the recommended binder base thickness of perpetual pavement.

5.5.1 Validation of binder base thickness obtained from proposed finite strain criteria using IITPAVE

The validation of the present method has been done in present study by using IITPAVE [51] software. The pavement thickness obtained using the present methodology has been used as an input parameter in IITPAVE [51] software for estimating RTS at the bottom of the bituminous binder base and the VCS on the top of the subgrade. The strain and thickness thus obtained against fatigue and rutting criteria have been presented in Table 5.6 (Appendix 4A) and Figure 5.10.The RTS obtained from IITPAVE [51] corresponding to binder base

thickness estimated using the present methodology based on finite fatigue strain was in the range between 94 to 91 µε for subgrade CBR ranging from 5% to 15% whereas the allowable fatigue strain of 80 µε was considered as input parameter for pavement design in the present method. Similarly, the VCS obtained from IITPAVE [51] on the top of the subgrade was found to vary between 182 to 141 µε. However, for subgrade CBR ranging from 5% to 15%, the allowable VCS of 200 µε was considered as an input parameter for perpetual pavement design in the present analysis. So, it is evident from the strain data presented in Table 5.6 (Appendix 4A) that the thickness of the binder base obtained using the finite strain based method is reasonably safe under rutting in comparison with IITPAVE [51] output but fails marginally under fatigue. In this backdrop, the allowable RTS at the bottom of the bituminous binder base may be revised and increased to 95 µε instead of 80 µε. Similarly, the recommended allowable VCS on the top of subgrade may be revised and reduced to 185 µε instead of 200 µε considered in the present analysis.

5.5.2 Validation of binder base thickness obtained from proposed finite load criteria using IITPAVE

The validation of perpetual pavement thickness obtained in present study based on finite load (300msa) criteria has been made in Table 5.7 (Appendix 4A) and Figure 5.11. The binder base thickness for different subgrade CBR has been back-calculated using IITPAVE [51] based on allowable fatigue strain corresponding to 300 msa and reported in Table 5.7 (Appendix 4A) and Figure 5.11. It is evident in Table 5.7 (Appendix 4A) that IITPAVE [51] generated binder base values are 9% more that than the value obtained from the present finite load based method and therefore may be considered close and comparable. The binder base thickness obtained using the present finite strain criteria ranged between 307 mm to 264 mm for subgrade CBR ranging from 5% to 15%, whereas the thickness of binder base obtained using IITPAVE [51] for the same CBR range varied between 340 mm to 289 mm. The reason of this variation may be due to the difference in boundary conditions considered in IITPAVE [51] software and the present analytical method which assumes the failure of pavement as linear and elastic.
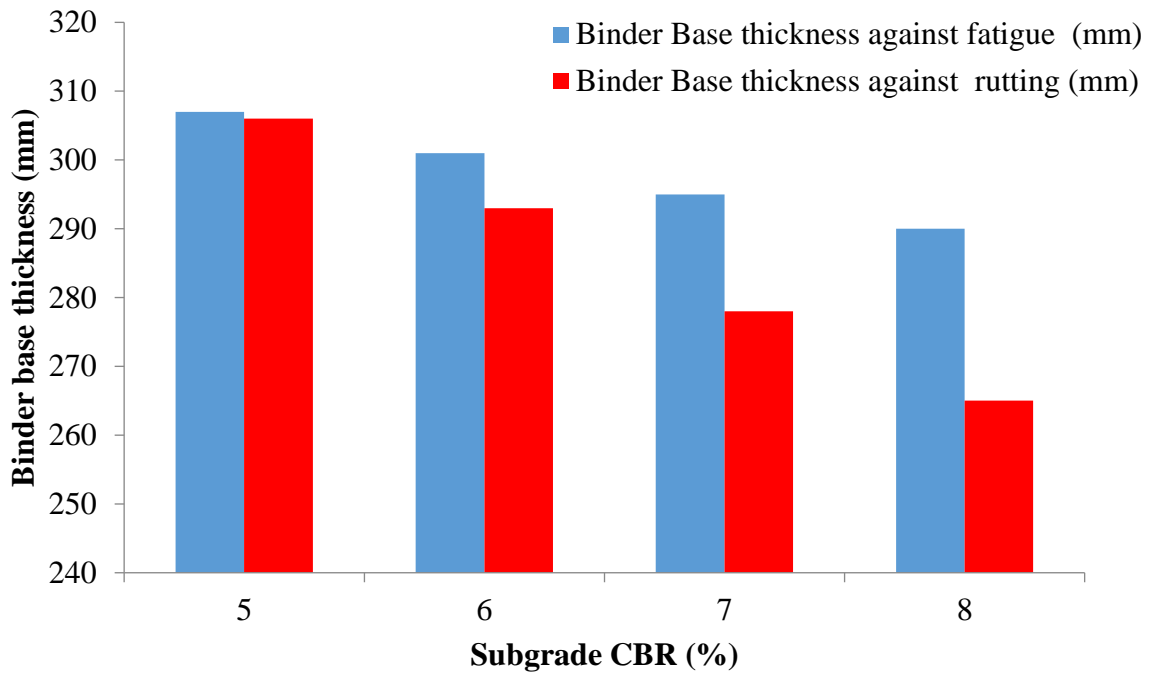
Figure 5.5: Binder base thickness of perpetual pavement of subgrade CBR from 5%-8% based on finite strain criteria
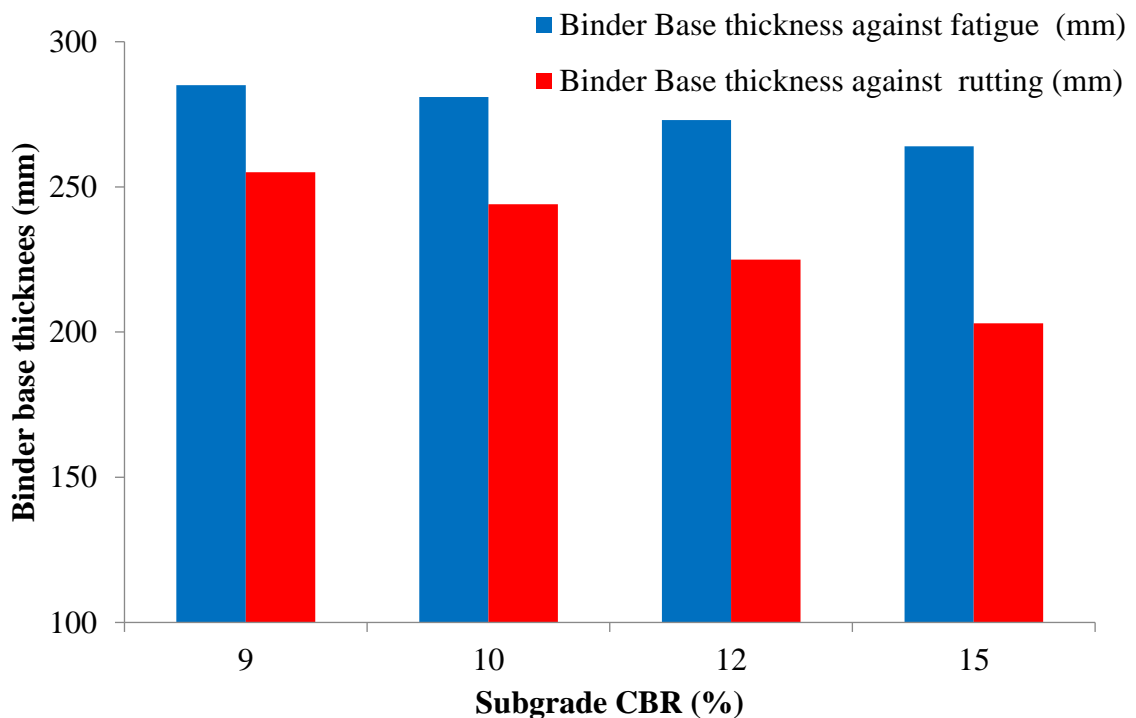
Figure 5.6: Binder base thickness of perpetual pavement of subgrade CBR from 9%-15% based on finite strain criteria
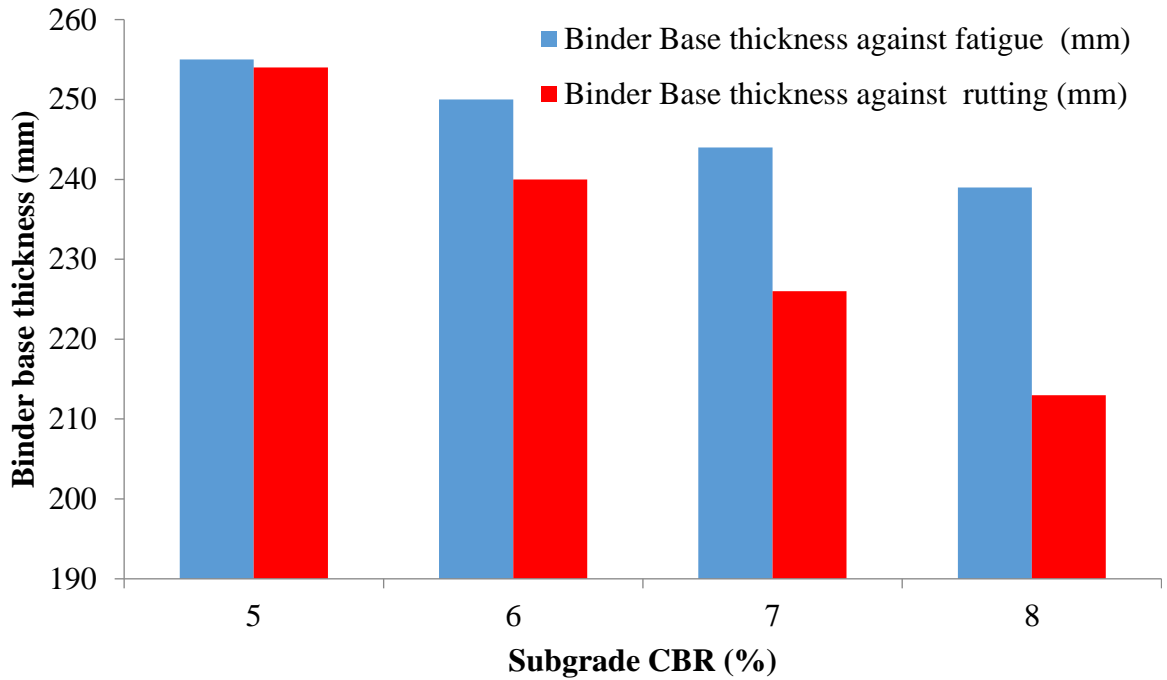
Figure 5.7: Binder base thickness for perpetual pavement of subgrade CBR 5%-8% based on finite load criteria
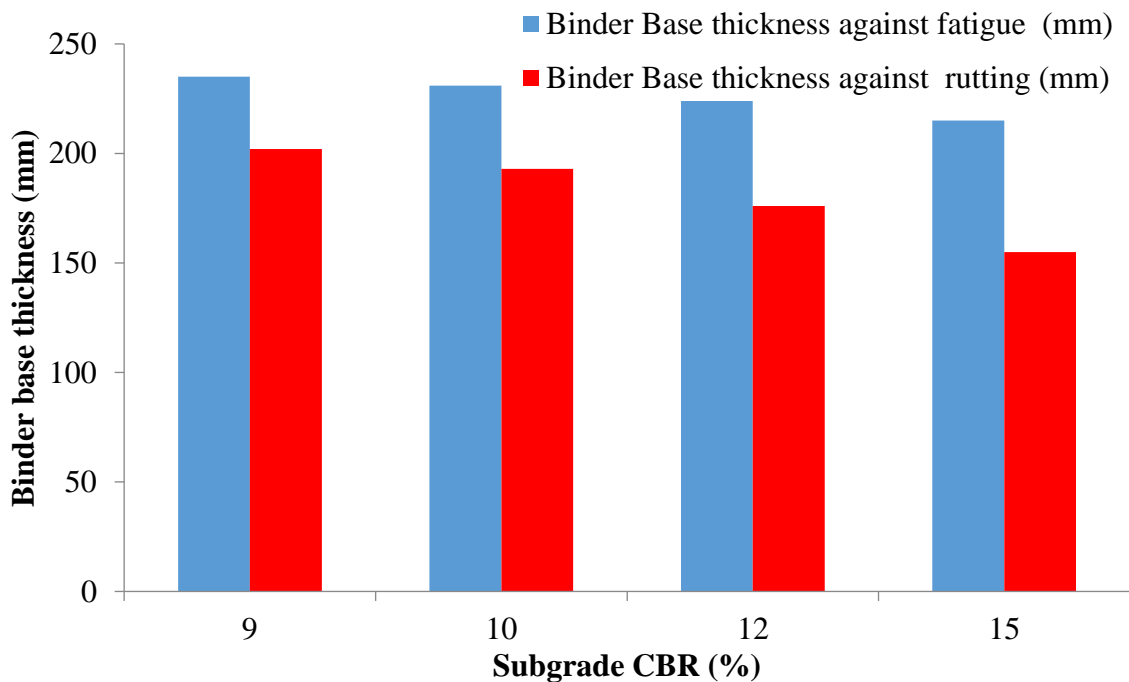
Figure 5.8: Binder base thickness for perpetual pavement of subgrade CBR 9%-15% based on finite load criteria
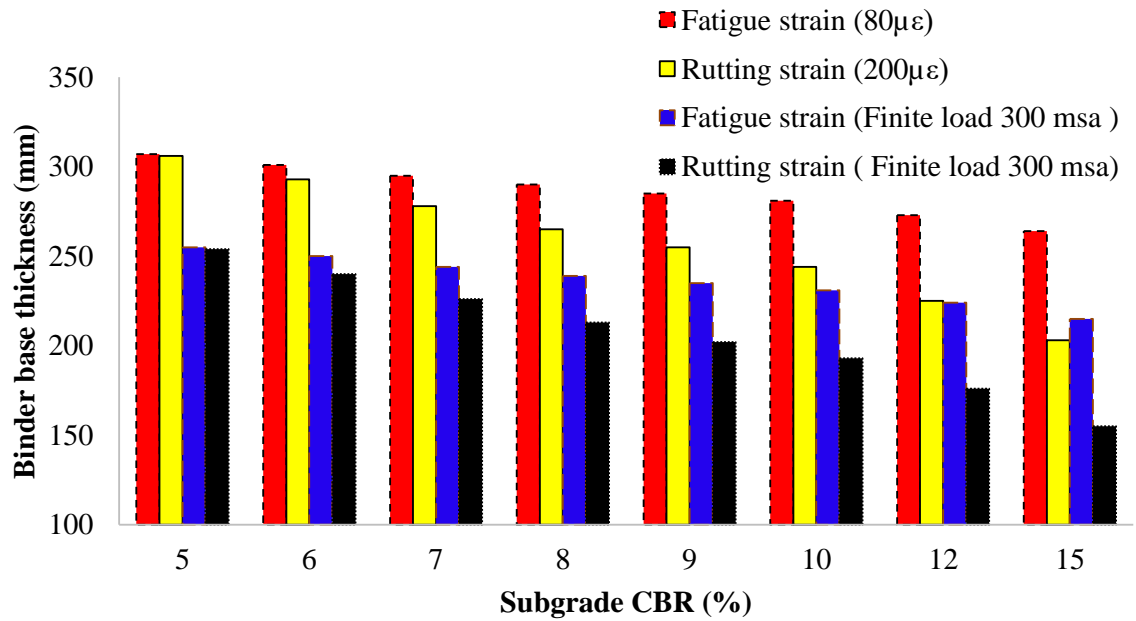
Figure 5.9: Recommended binder base thickness of perpetual pavement for subgrade CBR 5%-15% based on finite strain and load criteria
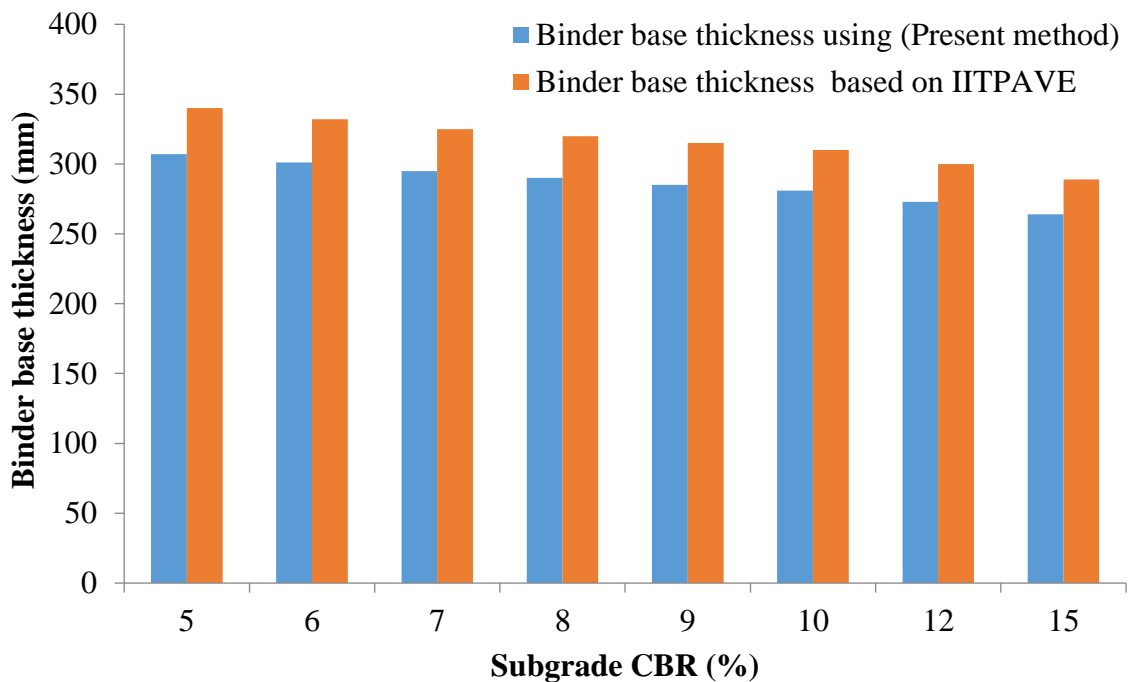
Figure 5.10: Comparison of binder base thickness using IITPAVE and present method based on finite strain criteria
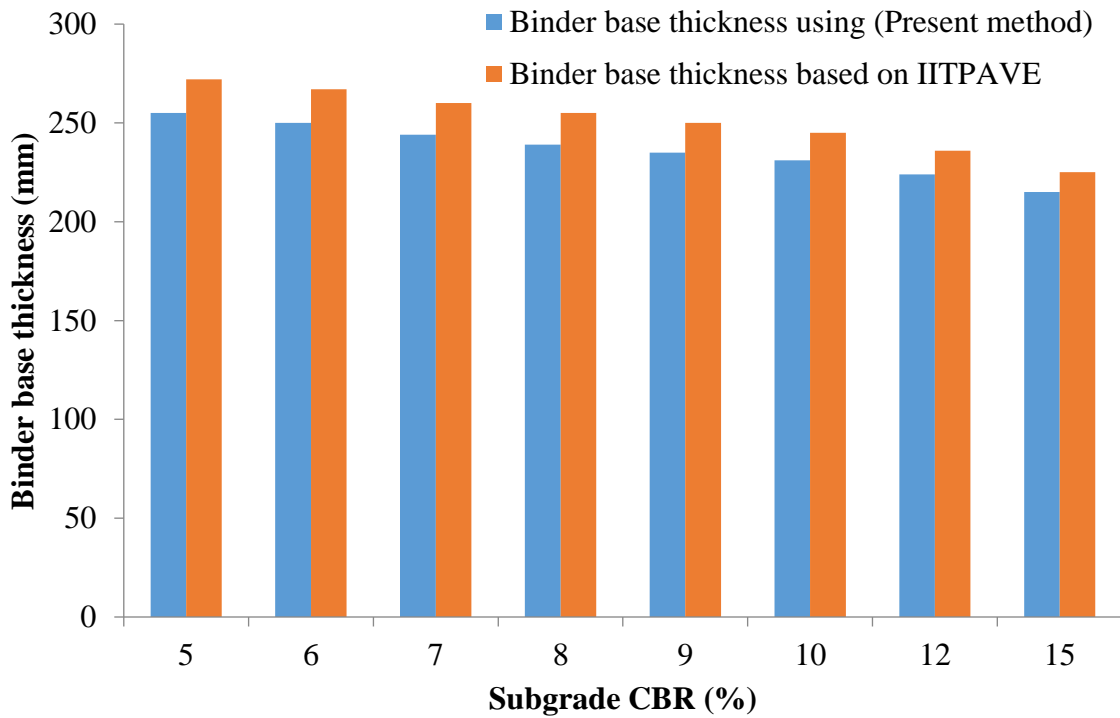
Figure 5.11: Comparison of binder base thickness using IITPAVE and present method based on finite axle load repetition

5.5.3 Validation of present method using IRC: 37-2018

The method proposed in this study for estimation of perpetual pavement thickness has also been used for the estimation of conventional bituminous road pavement thickness for its validation.

The thickness of binder base of pavement corresponding to specified axle load and subgrade CBR has been determined using the present methodology for comparative study with the recommended thickness as in IRC: 37-2018. The thickness of the binder base has been determined to limit fatigue failure by solving Equation 5.9 and Equation 5.13.Similarly, the thickness of the binder base has also been obtained in this study to limit failure of pavement against rutting by solving Equation 5.11 and Equation 5.15 for different axle load repetitions and subgrade strength. Thus the higher value of binder base obtained against fatigue and rutting has been considered as design thickness.

The thickness of the unbound granular layer in the present analysis has been considered as 450 mm for validation and the subgrade CBR of 5%, 8%,

and 10% were considered. The axle load range in the present analysis has been considered between 5-20 msa as lower axle load group and between 30-50 msa as higher axle load group. The design thickness of the binder base thus obtained using the present method has been compared with relevant layer thickness as recommended in IRC: 37-2018 and presented in Table 5.8 and Table 5.9 (Appendix 4A) and Figure 5.12 to Figure 5.15. It is evident from the data presented in Table 5.8 and Table 5.9 (Appendix 4A) that the binder base thickness obtained using the present method is reasonably close with respect to the binder base thickness recommended in IRC: 37-2018 for low to high CBR as well as for low to high axle load groups.

It may be noted that, for a lower axle load of 5 msa with subgrade CBR 5% and 8%, the variation in binder base thickness obtained by two different methods were in between 4.2% and 3.7% respectively.

However, for a higher axle load of 50 msa, the same variation in binder base for subgrade CBR 5% and 8% were found to 1.8% and 5.1% respectively. It has been found that the variation in binder base thickness between the two methods is marginal for higher subgrade CBR and for higher axle loads. In this backdrop, the observed convergence of binder base thickness justifies the acceptability of present method. Finally recommended binder base thickness for different subgrade CBR using present method have been presented in Table 5.10
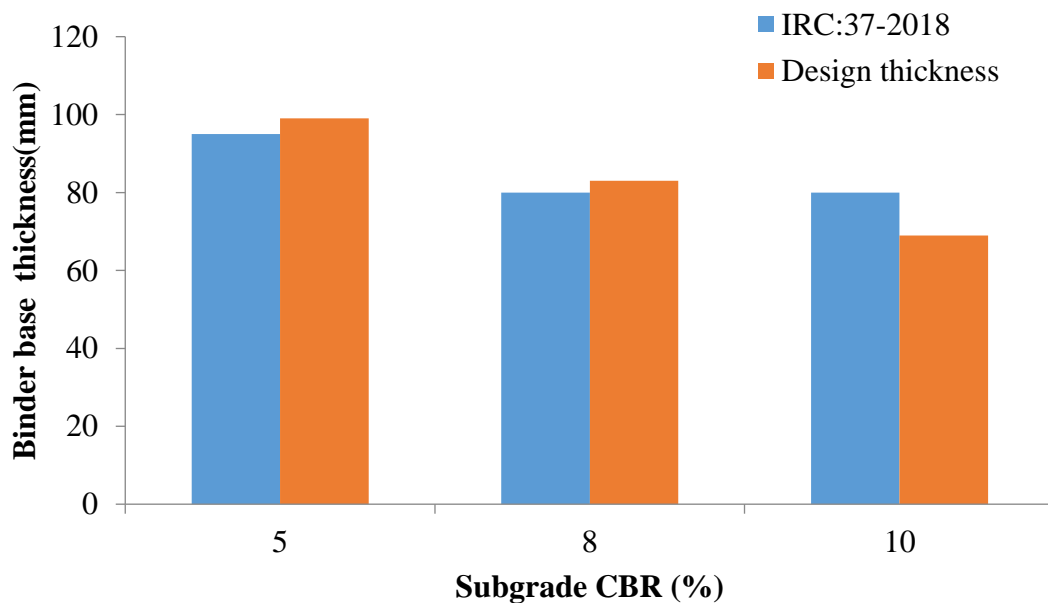
Figure 5.12: Comparison of binder base thickness using present method and IRC-37-2018 for subgrade CBR 5% - 10%and 5 msa axle load repetitions.
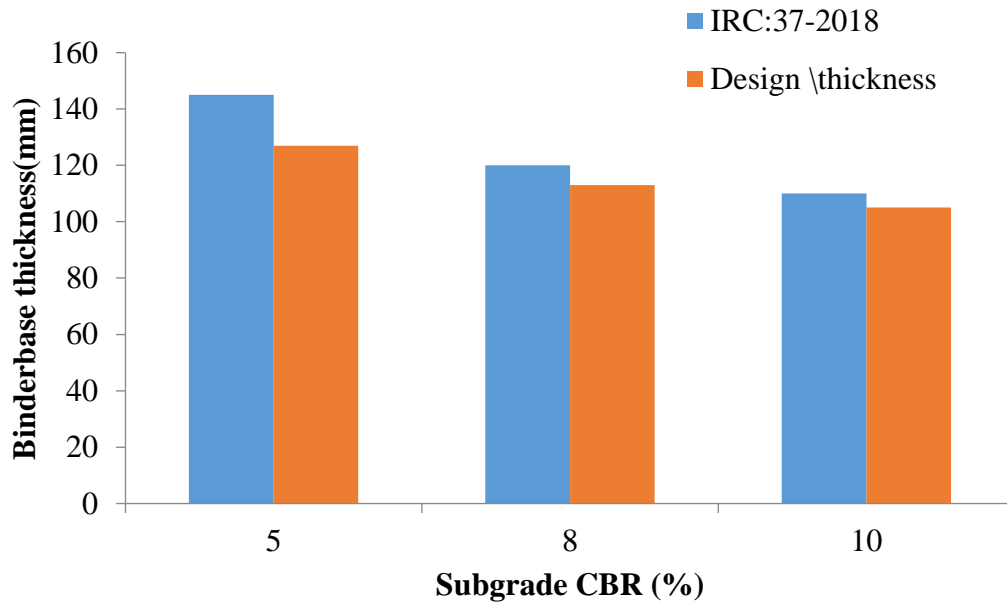
Figure 5.13: Comparison of binder base thickness using present method and IRC-37-2018 for subgrade CBR 5% - 10%and 20 msa axle load repetitions.
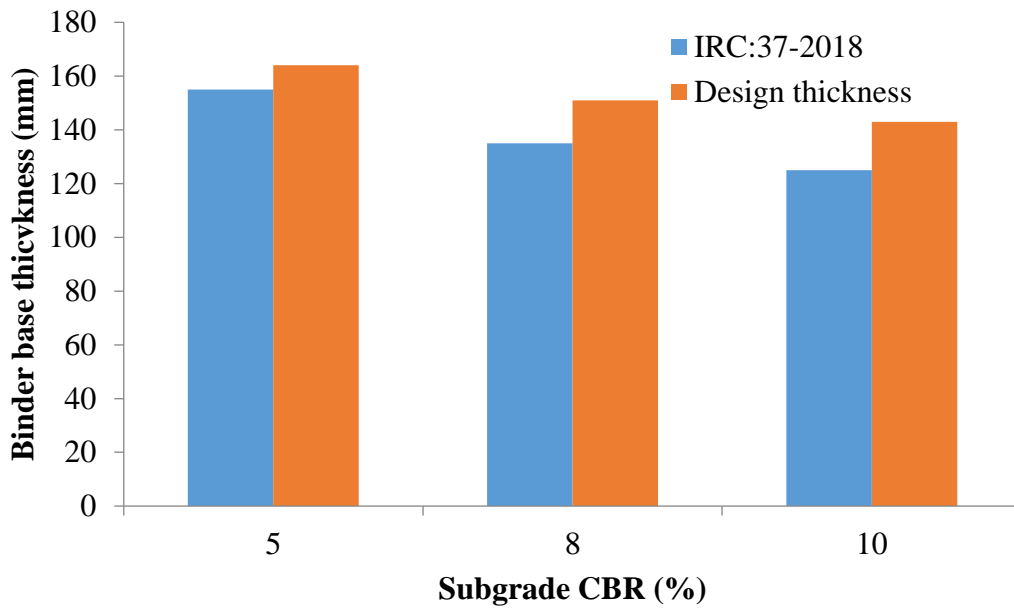
Figure 5.14: Comparison of binder base thickness using present method and IRC-37-2018 for subgrade CBR 5% - 10%and 30 msa axle load repetitions.
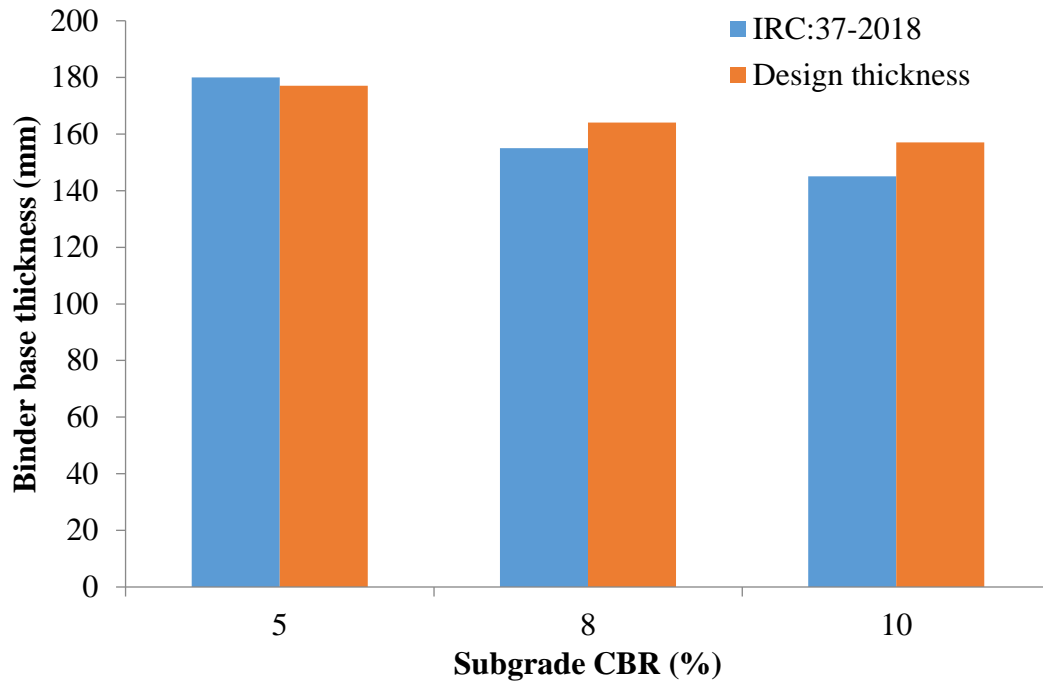
Figure 5.15: Comparison of binder base thickness using present method and IRC-37-2018 for subgrade CBR 5% - 10%and 50 msa axle load repetitions.

5.6   Concluding remarks

The methodology for perpetual pavement design proposed in this study can also be used for the estimation of conventional bituminous pavement thickness considering the pavement as a multi-layered system. The reliability of present method has been compared with IRC: 37-2018 and found to be satisfactory. It has been observed in the present analysis that the thickness of the binder base required to withstand fatigue is generally more than that required to withstand rutting under a specified axle load repetition. Therefore, it can be concluded that the performance of perpetual pavement is governed by its failure under fatigue.

It is relevant to mention that the thickness of the binder base in a perpetual road pavement obtained using 300 msa load appears to be less than the thickness obtained using finite strain-based criteria. For validation of the present method, fatigue and rutting strains were estimated using IITPAVE [51] for the pavement thickness obtained using present methodology. It has been found from the critical strain data, that the allowable RTS at the bottom of a bituminous base should be revised as 95$\mu\varepsilon$ instead of 80$\mu\varepsilon$ for perpetual pavement design.

Similarly, the allowable VCS on the top of the subgrade may be modified to 185µε instead of 200 µε. However, the allowable fatigue or rutting strains for the design of perpetual road pavement will increase if the design load of 300 msa is considered. Moreover, the thickness of the binder base obtained using IITPAVE [51] and the present study shows good convergence. Therefore, the present method may be considered as an alternative and reliable approach of Mechanistic- Empirical design of perpetual flexible pavement.

CHAPTER 6
MECHANISTIC EMPIRICAL DESIGN OF BITUMINOUS OVERLAY

6.1   Introduction

Repair of airport and road pavements has gained more importance over the years. Road connectivity in India has got major importance in its infrastructure development works in the last twenty years. With the increase in length of the major new road network, the need for repair of such pavements has also increased substantially. Particularly, the unanticipated impact of climate change and loading has been found to affect the serviceability of road pavement to a great extent. Therefore, prediction of terminal serviceability criteria and preparing a repair plan accordingly with appropriate materials has become the prime need of the hour in a pavement maintenance program. In this backdrop, an effective and innovative design of overlay is required to make the road pavements durable and functional. Design of overlay can be done either on stress, strain, or deflection-based criteria corresponding to expectedaxle load repetitions during its service life. Therefore , attempts have been made by several researchers to design bituminous overlay thickness on existing damaged flexible road pavement based on Empirical, Mechanistic, and Mechanistic-Empirical approaches. In this context, efforts have been taken in this study to design bituminous overlay thickness using interface deflectionat pavement overlay interface as a design parameter using a mechanistic-empirical approach.

The most sustainable way of pavement rehabilitation is to put an overlay on the top of a bituminous layer on an existing structurally weakpavement in today's world of severely depleting natural sources for construction. The thickness of overlay depends upon several parameters of existing in-situ pavement, amongst those, pavement modulus of different layers, the thickness of constituent layers, and projected traffic; Poisson's ratio are important. Current design procedure of Overlay design e.g. Asphalt Institute (AI) [10] method is based on semi-empirical and semi–mechanistic, resulting in either premature failure or overestimated pavement parameters thereby making it sometimes economically non-viable. Thus, the present study tries to include an alternative approach in the field of overlay design and present a comprehensive comparative analysis with respect to widely used AI [10] method.

The higher value of pavement deflection indicates lower strength of pavement and vice versa. Therefore, the damage and distress of pavement can be quantified using pavement deflection data. The objective of putting an overlay on the existing pavement is to limit stress, strain, and deflection at different layer interfaces of the multi-layered system in the pavement to make the pavement durable and functionally more efficient from its serviceability point of view. Several correlations have been developed between allowable numbers of load repetitions (Huang et al. 1984B.C.)[87-90] with allowable vertical stress and modulus of subgrade for analysis of pavement performance. An Empirical relationship (Ullidtz.1997)[181] based on the AASHTO [1,2,3] road test may be used to determine the stress developed on unbound materials before its failure. The regional factor in this relationship is an important parameter to be carefully chosen. NCHRP-128 guide may be referred for values in detail. Amongst those, Boussinesq's [34], Huang [87-90], and Danish [181] criteria are found to be effective in finding the stress level at the desired depth. Several researchers (Haung, Ullidtz, and Horak) [87-90, 181, 83-85] have found Odemark's method useful in transforming the depth into equivalent depth to be readily applicable for a homogeneous medium. Interface deflection (Huang 1969c [87-90], Solanki et al 2016 [168] Loganathan, et al 2019[108] ,Naughton et al 2019 [123] , Purakayastha et. al .202 0[137] is an important criterion for a two-layer new pavement or overlay design. Studies have also been carried out to find most sensitive [151] parameters for overlay design. Against this backdrop, present study is intended to make new contributions in the field of overlay design with special reference to AI [10] method.

6.2   Literature review

S.V.Dinesh et al. (2022) [157] proposed a study to use BBD and FWD as a non-destructive testing method to evaluate the structural condition of a pavement that deteriorated over time due to traffic movement. It was concluded that the FWD is more reliable as it reduces the overlay thickness with a better degree of traffic simulation. India's flexible pavements face deterioration due to heavy traffic, requiring evaluation and maintenance measures. Benkelman Beam Deflectometer (BBD) and Falling Weight Deflectometer (FWD) are widely used

non-destructive techniques. The study conducted in a 5 km National Highway stretch in Bangalore, Karnataka, developed a correlation between FWD and BBD, analyzing pavement structural evaluation using KGP-BACK and IIT-PAVE. A linear correlation was developed, with a coefficient of correlation (R2) of 0.8994. The study considers FWD as a reliable method for pavement structural evaluation and cost-effective, reducing desired overlay thickness.

Sahis,M.K. et al. (2021) [151] formulated to determine the appropriate thickness of bituminous overlay for existing flexible road pavement, aiming to minimize vertical stress at the interface between the pavement and overlay. This research treats the combination of new overlay and old pavement as a two-layered system. Vertical stress at the interface is calculated using Boussinesq's theory after transforming the system using Odemark's method. The calculated stress is then compared with allowable vertical stress from empirical data to estimate overlay thickness for various axle loads and pavement deflections. The paper compares the overlay thickness obtained from this approach with that from the Asphalt Institute method, finding reasonable agreement. The curvature of the overlay under wheel load, represented by the base layer index, is used as a performance measure. Comparative analysis between overlay thicknesses determined by stress-based and deflection-based criteria is provided, showing that stress-based methods produce reliable and crack-resistant overlay thickness estimates. Sensitivity analysis indicates that the bituminous mix modulus is more influential than axle load repetitions in estimating overlay thickness.

Singh and Sahoo (2020) [166] proposed a study for a two-layered low-volume flexible pavement. Rutting has been considered as the major mode of distress for this type of pavement. Single and standard axle dual wheel assembly was used in the study for the determination of interface deflection.The study analyzes two-layered flexible pavements for low volume roads, focusing on surface and interface deflections. The study proposes a new formulation to determine surface and interface deflections for single and standard axle dual wheel assembly in two-layered flexible pavement systems. The formulation considers factors like tire imprint, granular base course modulus, pavement thickness, and pavement and subgrade ratio. The effect of Poisson's ratio was considered insignificant. In this paper, reflection factors were generated in non-

dimensional charts as a function of pavement and subgrade modulus, pavement thickness, and tire width.

S.Purakayastha et al. (2020) [137] formulated a methodology for the determination of bituminous thickness using the M-E approach. The modular ratio has been used to determine the interface deflection of a two-layered flexible pavement to determine the overlay thickness of specified resilient modulus so that interface deflection becomes equal to allowable deflection.

T. Chopra et al. (2019)[167] proposed a study to ascertain the pavement management and maintenance from the response of the pavement against the applied load. FWD and KGPBACK were used to evaluate the performance of a certain road section in terms of deflection of the pavement response against applied load. The evaluated data were used to generate a highway development model to observe the effect of the bituminous overlay on different distresses cracking, raveling, rutting, roughness, etc.

S. Romanoschi et al. (2019) [147]studied that NDT testing such as falling weight was used widely to evaluate the structural capacity of pavement at different levels. The deflection bowl was drawn from different layer indexes obtained using FWD. The study further reveals that different parameters that developed during the study can be easily applied in the pavement management system database to obtain the most efficient maintenance strategy.

M.Belachia et al. (2019) [116] mentioned that for flexible pavement, permanent deformation can occur in terms of rutting due to the accumulation of strain in different layers of the materials. The study evaluated the deflection basin of pavement using a falling weight deflectometer, considering Boussinesq's equation and Odemark's layers transformation. The paper emphasized the importance of identifying and addressing flexible pavement deformation due to factors like traffic and environmental conditions. The study proposed efficient methods for analyzing and comparing deflection basins at the CTTP of Algiers using deflectographs and falling mass deflectometers. The results showed asphalt layer modules have a minimum average deflection variation of 8.80%, consistent with measured deflection. The study also verified degraded pavement reinforcement using ELMODE6 and ALIZEIII programs.

G. Hall et al. (2019) [173] proposed a study to evaluate the pavement condition using a falling weight deflectometer at a different location.Different

layer indexes such as BLI, MLI, and LLI, were evaluated from deflection determined at a different point to draw the deflection bowl. The study further reveals that a good correlation was found during the assessment of upper and lower layers using a falling weight deflectometer.

P.J.Gundaliya (2016) [168]applied a falling weight deflectometer to assess the current structural condition of an in-service pavement system.FWD was used to evaluate the deflection bowl index such as SCI, MLI, and LLI The study conclude that the SCI was found to be 240 microns above which the pavement conditioned termed as poor but below 100 microns it was good. Similar results were also obtained for MLI (140-100) and LLI for new pavement 14 and 20 for new pavement.

Sarker et al. (2016) [160] presented a mechanistic-empirical approach for overlay thickness designs of low-volume pavements through a combination of non-destructive deflection testing and pre-established pavement damage models e.g. AASHTO 1993 NDT method, IDOT modified layer coefficient method and Asphalt Institute deflection. The proposed method was found to be more reliable in terms of structural performance and economy.

T Van Phuc Le et al. (2016) [98] presented a regression model for asphalt concrete (AC) overlay thickness design based on a Mechanistic-Empirical pavement design guide to be used in urban roads of Seoul city. The regression model was verified by comparing the predicted and measured annual average daily truck traffic (AADTT) and AC overlay thickness. It is observed from the validation study that the regression model is capable of predicting the AC overlay thickness within a reasonable level of accuracy.

István Fi et al. (2013) [93] developed a mechanical–empirical-based asphalt overlay design procedure that considered equivalent pavement modulus to simplify the calculation. The current Hungarian asphalt overlay practice has also been presented. Overlay design methods vary across countries, but the current Hungarian standard considered in the study dates back several decades. To address new construction technologies and economics, a mechanical-empirical method was developed at the Highway Laboratory of BME. The method used in this paper uses the strain value at the bottom of the existing asphalt layer and the equivalent modulus of pavement structures to determine

the thickness of the overlaying binder course. The study reported asphalt overlay design curves, which can be used for pavement overlay design purposes.

R.Fortes et al. (2013) [109] proposed using a falling weight deflectometer to evaluate the structural condition of in-service pavement in Brazil. The deflection at the point of load application (D_0), is not enough to evaluate pavement structural conditions. The information on deflection basins can help in pavement rehabilitation and avoid premature failure.The study reveals that Brazil is increasingly using FWD equipment for deflection analysis and structural characterization of existing pavements, but it was indicated in the study that the association of maximum deflection (D0) alone may not be conclusive enough to diagnose the pavement's structural condition.The proposed methodology has proven promising, helping in troubleshooting pavement rehabilitation and avoiding premature failures in diagnosing faults. The paper considers studies that have shown that maximum deflection alone is not sufficient to characterize a pavement's condition. The paper concluded that these models can be verified in simplified form with FWD results, the evolution of structural parameters as a function of traffic and time, or to estimate pavement remaining life according to the deflection basin.

E. Horak (2008) [83] evaluated the structural performance of flexible pavement using a non-destructive testing method such as FWD. It was suggested that worldwide the FWD is used as a pavement rehabilitation device throughout the world. Different layers index such as BLI, MLI, and LLI can be used to generate the deflection basin using deflection from different radial distances from FWD. The paper establishes and verifies South African mechanistic rehabilitation design procedure using heavy vehicle simulators. Surface deflection basins were measured using road surface deflectometers or deflectographs. Typical South African pavement structures were analyzed, and the equivalent-layer-thickness (ELT) concept was investigated for its applicability. The study reveals that EL T represents pavement structural capacity, based on the effective elastic modulus of the subgrade. The paper concludes that overlays are crucial rehabilitation options, and the design-curve approach is suitable for overlay-design curves.

Abaza,K, A.,(2005) [6-7] proposed a study very similar to the mechanistic method of overlay design. The loss of strength indicator of

pavement is in terms of deflection. The performance parameters are converted into relative strength indicators and then converted into equivalent overlay thickness.Since, flexible pavement performance is crucial in design, this paper assesses surface condition over time by constructing a performance curve for each structure. The proposed approach compensates existing pavement structures for performance loss over specified service time using performance curve parameters. Performance parameters are converted into equivalent relative strength indicators, which are then used to calculate overlay thicknesses. The relative strength indicators used in this paper are structural number and gravel equivalent used by the American Association of State Highway and Transportation Officials and the California Department of Transportation design methods of flexible pavement, respectively.

M.S.Hoffman (2003) [82] undertaken a study to assess the structural requirements for a flexible pavement by analyzing deflection basin data obtained from Falling Weight Deflectometer (FWD) tests, employing a Mechanistic approach. YONPAVE software was utilized to determine the structural number of the pavement. Additionally, the study concluded that the deflection basin data from FWD can be utilized to derive effective structural numbers and subgrade moduli, offering insights into the structural performance of the pavement.

Horak (1988) [84] suggested an alternative index parameters for a deflection bowl by employing the concept of equivalent layer thickness. It demonstrates that vertical strain, as determined by equivalent layer thickness, offers a viable approach for estimating subgrade elastic modulus, which in turn aids in crafting overlay thickness design curves. While the modified structural number (SNC or SNP) exhibits noteworthy correlations with deflection bowl measurements obtained from falling weight deflectometer (FWD) tests, a considerable portion of the inherent structural insights within the deflection bowl remains untapped. In response, the study introduces and validates a singular relationship between the complete deflection bowl and the effective adjusted structural number (SNPeff). Although SNP and the structural condition index (SCI) are conventionally utilized for network assessments and initial project evaluations, they lack the ability to pinpoint the origins of distress. The research highlights that supplementing these indices with a comprehensive analysis of deflection bowl parameters significantly enhances investigative

capabilities. SNPeff and SCI can be computed based on SNPeff and SNP, respectively, for design purposes or as necessitated (SNPreq). However, neither SCI nor SNPeff can isolate the sources of distress within the pavement structure's depth. Consequently, the paper recommends augmenting SNPeff and SCI with the established structural benchmark methodology for deflection bowls, as it furnishes a structured three-tiered condition assessment framework, facilitating the identification of problematic zones and layer combinations potentially responsible for distress occurrences.

Hoffman (1860) [34] developed YONAPAVE software based on the FWD deflection basin considering the maximum deflection and variability along the section. In this method, the difference between desired effective structural number as per the AASTHO guide and the structural number calculated from the area of the deflection basin has been used to find thedesign overlay thickness.The current LADOTD overlay design method follows the 1993 AASHTO pavement design guide. The 1993 AASHTO overlay thickness design method utilizes the effective thickness approach. The required thickness of the asphalt concrete (AC) overlay is a function of the structural capacity required to meet future traffic demands and the structural capacity of the existing pavement.

AI (1983) [10] method is widely used for overlay thickness design which is based on representative rebound deflection and corresponding axle load repetitions. An equivalent pavement modulus of the existing pavement is calculated which play important role in the selection of overlay thickness.

Ghazi et al. (2020) [72] developed an experimental PSI pavement evaluation model based on regression analysis. The present serviceability rating (PSR) and the roughness were also measured along with linear fatigue and rutting cracking, rut depth, raveling, patching, debonding, and potholes for thirty-five numbers rural highways. Linear cracking and rut depth were identified as the most significant parameters and PSR found to be most affected by slope variance in the case of smooth pavement in comparison with rough pavement.

Moudjari et al. (2019) [116] proposed a more efficient technique to analyze the deflection basin don by Lacroix Deflectograph and Falling Weight Deflectometer (FWD). The study also presented an approach to find deflection based on back-calculation as obtained from FWD and ELMOND program which

includes analytical equation comprising Odemark's and Boussinesq's formula. A comparative study has also been carried out which shows the relevance of adopting such a simple analytical method in the field of structural evaluation of the flexible pavement.

B.H. Setiadji (2018) [163] evaluated critical parameters of the deflection bowl for optimum use in analyzing the different parameters of road pavement structure in detail. The study suggested a simplification and reformulation of the parameters to find the sub-grade modulus more accurately. The study reveals that NDT method that requires specialist expertise is widely used to assess road pavement condition, with load-deflection back calculation. The study suggests that to overcome this, deflection bowl parameter application could be an alternative since these parameters are easy to use but only indicate the structural layer condition, requiring careful consideration. The study evaluated the optimal usage of parameters against different road pavement structures, revealing the need for simplification and reformulation to improve ease of use, accuracy of subgrade modulus determination, and the ability to evaluate structures with less than four-layer numbers.

Fabricio Leiva -Villacorta et al. (2017) [104] established a correlation between the deflections of the pavement surface and the likelihood of permanent deformation. The proposed model has proven highly effective, requiring fewer parameters to predict deflection and the remaining lifespan of the pavement. AASHTOWare is a comprehensive pavement design software, utilizing the NCHRP mechanistic-empirical pavement design guide. It predicts pavement responses such as stresses, strains, and deflections based on traffic, climate, and materials parameters, projecting the development of key pavement distresses and smoothness loss over time for both asphalt concrete (AC) and Portland cement concrete (PCC) pavements. This state-of-the-art tool embodies the latest advancements in pavement design, offering features to optimize designs according to specific requirements and allowing users to evaluate and refine designs. Additionally, its database functionality enables the storage and reuse of finalized designs along with individual input pavement design parameters. This capability facilitates future designs, as well as the detection of distress, performance analysis, and long-term pavement management.

Sarkar et al. (2016) [159] presented a mechanistic-empirical approach for overlay thickness design for low volume pavements through a combination of non-destructive deflection testing and pre-established pavement damage models. The method was found to be more reliable in terms of structural performance and economy. The study reveals that the Illinois Department of Transportation (IDOT) employs an empirical design approach for overlay thickness designs of low volume roads, using modified layer coefficients for limited material types which is outdated and lacks testing for recycled and nontraditional construction materials. The study developed a mechanistic-empirical approach, using nondestructive deflection testing and pre-established pavement damage models for overlay thickness designs. Twenty pavement sections from six counties in Illinois were selected, and FWD tests were conducted to determine the structural conditions of existing pavement sections. The M-E Overlay Design method identified structural deficiencies, leading to more economical, safer, and reliable overlay solutions for low volume roads.

Saleh et al. (2016) [155] proposed a computational method for assessing the remaining service life of pavements based on rutting and fatigue criteria. This technique correlates normalized area with compressive strain at the subgrade surface and surface curvature with tensile strain at the asphalt bottom. It highlights the importance of utilizing reliable indicators for structural condition and service life estimation to guide funding and maintenance decisions for road assets at a network level.Computer simulations were employed to simulate surface deflection profiles and critical pavement responses across 2880 flexible pavement sections. The research established a strong correlation between normalized area and compressive strain at the subgrade surface, as well as between pavement surface curvature and the area under the pavement profile. These correlations were then utilized to assess the remaining service life in terms of rutting and fatigue.Furthermore, it was found that the normalized area ratio and normalized deflection ratio were robust indicators, insensitive to variations in subgrade conditions and applied loads, as well as pavement response. Consequently, the study concluded that these parameters can effectively rank and classify the structural condition of pavement networks, aiding in the prediction of remaining service life.

Sarker et. al(2015) [180] conducted to determine overlay thickness for a local transportation agency, employing a mechanistic-empirical approach. Deflection served as the key parameter to assess the condition of the existing pavement in service. Upon assessing pavement deflection through Falling Weight Deflectometer (FWD) testing, it was observed that the Illinois Department of Transportation (IDOT) utilized an outdated empirical design approach for determining structural overlay thickness on low volume roads, which involved modified layer coefficients for limited material types. In contrast, the study proposed a mechanistic-empirical approach, integrating nondestructive deflection testing and preestablished pavement damage models. Twenty pavement sections across six counties in Illinois, each with diverse structural and traffic characteristics, were selected for FWD tests. Overlay thickness requirements were determined using three methods: AASHTO 1993 NDT method, IDOT modified layer coefficient method, and Asphalt Institute deflection approach. The study concluded that the mechanistic-empirical overlay design method highlighted structural deficiencies in original pavement configurations, offering more cost-effective, safer, and dependable overlay solutions for low volume roads.

Loay et al (2011) [9] developed a two-dimensional finite element model, using ABAQUS software to find the effect of static repeated wheel load on rutting formation and pavement response. The FWD has been used for the validation of the results. This study developed a two-dimensional finite element model using ABAQUS software to investigate the impact of static repeated wheel load on rutting formation and pavement response. The study revealed that rut depth increases with increasing temperature, tire pressure, and subgrade strength. The results were compared with actual field measurements, but approximations and idealizations were inevitable. The study concluded that the linear-elastic perfectly-plastic Drucker-Prager model provided acceptable results.

6.3   Mechanistic-Empirical design of bituminous overlay for flexible road pavement based on vertical interface deflection

In pavement engineering, the interface-based deflection of overlay design plays a crucial role in ensuring the durability and performance of flexible

pavements. Flexible pavements, consisting of multiple layers of materials, are subject to various forms of distress over time due to traffic loads, environmental factors, and aging. One of the primary methods to address these issues is through overlay design, which involves placing a new layer of material over the existing pavement surface. However, the success of overlay design heavily relies on understanding the behavior of layer interface between the existing pavement and the overlay material.

Repair and retrofitting of flexible pavements are essential components of pavement maintenance and rehabilitation strategies. In these context, interface-based deflection analysis advocates on decisions regarding the selection of overlay materials, thicknesses, and required construction techniques to mitigate distress and extend pavement service life.

6.3.1 Objective

The objective of the present study is to develop a Mechanistic-Empirical approach for the design of a bituminous overlay using vertical interface deflection as a design parameter.

6.3.2 Methodology

In this study, the pavement with overlay has been considered as a two-layer system as shown in Figure 6.1. The top layer consists of bituminous overlay with thickness h_1 and resilient modulus E_1 is resting on an existing pavement layer of elastic modulus of E_2. The equivalent elastic modulus (E_2) of existing multilayered pavement has been estimated in this study on the basis of pavement deflection before overlay using Burmister's (1958) Equation [37-41].

$$E_2 = \frac{2(1-\nu^2)\, q\, a}{\delta} \qquad\qquad (6.1)$$

Where, a = Contact radius of the loaded area between tire and pavement

δ = Rebound deflection of pavement before the overlay

q = Contact stress on pavement due to wheel load

If ν = Equivalent poisons ratio of the multilayered system before overlay is assumed as 0.5 the Equation 6.1 may be expressed as

$$E_2 = \frac{1.5\,qa}{\delta} \tag{6.2}$$

In order to determine the vertical stress due to wheel load at pavement-overlay interface, the proposed two-layered system has been transformed into a homogenous system by using Odemark's [126] method.
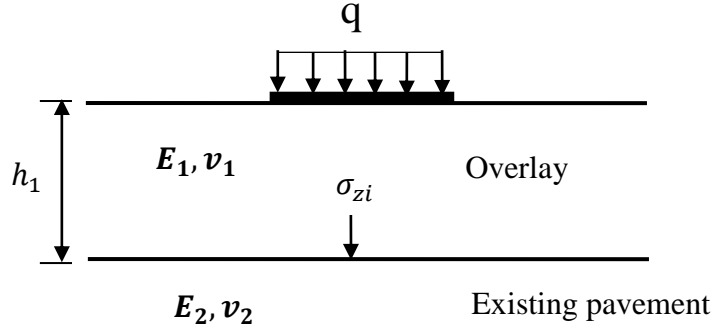
Figure 6.1 : Typical flexible pavement section in a two-layered system with overlay

6.3.2.1 Odemark's Method

If the poisons ratio of two layers are assumed approximately same , the equivalent thickness(h_e) corresponding to the two layered system may be expressed as (described in Chapter 2).

$$h_e = f h_1 \sqrt[3]{\frac{E_1}{E_2}} = k_1 \tag{6.3}$$

In present section, the top overlay layer followed by the bottom layer of in-situ road pavement has been considered as a two-layered system to estimate the interface deflection at pavement–overlay interface due to wheel load on overlay surface. The vertical interface deflection thus obtained has been considered in this study as the pavement deflection after putting overlay and characterized as a design parameter. It may be noted that the resilient modulus of the new overlay is reasonably high when compared with the elastic modulus of existing pavement under terminal serviceability conditions. Moreover, the distribution of stress in such a layered system reduces considerably at the layer interface resulting smaller vertical deflection at the pavement overlay interface. Therefore, the assumption to consider the interface deflection as pavement deflection in a two-layered system may be considered as reasonably good for estimation of overlay thickness.

6.3.2.2 Determination of vertical interface deflection in two-layered system

The vertical interface stress at the overlay pavement interface may be determined using Bousenesq's method after transforming the two-layered system into a homogeneous system using Odemark's approach. as explained in Equation 6.3.The vertical stress at a depth (z) due to a circular load intensity (q) acting on a radius (a) may be determined using Bousenesq's thory as shown in Equation 6.4a.

In this backdrop , substituting $z = h_e$, in eqn 6.4a   the vertical interface stress (σ_{zi}) may be determined from Equation 6.4b

$$\sigma_{zi} = q \left[1 - \frac{1}{\left(\sqrt{1 + \left(\frac{a}{z}\right)^2} \right)^3} \right] \tag{6.4a}$$

$$\sigma_{zi} = q \left[1 - \frac{1}{\left(\sqrt{1 + \left(\frac{a}{h_e}\right)^2} \right)^3} \right] \tag{6.4b}$$

It is relevant to mention that the effect of contact stress due to wheel load is reduced significantly at the overlay-pavement interface due to dispersion of stress in a layered medium from a higher(E_1) to lower (E_2)elastic modulus. Therefore, the reduction of vertical interface stress at the overlay pavement interface can be explained due to the increase in contact area for stress dispersion in a two-layered system as shown in Figure 6.2. The vertical stress at pavement overlay interface in a two-layered system becomes highest along the center of the loaded area at depth $z = h_e$. and has been used to determine the highest interface deflection for the design of overlay.
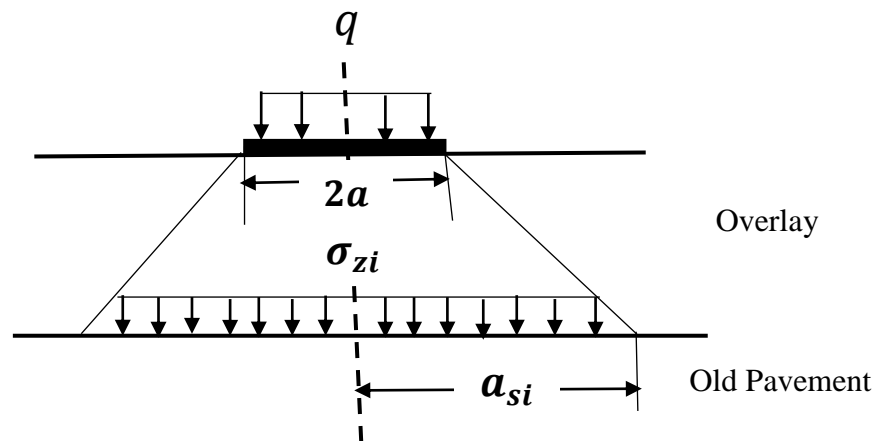
Figure 6.2: Dispersion of vertical interface stress in a two-layered system.

The radius of dispersed area (a_{si}) of vertical interface stress at the layer interface may be obtained from Equation 6.5.

From Figure 6.2,

$$\pi a^2\, q = \pi\, a_{si}{}^2\, \sigma_{zi} \tag{6.5}$$

Where, 'q' is the surface stress intensity acting on a circular plate of radius (a) on the overlay surface.

$$a_{si} = a\sqrt{\frac{q}{\sigma_{zi}}} \tag{6.6}$$

Therefore, the interface deflection (Burmister, 1943, 1945) [37-41] along the center of wheel load at a depth $z = h_e$ from the top of the existing pavement may be determined from Equation 6.7.

$$d_{si} = \frac{1.5\, a_{si}\, \sigma_{zi}}{E_2} \tag{6.7}$$

However, by substituting the value of a_{si} from Equation 6.6and substituting in Equation 6.7, the interface deflection at overlay- pavement interface (Biswas, 2005) [28] may be expressed as

$$d_{si} = \frac{1.5\, a\, \sqrt{q\, \sigma_{zi}}}{E_2} \tag{6.8}$$

The interface deflection thus obtained in a two-layered system has been made equal to the allowable deflection obtained from the AI [10] method to determine the required overlay thickness. The correlation between pavement deflection and axle load repetitions developed by (AI) [10] has been shown in Equation 6.9 which has been used in this study for the estimation of overlay thickness.

$$\delta_a = 26.32 \times (N)^{-0.2438} \tag{6.9}$$

Therefore by solving Equations (6.3,6.4,6.8, 6.9) the required overlay thickness for specified axle load repetitions may be obtained from Equation 6.10.

$$26.32 \times (N)^{-0.2438} = \frac{1.5a\sqrt{q\left[1 - \left(\dfrac{(k_1)}{\sqrt{a^2 + (k_1)^2}}\right)^3\right]q}}{E_2} \tag{6.10}$$

$$\text{Where, } K_1 = \left(f h_1 \sqrt[3]{\frac{E_1}{E_2}}\right)$$

The overlay thickness thus obtained using the present methodology has been compared with the overlay thickness obtained using AI [10] method.

6.3.2.3 Determination of overlay thickness by AI method

It is evident from the pavement failure study that pavement interface deflection plays an important role in controlling the distress during its design life. In the AI [10] method, a pavement system with overlay has also been considered as a two-layered system similar to the model proposed in this study. Expected deflection after overlay on flexible road pavement has been characterized as design rebound deflection (δ_a) which has been expressed by Equation 6.11as recommended in AI method.

$$\delta_a = \frac{(1.5)qa}{E_2}\left(\left\{1 - \left[1 + 0.8\left(\frac{h_1}{a}\right)^2\right]^{-0.5}\right\}\frac{E_2}{E_1} + \left\{1 + \left[0.8\frac{h_1}{a}\left(\frac{E_1}{E_2}\right)^{\frac{1}{3}}\right]^2\right\}^{-0.5}\right) \quad (6.11)$$

Therefore, by solving Equations 6.10 and Equation 6.11overlay thickness (h_1) with the required modulus (E_1) for specified axle load repetitions (N) may be obtained using rebound deflection of existing pavement before overlay. The overlay thickness thus obtained from the AI [10] method and using the present approach has been compared for lower axle load range (5 msa) to higher axle load range (50 msa) for validation of test results. The Flow diagram of adopted methodology of overlay design based on interface deflection has been shown in Figure 6.3.

```
┌─────────────────────────────────────────────────────┐
│       Interface deflection based overlay design       │
└─────────────────────────────────────────────────────┘
                          │
                          ▼
┌─────────────────────────────────────────────────────┐
│  Derivation and estimation of equivalent modulus of    │
│  existing pavement using rebound deflection data       │
│  before overlay for a specific subgrade CBR & axle     │
│  load repetitions                                      │
└─────────────────────────────────────────────────────┘
                          │
         ┌────────────────┼────────────────┐
         │                ▼                │
         │      ┌──────────────────────┐   │
         │      │      INPUT DATA       │   │
         ▼      │  Axle load repetitions,│  ▼
┌──────────┐    │    Poisson's ratio,    │ ┌──────────────┐
│ Interface-│◄──│    Tire pressure       │►│  Rebound     │
│ deflection│    │   Contact radius,     │ │  deflection  │
│ based     │    │  Bituminous mix modulus│ │  based       │
│ Design    │    └──────────────────────┘ │  AI method   │
└──────────┘                               └──────────────┘
      │           ┌──────────────────┐            │
      └───────────│ Overlay Thickness │────────────┘
                  └──────────────────┘
                          │
                          ▼
┌─────────────────────────────────────────────────────┐
│  Comparison of overlay thickness between Interface     │
│  deflection based and rebound deflection method        │
└─────────────────────────────────────────────────────┘
                          │
                          ▼
┌─────────────────────────────────────────────────────┐
│  Design of overlay thickness due to overstress by      │
│  Interface-deflection based approach.                  │
└─────────────────────────────────────────────────────┘
                          │
                          ▼
                  ╭──────────────────╮
                  │   Conclusions     │
                  ╰──────────────────╯
```

**Figure 6.3. Flow diagram of adopted methodology of overlay design based on
interface deflection**

6.3.2.4   Input parameters used in overlay design

The following input parameters have been used for comparative analysis of overlay thickness obtained from the present method with the AI [10] method. Deflection values (δ) before overlay have been considered from 0.5 mm to 5.0 mm. The equivalent modulus of existing pavement (E_2) has been calculated using Equation 2 for different rebound deflections before overlay. The modulus of the overlay layer (E_1) has been considered as 3500 MPa with Poisson's ratio (ν) as 0.5 for overlay and in-situ road pavement.. A wheel load of 40 kN with contact stress (q) of 0.483 MPa, has been considered with a radius of the contact between tire and pavement as 163mm. The design load in terms of axle load repetitions for overlay design has been considered between 0.5 msa to 50 msa.

6.3.3   Results and Discussion

In-situ road pavement is the foundation on which overlay is laid. Therefore the strength of in-situ pavement governs the thickness of the required overlay for an intended service period. In the present method, the thickness of the overlay has been designed to reduce higher surface deflection of damaged pavement to comparatively lower range of allowable deflection after overlay. Therefore, the top of existing pavement surface before overlay is the interface of the new overlay and old pavement. Therefore, the overlay design using the present method recommends to put appropriate thickness of bituminous overlay with the required modulus so that vertical interface deflection at the pavement-overlay interface can be reduced to an allowable limit after overlay.The thickness of bituminous overlay thus obtained from the AI method and present approach has been solved by MATHEMATICA programming tool for different pavement deflection and axle loads (N).The overlay thickness thus obtained are presented in Figure 6.4 to Figure 6.7.
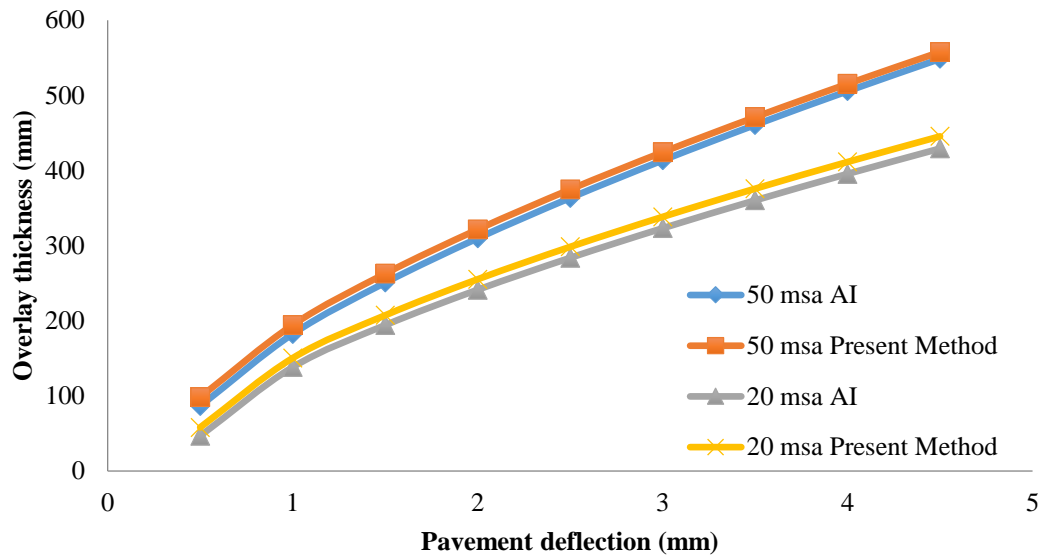
Figure 6.4.Comparison of overlay thickness between Asphalt Institute and present method for different axle load repetitions.
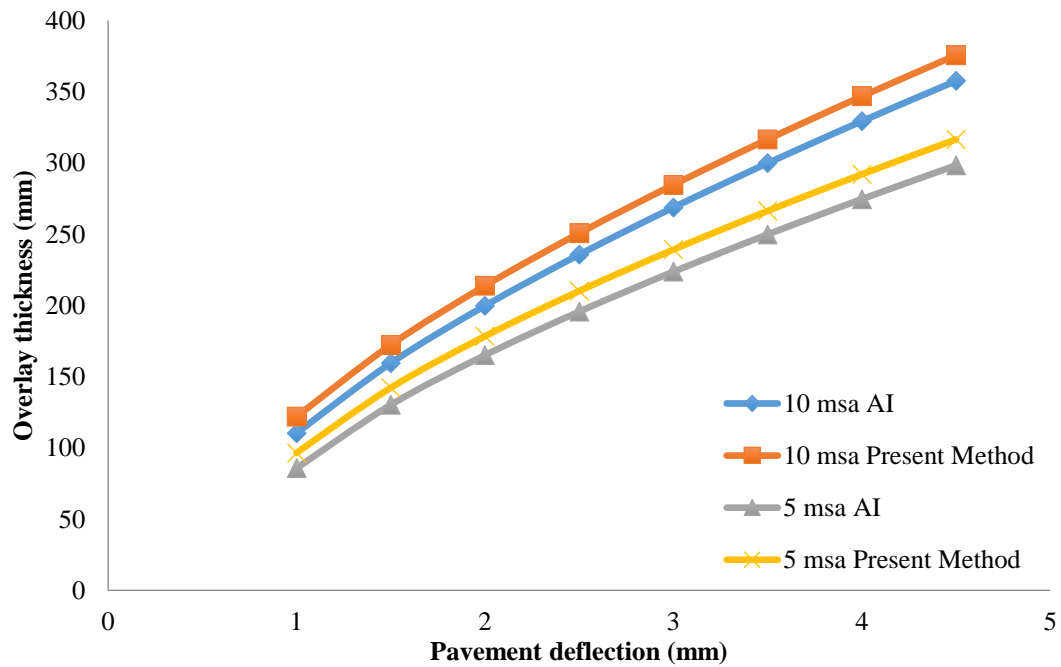
Figure 6.5 Comparison of overlay thickness between Asphalt Institute and present method for different axle load repetitions.
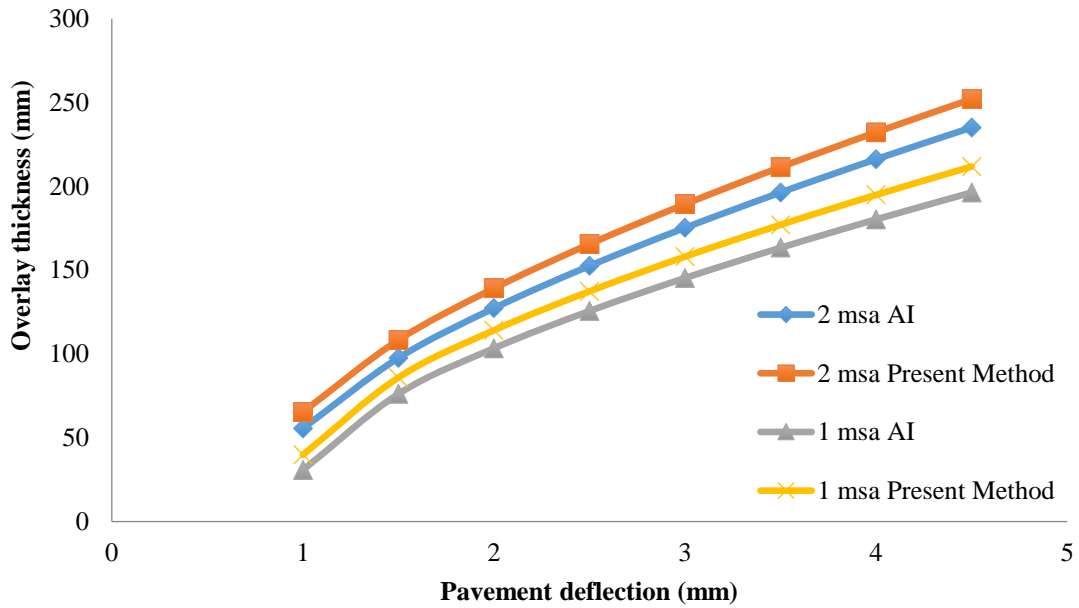
Figure 6.6 Comparison of overlay thickness between Asphalt Institute and present method for different axle load repetitions.
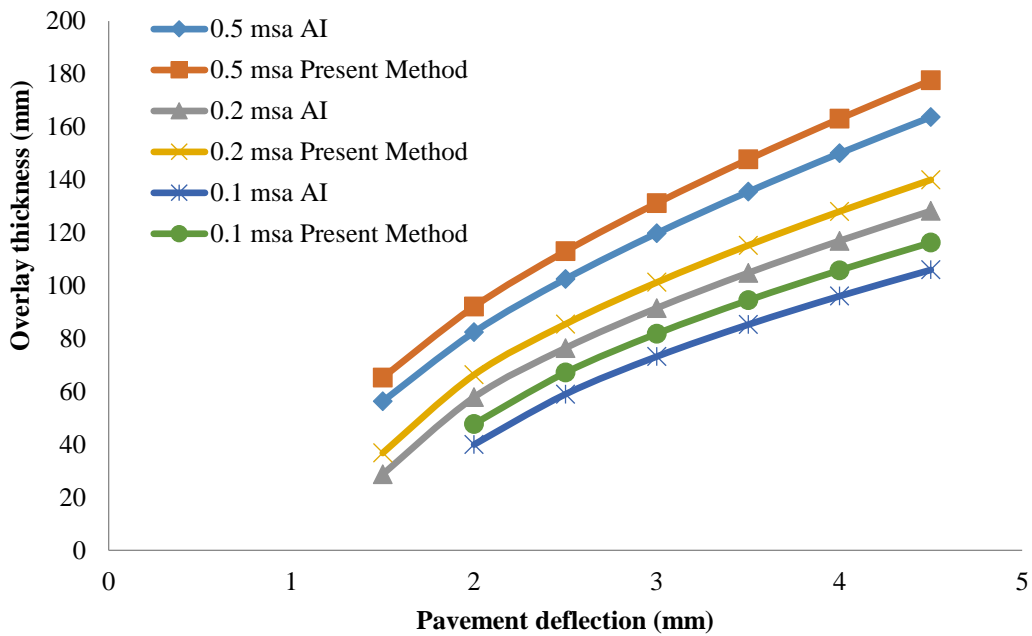
Figure 6.7 Comparison of overlay thickness between Asphalt Institute and the present method for different axle load repetitions.

The rebound deflection on the pavement before the overlay is an indicator of pavement strength. If the pavement deflection is large then the pavement strength can be considered relatively weak and vice versa. It is evident from those figures that the required overlay thickness increases with an increase in rebound deflection. The rate of increase of overlay thickness observed in the AI method and the present approach is reasonably close. However, the required overlay thickness obtained using the present method has been observed marginally higher than the thickness obtained from the AI method. The trend of variation of overlay thickness with rebound deflection was found similar for lower range of axle load (0.5 msa) as well as higher axle load range (50 msa). So, the sensitivity of pavement deflection on overlay thickness is comparable between the two methods. However, it is relevant to mention that the rate of increase of overlay thickness with respect to pavement deflection is reasonably high in high volume roads (50 msa) in comparision with low volume roads (0.5 msa). Therefore, it is advisable to put overlay when pavement deflections are within 2.5 to 3.0 mm, beyond which overlay thickness requirement may be too high. It has to be noted that the AI [10] method is principally based on a surface deflection on pavement but the present method has been proposed on vertical interface deflection at pavement-overlay interface. The significant convergence of results between the two methods thus indicates the reliability of the present method as an accepted Mechanistic-Empirical approach for overlay design.

It is has been found that the overlay thickness increases with the increase in axle load. In present study, dual wheel load range from 40 kN to 60 kN has been considered to evaluate the effect of overloading on bituminous overlay thickness. The change in overlay thickness for different wheel loads ranging from 40 kN to 60 kN with pavement deflection ranging between 0.5 mm to 4.5 mm have been presented in Table 6.1 to Table 6.3 (Appendix 5A) . It is evident that the effect of overloading in terms of increase in wheel load on overlay thickness is significant for the road pavement with higher deflection. Higher deflection of pavement generally indicates a higher extent of damage, which may require more-overlay thickness for specified axle load repetitions. However, the requirement of overlay thickness becomes comparatively less for

the road pavements showing smaller deflection. It is also evident from the data in Table 6.1(Appendix 5A), that for a high volume road with design traffic of 50 msa, the required change in overlay thickness for an increase in wheel load from 40 kN to 60 kN with a pavement deflection of 0.5 mm was found as 30 mm only. However, the overlay thickness increase under similar boundary conditions with a pavement deflection of 4.5 mm has been found as high as 169 mm, which emphasizes that early repair of pavement with less damage would require less overlay thereby incurring a lower expenditure for repair works.

The variation of overlay thickness thus found in the present study shows that the overlay thickness increaseswith the increase in wheel load on the pavement when the pavement deflection remains unchanged. However, the effect of change in overlay thickness is significantly higher for overloading when the pavement is severely damaged with higher deflection. Similarly, for low-volume roads with an axle load of 2 msa, it has been observed that the effect of increased wheel load from 40 to 60 kN on overlay thickness is less in comparison to high-volume roads. In this context, it can be concluded that the effect on overlay thickness due to change in wheel load and cumulative axle load repetitions are quantitatively different for low volume and high volume roads, which may be analyzed with a better degree of reliability using the present analytical approach.

In the present study, attempts have been made to assess the reduction in overlay life due to overloading on road pavement. The sections of overlay which were designed with an initial axle load of 50 msa, 10 msa, and 2 msa have been considered for estimation of reduction of overlay life if wheel loads are changed from 40kN to 60 kN. The reduction of overlay life has been estimated by back-calculation considering interface deflection as a design parameter for increased wheel load . The vertical interface deflection thus obtained using the present analytical approach with 60 kN wheel load has been used in the back-calculation of overlay age using Equation 6.9. Therefore, the modified overlay life thus obtained for wheel load of 40kN and 60 kN for pavement different deflections with different axle load repetitions have been presented in Table 6.4 to Table 6.6 (Appendix 5A).The modified overlay life was found to get reduced with respect to its assumed service life due to overloading. It has been found from those tables that the reduction of overlay age is significantly higher for the roads

with higher traffic volume with a lower pavement deflection. This means a moderately good overlay section will be severely affected due to overloading. It has been observed from the analysis that the reduction of overlay age due to overloading may be as high as 59% in a high volume road with a 50 msa repetitions with a pavement deflection of 1.0 mm whereas the overlay age reduction for a low volume road with an axle load of 2.0 msa was found 35% only. But when the pavement is badly damaged with a higher deflection , the reduction in overlay life for high and low-volume roads is comparable. However, the effect of overloading on overlay service life on damaged roads with higher deflection was found significant. It has been found that for the damaged pavement section with deflection ranging between 2.5 mm to 4.5 mm, the average reduction of overlay life 62 % which indicates the severity of damage of overlay for roads subjected under overloading. Against this backdrop, the effect of the different classes of axle and wheel loads on vehicle damage factors may be studied in future for the design of a bituminous overlay.Finally a Graphical User Interface (GUI) has been developed based on the algorithms as shown in Figure 6.3 using PYTHON and JAVA to make the overdesign process more user friendly.

6.3.4   Concluding remarks

It has been found in present study that the pavement with higher deflection is weak in strength and would require a higher thickness of overlay for specified service life and vice versa. The overlay thickness has been estimated in this study based on a Mechanistic- Empirical design approach, which closely matches the overlay thickness obtained from the AI [10] method. In this study, overlay thickness has been estimated for different ranges of axle load between 50 msa and 0.1 msa. However,   comparision of overlay thickness with the Asphalt Institute [10] method has been made in this study with low volume roads with axle load repetitions ranging from 0.1 msa to 2.0 msa as well as high volume roads ranging from 20 msa to 50 msa. However, it is relevant to mention that the rate of increase of overlay thickness with respect to pavement deflection is reasonably high in high-volume roads when compared with low-volume roads. The rate of change of overlay thickness for different pavement

deflections was found close between the present approach and the AI [10] method. Therefore, it can be concluded that the sensitivity of pavement deflection on overlay thickness is comparable between the two methods which justifies the reliability of the present method as an analytical approach for overlay design. In the present study, attempts are made to assess the reduction in overlay life due to overloading on road pavement. The reduction of overlay life has been estimated by back-calculation considering interface deflection as a design parameter. It has been observed that the reduction of overlay age is significantly higher for the roads with high traffic volume with even lower pavement deflection. But when the pavement is badly damaged with higher deflection, the reduction in overlay life for both high and low-volume roads are comparable and significant. In this backdrop, the effect of a different class of axle and wheel loads on vehicle damage factors for overlay design may be considered as future scope of work.

6.4   Mechanistic-Empirical design of overlay based on vertical interface stress

Estimation of overlay based on vertical interface stress has been discussed in this section. The focus is on estimating overlay thickness using vertical interface stress as a key factor. Interface stress, which refers to the force exerted between the overlay and the base layer, is highlighted as a crucial element influencing overlay thickness. Therefore, it's deemed as a significant parameter in overlay design.

Furthermore, the study also incorporates the consideration of the base layer index for validation purposes. This means that the present study takes into account the characteristics and properties of the base layer to ensure the accuracy and reliability of the overlay estimation method being discussed. By including the base layer index in the analysis, the study aims to validate and potentially enhance the effectiveness of the overlay design approach as proposed.

6.4.1 Objective

The objective of the present study is to determine the bituminous overlay thickness on the top of the in-service flexible road pavement by limiting the vertical interface stress at the pavement overlay interface.

6.4.2 Methodology

In present study, the overlay on the top of the existing flexible road pavement has been considered as a two-layered system. The system consists of a stiffer layer of the overlay on top with an elastic modulus (E_1) followed by weaker existing pavement with an elastic modulus of (E_2) which requires further strengthening. The equivalent elastic modulus of existing multilayered pavement has been estimated in this study based on pavement deflection before overlay by using Equation 6.12 recommended by Boussinesq's [34].

$$E_2 = \frac{2(1-v^2)qa}{\delta}$$ (6.12)

Where,

a = Contact radius of the loaded area between tire and pavement.

δ = Rebound deflection of pavement before the overlay

q = Contact stress on pavement due to wheel load.

v = Equivalent poisons ratio of the multilayered system before overlay which has been assumed as 0.5.

To determine the vertical stress by Boussinesq's [34] theory at pavement overlay interface along the centerline of the loaded area, the proposed two-layered system has been transformed into a homogenous system by using Odemark's [126] method.

6.4.2.1 Odemark's Method

If the Poison's ratios of the layers are assumed approximately the same for the two layers under consideration as shown Figure 6.1 the equivalent thickness corresponding to the two-layered system may be expressed as (described in Chapter 2)

$$h_e = f h_1 \sqrt[3]{\frac{E_1}{E_2}} \qquad\qquad (6.13)$$

6.4.2.2 Determination of interface stress using Danish correlation

To determine the vertical stress on the top of the existing pavement at pavement –overlay interface, Boussinesq's equation can be used after the transformation of the two-layered system into a homogeneous system. Therefore, vertical interface stress at the overlay-pavement interface at depth (z) for a uniformly distributed circular wheel load (q) when acts on the top of overlay, may be determined by Boussinesq's[34] Equation 6.14a.

$$\sigma_z = q\left[1 - \left(\frac{z}{\sqrt{a^2+z^2}}\right)^3\right] \qquad\qquad (6.14a)$$

Where a = Radius of contact between wheel load and overlay surface. Now substituting z = h_e, in Equation 6.14a Equation 6.14b may be obtained.

$$\sigma_z = q\left[1 - \left(\frac{h_e}{\sqrt{a^2+h_e^2}}\right)^3\right] \qquad\qquad (6.14b)$$

The principle followed in this study for the design of overlay is to limit the vertical interface stress on in-situ road pavement by putting the required thickness of overlay with the desired modulus. The correlation to determine the permissible vertical stress on the top of any unbound layer has been recommended in Danish (Ullidtz) [181] correlation and shown in Equation 6.15. According to Danish [181] correlation, the permissible vertical stress (σ_{zu}) depends on anticipated axle load repetitions before failure and the elastic modulus of the unbound layer.

$$\sigma_{zu} = 0.164 \times \left(\frac{N \times R}{10^6}\right)^{\frac{-1}{3.26}} \times \left(\frac{E_2}{160}\right)^{\alpha} \qquad\qquad (6.15)$$

Where N = Number of the load repetitions (msa) before failure of the granular unbound material.

R = the regional factor which has been assumed to be 2.75 for the semi-arid region in this study. [NCHRP-128 [181] guide may be referred for values in detail].

α = 1.16 if E≤ 160 MPa; else α= 1.00.

In present analysis, the value of modulus (E_2) has been obtained from Equation 6.12 using rebound deflection data before overlay.

Thereby solving Equations 6.14b and 6.15, the required thickness of overlay can be determined corresponding to different rebound deflection before overlay and anticipated axle load repetitions leading to failure. The overlay thicknesses thus obtained have been shown in Figure 6.9 to Figure 6.18.

6.4.2.3 Determination of interface stress using Huang's correlation

Moreover, Huang [87-90] has also recommended a correlation between the permissible vertical stresses (σ_{zh}) on top of existing damaged pavement as shown in Equation 6.16. The correlation relates the allowable number of axle repetitions to limit permanent deformation of pavement, and the modulus of existing damaged pavement. The existing damaged pavement has been considered as the foundation of paving layers, which can be idealized as homogeneous, elastic, isotropic, and semi-infinite.

$$\sigma_{zh} = \left[\frac{N}{4.873 \times 10^{-5} \times E_2^{3.583}} \right]^{\frac{-1}{3.734}} \tag{6.16}$$

Where N = allowable number of axle load repetitions (msa) to limit permanent deformation of pavement. E_2 = equivalent elastic modulus of the existing pavement estimated from rebound deflection.

Huang's formulation considers that the failure criterion of pavement is governed by the failure of its foundation when the actual stress on foundation due to wheel load repetitions exceeds the allowable value.

In the present analysis, the existing pavement with multilayered elastic materials including subgrade has been considered as the foundation of the overlay. Moreover, the existing pavement with a multilayered system has been characterized in this study by an equivalent elastic modulus (E_2) of a homogeneous medium based on rebound deflection before overlay as explained earlier in Equation 6.12. Therefore, the existing old pavement with the equivalent elastic modulus (E_2) may be considered as a homogeneous layer that acts as a foundation of overlay in a two-layered system. In this backdrop,

Huang's formulation to determine the permissible stress on subgrade has been used in this study to determine the permissible stress (α_{zh}) on the unbound layer in the pavement.

Therefore, by solving Equations 6.14b and 6.16 the overlay thickness may be determined corresponding to different pavement deflection before overlay for required axle load repetitions. The overlay thickness thus obtained based on permissible stress on unbound materials using Huang's correlation has also been presented in Figure 6.9 to Figure 6.18.To compare the overlay thickness using present methods, the thickness of overlay has also been estimated in this study using AI[10] method considering pavement deflection and axle load as a design parameter. The overlay thickness thus obtained from the AI [10] method has been compared with the overlay thickness estimated from two other stress-based approaches presented in the study.

6.4.2.4 Validation of overlay thicknesses obtained using present methodologies using deflection bowl as failure parameters

To assess the accuracy of overlay thicknesses obtained using present methodologies the curvature index in the form of Base Layer Index (BLI) [83-85] has been determined analytically in present study from the deflection basin of pavement after overlay under a wheel load and compared with acceptable standards.

The curvature of the deflection basin under a wheel load is an important indicator of the strength of the in-situ multilayered pavement. Therefore, to evaluate the durability and accuracy of overlay thickness, the Base layer Index (BLI) under wheel load has been considered as a design parameter in this study. The BLI is considered as an indicator of overlay performance, precisely against cracking, which can be obtained from the deflection basin of pavement. In this backdrop, the deflection basin of pavement after overlay has been estimated using a mechanistic approach which has been illustrated in this section. In present study, the value of BLI   has been estimated based on the correlation as shown in Equation 6.17.

$$BLI = d_o - d_{300} \tag{6.17}$$

In which, d_0, is the vertical interface deflection (in mm) at the overlay-pavement interface along the centerline of the loaded area and d_{300} is the vertical interface deflection (mm) at the overlay-pavement interface a radial distance of 300 mm from the centerline of the load.

6.4.2.5 Determination of vertical interface deflection at overlay pavement interface

In the present analysis, the section of overlay followed by the in-situ road pavement has been considered as a two-layered system to determine the interface deflection at the pavement overlay layer interface. The vertical interface deflection thus obtained on the top of the existing pavement after laying overlay has been assumed as the deflection of repaired pavement. Considering higher elastic modulus of overlay on top of existing pavement with lower elastic modulus, the assumption to consider the interface deflection as design deflection in a two-layered system is reasonably good for estimation of overlay thickness.

In order to determine the vertical interface deflection, the vertical interface stress at the overlay pavement interface has been determined using Boussinesq's method by transforming the two-layered systems using Odemark's approach as explained in Equation 6.4a and Equation 6.4b. The vertical interface stress (σ_{zo}) has been shown in Equation 6.18, which is the vertical stress along the centerline of the circularly loaded area at a depth $z = h_e$, where h_e is the transformed thickness of the overlay.

$$\sigma_{zo} = q \left[1 - \left(\frac{h_e}{\sqrt{a^2 + h^2_e}} \right)^3 \right] \tag{6.18}$$

However, using Boussinesq's [34] theory, the vertical interface stress $\sigma_{z_{ri}}$ at the overlay pavement interface at different radial distances (r_i) from the centerline of the loaded area may be determined using Equation 6.19.

$$\sigma_{z_{ri}} = \sigma_{zo} \left[\frac{1}{1 + \left(\frac{r_i}{h_e} \right)^2} \right]^{\frac{5}{2}} \tag{6.19}$$

In a falling weight deflectometer (FWD), the vertical deflection in constituent layers in a multilayered pavement is measured at different radial

distances ranging in between 0-1500 mm with suitable spacing of geophones to get the deflection basin under a wheel load. To estimate the deflection bowl of the pavement after overlay, the vertical interface stress and deflection at different radial distances have been obtained in present study analytically using Boussinesq's method. The vertical interface stress obtained at the pavement overlay interface has been used to determine the vertical interface deflection at different radial distance for estimation of the deflection bowl.

In order to determine the vertical interface stress, the effect of load dispersion from overlay surface to old pavement surface needs to be explained. It is known that the effect of wheel load stress at pavement surface gets reduced at the overlay-pavement interface due to dispersion of stress through a layered medium with a higher elastic modulus to a lower one. Therefore, the increase in a larger area for stress dispersion in a two-layered system results decrease in contact stress intensity at overlay- pavement interface as shown in Figure 6.2. However, the vertical interface stress along the center of the loaded area is the highest at depth $z = h_e$, which reduces with increase in radial distance (r) and has been used in Equation 6.22 for estimation of vertical interface deflection.

The radius of dispersed area a_{si} of vertical interface stress at the layer interface may be obtained from Equation 6.20.

From Figure 6.2, $\pi a^2 q = \pi a^2_{si}\sigma_{zri}$ (6.20)

Where q is the surface stress intensity due to wheel load, acting on a circular area of radius (a) on the pavement surface.

$$a_{si} = a \sqrt{\frac{q}{\sigma_{zri}}}$$ (6.21)

Therefore, the interface deflection at any radial distance on a horizontal plane at a depth $z = h_e$ from the top of overlay may be determined from Equation 6.22.

$$d_{ri} = \frac{1.5\, a_{si}\sigma_{zri}}{E_2}$$ (6.22)

However, by substituting the value a_{si} from Equation 6.21 into Equation 6.22 the interface deflection at different radial distances may be expressed as

$$d_{ri} = \frac{1.5\, a \sqrt{q\, \sigma_{zri}}}{E_2}$$ (6.23)

Therefore, the vertical interface deflection at a different radial distance may be obtained using Equation 6.23 from which BLI can be determined. The BLI thus obtained from Equation 6.23 may be expressed as Equation 6.24.

$$d_o - d_r = A\left[1 - \sqrt{B}\right] \tag{6.24}$$

Where,

$$A = \frac{1.5 \, a \, \sqrt{q\sigma_{z0}}}{E_2} \qquad \text{and} \qquad B = \left[\frac{1}{1+\left(\frac{r_i}{h_e}\right)^2}\right]^{\frac{5}{2}}$$

The estimated   BLI value for the pavement with different overlay thickness using different methods have been reported in this study using Equation 6.24 for comparative analysis. The flow diagram of the adopted methodology can be shown in Figure 6.8.

6.4.2.6 Input parameters used in overlay thickness design

Input parameters have been used in the present analysis for comparative study of overlay thickness as mentioned in section 6.3.2.4. Deflection values (δ) before overlay have been considered as 0.5, 1.0, 1.5, 2.0, 2.5, 3.0, 3.5 and 4.0 in mm.

6.4.3   Results and Discussion

Primarily, the overlay thickness based on surface deflection has been estimated from the AI [10] method for different axle load repetitions.

The overlay thickness thus obtained for different axle load repetitions using the AI [10] method and two other recommended stress-based methods have been presented through Figure 6.9 to Figure 6.18. It is evident from those figures that, increase in pavement deflection results higher thickness of overlay. However, the rate of increase of overlay thickness was found highest in the AI method with respect to other recommended models of overlay design in this study. It is relevant to mention that the deflection and the overlay thickness value at the point of intersection of three different curves reduce with the increase in axle load repetitions. This means the overlay thickness was found to be converging within a deflection range of 1.5 mm to 2.5 mm.

```
                          ┌─────────────────────┐
                          │    Overlay design   │
                          └─────────────────────┘
                                    │
                                    ▼
          ┌────────────────────────────────────────────────────┐
          │ Estimation of equivalent modulus of existing        │
          │ pavement using rebound deflection data before the   │
          │ overlay for a specific subgrade CBR & axle load     │
          │ repetitions                                         │
          └────────────────────────────────────────────────────┘
```

Estimation of equivalent modulus of existing pavement using
rebound deflection data before the overlay
for a specific subgrade CBR & axle load repetitions

INPUT DATA
Axle load repetition, Tire
Pressure, Contact radius,
Bituminous mix modulus

Stress based
design

Deflection
based design

Huang's correlation

Danish correlation

Overlay thickness

Asphalt institute (AI)
method

Overlay thickness

Comparison of overlay thickness between stress-based and deflection method

Determination of base layer index for different overlay thickness corresponding to
different axle load and rebound deflection

Comparison of a base layer index and
Conclusions

Figure 6.8: Flow diagram of the adopted methodology of overlay design based on interface vertical stress

However, the overlay thickness obtained by limiting the vertical interface stress using Danish [181] and Huang's [87-90] correlations is quite close for different axle load repetitions. Here, it is to be noted that the design of overlay in the AI [10] method is based on limiting the deflection on overlay whereas the methods proposed in the present study for estimation of overlay thickness are based on limiting vertical stress at overlay pavement interface. The overlay design curves obtained from the stress-based approach were found to intersect each other with a flatter gradient. It has also been observed that overlay thickness is higher for lower deflections with smaller axle load repetitions by two stress-based methods in comparison to the AI [10] method.
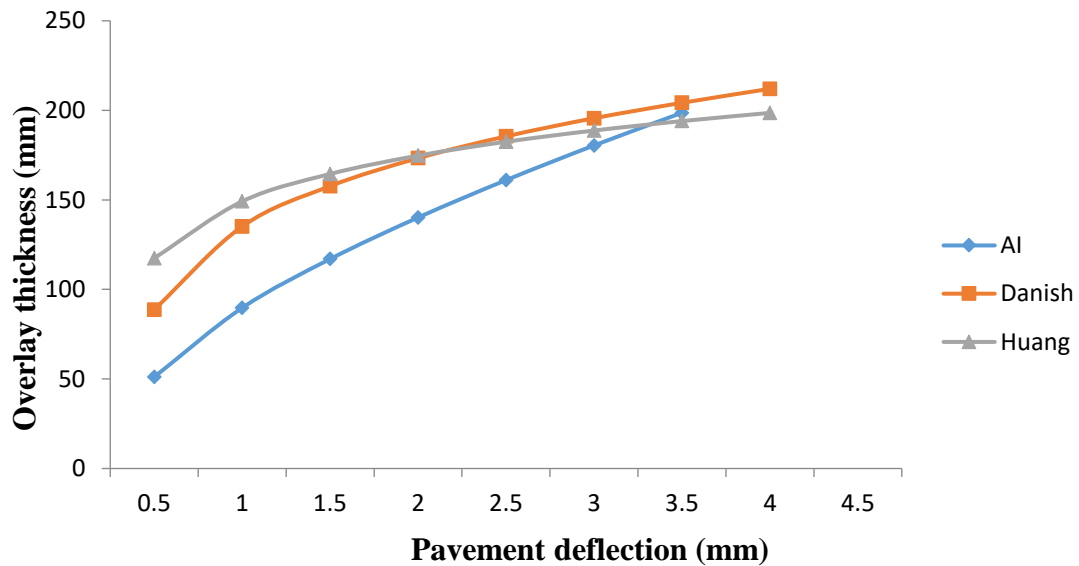
Figure 6.9: Variation of overlay thickness with pavement deflection (2 msa)
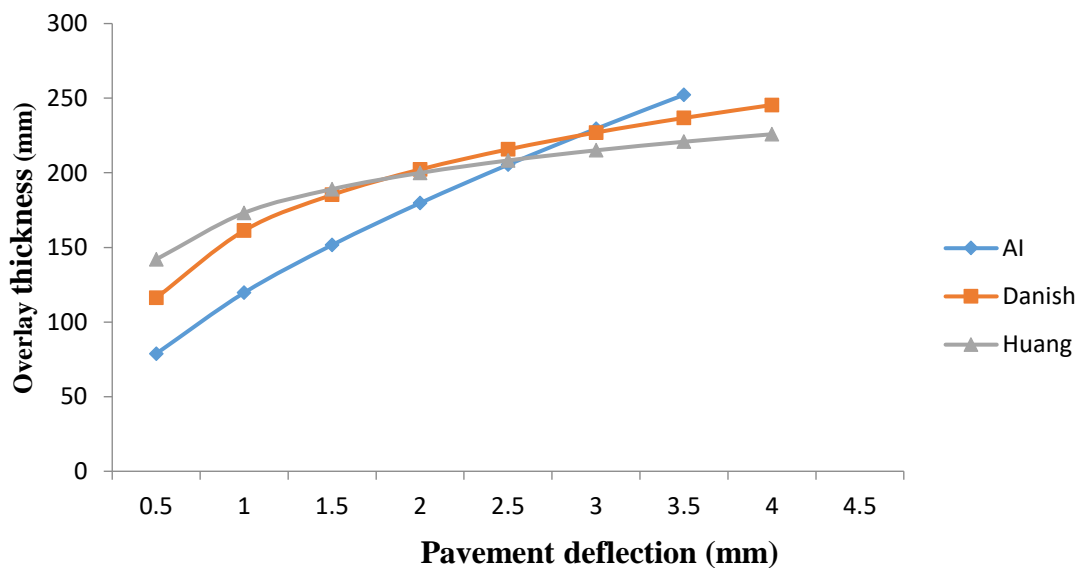
Figure 6.10: Variation of overlay thickness with pavement deflection (5 msa)
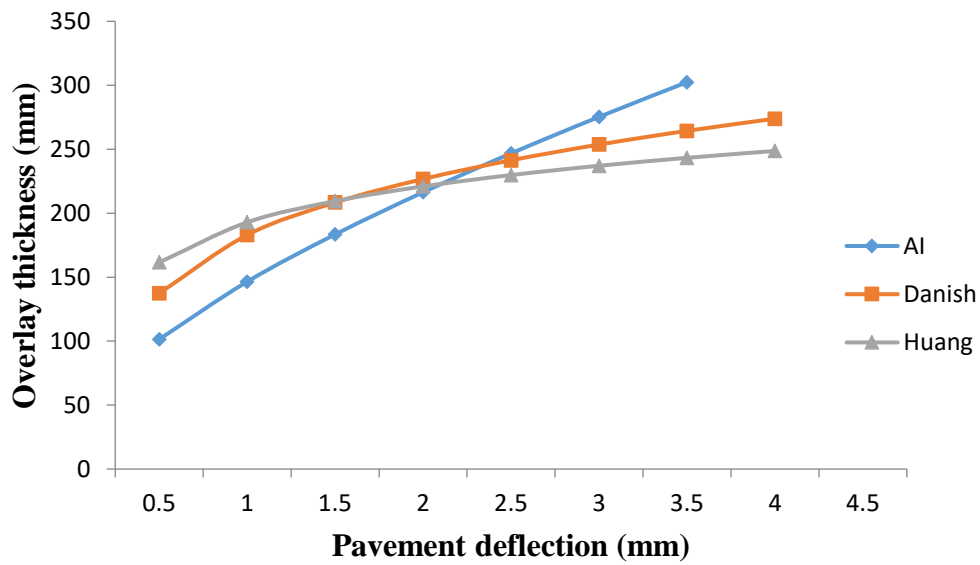
Figure 6.11: Variation of overlay thickness with pavement deflection (10 msa)
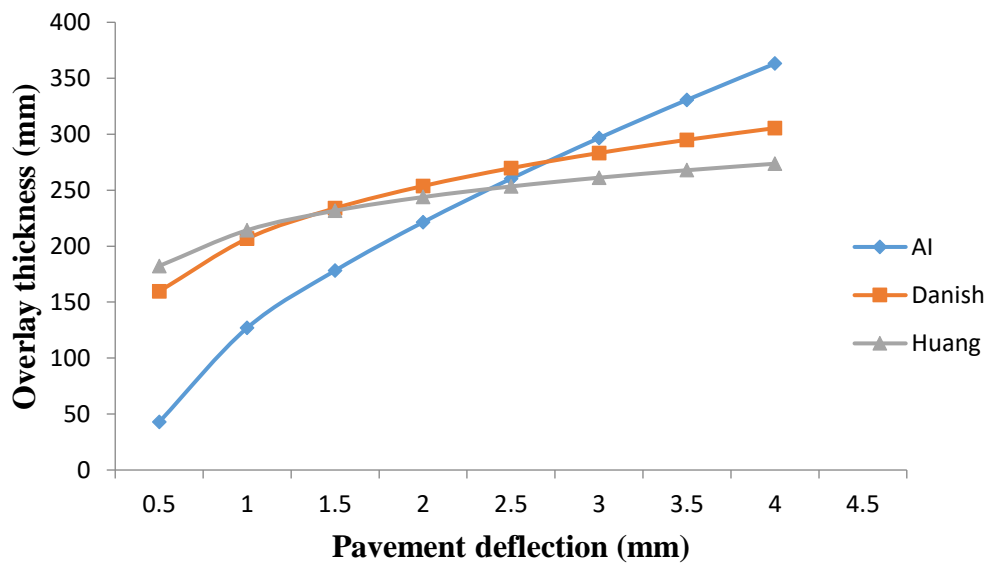
Figure 6.12: Variation of overlay thickness with pavement deflection (20 msa)
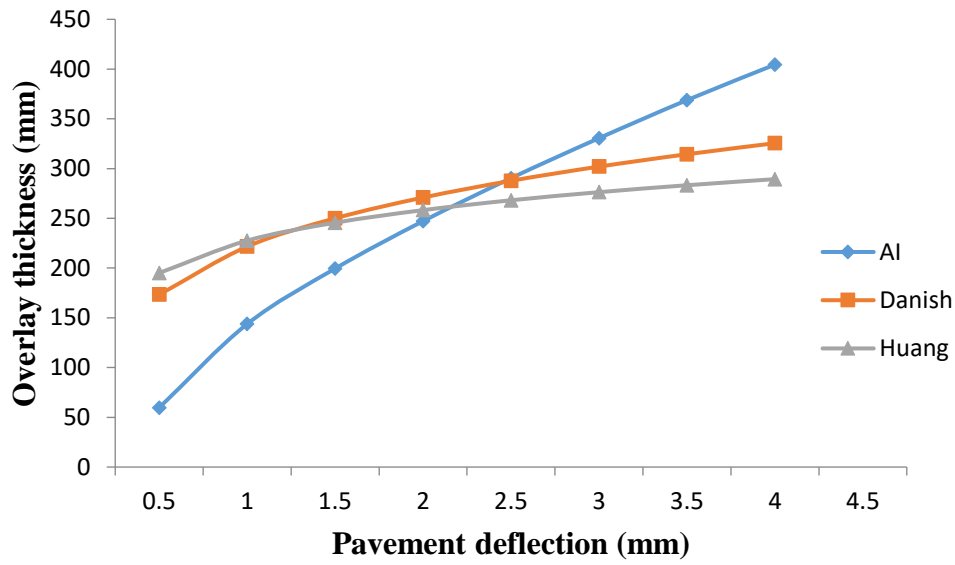
Figure 6.13: Variation of overlay thickness with pavement deflection (30 msa)
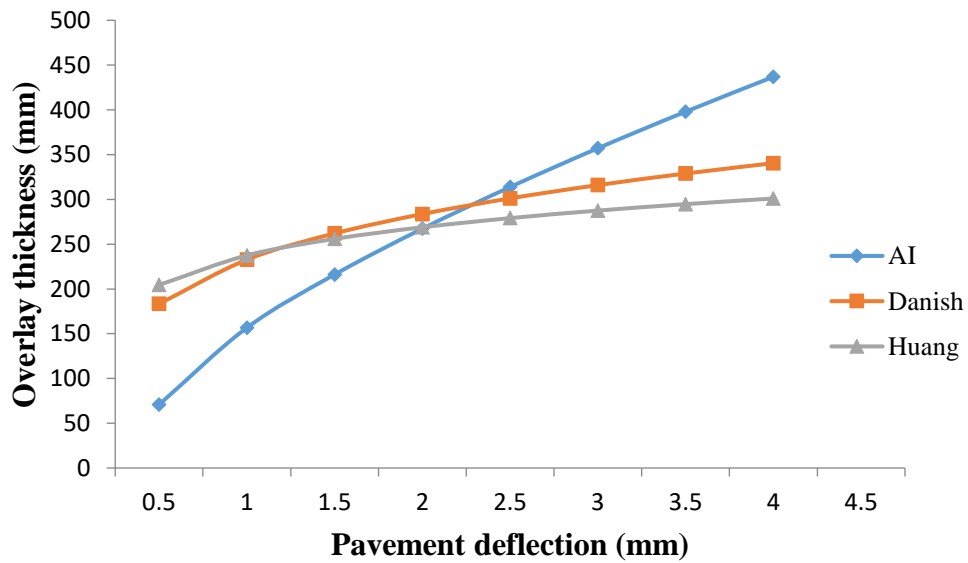
Figure 6.14: Variation of overlay thickness with pavement deflection (40 msa)

213
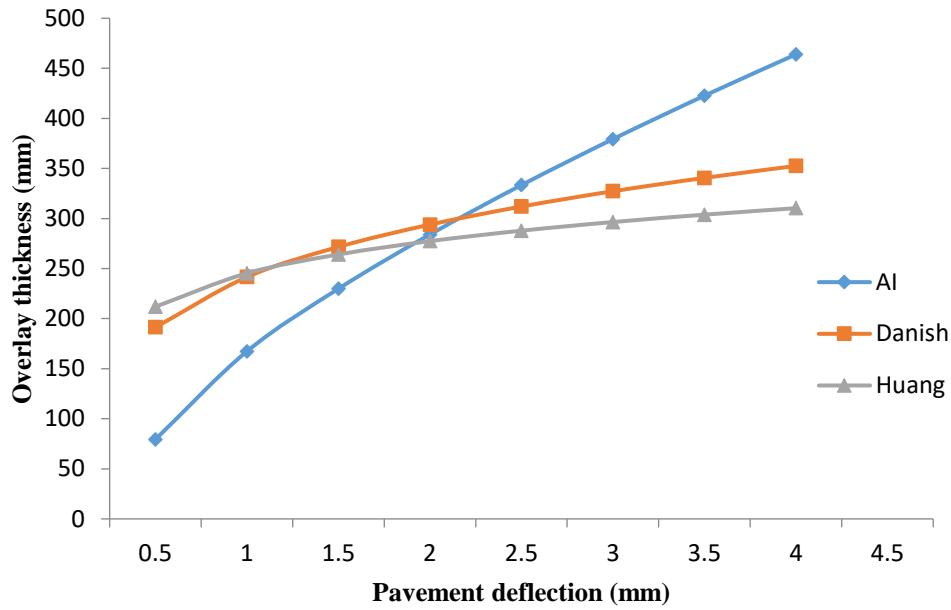
Figure 6.15: Variation of overlay thickness with pavement deflection (50 msa)
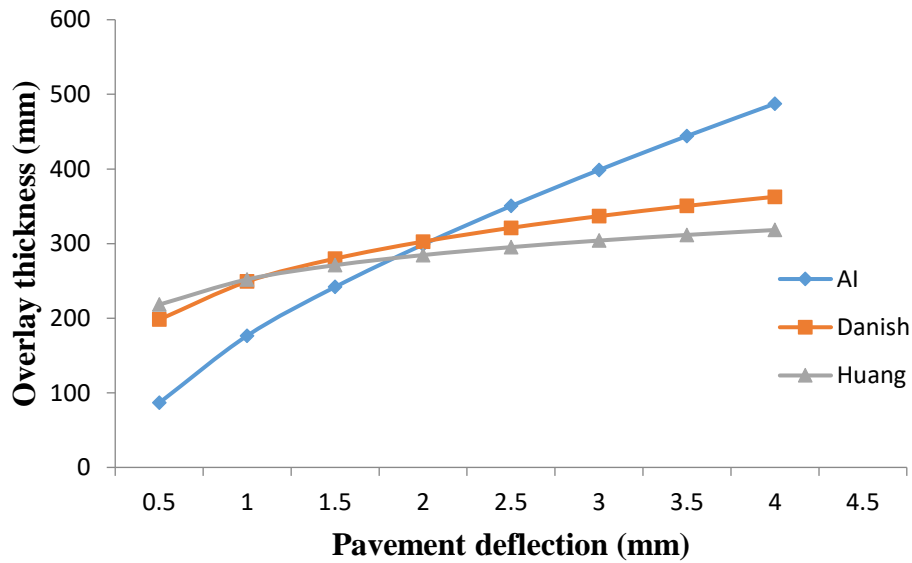
Figure 6.16: Variation of overlay thickness with pavement deflection (60 msa)
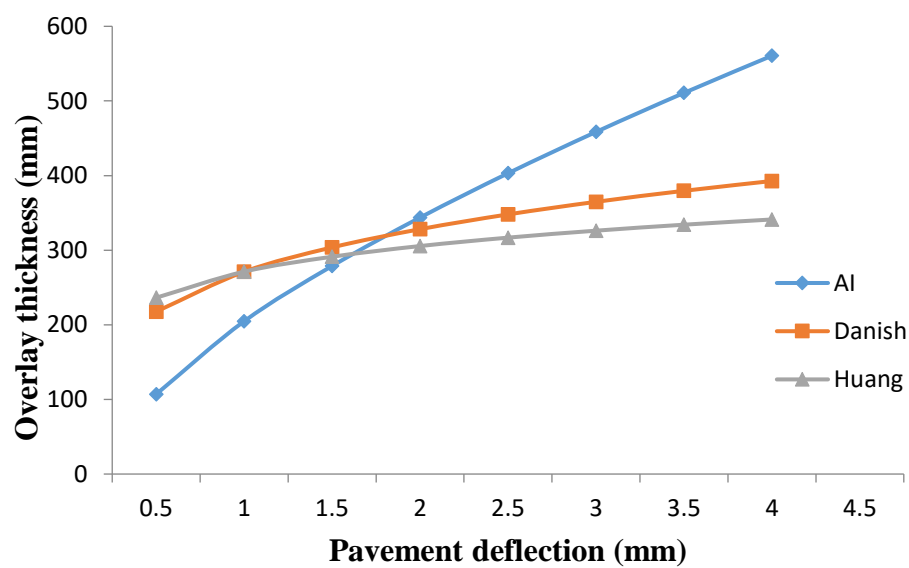
Figure 6.17: Variation of overlay thickness with pavement deflection (100 msa)
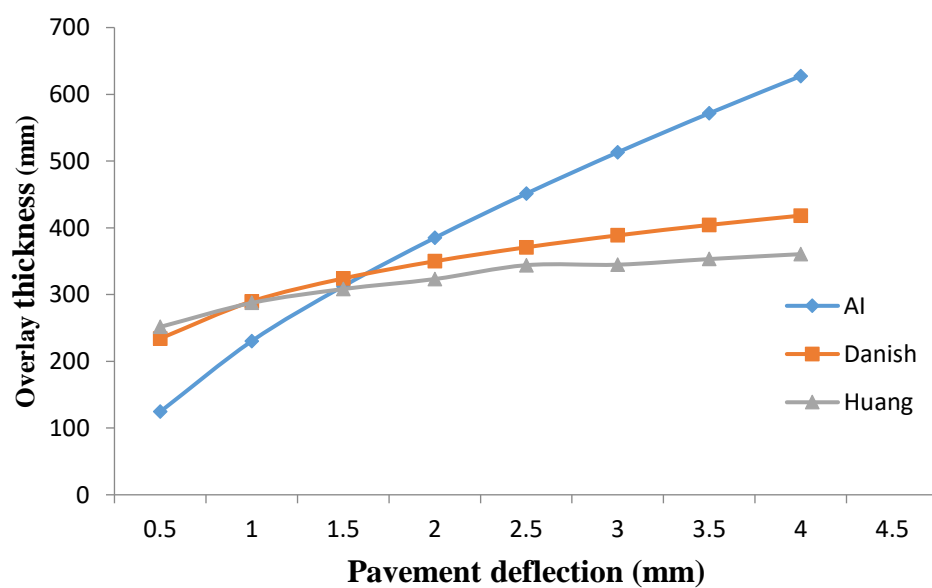
Figure 6.18: Variation of overlay thickness with pavement deflection (150 msa)

6.4.3.1 Validation of overlay thickness using deflection bowl

Detailed analysis of the deflection bowl may interpret the probable extent of damage and distress of road pavement. In present analysis, the deflection bowl parameters like Base Layer Index (BLI) has been considered for comparison and evaluation of safety of overlay thickness obtained using different methods. The allowable value of BLI has been suggested by Horak et al [83-85] as 0.20 mm for flexible pavement, which means the overlay thickness which shows a BLI less than 0.2 mm is well within a factor of safety in terms of its susceptibility to cracking. It is relevant to note that the BLI value depends on the modulus and thickness of the overlay, which changes with axle load repetitions and pavement deflection.
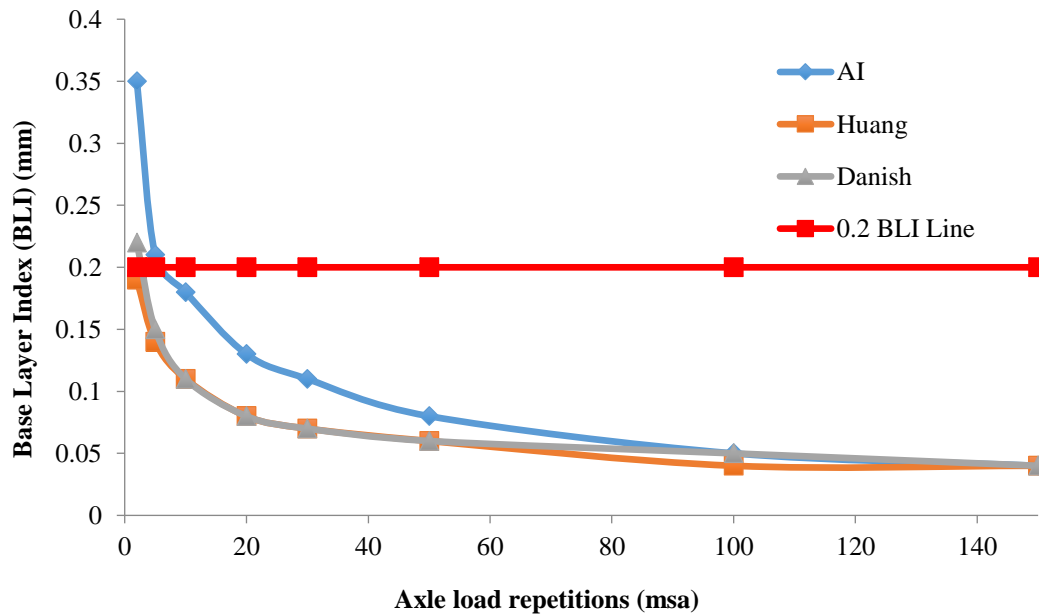
Figure 6.19: Variation of base layer index with axle load repetitions

In present study, the average BLI value for different pavement deflections ranging from 0.5 mm to 4.0 mm for a specified axle load repetition has been determined using a mechanistic approach. The summation of mean plus two times standard deviation of BLI values thus obtained for different pavement deflection has been defined as characteristic BLI in present analysis. The characteristic BLI values thus obtained from two stress-based methods and the deflection-based AI [10] method are presented in Table 6.7 (Appendix 5A).

The axle load variations from 2 to 150 msa have been considered for estimation of BLI in Table 6.7 (Appendix 5A). It has been found that the BLI values obtained for the overlay thickness estimated using the AI method ranges between 0.35 to 0.04 whereas the BLI has been found to range between 0.22 to 0.04 using Danish correlation and 0.19 to 0.03 using Huang's correlation. It has been observed from the data as presented in Table 6.7 (Appendix 5A), the overlay thickness obtained by all three methods is safe against cracking for the sections above the load range of 5msa. However, the overlay thickness estimated using the AI [10] method and Danish [181] correlation for a load range of 2 msa were found marginally unsafe under fatigue. The variation of BLI with axle load repetitions has been presented in Figure 6.19 from which it can be concluded that the overlay thickness obtained using two stress-based approaches in this study are reasonably safe in terms of cracking.

In this section, a sensitivity analysis has also been carried out to find the most dominant parameters between axle load repetitions and modulus of bituminous layer to affect the overlay thickness. For this purpose, initially, overlay thicknesses have been calculated by varying modulus of bituminous overlay from 3500 MPa to1750 MPa by keeping axle load repetitions constant. The variation of overlay modulus @10% from its initial modulus value of 3500MPa has been made in Table. 6.8 (Appendix 5A).

Similarly, by varying load repetition from 50-25 msa, the thickness of the overlay has been calculated for a constant modulus (3500 MPa) of overly. The variation of axle load repetitions @10% from its initial value of 50 msa has also been made in Table. 6.9 (Appendix 5A).

It can be observed from the results as shown in Table 6.8 and Table 6.9 (Appendix 5A), that the change in overlay thickness is higher for change in overlay modulus than axle load repetitions. Therefore it can be concluded from present comparative analysis that the overlay modulus is more sensitive for estimation of overlay thickness. Therefore, use of bituminous overlay mix with higher modulus is preferred in repair of in service flexible road pavements to ensure better durability.

6.4.4   Concluding remarks

It is evident from the results and discussion that, the design of overlay by limiting the vertical interface stress may be considered as a reliable method for strengthening existing bituminous road pavement. Comparative analysis of overlay thickness obtained from stress-based approach reveals that the rate of change of overlay thickness with pavement deflection is reasonably high in AI [10] method than two other stress-based methods. The durability of overlay has been characterized in this analysis by BLI value after determination of deflection bowl under a wheel load. It has been found that the overlay thickness obtained from the stress-based approach is reasonably safe in terms of cracking as evident from the curvature index of the deflection basin. It can be concluded from sensitivity analysis that the modulus of the bituminous mix is more sensitive to affect the overlay thickness than axle load repetitions, if other parameters remain unchanged. However, the design of overlay to limit rutting on pavement and a rigorous method of sensitivity analysis may be considered as future scope of the study.

CHAPTER 7

PREDICTION OF RESIDUAL LIFE OF PAVEMENT BY SURFACE DEFLECTION USING ODEMARK'S APPROACH

7.1   Introduction

Predicting the residual life of pavement is a crucial aspect of infrastructure management and maintenance. It helps transportation authorities and engineers make informed decisions regarding when and how to rehabilitate or replace deteriorating road surfaces. One effective method for estimating the remaining service life of a pavement is through surface deflection analysis, particularly by employing Odemark's [126] approach. Odemark's [126] approach is a widely recognized technique in the field of pavement engineering. It involves the measurement of surface deflections [94, 64, 26], which are deformations or depressions in the pavement caused by the weight of passing vehicles. By analyzing these deflections over time, engineers can gain valuable insights into the structural condition and remaining life of the pavement. Utilizing this predictive methodology in pavement engineering presents numerous benefits. Initially, it supports efficient maintenance procedures [64, 26] by accurately assessing the remaining lifespan [69,128] of pavements, enabling transportation authorities to allocate resources effectively, prioritizing critical areas. Secondly, it advances safety protocols by facilitating timely interventions to prevent hazardous road conditions, thereby reducing the frequency of accidents and associated injuries. Thirdly, it promotes environmental sustainability by optimizing pavement maintenance, thereby reducing the environmental impact of construction and demolition activities, promoting a more environmentally friendly approach to infrastructure management. Lastly, it aids in long-term [64, 26] infrastructure planning by providing authorities with insights into the expected lifespan of pavements, facilitating strategic planning and budget allocation.

Residual life of a pavement can be defined as the anticipated time period or standard axle load repetitions during which a pavement shall be free from functional or structural distress under normal conditions, provided that only routine maintenance is performed [20]. Residual life is calculated from the pavement condition during a specified year and the projected number of years until rehabilitation is required. Once Remaining life is obtained for each pavement section in the network, the sections are grouped into different categories [55]. Such categorization combines severity and extent of different

distresses and rate of deterioration. Prediction of remaining life also includes development of performance models and establishment of a threshold value for each distress type. Based on these threshold values, present distress level and using the deterioration model for the respective distress, the time for each distress to reach the threshold value can be determined[20].Therefore, calculation of remaining life is a complex process due to lack of adequate performance prediction models required for determining the timing of the rehabilitation project. In general, there are three estimation procedures of residual life of pavement, which include (i) functional failure-based approach, (ii) structural failure-based approach and (iii) functional and structural failure-based approaches [192-193]. Kansas Department of Transportation (KDOT) [183] uses an empirical equation, embedded in a probabilistic simulation, to compute remaining service life of flexible pavements based on surface conditions and deflection from the last sensor of a falling weight deflectometer (FWD). However, it is not feasible from time, cost, and safety points of view to use FWD in Indian road network either in national level or in regional level. Gedafa et al. (2008) [70] found no significant difference between the center deflection under the load plate of FWD and that from a rolling-wheel deflectometer (RWD). RWD is a state-of-the-art equipment to measure pavement surface deflection at the centre of the deflectometer at highway speed. The study revealed that RWD could be used to collect deflection data at the network level.

Surface deflection, gauged through non-destructive testing methods like the Falling Weight Deflectometer (FWD) or the Traffic Speed Deflectometer (TSD), serves as a pivotal indicator of the structural capacity and stiffness of the pavement layers. Odemark's [126] approach utilizes these deflection measurements to characterize the pavement's condition, incorporating factors such as load-bearing capacity, material properties, and environmental influences. Through the integration of advanced analytical tools and methodologies, our aim is to refine the accuracy of residual life predictions and contribute to the formulation of proactive pavement management strategies. The findings presented herein furnish valuable insights for transportation agencies, engineers, and decision-makers engaged in the preservation and optimization of pavement assets, ultimately enhancing the sustainability and efficiency of our

transportation infrastructure. In this context, this section delves into the utilization of Odemark's [126] approach for predicting the residual life of pavements based on surface deflection data.

7.2   Literature review

Chen et al. (2010) [44] performed an extensive review on pavement life expectancy models based on a new methodology of model classification. Accurate pavement performance life assessment is crucial for pavement management systems. Various models have been developed over the years, but lack of systematic classification and analysis hinders further research. The study performed reviewed flexible pavement life prediction models and introduced a new classification method for pavement engineers and depicted that predicting pavement remaining service life (RSL) is still in the preliminary stage. The study suggested that determination, unification of threshold values of pavement performance indices and the development of simple and reliable models requiring the data most PMS database has may be crucial for pavement life expectancy research in the future.

Abaza et al. (2004) [6] presented a deterministic performance prediction model for use in rehabilitation and management of flexible pavements. The model presented in the study uses the AASHTO serviceability concept for designing flexible pavements, introducing a performance curve based on the present serviceability index (PSI) which can be estimated using the AASHTO basic design equation. The paper suggests that the performance curve can be used in pavement rehabilitation and management applications, such as evaluating alternatives, developing asphaltic overlay procedures, and performing life-cycle analysis and also predict future conditions and estimation of transition probabilities in stochastic prediction models. These analyses and techniques presented in the study are useful for pavement engineers and the study also predicts that it can be an effective teaching tool for pavement design students.

Park S. H. et al. (2019) [129] suggested that flexible pavements require efficient and realistic prediction models for long-term degradation due to cracking, surface deformation, disintegration, and defects. These failures result from the pavement system's reactions to complex mechanical, thermo

mechanical, or chemical loads. Due to the complexity and uncertainty of pavement degradation, comprehensive and phenomenological studies are necessary to estimate pavement lifetime and evaluate conditions. The study developed three comparative models and applied it to pavement degradation data, with strengths and weaknesses in usability, implementation, and information requirements. The study focuses on the use of a gamma process model for predicting performance degradation and pavement lifetime, obtaining conditions and lifetime as probability distribution curves with time-varying parameters.

Bastola N R et al. (2023) [22] reported that DOTs in the South-Central States and abroad use NDT surface deflection bowl data to identify pavement sections for further investigation. The falling weight deflectometer (FWD) test is a common NDT-based test used to assess flexible pavement performance. The research used 3-D Move software to simulate deflection produced by FWD devices, reducing the need for lengthy field testing. The study validated deflection values and deflection bowl parameters, such as the normalized comprehensive deflection ratio and normalized comprehensive area ratio, to predict the remaining service life of flexible pavement structure which will help DOTs and transportation agencies initiate rehabilitation work efficiently and economically.

Loganathan et al. (2019)[108] proposed approach suggests minimizing the necessity for static Falling Weight Deflectometer (FWD) testing by employing advanced computer simulations to replicate the FWD deflection bowl observed in the field. Through these simulations, a simulated FWD deflection bowl is generated, facilitating the derivation of novel comprehensive parameters for pavement deflection bowl analysis. Specifically, the tensile strain at the bottom of the asphalt layer is effectively linked to the newly formulated normalized Comprehensive Area ratio parameter (CAR) and the number of load repetitions to fatigue failure (N_f). Utilizing the 3D-Move software package, a straightforward method is devised to predict the remaining service life of flexible pavement sections. The study focuses on developing the area ratio parameter using a 1524 mm deflection bowl length, demonstrating a strong correlation between the normalized comprehensive area ratio and the tensile strain at the bottom of the asphalt layer. Consequently, the research concludes

that these parameters offer a straightforward and dependable means of assessing the structural capacity of flexible pavement sections on a network-wide scale.

Elbagalati et al. (2016) [61] predicted in-service pavement structural capacity based on traffic-speed deflection measurements. The Rolling Wheel Deflectometer (RWD) has become a popular tool for predicting pavement structural capacity in Pavement Management Systems (PMS). This study aimed to develop a model that predicted pavement structural capacity at a 0.16 km interval using RWD measurements. The model showed acceptable accuracy with a Root Mean Square Error (RMSE) of 0.8 and coefficient of determination (R^2) of 0.80 in the validation stage. Core samples showed that predicted structurally-deficient sections suffered from asphalt stripping and material deterioration distresses. The developed model can be a valuable tool for predicting pavement structural condition at the network level in PMS.

Bryce et al. (2013)[36] suggested a network-level structural capacity indicator for asphalt pavements in Virginia, examining different indexes and decision-making approaches using deflection and distress data from Virginia's interstate highways. It demonstrates that the Structural Capacity Index, rooted in the structural number principle, yields network-level decisions consistent with the Virginia Department of Transportation's project-level activities in the 2008 construction season. The study assesses the index's sensitivity to input variables and establishes the influence of pavement structural capacity on the service life of maintenance treatments. Additionally, it provides equations for determining the service life of corrective maintenance treatments.

Gao et al. (2018) [69] proposed a damage model for asphalt mixtures based on dissipated energy to facilitate the efficient maintenance and repair of asphalt pavements by accurately predicting their remaining service life. This research conducted repeated indirect tensile tests (ITTs) on asphalt mixtures of varying ages to assess damage accumulation through dissipated energy in each loading cycle. The findings indicated minimal variability and high sensitivity to aging durations, with an exponential curve effectively describing the relationship between dissipated energy and loading cycles across different aging periods. Subsequently, a damage model incorporating dissipated energy was formulated and validated using asphalt mixtures of diverse ages and loading repetitions. Similar ITTs were conducted on samples extracted from Nanjing

Airport Expressway to determine parameters within the damage model. The study emphasized the significance of repeated ITTs on asphalt mixtures with varied aging durations to establish their damage curves based on dissipated energy. The adoption of an exponential function yielded well-fitted curves with low variability and heightened sensitivity to aging duration. Results demonstrated the model's efficacy in predicting the Remaining Service Life (RSL) of asphalt mixtures on the Nanjing Airport Expressway, offering valuable insights for maintenance decisions. However, the paper underscored the necessity for further research to ascertain the applicability of the method to other highways as well as urban and rural roads.

Biligiri K.P. et al. (2015) [26] developed a criterion for evaluating the remaining service life of existing roads based on their field fatigue cracking characteristics. Two base course layers were investigated: reference and modified stone mastic asphalt mixes. Field cores were estimated using fracture mechanics principles, and laboratory performance tests were conducted. The modified structure showed significantly longer fatigue life than the reference mix, indicating that laboratory procedures based on asphalt mixture properties' fracture and fatigue mechanics are useful for evaluating pavement mix performance in the field. The criteria developed in this study could serve as guidelines for agencies to understand asphalt materials' fatigue characterization and implement them as quality control tests to assess pavement design life.

Elkins et al. (2013) [64] reformulated pavement remaining service life framework. Effective pavement network management relies on predicting future construction events. The current RSL terminology has issues, complicating interpretation, interagency data exchange, and use. The paper suggests that to improve consistency, the term "RSI" should be replaced with "time remaining until a defined construction treatment is required." The approach unifies the outcome of different approaches by focusing on when and what treatments are needed and the service interruption created. A companion document (FHWA-HRT-13-050) provided step-by-step guidelines for implementing the RSI terminology.

Karballaeezadeh N et al. (2019) [94] developed an optimized support vector machine (SVM) approach to forecast the remaining service life (RSL) of pavement. Instead of relying on the traditional Heavy Weight Deflectometer

(HWD) test, this method harnessed particle filter techniques to fine-tune the SVM. By incorporating key parameters like pavement layer thickness and asphalt surface temperature, the model accurately projected the RSL on an annual basis. When compared against actual data, the model demonstrated a precision exceeding 95%. The findings propose that this approach offers a viable means to estimate the lifespan of in-use pavements, utilizing readily available weather data and pavement layer thickness information, possibly obtained through Ground Penetrating Radar (GPR) devices. Furthermore, it suggests that adopting this method could yield substantial cost savings and minimize traffic disruptions, enabling authorities and organizations to promptly assess pavement RSL.

Park et al. (2003) [128] suggested a methodology of advancement in forecasting methods for the remaining lifespan of flexible pavements involves utilizing multi load-level deflections obtained from falling-weight deflectometers (FWD). These methods integrate pavement response and performance models to anticipate critical pavement behaviors based on surface deflections and deflection basin parameters. Verification of the predictive procedure relies on pavement distress data and FWD multi load-level deflection data. This approach effectively forecasts fatigue cracking performance, with the exception of pavements experiencing high and rapidly escalating cracking in wet-freeze regions. The research findings demonstrate close agreement between predicted rut depths and measured rut depths across various levels of rutting potentials. Notably, the study highlights that single-load-level deflections consistently underestimate rut depths, underscoring the efficacy of multi load-level deflections in accurately estimating excessive rutting levels and enhancing the prediction accuracy of rutting potential in flexible pavements.

7.3   Objective

The objective of present study is to develop a Mechanistic – Empirical method to estimate residual life of an in-service pavement using surface deflection as design criteria. Moreover, present study is intended to establish correlation between residual life and pavement deflection using layer thickness, traffic and subgrade soil data.

7.3.1   Methodology

In present study, the pavement has been considered as three layer system as shown in Figure 7.1. The top layer consists of binder base with bituminous mix of thickness h_1 with elastic modulus (E_1). The intermediate layer is a combination of unbound granular base and granular sub-base with thickness of h_2 and elastic modulus (E_2) resting on sub-grade soil with a modulus of (E_3). Various research works [46, 48, 51,104] have already been done for design of flexible pavements that recommends the vertical compressive strain on the top of sub-grade or radial tensile strain at the bottom of bituminous layer as design criteria. Moreover, stress based or deflection based design criteria [27-33, 49-50] have also been evolved and are in use. Each of these methods recommends to limit the stress, strain or deflection in different layer interface to determine the required thickness and the moduli of constituent layers for a specified axle load repetitions. It has been assumed in present analysis that the pavement deforms in an elastic manner prior to failure. The analysis in the present study includes formulation of a model to determine the surface deflection of the pavement by Boussinesq's [34] approach after transforming the three-layer pavement system into a homogeneous system by Odemark's [126] method.
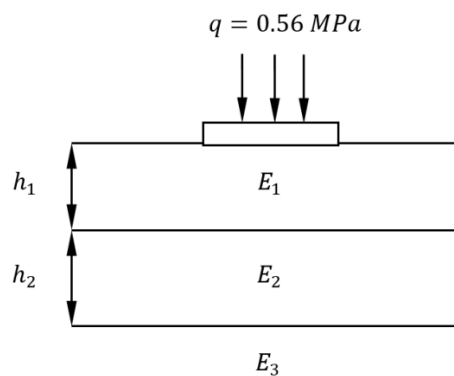
Figure 7.1: Typical section of a three-layered flexible pavement

7.3.1.1 Odemark's approach

The top layer of pavement consists of binder base with bituminous mix of thickness h_1 with elastic modulus (E_1) and Poisson ratio v_1 The intermediate

layer is a combination of unbound granular base and granular sub-base with thickness of h_2, Poisson ratio v_2 and elastic modulus (E_2) resting on sub-grade soil with a modulus of (E_3) with Poisson ratio v_3. Transformation of such three layered system into a homogenous system can be done with the concept of equivalent thickness (h_e) having modulus (E_3). Considering Poisson ratios of three layers are approximately equal, the following relationship can be established as transformed depth for the three layered system as (described earlier in Chapter 2 and Chapter 3)

$$h_e = f_1 \left[f\,h_1 \sqrt[3]{\frac{E_1}{E_2}} + h_2 \right] \sqrt[3]{\frac{E_2}{E_3}} \tag{7.1}$$

7.3.1.2 Determination of surface deflection and vertical strain on subgrade using Odemark –Boussinesq's formulation.

The surface deflection (d_z) of pavement may be obtained as a summation of compression of bituminous base, granular base and sub base and deflection at the top of subgrade along the centre of the loaded area. In this study, three-layered system has been transformed to a homogenous system as mentioned earlier using Odemark's [126] method and subsequently Boussinesq's [34] theory has been applied to determine the surface deflection of pavement in such homogeneous system. According to theory of elasticity the deflection at a depth 'z' in a homogenous mass can be expressed as Equation 7.2.

$$d_z = \frac{(1+v)qa}{E} \left[\frac{1}{\sqrt{1+\left(\frac{z}{a}\right)^2}} + (1-2v)\left(\sqrt{1+\left(\frac{z}{a}\right)^2} - \frac{z}{a} \right) \right] \tag{7.2}$$

By substituting 'z' = h_e Equation 7.2 can be transformed as in Equation 7.3.

$$d_z = \frac{(1+v)qa}{E} \left[\frac{1}{\sqrt{1+\left(\frac{h_e}{a}\right)^2}} + (1-2v)\left(\sqrt{1+\left(\frac{h_e}{a}\right)^2} - \frac{h_e}{a} \right) \right] \tag{7.3}$$

Similarly, using the equivalent depth h_e, the vertical compressive strain (ϵ_z) at the top of subgrade layer along the centreline of load may be obtained as

$$\epsilon_v = \frac{(1+v_3)qa}{E_3} \left[\frac{\frac{h_e}{a}}{\left\{1+\left(\frac{h_e}{a}\right)^2\right\}^{3/2}} + (1-2\,v_3)\left\{ \frac{\frac{h_e}{a}}{\left(1+\left(\frac{h_e}{a}\right)^2\right)^{1/2}} - 1 \right\} \right] \tag{7.4}$$

Where v_3 the Poisson ratio for the subgrade layer and q is the uniformly distributed load acting on an area of radius a.

It is to be noted that surface deflection on the pavement has been accepted as design criteria for design of overlay [91] and the same can be extended for the design of new pavement too. It is relevant to mention that the surface deflection of a pavement is the indicator of the damage of all the constituent layers of the pavement. However, the modulus of subgrade soil being the least amongst the resilient modulus of other constituent layers in the pavement, largely contributes its share in the surface deflection. Flow diagram of adopted methodology for estimation of residual life of flexible pavement is shown in Figure 7.2

7.3.2   Input design parameters

For determination of surface deflection of pavement, the diameter of the loaded area has been considered circular which carries a uniformly distributed load of 0.56 MPa [48,51] and acts on the top surface of the pavement as shown in Figure 7.1. The axle load for pavement design has been considered as 80kN, assuming that the contact area between the tire and pavement as circular and the diameter of the loaded area may be considered as 305.2 mm.

IRC-37: 2012 [48], a guideline for design of flexible road pavements in India formulated by the Indian Roads Congress (IRC) has been used in this study as a reference document to select pavement .sections for different CBR and axle load repetitions The thickness of constituent layers of pavement for different subgrade CBR and axle load repetitions which were recommended in the IRC guideline have been considered as input parameters in present analysis. The pavement thickness in the guideline has been based on limiting the vertical compressive strain on top of subgrade to limit rutting and the radial tensile strain at the bottom of bituminous base in order to limit cracking. It is important to note that the pavement surface deflection as a failure parameter is usually accepted for back calculation of layer modulus for use in iteration technique. However, in the present work, the pavement section which was designed on the basis of strain based criteria has been considered for deflection analysis.
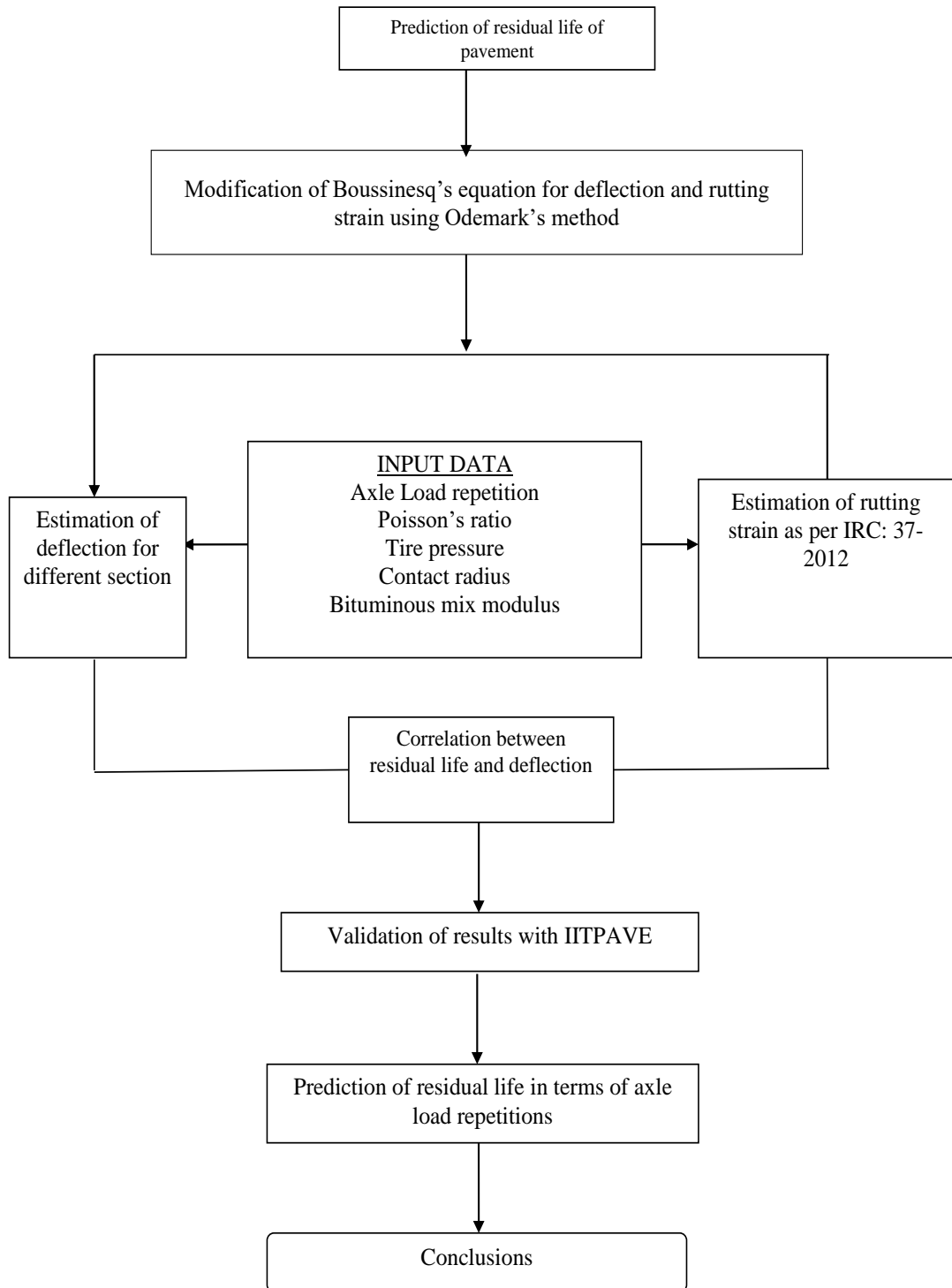
Figure 7.2 Flow diagram of adopted methodology for estimation of residual life of flexible pavement

The vertical compressive strain on the top of the subgrade in a three layer system has been determined in the present work using Equation 7.4 for which the three layered system has been transformed in to a homogeneous system with an equivalent depth as explained in Equation 7.2 .The surface deflection on pavement has also been estimated using Equation 7.3. The allowable axle load repetitions against rutting failure corresponding to a specific vertical compressive strain has been obtained using Equation 7.5 at 90% reliability level.

$$N = 1.41 \times 10^{-8}(\epsilon_v)^{-4.5337} \tag{7.5}$$

Where, *N*= number of cumulative standard axles (msa) before failure in rutting. In present analysis, the pavement life before failure in rutting has been termed as residual life which can be determined from proposed correlations of deflection and axle load repetitions.

However, according to IRC: 37-2012 [48], the combined elastic modulus of granular base and sub-base layer may be expressed as

$$E_2 = 0.2 \, (h_2)^{0.45} E_3 \, (MPa) \tag{7.6}$$

Where *h₂* = total thickness of granular base and sub-base (mm) and elastic modulus of pavement subgrade can be expressed as

$$E_3 = 10(CBR) \quad (MPa) \text{ if } CBR \leq 5\% \tag{7.7}$$

$$E_3 = 17.6(CBR)^{0.64} \; (MPa) \text{ if } CBR > 5\% \tag{7.8}$$

In this backdrop, correlation between axle load repetitions, which has been obtained using Equation 7.5 and the surface deflection using Equation 7.3 for different subgrade CBR have been established and presented in this study. The assumption made in this formulation emphasises the predominating mode of failure of pavement as rutting, which has a strong correlation with vertical compressive strain on the top of subgrade and the surface deflection of the pavement.

The initial thickness of the pavement section has been considered as per the recommendation of IRC: 37-2012 [48] for specific axle load repetitions and subgrade CBR. In the present work, subgrade CBR of 3%, 5%, 7% and 10% have been considered for different axle load repetitions ranging between 2 msa and 150 msa.

Therefore, the surface deflection determined using present approach for different pavement thickness for a specific axle load repetition and subgrade CBR may be considered as allowable deflection, a design criteria for pavement evaluation. Variations of surface deflection with axle load repetitions for different subgrade strength thus obtained, are presented in Figure 7.3.

It is relevant to note that the Benkelman beam rebound deflection measurements are taken on pavements till the presence of bituminous mix on wearing course. The need of estimation of residual life of bituminous pavement becomes important when there are visible damage and distress in the pavement structure. In this study, it has been assumed that the need of repair of pavement becomes urgent when the bituminous wearing course becomes functionally non-existent and propagation of damage and distress in binder course are significant.

7.4   Results and Discussion

It is evident from the results obtained that the allowable deflection on pavement reduces with the increase in axle load repetitions. The research works [191-193] so far conducted reveals that the allowable pavement deflection varies with standard axle load repetition. However, the present work reveals that the allowable deflection on pavement is also dependent on pavement subgrade CBR besides axle load repetitions. The more is the subgrade strength, the less will be the allowable deflection for a specified axle load repetitions. The deflection of an in-service pavement is obtained by any in-situ non-destructive test, which may be used to find out the residual life of pavement as illustrated in present work. If the measured surface deflection is more than the allowable surface deflection for a specific subgrade, then the residual life of the pavement will be substantially less as the slope of the curves indicating the variation of residual life with surface deflection are stiff. It has been accepted that the strength of subgrade in pavement affects largely the surface deflection of the pavement. Therefore, the deflection based pavement evaluation should be correlated with its subgrade CBR and such correlations are presented in this study. It is to be noted that determination of subgrade strength either in field or in laboratory can be done easily with a better degree of reliability and therefore may be used in those correlations to estimate residual life with a better reliability. The residual life of pavement has been characterised as the number of standard axle load

repetitions on pavement before its failure in rutting corresponding to an allowable deflection for a typical subgrade as shown in Figure 7.3. It is relevant to mention that a terminal surface deflection may also be explained from the conceptual framework of present work corresponding to a minimum axle load repetition, which may allow a time period for preparation of repair by the highway administration.

Boussineq's -Odemark's [34,126] methodology to predict the residual life of pavement using surface deflection has advantages, but it also has limitations. However, it should be emphasized that the current model does not sufficiently account for the aging impacts of pavement materials over time. As pavements age, the material qualities change, altering structural behavior and failure mechanisms that may not be adequately addressed in the current model. If the change in depth of the bituminous layer thickness and related modulus had been taken into account, the deflection versus load characteristic would have been much more realistic than illustrated in Figure 7.3.

To ensure accurate predictions, the model may need to be calibrated and validated using local or site-specific data. Without sufficient validation, generalizations from one site or set of conditions to another may result in incorrect residual life estimations. A representative core sample is particularly recommended for this purpose and for estimating input parameters.

It is crucial to note that advances in pavement engineering and research may eventually address some of these constraints. When using present approach for forecasting the residual life of pavements, users should take caution and keep these limitations in mind.

7.4.1 Validation of proposed model

To validate the proposed methodology few pavement section corresponding to CBR 15%, 10%, 8% and 5% from IRC: 37-2012 [48] have been analyzed by IITPAVE for estimation of pavement deflection for different axle load repetitions. The deflection thus obtained using IITPAVE and present method have been shown in Figure 7.4 to Figure 7.7. It is evident from these figures that both method yield almost similar deflection and strain which in other way proves the acceptability of present method.
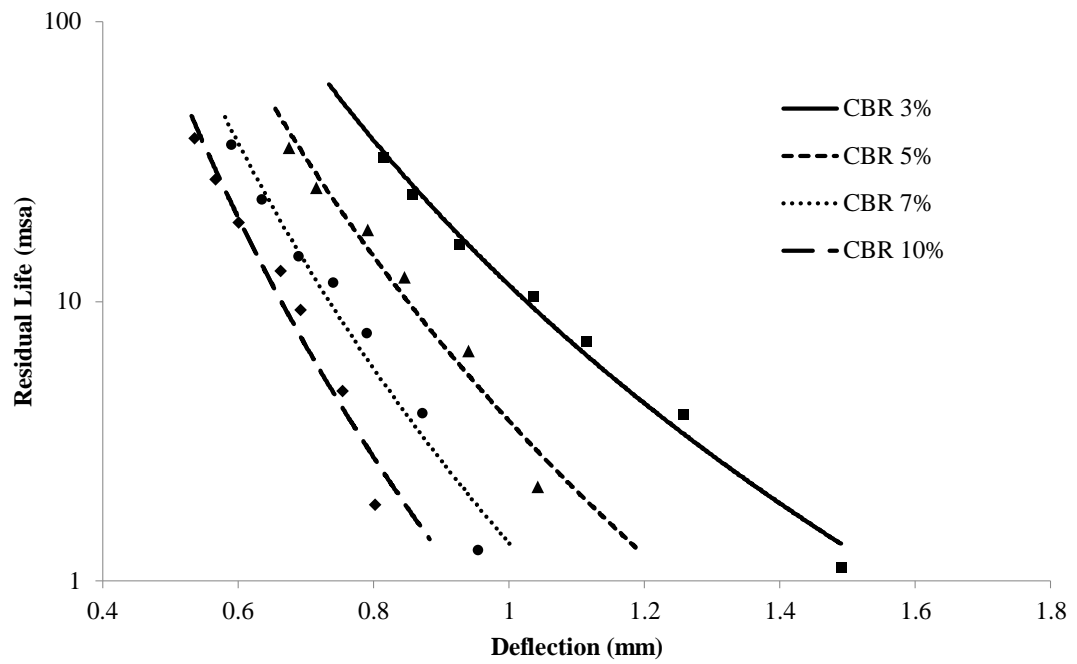
Figure 7.3: Variation of residual life of pavement and deflection for different subgrade CBR (%)
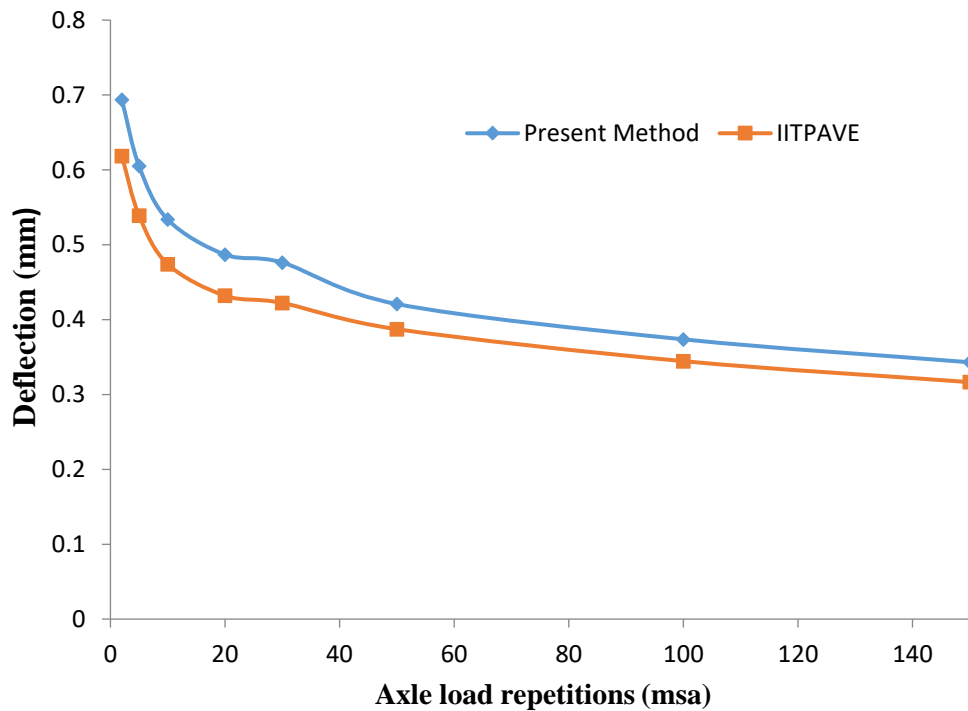
Figure 7.4: Comparison of variation of deflection with axle load repetitions between present method and IITPAVE for 15 % subgrade CBR
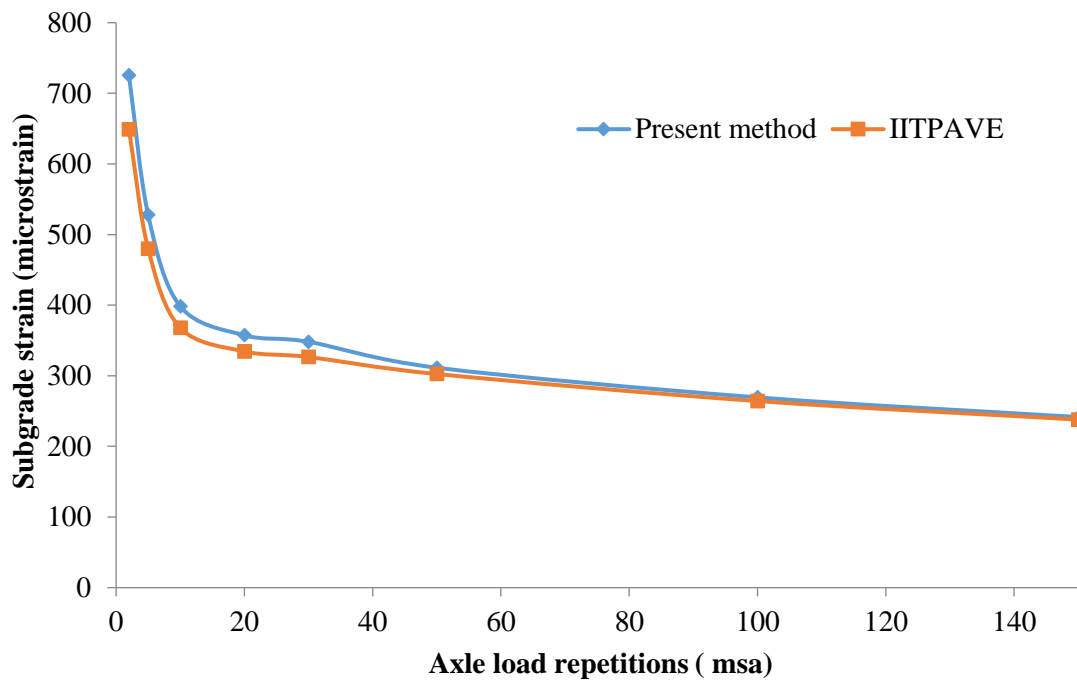
Figure 7.5: Comparison of variation of subgrade strain with axle load repetitions between present method and IITPAVE for 10 % subgrade CBR
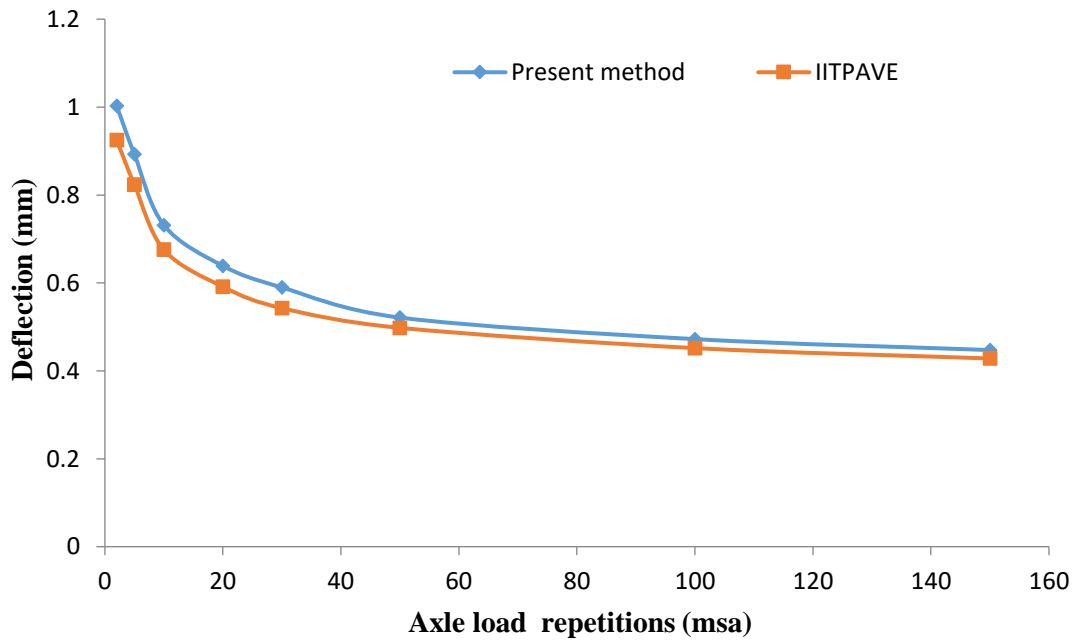
Figure 7.6: Comparison of variation of deflection with axle load repetitions between present method and IITPAVE for 8% subgrade CBR
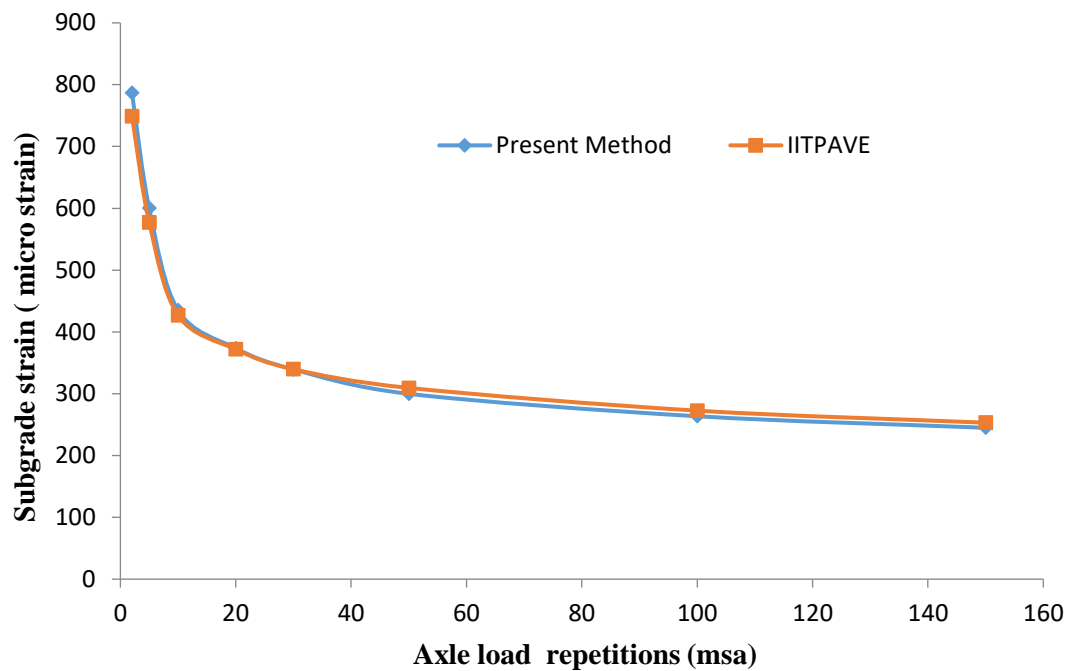
Figure 7.7: Comparison of variation of subgrade strain with axle load repetitions between present method and IITPAVE for 5 % subgrade CBR

7.5   Concluding remarks

The findings of the present study may be considered as an indicative model for determination of residual life of a bituminous road pavement using surface deflection as an effective parameter. Estimation of residual life of pavement is an important aspect of pavement management in terms of adopting appropriate repair and rehabilitation program of the pavement. It has been observed that the residual life of pavement may be obtained from the pavement deflection using the methodologies and model suggested in this study. It has also been found that the allowable deflection on pavement depends on pavement subgrade CBR and axle load repetitions. A concept of terminal surface deflection, the threshold value of deflection beyond which the pavement section shall deemed to be deficient from functional and structural point of view may be determined from present study. Terminal deflection on the pavement thus obtained emphasises the need for immediate repair of pavement section.

CHAPTER 8
CONCLUSIONS AND FUTURE SCOPES OF WORK

8.1   Conclusions

A strain and stress based Mechanistic- Empirical approach has been used in present study to determine the compacted subgrade thickness on the top of a weak natural subgrade as a measure of ground improvement for specified axle load repetitions. It has been found that the thickness of compacted subgrade increases with the increase in axle load and decrease in strength of natural subgrade. It has also been found that the increase of thickness of compacted subgrade is significant of upto 50 msa load repetitions beyond which it becomes less significant. It is observed in this study that the compacted subgrade thickness, as per strain-based criteria, exceeds that of stress-based approach.

Furthermore, the study includes the importance of axle load repetitions as an input variable for determination of compacted subgrade thickness. Moreover, the study concludes that the provision of IRC: 37-2018 or MORD specifications to provide 500 mm thickness of compacted subgrade without considering axle load repetitions, may lead to either an under-designed or over-designed section, resulting in an unsafe or uneconomical pavement in terms of rutting failure. Hence, it is recommended to modify the provision of a fixed thickness of compacted subgrade in the light of present analysis.

A deflection based method for estimation of compacted subgrade thickness may also be used to achieve a required effective CBR of subgrade for design of flexible road pavement. It has been found that the depth of borrow materials are based on input variables like natural subgrade CBR, compacted soil subgrade CBR, and effective CBR. It is important to note that when the natural subgrade CBR is below 5%, subgrade improvement is required to enhance its strength and extend service life against rutting. Present study reveals substantial variations in the thickness of compacted subgrade up to a CBR of 20% for borrowed soil, beyond which the variations are less significant. The study also suggests that the future efforts should focus on estimating depth of compacted subgrade with required effective CBR for a projected service life of the pavement.

In this study, stress based low volume pavement design has been proposed which reveals the sensitivity of pavement thickness variation on soft soil compared to hard soil. The suggested pavement design method recommends

determination of granular base thickness with different elastic moduli. The outcomes of proposed stress-based pavement design model are comparable with other results obtained from mechanistic, empirical, and mechanistic-empirical approaches.

The study further includes the application of a concentration factor for determination of vertical stress using the modified Boussinesq's equation in a layered system. The pavement thickness obtained from present analytical approach based on concentration factor closely matches with findings from other Mechanistic-Empirical based approach.

Further, the study has been aimed to develop a Mechanistic-Empirical approach to determine required optimum thickness of bituminous and granular layer against rutting and fatigue in a flexible road pavement. It has been found that the variation of granular layer thickness is more sensitive than the bituminous layer thickness on pavement performance in terms of rutting. The pavement deflection obtained for the estimated thickness of granular and bituminous layer using present methodology was found close to those obtained using IITPAVE and KENPAVE. In this context, the proposed method may be considered as an acceptable and reliable approach in pavement design. However, the effect of variation of modulus of pavement layers on pavement thickness need to be considered in future to increase the reliability of the method.

A strain based methodology for perpetual pavement design has also been proposed in this study, which can be used for the estimation of conventional bituminous pavement thickness considering the pavement as a multi-layered system. The reliability of the method has been compared with IRC: 37-2018 and found to be satisfactory. It has been observed in the present analysis that the thickness of the binder base required to withstand fatigue is generally more than that of rutting under a specified axle load repetition. Therefore, it can be concluded that the service life of perpetual pavement is governed by its failure under fatigue.

It is relevant to mention that the thickness of the binder base in a perpetual road pavement obtained using 300 msa load appears to be less than the thickness obtained using finite strain-based criteria. For validation of the present method, fatigue and rutting strains were estimated using IITPAVE for the

pavement thickness obtained using present methodology. It has been found from the analysis that the allowable radial tensile strain at the bottom of a bituminous layer to withstand fatigue should be revised as 95με instead of 80με for perpetual pavement design. Similarly, the allowable vertical compressive strain on the top of the subgrade may be modified to 185με instead of 200με. Moreover, the thickness of the binder base obtained from present study shows good convergence with the binder base thickness obtained using IITPAVE. Therefore, the present method may be considered as a reliable approach of Mechanistic- Empirical design of perpetual road pavement.

Overlay thickness design has also been discussed in present study. It has been found that the pavement with higher deflection is weak in strength and would require a higher thickness of overlay for specified service life and vice versa. The overlay thickness has been estimated in this study based on vertical interface deflection, which closely matches with the overlay thickness obtained from the Asphalt Institute method. Comparison of overlay thickness with the Asphalt Institute method has been made in this study for both low as well as high volume roads.

However, it is relevant to mention that the rate of increase of overlay thickness with respect to pavement deflection is reasonably high in high-volume roads with respect to low-volume roads. The rate of change of overlay thickness for different pavement deflections have been found close between the present approach and the Asphalt Institute method. Therefore, it can be concluded that the sensitivity of pavement deflection on overlay thickness is comparable between the two methods and justifies the reliability of the present method as an analytical approach for estimation of overlay thickness.

In the present study, attempts have also been made to assess the reduction in overlay life due to overloading on road pavement. It has been observed that the reduction of overlay age is significantly higher for the roads with high axle load repetition. But when the pavement is severely damaged showing higher deflection, the reduction in overlay life for both high and low-volume roads are comparable and significant. In this backdrop, the effect of different classes of axle and wheel loads on vehicle damage factors for overlay design may be considered as future scope of work.

It is also evident, that the design of overlay thickness by limiting the vertical interface stress may be considered as a reliable method for strengthening existing bituminous road pavement. Comparative analysis of overlay thickness obtained from stress-based approach reveals that the rate of change of overlay thickness with pavement deflection is reasonably high in AI method than two other stress-based methods. The durability of overlay has been characterized in this study by BLI value after determination of deflection bowl under a wheel load. It has been found that the overlay thickness obtained from the stress-based approach is reasonably safe in terms of cracking as evident from the curvature index of the deflection basin. It can be concluded from sensitivity analysis that the modulus of the bituminous mix is more sensitive to affect the overlay thickness than axle load repetitions, when other parameters remain unchanged. However, the design of overlay to limit rutting on pavement, a rigorous method of sensitivity analysis may be considered as future scope of the study.

Finally, an indicative model for determination of residual life of a bituminous road pavement has also been developed using surface deflection as a design parameter. It has been found that the allowable deflection on pavement depends on pavement subgrade CBR in addition to axle load repetitions. A concept of terminal surface deflection, the threshold value of deflection beyond which the pavement section shall deemed to be deficient from functional and structural point of view may be estimated from present study.

Moreover, in present study an attempt has been made to develop all the algorithm that leverages MATHEMATICA as a powerful calculation tool, PYTHON as a backend program and JAVA as language to develop Graphical User Interface (GUI). These algorithms have been worked out to streamline the process of translating few solutions of doctoral thesis into functional software, showcasing the integration of advanced mathematical capabilities offered by MATHEMATICA and the versatility of PYTHON for seamless program execution and user interaction. This attempt marks a significant advancement in the intersection of academic research and practical software development, providing a robust and efficient solution for the transformation of theoretical concepts into tangible, user-friendly applications.

8.2   Future scope of work

The scope of future work on flexible pavements involves addressing various aspects related to the design, construction, maintenance, and performance of flexible road pavement. The key areas that researchers and practitioners may focus on:

1. Enhancements in probabilistic modeling techniques can be pursued to better capture uncertainties in real-life situations. This includes refining models that account for environmental factors and traffic loads, ensuring a more realistic assessment of pavement performance during climate change.

2. Implementation of a strain-based design approach, which involves design of the pavement structure based on the strains experienced by the materials under dynamic load. Calibration of design parameters to ensure that the pavement can accommodate expected strains without experiencing excessive deformation or damage.

3. Integration of advanced technologies, such as intelligent transportation systems (ITS) and sensors, for real-time monitoring of pavement performance. Utilization of data-driven approaches for continuous improvement and adaptation of pavement designs.

4. Evaluation of the economic feasibility and cost-effectiveness of the proposed design approach. Consideration of initial construction costs, as well as life-cycle costs, to ensure the overall economic sustainability of the pavement.

5. The importance of load characterization, especially considering load from tandem and tridem axles in the Indian context, highlights an important area for future study. Researchers should inquire into the effects of factors such as tire pressure, wheel load, and axle configuration, on vehicle damage factor with reference to design of road pavements. This analysis will provide valuable insights into assessing and mitigating the extent of pavement damage caused by different vehicular loads.

6. Analysis of behaviour of multilayered road pavements using non-linear elastic approach and FEM based analysis.

7. Continued exploration of optimization algorithms within reliability-based design can lead to further improvements in the efficiency of design parameters. This could contribute to more resource-efficient designs, reducing construction costs while maintaining the desired level of pavement performance.

8. The future scope involves implementing comprehensive monitoring systems to assess the long-term performance of pavements under varying conditions. This continuous evaluation would aid in refining reliability-based design approaches and ensuring designs meet performance criteria throughout the entire pavement life cycle.

APPENDICES

Appendix 1A

Table 2.1: Depth of borrow material for compacted subgrade on

2% natural subgrade CBR.

Borrow material CBR (%)	Depth of borrow material to achieve effective CBR (%)									
	5%	**6%**	**7%**	**8%**	**9%**	**10%**	**12%**	**15%**	**13%**	**14%**
7	837.9	1808.0	NA	NA	NA	NA	NA	NA	NA	NA
8	618.3	1020.5	2317.3	NA	NA	NA	NA	NA	NA	NA
9	509.7	755.0	1285.8	2869.0	NA	NA	NA	NA	NA	NA
10	444.3	620.5	939.2	1572.0	3461.3	NA	NA	NA	NA	NA
11	400.3	538.6	764.1	1136.0	1876.6	4090.7	NA	NA	NA	NA
12	368.4	483.1	657.8	916.9	1345.7	2199.6	NA	NA	NA	NA
13	344.0	442.8	586.1	784.0	1078.5	1566.7	5454.0	NA	NA	NA
14	324.8	412.1	534.2	694.6	917.0	1248.6	2896.0	NA	6184.1	NA
15	309.2	387.8	494.7	630.0	808.5	1056.5	2042.0	NA	3268.6	6945.0
16	296.1	368.0	463.6	581.0	730.2	927.6	1613.0	7735.3	2294.5	3655.8
17	285.0	351.6	438.4	542.5	671.0	834.8	1354.0	4057.4	1805.8	2557.1
18	275.5	337.7	417.4	511.3	624.5	764.6	1181.0	2829.2	1511.5	2006.3
19	267.2	325.7	399.7	485.5	586.9	709.6	1056.0	2213.6	1314.4	1674.6
20	259.8	315.2	384.6	463.7	555.9	665.2	962.0	1843.1	1172.9	1452.6
30	215.3	254.4	300.3	348.9	401.0	457.4	587.0	839.6	661.5	745.2
40	193.1	225.5	262.5	300.5	340.0	381.3	471.0	627.1	519.3	571.3
50	179.0	207.7	239.9	272.5	305.7	339.8	411.0	530.4	449.4	489.0

Table 2.2: Depth of borrow material for compacted subgrade on 3% natural subgrade CBR.

Borrow material CBR (%)	Depth of borrow material to achieve effective CBR (%)									
	5%	6%	7%	8%	9%	10%	12%	13%	14%	15%
7	837.9	1808.0	NA	NA	NA	NA	NA	NA	NA	NA
8	618.3	1020.5	2317.3	NA	NA	NA	NA	NA	NA	NA
9	509.7	755.0	1285.8	2869.0	NA	NA	NA	NA	NA	NA
10	444.3	620.5	939.2	1572.0	3461.3	NA	NA	NA	NA	NA
11	400.3	538.6	764.1	1136.0	1876.6	4090.7	NA	NA	NA	NA
12	368.4	483.1	657.8	916.9	1345.7	2199.6	NA	NA	NA	NA
13	344.0	442.8	586.1	784.0	1078.5	1566.7	5454.0	NA	NA	NA
14	324.8	412.1	534.2	694.6	917.0	1248.6	2896.0	NA	6184.1	NA
15	309.2	387.8	494.7	630.0	808.5	1056.5	2042.0	NA	3268.6	6945.0
16	296.1	368.0	463.6	581.0	730.2	927.6	1613.0	7735.3	2294.5	3655.8
17	285.0	351.6	438.4	542.5	671.0	834.8	1354.0	4057.4	1805.8	2557.1
18	275.5	337.7	417.4	511.3	624.5	764.6	1181.0	2829.2	1511.5	2006.3
19	267.2	325.7	399.7	485.5	586.9	709.6	1056.0	2213.6	1314.4	1674.6
20	259.8	315.2	384.6	463.7	555.9	665.2	962.0	1843.1	1172.9	1452.6
30	215.3	254.4	300.3	348.9	401.0	457.4	587.0	839.6	661.5	745.2
40	193.1	225.5	262.5	300.5	340.0	381.3	471.0	627.1	519.3	571.3
50	179.0	207.7	239.9	272.5	305.7	339.8	411.0	530.4	449.4	489.0

Table 2.3: Depth of borrow material for compacted subgrade on 4% natural subgrade CBR.

Borrow material CBR (%)	Depth of borrow material to achieve effective CBR (%)									
	5%	6%	7%	8%	9%	10%	12%	13%	14%	15%
7.0	267.0	626.7	NA	NA	NA	NA	NA	NA	NA	7.0
8.0	202.1	368.7	871.6	NA	NA	NA	NA	NA	NA	8.0
9.0	169.7	280.3	501.6	1141.0	NA	NA	NA	NA	NA	9.0
10.0	150.1	235.0	375.9	644.6	1434.4	NA	NA	NA	NA	10.0
11.0	136.7	207.1	311.7	476.9	798.4	1750.8	NA	NA	NA	11.0
12.0	126.9	188.0	272.5	391.7	584.1	962.7	NA	NA	NA	12.0
13.0	119.4	174.1	245.8	339.8	475.8	698.0	2449.0	NA	NA	13.0
14.0	113.4	163.4	226.4	304.6	410.0	564.4	1322.0	2828.1	NA	14.0
15.0	108.5	154.9	211.5	279.1	365.5	483.4	945.0	1516.8	3227.0	15.0
16.0	104.4	147.9	199.7	259.7	333.3	428.8	755.0	1077.9	1721.0	16.0
17.0	100.9	142.0	190.1	244.3	308.9	389.4	641.0	857.4	1217.0	17.0
18.0	97.9	137.1	182.1	231.8	289.6	359.6	564.0	724.3	964.0	18.0
19.0	95.2	132.8	175.2	221.4	273.9	336.0	508.0	635.1	811.5	19.0
20.0	92.9	129.0	169.4	212.6	260.9	317.0	466.0	570.8	709.2	20.0
30.0	78.3	106.6	136.1	165.3	195.2	226.7	297.0	336.3	381.4	30.0
40.0	70.8	95.6	120.7	144.8	168.6	192.8	244.0	270.7	299.4	40.0
50.0	66.0	88.7	111.3	132.6	153.3	173.9	216.0	237.6	260.1	50.0

Table 2.4: Depth of borrow material for compacted subgrade on 5% natural subgrade CBR.

Borrow material CBR (%)	Depth of borrow material to achieve effective CBR (%)									
	5%	6%	7%	8%	9%	10%	12%	13%	14%	15%
7	NA	320.6	NA	NA	NA	NA	NA	NA	NA	7
8	NA	182.8	518.9	NA	NA	NA	NA	NA	NA	8
9	NA	136.6	301.1	727.4	NA	NA	NA	NA	NA	9
10	NA	113.6	226.3	417.0	953.2	NA	NA	NA	NA	10
11	NA	99.6	188.1	311.0	538.4	1197.0	NA	NA	NA	11
12	NA	90.2	164.8	257.0	397.7	667.4	NA	NA	NA	12
13	NA	83.3	148.9	223.9	326.2	488.4	1740.0	NA	NA	13
14	NA	78.1	137.3	201.4	282.5	397.6	949.5	2037.2	NA	14
15	NA	73.9	128.5	185.1	253.0	342.5	684.0	1102.7	2350.8	15
16	NA	70.5	121.5	172.6	231.5	305.2	550.1	789.3	1263.7	16
17	NA	67.6	115.7	162.7	215.2	278.2	469.0	631.5	899.6	17
18	NA	65.2	110.9	154.7	202.2	257.7	414.5	536.1	716.5	18
19	NA	63.1	106.8	148.0	191.7	241.5	375.1	472.0	605.9	19
20	NA	61.3	103.3	142.3	183.0	228.4	345.3	425.8	531.6	20
30	NA	50.4	83.3	111.5	138.5	165.6	224.0	256.5	292.3	30
40	NA	45.1	74.0	98.0	120.2	141.7	185.3	208.0	231.8	40
50	NA	41.8	68.3	90.0	109.6	128.4	165.0	183.6	202.6	50

Table 2.5: Depth of borrow material for compacted subgrade on 6% natural subgrade CBR.

Borrow material CBR (%)	Depth of borrow material to achieve effective CBR (%)									
	5%	6%	7%	8%	9%	10%	12%	13%	14%	15%
7	NA	NA	NA	NA	NA	NA	NA	NA	NA	7
8	NA	359.3	NA	NA	NA	NA	NA	NA	NA	8
9	NA	201.8	551.0	NA	NA	NA	NA	NA	NA	9
10	NA	148.7	315.6	751.7	NA	NA	NA	NA	NA	10
11	NA	122.3	234.8	427.0	967.5	NA	NA	NA	NA	11
12	NA	106.4	193.7	316.1	542.9	NA	NA	NA	NA	12
13	NA	95.8	168.6	259.6	398.8	1447.0	NA	NA	NA	13
14	NA	88.0	151.6	225.2	325.6	794.6	1710.8	NA	NA	14
15	NA	82.2	139.3	201.8	281.0	574.8	931.1	1989.5	NA	15
16	NA	77.5	129.9	184.8	250.9	463.8	669.2	1074.7	2282.9	16
17	NA	73.7	122.4	171.9	229.0	396.4	537.1	767.9	1225.3	17
18	NA	70.6	116.4	161.7	212.3	351.0	457.1	613.4	871.0	18
19	NA	67.9	111.3	153.4	199.2	318.2	403.3	520.0	692.8	19
20	NA	65.6	107.0	146.5	188.5	293.4	364.4	457.2	585.2	20
30	NA	52.6	83.8	111.1	137.4	191.9	221.7	254.2	290.1	30
40	NA	46.5	73.7	96.6	117.8	159.3	180.5	202.5	225.5	40
50	NA	42.9	67.6	88.1	106.8	142.2	159.7	177.4	195.5	50

Table 2.6: Depth of borrow material for compacted subgrade on 7% natural subgrade CBR.

Borrow material CBR (%)	Depth of borrow material to achieve effective CBR (%)									
	5%	6%	7%	8%	9%	10%	12%	13%	14%	15%
7	NA	NA	NA	NA	NA	NA	NA	NA	NA	7
8	NA	NA	NA	NA	NA	NA	NA	NA	NA	8
9	NA	NA	379.6	NA	NA	NA	NA	NA	NA	9
10	NA	NA	208.9	565.3	NA	NA	NA	NA	NA	10
11	NA	NA	151.3	319.9	757.9	NA	NA	NA	NA	11
12	NA	NA	122.9	235.6	427.1	NA	NA	NA	NA	12
13	NA	NA	106.0	192.8	314.1	1182.8	NA	NA	NA	13
14	NA	NA	94.7	166.8	256.6	653.6	1416.5	NA	NA	14
15	NA	NA	86.6	149.3	221.5	474.8	775.6	1664.1	NA	15
16	NA	NA	80.5	136.6	197.8	384.1	559.7	903.9	1925.3	16
17	NA	NA	75.7	127.0	180.6	329.0	450.6	648.4	1038.5	17
18	NA	NA	71.8	119.4	167.5	291.8	384.4	519.5	741.0	18
19	NA	NA	68.5	113.2	157.2	265.0	339.8	441.5	591.1	19
20	NA	NA	65.8	108.0	148.9	244.5	307.6	389.0	500.5	20
30	NA	NA	51.1	81.8	108.7	161.0	188.7	218.5	251.1	30
40	NA	NA	44.6	71.0	93.3	134.0	154.2	174.8	196.2	40
50	NA	NA	40.9	64.8	84.6	119.8	136.7	153.5	170.5	50

Table 2.7: Design Subgrade CBR values for borrow material of compacted thickness of 500 mm

500 mm Borrow material	Effective CBR (%) obtained using natural subgrade CBR (%)					
	1.50%		2.0%		2.50%	
	Present method	IRC	Present method	IRC	Present method	IRC
7	4.05	4.05	4.46	4.49	4.76	4.82
8	4.28	4.27	4.73	4.74	5.23	5.29
9	4.49	4.47	4.97	4.99	5.67	5.73
10	4.69	4.76	5.43	5.44	6.10	6.39
11	4.87	4.85	5.78	5.77	6.50	6.53
12	5.17	4.99	6.11	6.07	6.89	6.91
13	5.43	5.34	6.43	6.36	7.27	7.28
14	5.68	5.58	6.74	6.69	7.63	7.65
15	5.92	5.8	7.04	6.96	7.99	7.97
16	6.15	6.02	7.33	7.24	8.33	8.31
17	6.37	6.23	7.62	7.49	8.66	8.63
18	6.59	6.47	7.89	7.77	8.98	8.93
19	6.80	6.63	8.15	8.00	9.30	9.29
20	7.00	6.81	8.41	8.26	9.61	9.52
30	8.80	8.51	10.70	10.50	12.34	12.13
40	10.29	9.92	12.61	12.25	14.64	14.30
50	11.57	11.12	14.27	13.80	16.65	16.19

Table 2.8: Design Subgrade CBR values for borrow material of compacted thickness of 500 mm

| 500 mm Borrow material | Effective CBR (%) obtained using natural subgrade CBR (%) | | | | | |
| | 3.00% | | 5.00% | | 7.00% | |
	Present method	IRC	Present method	IRC	Present method	IRC
7	5.16	5.25	6.28	6.43	6.71	6.87
8	5.68	5.77	6.97	7.14	7.47	7.65
9	6.18	6.27	7.63	7.81	8.19	8.39
10	6.66	7.02	8.26	8.84	8.89	9.34
11	7.11	7.2	8.88	9.07	9.57	9.8
12	7.55	7.54	9.47	9.67	10.23	10.48
13	7.98	8.03	10.05	10.25	10.88	11.12
14	8.39	8.45	10.62	10.77	11.51	11.77
15	8.79	8.83	11.17	11.38	12.12	12.39
16	9.18	9.21	11.70	11.90	12.72	13.00
17	9.56	9.57	12.23	12.43	13.31	13.58
18	9.93	9.94	12.74	12.95	13.88	14.16
19	10.29	10.28	13.24	13.49	14.44	14.72
20	10.64	10.62	13.73	13.92	15.00	15.29
30	13.78	13.62	18.20	18.32	20.05	20.32
40	16.44	16.16	22.06	22.08	24.47	24.64
50	18.77	18.37	25.51	25.43	28.44	28.52

Table 2.9: Variation of compacted subgrade thickness with CBR range from 5% to 15% with different load repetitions on 2% natural subgrade CBR.

Natural Subgrade CBR (2%) with load intensity 0.25 MPa					
Axle load repetitions (msa)	Thickness of compacted subgrade (mm)				
	5%	8%	10%	12%	15%
2	544	495	472	454	432
5	605	550	525	505	481
10	656	596	568	547	521
20	710	645	615	592	564
30	743	676	644	620	591
50	788	716	683	657	626
100	852	774	738	710	677
150	892	810	773	743	709

Table 2.10: Variation of compacted subgrade thickness with CBR range from 5% to 15% with different load repetitions on 3% natural subgrade CBR.

Natural Subgrade CBR (3%) with load intensity 0.25 MPa					
Axle load repetitions (msa)	Compacted subgrade CBR				
	5%	8%	10%	12%	15%
2	501	456	434	418	398
5	559	508	484	466	444
10	607	551	526	506	482
20	658	598	570	548	523
30	689	626	597	575	548
50	731	664	634	609	581
100	792	719	686	660	629
150	829	753	718	691	659

Table 2.11: Variation of compacted subgrade thickness with CBR range from 5% to 15% with different load repetitions on 4% natural subgrade CBR.

Natural Subgrade CBR (4%) with load intensity 0.25 MPa					
Axle load repetitions (msa)	**Compacted subgrade CBR**				
	5%	**8%**	**10%**	**12%**	**15%**
2	470	428	408	392	374
5	526	478	456	439	418
10	572	520	496	477	455
20	621	565	538	518	494
30	652	592	565	543	518
50	692	629	600	577	550
100	750	682	650	625	596
150	786	714	681	655	625

Table 2.12: Variation of compacted subgrade thickness (mm) with CBR range from 8% to 15% with different load repetitions on 5% natural subgrade CBR.

Natural Subgrade CBR (5%) with load intensity 0.25 MPa					
Axle load repetitions (msa)	**Compacted subgrade CBR**				
	5%	**8%**	**10%**	**12%**	**15%**
2	NA	405	386	372	354
5	NA	455	434	417	398
10	NA	496	473	455	433
20	NA	539	514	495	472
30	NA	566	540	519	495
50	NA	601	574	552	526
100	NA	653	622	599	571
150	NA	684	653	628	598

Table 2.13: Variation of compacted subgrade thickness (mm) with CBR range from 8% to 15% with different load repetitions on 6% natural subgrade CBR.

Natural Subgrade CBR (6%) with load intensity 0.25 MPa					
Axle load repetitions (msa)	Compacted subgrade CBR				
	5%	8%	10%	12%	15%
2	NA	395	376	362	345
5	NA	444	424	407	388
10	NA	484	462	444	424
20	NA	527	503	484	461
30	NA	554	528	508	484
50	NA	589	562	540	515
100	NA	639	610	586	559
150	NA	671	640	615	587

Table 2.14: Variation of compacted subgrade thickness (mm) with CBR range from 8% to 15% with different load repetitions for 7% natural subgrade CBR.

Natural Subgrade CBR (7%) with load intensity 0.25 MPa					
Axle load repetitions (msa)	Compacted subgrade CBR				
	5%	8%	10%	12%	15%
2	NA	385	365	353	336
5	NA	434	414	398	379
10	NA	473	451	434	414
20	NA	516	492	473	451
30	NA	542	517	497	474
50	NA	577	550	529	504
100	NA	627	598	575	548
150	NA	658	627	603	575

Table 2.15: Variation of compacted subgrade thickness (mm) with CBR range from 5% to 15% with different load repetitions on 2% natural subgrade CBR.

Natural Subgrade CBR (2%) with load intensity 0.375 MPa					
Axle load repetitions (msa)	Compacted subgrade CBR (%)				
	5%	8%	10%	12%	15%
2	673	612	583	561	535
5	747	679	648	623	593
10	808	735	701	674	643
20	874	795	758	729	695
30	915	832	793	763	727
50	969	881	840	808	770
100	1048	952	908	873	833
150	1096	996	950	914	871

Table 2.16: Variation of compacted subgrade thickness with CBR range from 5% to 15% with different load repetitions on 3% natural subgrade CBR.

Natural Subgrade CBR (3%) with load intensity 0.375 MPa					
Axle load (msa)	Compacted subgrade CBR (%)				
	5%	8%	10%	12%	15%
2	626	566	540	519	495
5	696	630	601	578	551
10	754	682	650	626	597
20	816	738	704	677	646
30	855	773	737	709	676
50	906	820	781	752	717
100	980	886	845	813	775
150	1026	928	885	851	811

Table 2.17: Variation of compacted subgrade thickness with CBR range from 5% to 15% with different load repetitions on 4% natural subgrade CBR.

Natural Subgrade CBR (4%) with load intensity 0.375 MPa					
Axle load repetitions (msa)	**Compacted subgrade CBR (%)**				
	5%	**8%**	**10%**	**12%**	**15%**
2	591	534	510	490	467
5	658	596	568	546	521
10	714	646	616	592	566
20	774	700	667	642	612
30	811	733	699	672	641
50	860	778	741	713	680
100	930	842	802	772	736
150	974	881	840	808	770

Table 2.18: Variation of compacted subgrade thickness (mm) with CBR range from 8% to 15% with different load repetitions on 5% natural subgrade CBR.

Natural Subgrade CBR (5%) with load intensity 0.375 MPa					
Axle load repetitions (msa)	**Compacted subgrade CBR (%)**				
	5%	**8%**	**10%**	**12%**	**15%**
2	NA	510	486	468	446
5	NA	569	543	522	498
10	NA	618	589	567	540
20	NA	670	639	615	586
30	NA	703	670	645	615
50	NA	746	711	684	652
100	NA	808	770	741	706
150	NA	846	807	776	740

Table 2.19: Variation of compacted subgrade thickness (mm) with CBR range from 8% to 15% with different load repetitions on 6% natural subgrade CBR.

Natural Subgrade CBR (6%) with load intensity 0.375 MPa					
Axle load repetitions (msa)	Compacted subgrade CBR (%)				
	5%	8%	10%	12%	15%
2	NA	498	475	457	436
5	NA	557	531	511	487
10	NA	605	577	555	529
20	NA	657	626	602	574
30	NA	689	657	632	602
50	NA	731	697	671	639
100	NA	792	755	727	693
150	NA	830	791	761	725

Table 2.20: Variation of compacted subgrade thickness (mm) with CBR range from 8% to 15% with different load repetitions on 7% natural subgrade CBR.

Natural Subgrade CBR (7%) with load intensity 0.375 MPa					
Axle load repetitions (msa)	Compacted subgrade CBR (%)				
	5%	8%	10%	12%	15%
2	NA	487	465	447	426
5	NA	545	520	500	477
10	NA	593	565	544	519
20	NA	644	614	590	563
30	NA	675	644	620	591
50	NA	717	684	658	627
100	NA	777	741	713	680
150	NA	815	777	747	712

Table 2.21: Comparison of strain based compacted Subgrade thickness between present method and IITPAVE with 2% natural subgrade CBR

| Axle load repetitions (msa) | Thickness of compacted subgrade (mm) for 2% Natural subgrade CBR with load intensity 0.25MPa | | | |
| | 5% | | 8% | |
	Present method	IITPAVE	Present method	IITPAVE
2	544	630	495	590
5	605	695	550	655
10	656	750	596	705
20	710	820	645	760
30	743	855	676	800
50	788	910	716	850
100	852	980	774	910
150	892	1020	810	960

Table 2.22: Comparison of strain based compacted Subgrade thickness between present method and IITPAVE with 5% natural subgrade CBR

| Axle load repetitions (msa) | Thickness of compacted subgrade (mm) for 5% Natural subgrade CBR with load intensity 0.25MPa | | | |
| | 10% | | 15% | |
	Present method	IITPAVE	Present method	IITPAVE
2	386	415	372	395
5	434	465	417	445
10	473	505	455	480
20	514	560	495	525
30	540	590	519	555
50	574	620	552	590
100	622	670	599	640
150	653	700	628	675

Table:2.23: Comparison of strain based compacted Subgrade thickness between present method and IITPAVE with 7% natural subgrade CBR

Thickness of compacted subgrade (mm)for 7% Natural subgrade CBR with load intensity 0.25MPa				
Axle load repetitions (msa)	10%		15%	
	Present method	IITPAVE	Present method	IITPAVE
2	365	380	432	360
5	414	430	481	410
10	451	470	521	455
20	492	510	564	490
30	517	535	591	510
50	550	570	626	550
100	598	620	677	595
150	627	650	709	620

Table: 2.24: Comparison of strain based compacted Subgrade thickness between present method and IITPAVE with 2% natural subgrade CBR

Thickness of compacted subgrade (mm) for 2% Natural subgrade CBR with load intensity 0.375MPa				
Axle load repetitions (msa)	5%		8%	
	Present method	IITPAVE	Present method	IITPAVE
2	673	780	612	730
5	747	860	679	810
10	808	920	735	875
20	874	995	795	945
30	915	1050	832	990
50	969	1100	881	1050
100	1048	1195	952	1120
150	1096	1255	996	1180

Table: 2.25: Comparison of strain based compacted Subgrade thickness between present method and IITPAVE with 5% natural subgrade CBR

| Axle load repetitions (msa) | Thickness of compacted subgrade (mm) for 5% Natural subgrade CBR with load intensity 0.375MPa | | | |
| | 10% | | 15% | |
	Present method	IITPAVE	Present method	IITPAVE
2	486	525	446	500
5	543	585	498	560
10	589	630	540	610
20	639	685	586	660
30	670	720	615	690
50	711	760	652	730
100	770	820	706	795
150	807	860	740	830

Table: 2.26: Comparison of strain based compacted Subgrade thickness between present method and IITPAVE with 7% natural subgrade CBR

| Axle load repetitions (msa) | Thickness of compacted subgrade (mm)for 7% Natural subgrade CBR with load intensity 0.375MPa | | | |
| | 10% | | 15% | |
	Present method	IITPAVE	Present method	IITPAVE
2	465	480	426	460
5	520	540	477	517
10	565	590	519	560
20	614	640	563	615
30	644	675	591	642
50	684	715	627	680
100	741	775	680	740
150	777	810	712	775

Table 2.27: Variation of compacted subgrade thickness (mm) with CBR range from 5% to 15% with different load repetitions for 2% natural subgrade CBR.

Natural Subgrade CBR (2%) , Load intensity = 0.25 MPa					
Axle load repetitions (msa)	Compacted subgrade CBR (%)				
	5%	8%	10%	12%	15%
2	403	366	349	336	320
5	460	418	399	384	366
10	508	462	440	424	404
20	560	509	486	467	445
30	593	539	514	494	471
50	637	579	552	531	506
100	701	637	608	584	557
150	741	674	642	618	589

Table 2.28: Variation of compacted subgrade thickness (mm) with CBR range from 5% to 15% with different load repetitions for 3% natural subgrade CBR.

Natural Subgrade CBR (3%) , Load intensity = 0.25 MPa					
Axle load repetitions (msa)	Compacted subgrade CBR (%)				
	5%	8%	10%	12%	15%
2	371	337	322	309	295
5	426	387	369	355	339
10	472	429	409	393	375
20	522	474	452	435	415
30	553	503	479	461	440
50	595	540	515	496	473
100	656	596	568	547	521
150	694	631	601	578	552

Table 2.29: Variation of compacted subgrade thickness (mm) with CBR range from 5% to 15% with different load repetitions for 4% natural subgrade CBR.

Natural Subgrade CBR (4%) , Load intensity = 0.25 MPa					
Axle load repetitions (msa)	Compacted subgrade CBR(%)				
	5%	8%	10%	12%	15%
2	347	316	301	289	275
5	401	365	348	334	319
10	446	405	386	372	354
20	494	449	428	412	393
30	525	477	455	437	417
50	565	514	490	471	449
100	624	567	541	520	496
150	661	601	573	551	525

Table 2.30: Variation of compacted subgrade thickness (mm) with CBR range from 8% to 15% with different load repetitions for 5% natural subgrade CBR.

Natural Subgrade CBR (5%) , Load intensity = 0.25 MPa					
Axle load repetitions (msa)	Compacted subgrade CBR (%)				
	5%	8%	10%	12%	15%
2	NA	298	284	273	260
5	NA	346	330	318	303
10	NA	386	368	354	338
20	NA	430	410	394	376
30	NA	457	435	419	399
50	NA	492	470	452	431
100	NA	545	519	500	476
150	NA	577	551	530	505

Table 2.31: Variation of compacted subgrade thickness (mm) with CBR range from 8% to 15% with different load repetitions for 6% natural subgrade CBR.

Axle load repetitions (msa))	Natural Subgrade CBR (6%) , Load intensity = 0.25 MPa				
	Compacted subgrade CBR (%)				
	5%	8%	10%	12%	15%
2	NA	289	276	265	253
5	NA	338	322	310	295
10	NA	378	360	346	330
20	NA	420	401	386	368
30	NA	447	426	410	391
50	NA	483	460	443	422
100	NA	534	510	490	467
150	NA	567	540	520	496

Table 2.32: Variation of compacted subgrade thickness (mm) with CBR range from 8% to 15% with different load repetitions for 2% natural subgrade CBR.

Axle load repetitions (msa)	Natural Subgrade CBR (7%) , Load intensity = 0.25 MPa				
	Compacted subgrade CBR (%)				
	5%	8%	10%	12%	15%
2	NA	281	268	257	245
5	NA	329	314	302	288
10	NA	369	352	338	323
20	NA	411	392	377	360
30	NA	438	418	402	383
50	NA	473	451	434	414
100	NA	525	500	481	459
150	NA	557	531	510	487

Table 2.33: Variation of compacted subgrade thickness (mm) with CBR range from 5% to 15% with different axle load repetitions on 2% natural subgrade CBR.

Natural Subgrade CBR (2%) , Load intensity = 0.375 MPa					
Axle load repetitions (msa)	Compacted subgrade CBR (%)				
	5%	8%	10%	12%	15%
2	501	456	434	418	398
5	571	519	494	476	453
10	629	571	545	524	500
20	692	629	600	577	550
30	732	665	634	610	582
50	785	713	680	654	624
100	863	784	748	719	686
150	912	829	791	760	725

Table 2.34: Variation of compacted subgrade thickness (mm) with CBR range from 5% to 15% with different axle load repetitions on 3% natural subgrade CBR.

Natural Subgrade CBR (3%) , Load intensity = 0.375 MPa					
Axle load repetitions (msa)	Compacted subgrade CBR (%)				
	5%	8%	10%	12%	15%
2	465	423	403	388	370
5	532	483	461	443	422
10	587	533	509	489	466
20	647	588	561	539	514
30	685	622	593	571	544
50	735	668	637	613	584
100	809	736	701	675	643
150	856	778	742	713	680

Table 2.35: Variation of compacted subgrade thickness (mm) with CBR range from 5% to 15% with different axle load repetitions on 4% natural subgrade CBR.

Natural Subgrade CBR (4%) , Load intensity = 0.375 MPa					
Axle load repetitions (msa)	Compacted subgrade CBR (%)				
	5%	8%	10%	12%	15%
2	440	400	381	366	349
5	504	458	437	420	400
10	557	507	483	465	443
20	616	559	533	513	489
30	652	593	565	544	518
50	701	637	607	584	557
100	772	702	669	644	614
150	817	743	708	681	649

Table 2.36: Variation of compacted subgrade thickness (mm) with CBR range from 8% to 15% with different axle load repetitions on 5% natural subgrade CBR.

Natural Subgrade CBR (5%) , Load intensity = 0.375 MPa					
Axle load repetitions (msa)	Compacted subgrade CBR (%)				
	5%	8%	10%	12%	15%
2	381	363	349	333	381
5	438	418	402	383	438
10	486	463	445	425	486
20	537	512	493	470	537
30	570	543	522	498	570
50	613	584	562	536	613
100	676	644	620	591	676
150	716	682	656	626	716

Table 2.37: Variation of compacted subgrade thickness (mm) with CBR range from 8% to 15% with different axle load repetitions on 6% natural subgrade CBR.

Natural Subgrade CBR (6%) , Load intensity = 0.375 MPa					
Axle load repetitions (msa)	Compacted subgrade CBR (%)				
	5%	8%	10%	12%	15%
2	372	355	341	325	372
5	429	409	393	375	429
10	476	454	436	416	476
20	527	503	483	461	527
30	559	533	513	489	559
50	602	574	552	526	602
100	664	633	609	581	664
150	703	670	645	615	703

Table 2.38: Variation of compacted subgrade thickness (mm) with CBR range from 8% to 15% with different axle load repetitions on 7% natural subgrade CBR.

Natural Subgrade CBR (7%) , Load intensity = 0.375 MPa					
Axle load repetitions (msa)	Compacted subgrade CBR (%)				
	5%	8%	10%	12%	15%
2	NA	363	346	333	318
5	NA	420	400	385	367
10	NA	466	445	428	408
20	NA	517	493	474	452
30	NA	549	523	503	480
50	NA	591	563	542	517
100	NA	653	622	599	571
150	NA	691	659	634	605

Table 2.39: Variation of compacted subgrade thickness (mm) based on stress and strain approach for compacted CBR range from 5% to 15% with axle load repetitions on 2% natural subgrade CBR.

Axle load repetitions (msa)	Thickness of compacted subgrade (mm) on 2% Natural subgrade CBR and compacted subgrade CBR of									
	5%		8%		10%		12%		15%	
	Strain	Stress	Strain	Stress	Strain	Stress	Strain	Stress	Strain	Stress
2	544	403	495	366	472	349	454	336	432	320
5	605	460	550	418	525	399	505	384	481	366
10	656	508	596	462	568	440	547	424	521	404
20	710	560	645	509	615	486	592	467	564	445
30	743	593	676	539	644	514	620	494	591	471
50	788	637	716	579	683	552	657	531	626	506
100	852	701	774	637	738	608	710	584	677	557
150	892	741	810	674	773	642	743	618	709	589

Table 2.40: Variation of compacted subgrade thickness (mm) based on stress and strain approach for compacted CBR range from 5% to 15% with axle load repetitions on 4% natural subgrade CBR.

Axle load repetitions (msa)	Thickness of compacted subgrade (mm) on 4% Natural subgrade CBR and compacted subgrade CBR of									
	5%		8%		10%		12%		15%	
	Strain	Stress	Strain	Stress	Strain	Stress	Strain	Stress	Strain	Stress
2	470	347	428	316	408	301	392	289	374	275
5	526	401	478	365	456	348	439	334	418	319
10	572	446	520	405	496	386	477	372	455	354
20	621	494	565	449	538	428	518	412	494	393
30	652	525	592	477	565	455	543	437	518	417
50	692	565	629	514	600	490	577	471	550	449
100	750	624	682	567	650	541	625	520	596	496
150	786	661	714	601	681	573	655	551	625	525

Table 2.41: Variation of compacted subgrade thickness (mm) based on stress and strain approach for compacted CBR range from 5% to 15% with axle load repetitions on 5% natural subgrade CBR.

| Axle load repetitions (msa) | Thickness of compacted subgrade (mm) on 5% Natural subgrade CBR and compacted subgrade CBR of | | | | | | | | | |
| | 5% | | 8% | | 10% | | 12% | | 15% | |
	Strain	Stress	Strain	Stress	Strain	Stress	Strain	Stress	Strain	Stress
2	NA	NA	405	298	386	284	372	273	354	260
5	NA	NA	455	346	434	330	417	318	398	303
10	NA	NA	496	386	473	368	455	354	433	338
20	NA	NA	539	430	514	410	495	394	472	376
30	NA	NA	566	457	540	435	519	419	495	399
50	NA	NA	601	492	574	470	552	452	526	431
100	NA	NA	653	545	622	519	599	500	571	476
150	NA	NA	684	577	653	551	628	530	598	505

Table 2.42: Variation of compacted subgrade thickness (mm) based on stress and strain approach for compacted CBR range from 5% to 15% with axle load repetitions on 7% natural subgrade CBR.

| Axle load repetitions (msa) | Thickness of compacted subgrade (mm) on 7% Natural subgrade CBR and compacted subgrade CBR of | | | | | | | | | |
| | 5% | | 8% | | 10% | | 12% | | 15% | |
	Strain	Stress	Strain	Stress	Strain	Stress	Strain	Stress	Strain	Stress
2	NA	NA	385	281	365	268	353	257	336	245
5	NA	NA	434	329	414	314	398	302	379	288
10	NA	NA	473	369	451	352	434	338	414	323
20	NA	NA	516	411	492	392	473	377	451	360
30	NA	NA	542	438	517	418	497	402	474	383
50	NA	NA	577	473	550	451	529	434	504	414
100	NA	NA	627	525	598	500	575	481	548	459
150	NA	NA	658	557	627	531	603	510	575	487

Table 2.43: Variation of compacted subgrade thickness (mm) based on stress and strain approach for compacted CBR range from 5% to 15% with axle load repetitions on 2% natural subgrade CBR.

Axle load repetitions (msa)	Thickness of compacted subgrade (mm) on 2% Natural subgrade CBR and compacted subgrade CBR of									
	5%		8%		10%		12%		15%	
	Strain	Stress	Strain	Stress	Strain	Stress	Strain	Stress	Strain	Stress
2	673	501	612	456	583	434	561	418	535	399
5	747	571	679	519	648	494	623	476	593	453
10	808	629	735	571	701	545	674	524	643	500
20	874	692	795	629	758	600	729	577	695	550
30	915	732	832	665	793	634	763	610	727	582
50	969	785	881	713	840	680	808	654	770	624
100	1048	863	952	784	908	748	873	719	833	636
150	1096	912	996	829	950	791	914	760	871	725

Table 2.44: Variation of compacted subgrade thickness (mm) based on stress and strain approach for compacted CBR range from 5% to 15% with axle load repetitions on 4% natural subgrade CBR.

Axle load repetitions (msa)	Thickness of compacted subgrade (mm) on 4% Natural subgrade CBR and compacted subgrade CBR of									
	5%		8%		10%		12%		15%	
	Strain	Stress	Strain	Stress	Strain	Stress	Strain	Stress	Strain	Stress
2	591	440	534	400	510	381	490	366	467	349
5	658	504	596	458	568	437	546	420	521	400
10	714	557	646	507	616	483	592	465	566	443
20	774	616	700	559	667	533	642	513	612	489
30	811	652	733	593	699	565	672	544	641	518
50	860	701	778	637	741	607	713	584	680	557
100	930	772	842	702	802	669	772	644	736	614
150	974	817	881	743	840	708	808	681	770	649

Table 2.45: Variation of compacted subgrade thickness (mm) based on stress and strain approach for compacted CBR range from 5% to 15% with axle load repetitions on 5% natural subgrade CBR.

Axle load repetitions (msa)	Thickness of compacted subgrade (mm) on 5% Natural subgrade CBR and compacted subgrade CBR of									
	5%		8%		10%		12%		15%	
	Strain	Stress	Strain	Stress	Strain	Stress	Strain	Stress	Strain	Stress
2	NA	NA	510	381	486	363	468	349	446	333
5	NA	NA	569	438	543	418	522	402	498	383
10	NA	NA	618	486	589	463	567	445	540	425
20	NA	NA	670	537	639	512	615	493	586	470
30	NA	NA	703	570	670	543	645	522	615	498
50	NA	NA	746	613	711	584	684	562	652	536
100	NA	NA	808	676	770	644	741	620	706	591
150	NA	NA	846	716	807	682	776	656	740	626

Table 2.46: Variation of compacted subgrade thickness (mm) based on stress and strain approach for compacted CBR range from 5% to 15% with axle load repetitions on 7% natural subgrade CBR.

Axle load repetitions (msa)	Thickness of compacted subgrade (mm) on 7% Natural subgrade CBR and compacted subgrade CBR of									
	5%		8%		10%		12%		15%	
	Strain	Stress	Strain	Stress	Strain	Stress	Strain	Stress	Strain	Stress
2	NA	NA	487	363	465	346	447	333	426	318
5	NA	NA	545	420	520	400	500	385	477	367
10	NA	NA	593	466	565	445	544	428	519	409
20	NA	NA	644	517	614	493	590	474	563	452
30	NA	NA	675	549	644	523	620	503	591	480
50	NA	NA	717	591	684	563	658	542	627	517
100	NA	NA	777	653	741	622	713	599	680	571
150	NA	NA	815	691	777	659	747	634	712	605

Table 2.47: Stress based comparison of compacted subgrade thickness (mm) for 5% and 8% CBR with natural subgrade CBR of 2% based on present method and IITPAVE

Thickness of compacted subgrade (mm) on 2% Natural subgrade CBR with load intensity = 0.25 MPa				
Axle load repetitions (msa)	**(5%)**		**8%**	
	Present method	**IITPAVE**	**Present method**	**IITPAVE**
2	403	460	366	430
5	460	520	418	490
10	508	580	462	550
20	560	650	509	600
30	593	670	539	640
50	637	730	579	690
100	701	805	637	753
150	741	850	674	795

Table 2.48: Stress based comparison of compacted subgrade thickness (mm) for 10% and 12% CBR with natural subgrade CBR of 5% based on present method and IITPAVE

Thickness of compacted subgrade (mm) on 5% Natural subgrade CBR with load intensity = 0.25 MPa				
Axle load repetitions (msa)	**10%**		**12%**	
	Present method	**IITPAVE**	**Present method**	**IITPAVE**
2	284	305	273	293
5	330	351	318	345
10	368	393	354	381
20	410	440	394	425
30	435	470	419	450
50	470	500	452	490
100	519	550	500	550
150	551	585	530	595

Table 2.49: Stress based comparison of compacted subgrade thickness (mm) for 10% and 15% CBR with natural subgrade CBR of 7% based on present method and IITPAVE

| Axle load repetitions (msa) | Thickness of compacted subgrade (mm) on 7% Natural subgrade CBR with load intensity = 0.25 MPa | | | |
| | 10% | | 15% | |
	Present method	IITPAVE	Present method	IITPAVE
2	268	277	245	263
5	314	327	288	310
10	352	365	323	350
20	392	410	360	387
30	418	435	383	410
50	451	470	414	450
100	500	520	459	490
150	531	550	487	530

Table 2.50: Stress based comparison of compacted subgrade thickness (mm) for 5% and 8% CBR with natural subgrade CBR of 2% based on present method and IITPAVE

| Axle load repetitions (msa) | Thickness of compacted subgrade (mm) on 2% Natural subgrade CBR with load intensity = 0.375 MPa | | | |
| | 5% | | 8% | |
	Present method	IITPAVE	Present method	IITPAVE
2	501	575	456	540
5	571	645	519	610
10	629	720	571	690
20	692	790	629	740
30	732	830	665	770
50	785	890	713	850
100	863	970	784	910
150	912	1040	829	970

Table 2.51: Stress based comparison of compacted subgrade thickness (mm) for 10% and 15% CBR with natural subgrade CBR of 5% based on present method and IITPAVE

Axle load repetitions (msa)	10%		15%	
	Present method	IITPAVE	Present method	IITPAVE
2	363	390	333	370
5	418	445	383	420
10	463	490	425	470
20	512	550	470	520
30	543	580	498	550
50	584	622	536	590
100	644	690	591	660
150	682	730	626	700

Thickness of compacted subgrade (mm) on 5% Natural subgrade CBR with load intensity = 0.375 MPa

Table 2.52: Stress based comparison of compacted subgrade thickness (mm) for 10% and 15% CBR with natural subgrade CBR of 7% based on present method and IITPAVE

Axle load repetitions (msa)	10%		15%	
	Present method	IITPAVE	Present method	IITPAVE
2	346	360	318	340
5	400	420	367	398
10	445	465	409	440
20	493	510	452	490
30	523	545	480	520
50	563	600	517	565
100	622	650	571	615
150	659	690	605	660

Thickness of compacted subgrade (mm) on 7% Natural subgrade CBR with load intensity = 0.375 MPa

Appendix 3A

Table 3.1: Comparison of pavement thickness with IRC: SP-72-2007 for 100 mm granular subbase.

Axle load repetitions (ESAL)	Base thickness (mm) for 2% subgrade		Base thickness (mm) for (3-4)% subgrade		Base thickness (mm) for (5-6)% subgrade		Base thickness (mm) for (7-9)% subgrade	
	Present Study	IRC:SP:72	Present Study	IRC:SP:72	Present Study	IRC:SP:72	Present Study	IRC:SP:72
20000	288	300	231	200	172	175	114	150
40000	329	325	274	275	221	250	181	175
80000	373	375	318	325	268	275	234	225
150000	417	425	361	375	312	300	280	275
250000	456	475	398	425	349	325	319	300
450000	503	550	443	475	394	375	364	325
800000	554	650	491	650	441	425	411	375
1000000	575	650	510	650	459	425	429	375

Table 3.2: Comparison of pavement thickness with IRC: SP-72-2007 for 150 mm granular subbase.

Axle load repetitions (ESAL)	Base thickness (mm) for 2% subgrade		Base thickness (mm) for (3-4)% subgrade		Base thickness (mm) for (5-6)% subgrade		Base thickness (mm) for (7-9)% subgrade	
	Present Study	IRC:SP:72	Present Study	IRC:SP:72	Present Study	IRC:SP:72	Present Study	IRC:SP:72
20000	271	300	208	200	132	175	NA	150
40000	312	325	252	275	191	250	134	175
80000	356	375	297	325	242	275	200	225
150000	399	425	340	375	288	300	251	275
250000	437	475	377	425	325	325	291	300
450000	484	550	422	475	371	375	338	325
800000	533	650	469	650	417	425	385	375
1000000	554	650	488	650	436	425	404	375

Table 3.3: Comparison of pavement thickness between Kentucky's design and present analysis

Method	N_S	(z/a) values for different CBR								
		2%	3%	4%	5%	6%	7%	8%	9%	10%
Kentucky	20 msa	3.76	3.20	2.91	2.73	2.57	2.47	2.35	2.28	2.22
Present work		3.75	3.42	3.2	3.03	2.96	2.89	2.83	2.78	2.73
Kentucky	10 msa	3.55	3.03	2.73	2.56	2.44	2.33	2.23	2.16	2.08
Present work		3.09	2.9	2.74	2.67	2.61	2.55	2.51	2.46	3.09
Kentucky	2 msa	3.09	2.64	2.38	2.23	2.10	2.01	1.95	1.85	1.78
Present work		2.45	2.28	2.15	2.09	2.03	1.98	1.95	1.91	2.45
Kentucky	1 msa	2.84	2.44	2.21	2.02	1.90	1.91	1.75	1.67	1.62
Present work		2.41	2.04	1.92	1.87	1.82	1.77	1.73	1.70	1.61

Table 3.4: Comparison of pavement thickness with Corps of Engineers and Wyoming Design Chart

Agency	(z/a) values for different CBR							
	3%	4%	5%	6%	7%	8%	9%	10%
Corps of Engineers	2.37	2.05	1.82	1.64	1.50	1.41	1.31	1.27
Present method with 1 msa axle load	2.04	1.92	1.87	1.82	1.77	1.73	1.7	1.68
Wyoming Design Chart	2.84	2.44	2.17	2.0	1.85	1.74	1.64	1.56

Table 3.5: Comparison of pavement thickness with IRC: SP-72-2007

Pavement thickness (z/a) for 1msa load		
Subgrade CBR	Present work	IRC:SP-72-2007
2%	1.91	2.79
3-4%	1.70	2.16
5-6%	1.45	1.41

Table 4.1: Optimum thickness of bituminous layer and granular layer for 5% effective CBR considering load repetitions 5msa to 50 msa.

Optimum thickness of bituminous (h_1) (mm) and granular layer (h_2) (mm) for 5% effective subgrade CBR under different axle loads											
5 msa		10 msa		20 msa		30msa		40 msa		50 msa	
h_1	h_2	h_1	h_2	h_1	h_2	h_1	h_2	h_1	h_2	h_1	h_2
150	280	160	307	164	361	165	394	168	418	185	413

Table 4.2: Optimum thickness of bituminous layer and granular layer for 6% effective CBR considering load repetitions 5 msa to 50 msa.

Optimum thickness of bituminous (h_1) (mm) and granular layer (h_2) (mm) for 6% effective subgrade CBR under different axle loads											
5 msa		10 msa		20 msa		30msa		40 msa		50 msa	
h1	h2	h1	h2	h1	h2	h1	h2	h1	h2	h1	h2
140	284	150	309	160	361	170	365	170	369	180	364

Table 4.3: Optimum thickness of bituminous layer and granular layer for 7% effective CBR considering load repetitions 5 msa to 50 msa.

Optimum thickness of bituminous (h_1) (mm) and granular layer (h_2) (mm) for 7% effective subgrade CBR under different axle loads											
5 msa		10 msa		20 msa		30msa		40 msa		50 msa	
h_1	h_2	h_1	h_2	h_1	h_2	h_1	h_2	h_1	h_2	h_1	h_2
140	265	160	266	170	293	160	346	170	347	170	364

Table 4.4: Optimum thickness of bituminous layer and granular layer for 8% effective CBR considering load repetitions 5 msa to 50 msa.

Optimum thickness of bituminous (h_1) (mm) and granular layer (h_2) (mm) for 8% effective subgrade CBR under different axle loads											
5 msa		10 msa		20 msa		30msa		40 msa		50 msa	
h_1	h_2	h_1	h_2	h_1	h_2	h_1	h_2	h_1	h_2	h_1	h_2
140	249	150	272	170	275	160	327	160	349	170	344

Table 4.5: Optimum thickness of bituminous layer and granular layer for 9% effective CBR considering load repetitions 5msa to 50 msa.

Optimum thickness of bituminous (h_1) (mm) and granular layer (h_2) (mm) for 9% effective subgrade CBR under different axle loads											
5 msa		10 msa		20 msa		30msa		40 msa		50 msa	
h_1	h_2	h_1	h_2	h_1	h_2	h_1	h_2	h_1	h_2	h_1	h_2
140	236	150	258	170	260	160	311	160	332	170	327

Table 4.6: Optimum thickness of bituminous layer and granular layer for 10% effective CBR considering load repetitions 5msa to 50 msa.

Optimum thickness of bituminous (h_1) (mm) and granular layer (h_2) (mm) for 10% effective subgrade CBR under different axle loads											
5 msa		10 msa		20 msa		30msa		40 msa		50 msa	
h_1	h_2	h_1	h_2	h_1	h_2	h_1	h_2	h_1	h_2	h_1	h_2
140	224	150	245	160	269	150	319	160	318	170	291

Table 4.7: Optimum thickness of bituminous layer and granular layer for 12% effective CBR considering load repetitions 5msa to 50 msa.

Optimum thickness of bituminous (h_1) (mm) and granular layer (h_2) (mm) for 12% effective subgrade CBR under different axle loads											
5 msa		10 msa		20 msa		30msa		40 msa		50 msa	
h_1	h_2	h_1	h_2	h_1	h_2	h_1	h_2	h_1	h_2	h_1	h_2
130	205	130	246	150	247	140	295	140	314	150	309

Table 4.8: Optimum thickness of bituminous layer and granular layer for 15% effective CBR considering load repetitions 5msa to 50 msa.

Optimum thickness of bituminous (h_1) (mm) and granular layer (h_2) (mm) for 15% effective subgrade CBR under different axle loads											
5 msa		10 msa		20 msa		30msa		40 msa		50 msa	
h_1	h_2	h_1	h_2	h_1	h_2	h_1	h_2	h_1	h_2	h_1	h_2
110	224	130	221	140	242	130	288	140	286	140	300

Table 4.9: Comparison of deflection data obtained from present analysis, IITPAVE and KENPAVE for 3% subgrade CBR

Axle load repetition (msa)	Bituminous layer thickness (h_1) (mm)	Granular layer thickness (h_2) (mm)	Deflection for 3% subgrade CBR		
			Present analysis(mm)	IIT PAVE (mm)	KENPAVE (mm)
2	129	360	1.12	1.15	1.09
5	150	378	0.99	1.03	0.98
10	162	410	0.92	0.95	0.91
20	183	420	0.84	0.88	0.81
30	193	425	0.81	0.84	0.78
50	205	451	0.77	0.80	0.74
100	229	470	0.69	0.73	0.65
150	238	490	0.66	0.70	0.62

Table 4.10: Comparison of deflection data obtained from present analysis, IITPAVE and KENPAVE for 5% subgrade CBR

Axle load repetition (msa)	Bituminous layer thickness (h_1) (mm)	Granular layer thickness (h_2) (mm)	Deflection for 5% subgrade CBR		
			Present analysis(mm)	IIT PAVE (mm)	KENPAVE (mm)
2	104	315	0.90	0.91	0.87
5	128	315	0.80	0.81	0.76
10	145	330	0.73	0.74	0.70
20	160	348	0.67	0.69	0.65
30	170	350	0.65	0.66	0.62
50	188	360	0.60	0.62	0.58
100	204	386	0.56	0.57	0.54
150	218	390	0.54	0.55	0.50

Table 4.11: Comparison of deflection data obtained from present analysis, IITPAVE and KENPAVE for 10% subgrade CBR

Axle load repetition (msa)	Bituminous layer thickness (h_1) (mm)	Granular layer thickness (h_2) (mm)	Deflection for 10% subgrade CBR		
			Present analysis(mm)	IIT PAVE (mm)	KENPAVE (mm)
2	NA	NA	NA	NA	NA
5	98	290	0.68	0.68	0.65
10	120	290	0.62	0.61	0.59
20	142	290	0.56	0.56	0.54
30	151	300	0.53	0.54	0.51
50	165	310	0.50	0.51	0.47
100	186	320	0.46	0.47	0.44
150	197	328	0.44	0.45	0.42

Table 4.12: Comparison of pavement thickness obtained from different design approaches

Axle load repetitions (msa) = 30 Subgrade modulus (MPa) = 50	Pavement thickness		Axle load repetitions (msa) = 50 Subgrade Modulus (MPa) = 30	Pavement thickness	
	Bituminous layer (mm)	Granular layer (mm)		Bituminous layer (mm)	Granular layer (mm)
Narasimham, K.V. et al (2001)	180	370	I. Ghosh et al (2005)	210	410
Present analysis	200	355	Present analysis	205	451

Table 5.1: Binder base thickness for perpetual pavement for subgrade CBR from 5%-8% based on finite strain criteria

Subgrade CBR (%)	Binder Base thickness (mm) against fatigue	Binder Base thickness (mm) against rutting	Design thickness (mm) of binder Base
5	307	306	307
6	301	293	301
7	295	278	295
8	290	265	290

Table 5.2: Binder base thickness of perpetual pavement for subgrade CBR from 9%-15% based on finite strain criteria

Subgrade CBR (%)	Binder Base thickness (mm) against fatigue	Binder Base thickness (mm) against rutting	Design thickness (mm) of binder Base
9	285	255	285
10	281	244	281
12	273	225	273
15	264	203	264

Table 5.3: Binder base thickness for perpetual pavement for subgrade CBR 5%-8% based on finite load criteria

Subgrade CBR (%)	Binder Base thickness (mm) against fatigue	Binder Base thickness (mm) against rutting	Design thickness (mm) of binder Base
5	255	254	255
6	250	240	250
7	244	226	244
8	239	213	239

Table 5.4: Binder base thickness for perpetual pavement for subgrade CBR 9%-15% based on finite load criteria

Subgrade CBR (%)	Binder Base thickness (mm) against fatigue	Binder Base thickness (mm) against rutting	Design thickness (mm) of binder Base
9	235	202	235
10	231	193	231
12	224	176	224
15	215	155	215

Table 5.5: Recommended binder base thickness of perpetual pavement for subgrade CBR 5%-15% based on finite strain and load criteria

Subgrade CBR (%)	Binder base thickness (mm) under finite strain criteria		Binder base thickness (mm) under finite load criteria		Design thickness (mm)
	Fatigue	Rutting	Fatigue	Rutting	
5	307	306	255	254	307
6	301	293	250	240	301
7	295	278	244	226	295
8	290	265	239	213	290
9	285	255	235	202	285
10	281	244	231	193	281
12	273	225	224	176	273
15	264	203	215	155	264

Table 5.6: Comparison of binder base thickness using IITPAVE and present method based on finite strain criteria

Subgrade CBR (%)	Design Binder base thickness (mm) using (Present method)	Design Binder base thickness (mm) based on IIT PAVE (Corresponding to 80με fatigue strain)	IITPAVE calculated critical strain	
			Fatigue strain (με)	Rutting strain (με)
5	307	340	94	182
6	301	332	93	176
7	295	325	93	170
8	290	320	93	164
9	285	315	93	160
10	281	310	93	156
12	273	300	92	149
15	264	289	91	141

Table 5.7: Comparison of binder base thickness using IITPAVE and present method based on finite axle load repetitions

Subgrade CBR (%)	Design Binder base layer thickness (mm) using (Present method)	Design Binder base layer thickness (mm) based on IIT PAVE (Corresponding to 300msa axle load)	IITPAVE calculated critical strain	
			Fatigue strain (µε)	Rutting strain (µε)
5	255	272	123	230
6	250	267	123	220
7	244	260	123	213
8	239	255	122	206
9	235	250	121	199
10	231	245	121	194
12	224	236	120	185
15	215	225	119	174

Table 5.8: Comparison of binder base thickness using present method and IRC-37-2018 for different subgrade CBR and axle load repetitions

Subgrade CBR (%)	Axle load repetitions (5msa) Binder base thickness (mm) using Present Method				Axle load repetitions (20msa) Binder base thickness (mm) using Present Method			
	IRC:37-2018	Fatigue	Rutting	Design thickness	IRC:37-2018	Fatigue	Rutting	Design thickness
5	95.0	99	73	99	145	127	90	127
8	80.0	83	46	83	120	113	59	113
10	80.0	69	31	69	110	105	43	105

Table 5.9: Comparison of binder base thickness using present method and IRC-37-2018 for different subgrade CBR and axle load repetitions.

Subgrade CBR (%)	Axle load repetitions (30 msa)				Axle load repetitions (50msa)			
	Binder base thickness (mm) using Present Method				Binder base thickness (mm) using Present Method			
	IRC:37-2018	Present Method			IRC:37-2018	Present Method		
		Fatigue	Rutting	Design thickness		Fatigue	Rutting	Design thickness
5	155	164	145	164	180	177	157	177
8	135	151	115	151	155	164	123	164
10	125	143	98	143	145	157	106	157

Table 5.10: Recommended binder base thickness obtained using present method

Subgrade CBR (%)	5	6	7	8	9	10	12	15
Binder base thickness (mm) using (Present Method)	307	301	295	290	285	281	273	264

Appendix 5A

Table 6.1 Variation of overlay thickness for different axle loads considering 50 msa load repetitions

Pavement deflection (mm)	Overlay thickness (mm) for different axle loads considering 50 msa load repetitions		
	40kN	50kN	60kN
0.5	98	113	128
1.0	194	224	253
1.5	263	303	342
2.0	322	371	419
2.5	375	433	489
3.0	424	490	553
3.5	471	544	614
4.0	515	595	672
4.5	558	644	727

Table 6.2 Variation of overlay thickness for different axle loads considering 10 msa load repetitions

Pavement deflection (mm)	Overlay thickness (mm) for different axle loads considering 10 msa load repetitions		
	40kN	50kN	60kN
1.0	122	141	159
1.5	172	199	225
2.0	214	247	279
2.5	251	289	327
3.0	285	329	371
3.5	317	365	413
4.0	347	400	452
4.5	376	434	490

Table 6.3 Variation of overlay thickness for different axle loads considering 2 msa load repetitions

Pavement deflection (mm)	Overlay thickness (mm) for different axle loads considering 2msa load repetitions		
	40kN	**50kN**	**60kN**
1.0	65	75	85
1.5	108	125	141
2.0	139	161	181
2.5	165	191	216
3.0	189	219	247
3.5	211	244	276
4.0	232	268	303
4.5	252	291	329

Table 6.4 Reduction of overlay life due to overloading with an initial design life of 50 msa

Pavement deflection (mm)	Design overlay thickness (mm)	Overlay life (msa)with a wheel load of		Reduction of overlay life (msa)	Reduced overlay life (%)
		40kN	**60kN**		
1.0	194	50	21	29	59
2.5	375	50	19	31	63
4.5	558	50	18	32	63

Table 6.5 Reduction of overlay life due to overloading with an initial design life of 10 msa

Pavement deflection (mm)	Design overlay thickness (mm)	Overlay life (msa) with a wheel load of		Reduction of overlay life (msa)	Reduced overlay life (%)
		40kN	**60kN**		
1.0	122	10	5	5	52
2.5	251	10	4	6	62
4.5	376	10	4	6	63

Table 6.6 Reduction of overlay life due to overloading with an initial design life of 2msa

Pavement deflection (mm)	Design overlay thickness (mm)	Overlay life (msa) with a wheel load of		Reduction of overlay life(msa)	Reduced overlay life (%)
		40kN	60kN		
1.0	65	2	1.31	0.690	35
2.5	165	2	0.79	1.210	61
4.5	252	2	0.74	1.260	63

Table 6.7 Comparison of BLI for overlay estimated using AI method, Danish and Huang's stress-based approach

Axle load repetitions (msa)	Asphalt Institute method	Danish stress-based method	Huang's stress-based method
	Base layer index	Base layer index	Base layer index
2	0.35	0.22	0.19
5	0.21	0.15	0.14
10	0.18	0.11	0.11
20	0.13	0.08	0.08
30	0.11	0.07	0.07
50	0.08	0.06	0.06
100	0.05	0.05	0.04
150	0.04	0.04	0.04

Table 6.8 Overlay thickness for change in elastic modulus value of bituminous layer for 50 msa load repetitions

Pavement deflection (d_0) (mm)	Axle load repetitions (50msa)					
	Modulus of bituminous mixture (MPa)					
	3500	3150	2800	2450	2100	1750
0.5	86	90	94	99	105	113
1.0	182	190	199	210	224	244
1.5	251	261	274	290	311	339
2.0	310	323	340	360	386	421
2.5	363	380	399	423	454	497
3.0	413	432	454	482	518	567
3.5	461	481	506	538	578	634
4.0	506	528	556	591	635	697

Table 6.9 Overlay thickness for variation in load repetition for the standard value of modulus of bituminous layer (E_1 = 3500 MPa)

Pavement deflection (d_0) (mm)	Modulus of bituminous mix (E_1 = 3500 MPa)					
	Axle load repetitions (msa)					
	50	45	40	35	30	25
0.5	86	82	77	71	65	57
1.0	182	177	171	164	157	148
1.5	251	243	236	227	217	207
2.0	310	301	291	281	269	256
2.5	363	353	342	330	316	301
3.0	413	402	389	375	360	343
3.5	461	448	434	418	401	382
4.0	506	491	476	459	441	420

REFERENCES

References

1.   AASHTO (2019) American Association of state Highway and Transportation Officials), Guideline for Geometric Design of Low Volume Road, Washington, DC

2.   AASHTO (1997). AASHTO Standard T97-97, ''Flexural Strength of Concrete (Using Simple Beam with Third-Point Loading),'' American Association of State Highway and Transportation Officials, Washington, DC.

3.   AASHTO (2002). AASHTO Standard T198-02, ''Splitting Tensile Strength of Cylindrical Concrete Samples,'' American Association of State Highway and Transportation Officials, Washington, DC.

4.   AASHTO, G. (1993). Guide for design of pavement structures. American Association of State Highway and Transportation Officials, Washington, DC.

5.   Abadin, M. J., & Hayano, K. (2022). Investigation of premature failure mechanism in pavement overlay of national highway of Bangladesh. Construction and Building Materials, 318, 126194.

6.   Abaza, K. A. (2004). Deterministic performance prediction model for rehabilitation and management of flexible pavement. International Journal of Pavement Engineering, 5(2), 111-121.

7.   Abaza, K. A. (2005). Performance-based models for flexible pavement structural overlay design. Journal of Transportation Engineering, 131(2), 149-159.

8.   Abaza, K. A., & Abu-Eisheh, S. A. (2003). An optimum design approach for flexible pavements. International Journal of Pavement Engineering, 4(1), 1-11.

9.   Al Khateeb, Loay. (2011). "Rutting Prediction of Flexible Pavements Using Finite Element Modeling". Jordan Journal of Civil Engineering. 5. 173 - 190.

10.   Al. (1983). Asphalt Overlays for Highway and Street Rehabilitation, Manual Series No. 17; Asphalt Institute.

11.   Alessandra Bianchini, Carlos R. Gonzalez & Haley P. Bell. (2018). "Correction for the asphalt overlay thickness of flexible pavements considering pavement Conditions." International Journal of Pavement Engineering, 19:7, 577-585, DOI: 10.1080/10298436.2016.1198480.

12.   Alnedawi, A., Al-Ameri, R., & Nepal, K. P. (2019). Neural network-based model for prediction of permanent deformation of unbound granular materials. Journal of Rock Mechanics and Geotechnical Engineering, 11(6), 1231-1242.

13. Alnedawi, A., Nepal, K. P., & Al-Ameri, R. (2019). Permanent deformation prediction model of unbound granular materials for flexible pavement design. Transportation Infrastructure Geotechnology, 6, 39-55.

14. Alzaim, M., Gedik, A., & Lav, A. H. (2020). Effect of modulus of bituminous layers and utilization of capping layer on weak pavement subgrades. Civil Engineering Journal, 6(7), 1286-1299.

15. Amakye, S. Y., Abbey, S. J., Booth, C. A., & Oti, J. (2022). Performance of Sustainable Road Pavements Founded on Clay Subgrades Treated with Eco-Friendly Cementitious Materials. Sustainability, 14(19), 12588.

16. Amakye, S. Y., Abbey, S. J., Booth, C. A., & Oti, J. (2022). Road Pavement Thickness and Construction Depth Optimization Using Treated and Untreated Artificially-Synthesized Expansive Road Subgrade Materials with Varying Plasticity Index. Materials, 15(8), 2773.

17. American Association of State Highway and Transportation Officials. Operating Subcommittee on Roadway Design. (1974).

18. AASHTO Interim Guide for Design of Pavement Structures, 1972. American Association of State Highway and Transportation Officials.

19. Bagui, S. K. (2012). Pavement design for rural low volume roads using cement and lime treatment base. Jordan Journal of Civil Engineering, 6(3), 293-303.

20. Baladi, G. Y. (1991). Analysis of pavement distress data, pavement distress indices, and remaining service life. An Advanced Course in Pavement Management Systems, FHWA, Boston, MA.

21. Basic road statistics of India (2017-18), "Government of India, Ministry of Road Transport and Highways Transport Research wing".

22. Bastola NR, Souliman MI, Dessouky S and Daoud R (2022) Structural health assessment of pavement sections in the southern central United States using FWD parameters. Front. Built Environ. 8:1026469. doi: 10.3389/fbuil.2022.1026469

23. Behiry, A. E. A. E. M. (2012). Fatigue and rutting lives in flexible pavement. Ain Shams Engineering Journal, 3(4), 367-374.

24. Benkelman, A. C., Kingham, R. I., & Fang, H. Y. (1962). Special Deflection Studies on Flexible Pavement. HRB Spec. Rept, 73, 102-125.

25. Beriha, B., Sahoo, U. C., & Steyn, W. J. (2019). Determination of endurance limit for different bound materials used in pavements: a review. International Journal of Transportation Science and Technology, 8(3), 263-279.

26. Biligiri, K. P., & Said, S. H. (2015). Prediction of the remaining fatigue life of flexible pavements using laboratory and field correlations. Journal of Materials in Civil Engineering, 27(7), 04014201.

27. Biswas, P & Sahis, Manoj & Mandal, G & Majumder, D. (2017). A mechanistic empirical design concept for low volume flexible pavement using unbound granular materials with application of concentration factor in a layered system. 531-536. 10.1201/9781315100333-76.

28. Biswas, P. P. (2005). Mechanistic-Empirical Design of bituminous pavement using concentration factor in a two-layered system. (Ph.D. thesis), Jadavpur University, Kolkata, India, 2005.

29. Biswas, P. P., & Das, S. C. (1999). Geotechnical aspects on failure of flexible pavements. In Twelfth European Conference on Soil Mechanics and Geotechnical Engineering (Proceedings) The Netherlands Society of Soil Mechanics and Geotechnical Engineering; Ministry of Transport, Public Works and Water Management; AP van den Berg Machine fabriek; Fugro NV; GeoDelft; Holland Rail consult (No. Volume 2).

30. Biswas, P. P., Das, S. C., & Saraswati, S. (1998). A Model on Prediction of Flexible Pavement Behaviour. Indian Highways, 26(9).

31. Biswas, P. P., Das, S.C., and Saraswati, S. (1998b). "Influence of subgrade strength on vertical compressive strain in a two layered system." International Conference on Theoretical, Applied and Computational Mechanics, IIT Kharagpur, India.

32. Biswas, P. P., Sahis, M. K., & Sengupta, A. (2021). Determination of Compacted Subgrade Thickness on Weak Subgrade Using Odemark's Method Based on Mechanistic-Empirical Design Approach. In Proceedings of the Indian Geotechnical Conference 2019: IGC-2019 Volume V (pp. 79-87). Springer Singapore.

33. Biswas.P.P, Sahis.M.K., Mondal.G.C, & Majumdar.D. (2016), "Design of Low Volume Rural Roads with Unbound Granular Materials using Odemark's Method", International Journal of Engineering Research & Technology (IJERT) Volume 05, Issue 06.

34. Boussinesq.V.J. (1885) "Application des Potentielsal'etude de l'equilibre, et du movement des solid eselastiques avec des notes etenduessur divers points de physique mathematique et d'analyse.Gauthier-Villars." Paris.

35. Brito, L. A. T., Dawson, A. R., & Kolisoja, P. J. (2009). Analytical evaluation of unbound granular layers in regard to permanent deformation. Proceedings of the 8th International on the Bearing Capacity of Roads, Railways, and Airfields (BCR2A'09), Champaign IL, USA, 187-196.

36. Bryce, J., Flintsch, G., Katicha, S., & Diefenderfer, B. (2013). Enhancing network-level decision making through the use of a structural capacity index. Transportation research record, 2366(1), 64-70.

37. Burmister, D. M. (1943). "The Theory of Stresses and Displacements in Layered Systems and Applications to the Design of Airport Runways." Proceedings, Highway Research Board, Vol. 23, pp. 126-144.

38. Burmister, D. M. (1945). The general theory of stresses and displacements in layered systems. I. Journal of applied physics, 16(2), 89-94.

39. Burmister, D. M. (1956). Stress and displacement characteristics of a two-layer rigid base soil system: influence diagrams and practical applications. In Highway Research Board Proceedings (Vol. 35).

40. Burmister, D. M. (1958). Evaluation of pavement systems of the WASHO road test by layered system methods. Highway Research Board Bulletin, (177).

41. Burmister, D. M., Palmer, L. A., Barber, E. S., & Middle brooks, T. A. (1944). The theory of stress and displacements in layered systems and applications to the design of airport runways. In *Highway Research Board Proceedings* (Vol. 23).

42. Cao, W., Norouzi, A., & Kim, Y. R. (2016). Application of viscoelastic continuum damage approach to predict fatigue performance of Binzhou perpetual pavements. Journal of Traffic and Transportation Engineering (English Edition), 3(2), 104-115.

43. Carpenter, S. H., &Shen, S. (2006). Dissipated energy approach to study hot-mix asphalt healing in fatigue. Transportation Research Record, 1970(1), 178-185.

44. Chen, Can & Zhang, Jie. (2010). A Review on Flexible Pavement Performance Life Assessment. Geotechnical Special Publication. 2561-2570. 10.1061/41095(365)260.

45. Claessen, A. I. M., Edwards, J. M., Sommer, P., & Uge, P. (1977, January). Asphalt pavement design--the shell method. In Volume I of proceedings of 4th International Conference on Structural Design of Asphalt Pavements, Ann Arbor, Michigan, August 22-26, 1977 (No. Proceeding).

46. Congress, I. R. (1981). Tentative guidelines for strengthening of flexible road pavements using Benkelman beam deflection technique. IRC: 81-1981.

47. Congress, I. R. (2001). Guidelines for the design of flexible pavements. Indian code of practice, IRC, 37.

48. Congress, I. R. (2012). IRC: 37-2012, Guidelines for the Design of Flexible Pavements. In Indian Roads Congress, New Delhi, India.

49. Congress, I. R. (2015). Guidelines for the design of flexible pavements for low volume rural roads. IRC SP, 72.

50. Congress, I. R. (2015). Guidelines for the design of flexible pavements for low volume rural roads. IRC SP, 72.

51. Congress, I. R. (2018). IRC: 37: 2018-Guidelines for the design of flexible pavements. IRC, New Delhi, India.

52. Dalla Valle, P., & Thom, N. (2018). Improvement to method of equivalent thicknesses (MET) for calculation of critical strains for flexible pavements. International Journal of Pavement Engineering, 19(12), 1053-1060.

53. Das, A. (2015). Structural design of asphalt pavements: Principles and practices in various design guidelines. Transportation in Developing Economies, 1, 25-32.

54. Dawson, A. R., Kolisoja, P., Vuorimies, N., & Saarenketo, T. (2007). Design of low-volume pavements against rutting: simplified approach. Transportation research record, 1989(1), 165-172.

55. Dicdican, R. Y., Haimes, Y. Y., & Lambert, J. H. (2004). Risk-based asset management methodology for highway infrastructure systems (No. FHWA/VTRC 04-CR11). Virginia Transportation Research Council.

56. Dilip, D. M., & Babu, G. S. (2023). System reliability-based design optimization of flexible pavements using adaptive meta-modelling techniques. Construction and Building Materials, 367, 130351.

57. Dilip, Deepthi & Babu, G.. (2022). System Reliability-Based Design Optimization of Flexible Pavements Using Adaptive Meta-Modelling Techniques. SSRN Electronic Journal. 10.2139/ssrn.4141926.

58. E.Horak. (2006). Application of Equivalent-Layer- Thickness Concept in a Mechanistic Rehabilitation Design Procedure. Transportation Research Record 1207, pp 69-74.

59. El-Ashwah, A. S., Mousa, E., El-Badawy, S. M., & Abo-Hashema, M. A. (2022). Advanced characterization of unbound granular materials for pavement structural design in Egypt. International Journal of Pavement Engineering, 23(2), 476-488.

60. El-Badawy, S. M., & Kamel, M. A. (2011). Assessment and improvement of the accuracy of the Odemark transformation method. *International Journal of Advanced Engineering Sciences and Technologies*, *5*(2), 105-110.

61. Elbagalati, O., Elseifi, M. A., Gaspard, K., & Zhang, Z. (2016). Prediction of in-service pavement structural capacity based on traffic-speed deflection measurements. Journal of Transportation Engineering, 142(11), 04016058.

62. El-Hakim, M. Y., & Tighe, S. (2012). Perpetual pavement designs: The sustainable alternative for highway design. In Proceedings of the 2012 Annual Conference of the Canadian Society for Civil Engineering, Volume 2 (pp. 1585-1594). Canadian Society for Civil Engineering.

63. El-Hakim, M. Y., & Tighe, S. L. (2012). Sustainability of perpetual pavement designs: Canadian perspective. Transportation research record, 2304(1), 10-16.

64. Elkins, G. E., Thompson, T., Groeger, J., Visintine, B. A., & Rada, G. R. (2013). Reformulated pavement remaining service life framework (No. FHWA-HRT-13-038). United States. Federal Highway Administration. Office of Infrastructure Research and Development.

65. Erlingsson, S., Rahman, S., & Salour, F. (2017). Characteristic of unbound granular materials and subgrades based on multi stage RLT testing. Transportation Geotechnics, 13, 28-42.[28].Transport in INDIA, Wikipedia (Total goods and passengers travel through INDIA, by roads)

66. Falla, G. C., Leischner, S., Blasl, A., &Erlingsson, S. (2017). Characterization of unbound granular materials within a mechanistic design framework for low volume roads. Transportation Geotechnics, 13, 2-12.

67. Foster, C. R., &Ahlvin, R. G. (1954). Stresses and deflections induced by a uniform circular load. In Highway Research Board Proceedings (Vol. 33).

68. Foster, C. R., &Ahlvin, R. G. (1958). Development of multiple-wheel CBR design criteria. Journal of the Soil Mechanics and Foundations Division, 84(2), 1647-1.

69. Gao, Y., Geng, D., Huang, X., Cao, R., & Li, G. (2018). Prediction of remaining service life of asphalt pavement using dissipated energy method. Journal of Transportation Engineering, Part B: Pavements, 144(2), 04018011.

70. Gedafa, D. S., Hossain, M., Miller, R. W., & Steele, D. (2008). Network level pavement structural evaluation using rolling wheel deflectometer (No. 08-2648).

71. Ghanizadeh, A. R. (2016). An optimization model for design of asphalt pavements based on IHAP code number 234. Advances in Civil Engineering, 2016.

72. Ghazi G. Al-Khateeb and Nagham Y. Khadour (2020) Distress-based PSI Models for Asphalt Pavements of Rural Highways. Jordan Journal of Civil Engineering, Volume 14, No. 2, 2020 - 281 – 293.

73. Ghosh.I et al (2005) .Reliability Analysis of Pavements-State of the Art, Proceedings of All India Science, Technology and Engineering Students Academic Meet 2005, Bengal Engineering and Science University, Shibpur, Howrah, India,(2005) pp. 84-89.

74. González, A., Chamorro, A., Barrios, I., & Osorio, A. (2018). Characterization of unbound and stabilized granular materials using field strains in low volume roads. Construction and Building Materials, 176, 333-343.

75. Gregory, L. L. (1959). The history of Big Horn County, Wyoming. University of Wyoming.

76. Gupta, A., Kumar, P., & Rastogi, R. (2011). Pavement deterioration and maintenance model for low volume roads. International Journal of Pavement Research and Technology, 4(4), 195.

77. Gupta, A., Kumar, P., & Rastogi, R. (2015). Mechanistic–Empirical approach for design of low volume pavements. International Journal of Pavement Engineering, 16(9), 797-808.

78. Hall, K. D., & Elliott, R. P. (1992). ROADHOG- A flexible pavement overlay design procedure (with discussion and closure) (No. 1374).

79. Harichandran, R. S., Baladi, G. Y., & Yeh, M. S. (1989). Development of a computer program for design of pavement systems consisting of layers of bound and unbound materials. Final report (No. FHWA-MI-RD-89-02)..

80. Harris, F. A. (1956). Selection and Design of Semi-Flexible and Conventional Type Pavements. In HRB Proc (Vol. 35, pp. 110-138).

81. Hoffman, M. S. (2008). Extension of the YONAPAVE Method for Determining Flexible Pavements Overlay Thickness from Falling-Weight Deflectometer Deflections.

82. Hoffman, M. S. (2003). Direct method for evaluating structural needs of flexible pavements with falling-weight deflectometer deflections. Transportation Research Record, 1860(1), 41-47.

83. Horak, E. (2008). Benchmarking the structural condition of flexible pavements with deflection bowl parameters. Journal of the South African Institution of Civil Engineering, Vol 50 No 2, 2008, Pages 2–9, Study 652.

84. Horak, E.(1988).Application of Equivalent-Layer-Thickness concept in a mechanistic rehabilitation design procedure, Transp. Res. Rec. 1207 (1988) 69–75.

85. Horak, Emile, Hefer, Arno, Maina, James, Emery, Steve & Kubu,. (2014). Structural number determined with the falling weight deflectometer and used as benchmark Methodology. December 2014, DOI: 10.13140/2.1.1459.6165, Conference: CEEE 2014 Hong Kong, At Kowloon, Hong Kong, Volume: Proceedings.

86. https://morth.nic.in/sites/default/files/circulars_document/request-by-bidurkant.pdf

87. Huang, Y,H .(2004)."Pavement Analysis and Design." Pearson Prentice Hall, 2004, Edition: 2, ISBN: 0131424734, 9780131424739.

88. Huang, Y. H. (1969). Influence charts for two-layer elastic foundations. Journal of the Soil Mechanics and Foundations Division, 95(2), 709-713.

89. Huang, Y. H. (1984). KENTRACK, a computer program for hot-mix asphalt and conventional ballast railway track beds (No. 105).

90. Huang, Y. H., Lin, C., & Rose, J. G. (1984). Asphalt pavement design: Highway versus railroad. Journal of Transportation Engineering, 110(2), 276-282.

91. Islam, S., Hossain, M., Jones, C. A., Bose, A., Barrett, R., & Velasquez Jr, N. (2019). Implementation of AASHTOWare Pavement ME Design Software for Asphalt Pavements in Kansas. Transportation Research Record, 2673(4), 490-499.

92.   Islam, S., Sufian, A., Hossain, M., Miller, R., & Leibrock, C. (2020). Mechanistic-Empirical design of perpetual pavement. Road Materials and Pavement Design, 21(5), 1224-1237.

93.   István Fi, I., Szentpéteri, I. (2013). A Mechanistic-Empirical Approach for Asphalt Overlay Design of Asphalt Pavement Structure. Periodica polytechnic, Civil Engineering 58/1 (2014) 55–62, DOI: 10.3311/PPci.7408.

94.   Karballaeezadeh, N., Mohammadzadeh S, D., Shamshirband, S., Hajikhodaverdikhan, P., Mosavi, A., &Chau, K. W. (2019). Prediction of remaining service life of pavement using an optimized support vector machine (case study of Semnan–Firuzkuh road). Engineering Applications of Computational Fluid Mechanics, 13(1), 188-198.

95.   Kentucky, 1976, "A Flexible Pavement Design and Management System, Bureau of Highways, Department of Transportation", CommonWealth of Kentucky, 4th International Conference on Structural Design of Asphalt Pavement.

96.   Khiavi, A. K., & Ameri, M. (2013). Laboratory evaluation of strain controlled fatigue criteria in hot mix asphalt. Construction and Building Materials, 47, 1497-1502.

97.   Khweir, K., A. (2012). United Kingdom Overlay Design of Flexible Pavement: Determination of the Important Parameters.Eng1, DOI: 10.1061/(ASCE)TE.1943-5436.0000340.

98.   Kim, W. J., Park, C. K., Son, T. T., Phuc, L. V., & Lee, H. J. (2017). Improvement and Validation of an Overlay Design Equation in Seoul. International Journal of Highway Engineering, 19(5), 49-58.

99.   Kinchen, R. W., & Temple, W. H. (1980). Asphaltic concrete overlays of rigid and flexible pavements (No. Research Report No. FHWA/LA-80/147). Louisiana. Department of Highways. Research and Development Section.

100. Kollaros, G., Athanasopoulou, A., & Kokkalis, A. (2017). Perpetual flexible pavement design life. In Bearing Capacity of Roads, Railways and Airfields (pp. 537-542). CRC Press.

101. Kulkarni, S., & Ranadive, M. (2021, May). Effect of change in the resilient modulus of bituminous mix on the design of flexible perpetual pavement. In Techno-Societal 2020: Proceedings of the 3rd International Conference on Advanced Technologies for Societal Applications—Volume 1 (pp. 829-838). Cham: Springer International Publishing.

102. Le, V. P., Lee, H.J., Flores, J.M., Baek, J., Park, H.M (2016) Development of a simple asphalt concrete overlay design scheme based on a mechanistic-empirical approach, Road Materials and Pavement Design, 18:3, 630-645, DOI: 10.1080/14680629.2016.1182059.

103. Lee, S. I., Carrasco, G., Mahmoud, E., &Walubita, L. F. (2020). Alternative structure and material designs for cost-effective perpetual pavements in Texas. Journal of Transportation Engineering, Part B: Pavements, 146(4), 04020071.

104. Leiva-Villacorta, F., Vargas-Nordcbeck, A., & Aguiar-Moya, J. P. (2017). Permanent deformation and deflection relationship from pavement condition assessment. International Journal of Pavement Research and Technology, 10(4), 352-359.

105. Li, X. Y., Zhang, R., Zhao, X., & Wang, H. N. (2014). Sensitivity analysis of flexible pavement parameters by mechanistic-empirical design guide. Applied Mechanics and Materials, 590, 539-545.

106. Liao, J., &Sargand, S. (2010). Viscoelastic FE modeling and verification of a US 30 perpetual pavement test section. Road materials and pavement design, 11(4), 993.

107. Lister, N. W., & Powell, W. D. (1987). Design practice for bituminous pavements in the United Kingdom. In International Conference on The Structural Design.

108. Loganathan, K., Isied, M. M., Coca, A. M., Souliman, M. I., Romanoschi, S., & Dessouky, S. (2019). Development of comprehensive deflection parameters to evaluate the structural capacity of flexible pavements at the network level. International Journal of Pavement Research and Technology, 12, 347-355.

109. Lopes, F. M. and R. Fortes. (2013). Flexible pavements – structural evaluation based on deflection basin parameters. International Journal of Pavements Conference, São Paulo, Brazil, pp-163-1-8.

110. M. Robbins, M., H. Tran, N., H. Timm, D., & Richard Willis, J. (2015). Adaptation and validation of stochastic limiting strain distribution and fatigue ratio concepts for perpetual pavement design. Road Materials and Pavement Design, 16(sup2), 100-124.

111.   Maji, A., & Das, A. (2008). Reliability considerations of bituminous pavement design by mechanistic–empirical approach. International Journal of Pavement Engineering, 9(1), 19-31.

112.   Mazumder, M., Kim, H., & Lee, S. J. (2015). Perpetual pavement: future pavement network. J. Adv. Constr. Mater, 19(1), 35-49.

113.   Ministry of Rural Development. Specification for Rural Roads, Indian Road Congress (2014).

114.   Mishra, S., Sachdeva, S. N., & Manocha, R. (2019). Subgrade soil stabilization using stone dust and coarse aggregate: a cost effective approach. International Journal of Geosynthetics and Ground Engineering, 5, 1-11.

115.   Moayed, R. Z., Allahyari, F., & Nazari, M. (2012). Effect of the sand layer thickness on the CBR values of two layered subgrade. In Proceedings of 3rd international conference on new developments in soil mechanics and geotechnical engineering. Near East University, Nicosia, North Cyprus (pp. 437-444).

116.   Moudjari, Maroua & Belachia, Mouloud. (2019). Comparative Study of the Deflection of a Flexible Pavement Under the Effect of a Low Traffic. International Review of Civil Engineering (IRECE). 10. 249. 10.15866/irece.v10i5.16539.

117.   Mu, Y., Fang, L., & Liu, J. (2018). Simulation and Study of the Incinerator's Combustion Control System. In Proceedings of 2017 Chinese Intelligent Systems Conference: Volume II (pp. 453-462). Springer Singapore.

118.   Mukabi, J. N. (2015). Quantitative Delineation of the Structural Role of the Subgrade Stiffness and Thickness in Pavements. Electronic Pre-Print: dr. eng.mukabi@ academia. edu website.

119.   Mukabi, J. N. (2016). Mechanistic Approach of Determining Structural Subgrade Thickness. Electronic Pre-Print: dr. eng.mukabi@ academia. edu website.

120.   Narasimham, K. V., Misra, R., & Das, A. (2001). Optimization of bituminous pavement thickness in mechanistic pavement design. International Journal of Pavement Engineering and Asphalt Technology, 2(2), 59-72.

121.   Nataatmadja, A., Tao, S. Y., & Chim, K. (2012, September). Design subgrade CBR for flexible pavements: Comparison of predictive methods. In ARRB Conference, 25th, 2012, Perth, Western Australia, Australia.

122. National Cooperative Highway Research Program (NCHRP) (1972). 128 Report Evaluation of AASHO Interim Guides for Design of Pavement Structures. Highway Research Board.

123. Naughton, P., Hall, Gerard. (2019). Pavement condition from falling-weight deflectometer testing. Proceedings of the Irish Transport Research Network Conference, September 2019, Belfast.

124. Newcomb, D. E., Buncher, M., & Huddleston, I. J. (2001). Concepts of perpetual pavements. Transportation Research Circular, 503, 4-11.

125. Newcomb, D. E., Willis, R., &Timm, D. H. (2010). Perpetual asphalt pavements: A synthesis.

126. Odemark, N. (1949). Investigations as to the Elastic Properties of Soils and Design of Pavements According to the Theory of Elasticity (No.Meddelande 77).

127. Operational Manual (2005). National Rural Road Development Agency. February '2005.

128. Park, H.M., & Kim, Y.R. (2003). Prediction of Remaining Life of Asphalt Pavement with Falling-Weight Deflectometer Multi load -Level Deflections. Transportation Research Record, 1860, 48 - 56.

129. Park, S. H., & Kim, J. H. (2019). Comparative analysis of performance prediction models for flexible pavements. Journal of Transportation Engineering, Part B: Pavements, 145(1), 04018062.

130. Peddinti, P. R., & Sireesh Saride, B. M. (2017, December). Effect of Probability Density Functions on Reliability Analysis of Flexible Pavement. In Indian Geotechnical Conference, GeoNEst (pp. 14-16)..

131. Powell, W. D., Potter, J. F., Mayhew, H. C., & Nunn, M. E. (1984). The structural design of bituminous roads (No. LR 1132 Monograph).

132. Pratama, S., Cahyono, A. D., Saputra, C. D., Lestari, L. B., Laso, P. B., Putri, F. A., & Febyningtyas, P. R. (2022). An Easy Way To Determine The Flexural Quality Of Asphalt Is Using ASTM D113–07 and SNI 2432: 2011. Civilla: Journal Teknik Sipil Universitas Islam Lamongan, 7(1), 1-12.

133. Pratibha, R., SivakumarBabu, G. L., & Madhavi Latha, G. (2015). Stress–strain response of unbound granular materials under static and cyclic loading. Indian Geotechnical Journal, 45, 449-457.

134. Priyanka, B. A., Sarang, G., & Ravi Shankar, A. U. (2019). Evaluation of Superpave mixtures for perpetual asphalt pavements. Road Materials and Pavement Design, 20(8), 1952-1965.

135. Prowell, B. (2010). Validating the Fatigue Endurance Limit for Asphalt Pavements. HMAT: Hot Mix Asphalt Technology.

136. Pryke, A., Evdorides, H., & Ermaileh, R. A. (2006, July). Optimization of pavement design using a genetic algorithm. In 2006 IEEE International Conference on Evolutionary Computation (pp. 1095-1098). IEEE.

137. Purakayastha, S., Biswas, P. P., & Sahis, M. K. (2020). Determination of bituminous overlay thickness of flexible pavement by mechanistic-empirical approach based on concentration factor. International Journal of Pavement Research and Technology, 13, 222-227.

138. Purakayastha, S., Biswas, P. P., Sahis, M. K., & Mondal, G. C. (2022). Characterization of Layer Index in Bituminous Pavement Using Mechanistic-Empirical Approach Based on Concentration Factor in a Layered System. In Proceedings of the RILEM International Symposium on Bituminous Materials: ISBM Lyon 2020 1 (pp. 347-354). Springer International Publishing.

139. Putri, E. E., Rao, N. K., & Mannan, M. A. (2017). Determination of pavement thickness based on threshold stress of the subgrade soil. Int. J. Civil Eng. Technol, 8(10), 753-761.

140. Qadir, A., Gazder, U., & Ali, S. (2018). Comparison of SBS and PP fibre asphalt modifications for rutting potential and life cycle costs of flexible pavements. Road Materials and Pavement Design, 19(2), 484-493.

141. Rabbi, M. F., & Mishra, D. (2021). Using FWD deflection basin parameters for network-level assessment of flexible pavements. International Journal of Pavement Engineering, 22(2), 147-161.

142. Rada, G. R., Smith, D. R., Miller, J. S., &Witczak, M. W. (1990). Structural design of concrete block pavements. Journal of transportation engineering, 116(5), 615-635.

143. Rahman, M. S., & Erlingsson, S. (2015). Predicting permanent deformation behaviour of unbound granular materials. International Journal of Pavement Engineering, 16(7), 587-601.

144. Rajbongshi, P., & Das, A. (2008). Optimal asphalt pavement design considering cost and reliability. Journal of Transportation Engineering, 134(6), 255-261.

145. Reddy, K. S. (1993). Analytical evaluation of bituminous pavements (Doctoral dissertation, IIT, Kharagpur).

146. Reddy, M. A., Reddy, K. S., & Pandey, B. B. (2001). Design CBR of subgrade for flexible pavements. Highway Research Bulletin, 2001, 61-69.

147. Romanoschi, S. A., Gisi, A. J., Portillo, M., & Dumitru, C. (2008). First findings from the Kansas perpetual pavements experiment. Transportation Research Record, 2068(1), 41-48.

148. Ruge, Juan & Rondón-Quintana, Hugo & Bastidas-Martínez, J. (2022). Assessment of the asphalt mixtures properties subjected to a flexural strength. Journal of Physics: Conference Series. 2153. 012001. 10.1088/1742-6596/2153/1/012001.

149. Sabouri, M. (2020). An investigation on perpetual asphalt pavements in Minnesota. International Journal of Pavement Research and Technology, 13, 247-254.

150. Sahis, M. K., & Biswas, P. P. (2021). Optimization of bituminous pavement thickness using mechanistic-empirical strain-based design approach. Civil Engineering Journal, 7(5), 804-815.

151. Sahis, M. K., Biswas, P. P., & Saha, G. (2021). Mechanistic-Empirical Design of Overlay Based on Vertical Interface Stress and Curvature Index of Deflection Basin. Jordan Journal of Civil Engineering, 15(3).

152. Sahis, M. K., Biswas, P. P., Sadhukhan, S., & Saha, G. (2023). Mechanistic-empirical Design of Perpetual Road Pavement Using Strain-based Design Approach. Periodica Polytechnica Civil Engineering, 67(4), 1105-1114.

153. Sahoo, U. C., & Reddy, K. S. (2011). Performance criterion for thin-surface low-volume roads. Transportation research record, 2203(1), 178-185.

154. Sakhaeifar, M. S., Brown, E. R., Tran, N., & Dean, J. (2013). Evaluation of long-lasting perpetual asphalt pavement with life-cycle cost analysis. Transportation research record, 2368(1), 3-11.

155. Saleh Mofreh (2016). "A Mechanistic-Empirical Approach for the Evaluation of the Structural Capacity and Remaining Service Life of Flexible Pavements at the Network Level." Canadian Journal of Civil Engineering. University of Canterbury, Civil, and Natural Resources.

156. Sanchez-Silva, M., Arroyo, O., Junca, M., Caro, S., & Caicedo, B. (2005). Reliability based design optimization of asphalt pavements. The International Journal of Pavement Engineering, 6(4), 281-294.

157. Sanjay, R., Tejeshwini, S., Mamatha, K. H., & Dinesh, S. V. (2022). Comparative study on structural evaluation of flexible pavement using BBD and FWD. Materials Today: Proceedings, 60, 608-615.

158. Saride, S., Peddinti, P. R., & Basha, M. B. (2019). Reliability perspective on optimum design of flexible pavements for fatigue and rutting performance. Journal of Transportation Engineering, Part B: Pavements, 145(2), 04019008.

159. Sarker, P., & Tutumluer, E.(2015). Development of improved overlay thickness design alternatives for local roads. Illinois Center for Transportation Series No. 15-008/Research Report No. FHWA-ICT-15-008.

160. Sarker, P., Tutumluer, E., & Lackey, S. (2016). Nondestructive Deflection Testing based Mechanistic-Empirical Overlay Thickness Design Approach for Low Volume Roads: Case Studies. Procedia engineering, 143, 945-953.

161. Scheer, M. J. (2013). Impact of Pavement Thickness on Load Response of Perpetual Pavement (Doctoral dissertation, Ohio University).

162. Selvaraj, I. (2006). A practical guide to low-volume road perpetual pavement design.

163. Setiadji, Bh. (2018). Application of deflection bowl parameters for assessing different structures of road pavement. MATEC Web of Conferences. 195. 04002.10.1051/matecconf/201819504002.

164. Shell, 1985. Shell Pavement Design Manual −Asphalt Pavements and Overlay for Road Traffic, Shell International Petroleum, London.

165. Sidess, A., & Uzan, J. (2009). A design method of perpetual flexible pavement in Israel. International Journal of Pavement Engineering, 10(4), 241-249.

166. Singh, A. K., &Sahoo, J. P. (2020). Analysis and design of two layered flexible pavement systems: A new mechanistic approach. Computers and Geotechnics, 117, 103238.

167. Singh, A., Sharma, A., & Chopra, T. (2020). Analysis of the flexible pavement using falling weight deflectometer for Indian National Highway road network. Transportation Research Procedia, 48, 3969-3979.

168. Solanki, U., Gundaliya, P., & Barasara, M. (2016). Structural evaluation of flexible pavement using falling-weight deflectometer. In Multi-disciplinary Sustainable Engineering: Current and Future Trends (pp. 141-146). CRC Press.

169. Soós, Z., &Tóth, C. (2017). Simple overlay design method for thick asphalt pavements based on the method of equivalent thicknesses. Periodica Polytechnica Civil Engineering, 61(3), 389-397.

170. Subagio, B. S., Cahyanto, H. T., Rachman, A., & Mardiyah, S. (2005). Multi-Layer Pavement Structural Analysis Using Method of Equivalent Thickness Case Study: Jakarta-Cikampek Toll Road. Journal of the Eastern Asia Society for Transportation Studies, 6, 55-65.

171. Sultan, S. A., & Guo, Z. (2016). Evaluating life cycle costs of perpetual pavements in China using operational pavement management system. International Journal of Transportation Science and Technology, 5(2), 103-109.

172. Tarefder, R. A., & Bateman, D. (2012). Design of optimal perpetual pavement structure. Journal of transportation engineering, 138(2), 157-175.

173. Tarefder, R. A., Saha, N., Hall, J. W., & Ng, P. T. (2008). Evaluating weak subgrade for pavement design and performance prediction: A case study of US 550. Journal of Geo-Engineering, 3(1), 13-24.

174. Thompson, M. R., & Carpenter, S. H. (2006, September). Considering hot-mix-asphalt fatigue endurance limit in full-depth mechanistic-empirical pavement design. In Proc., International Conference on Perpetual Pavement.

175. Thube, D. T. (2006). Performance based maintenance management for rural roads. Unpublished thesis (PhD).Indian Institute of Technology Roorkee, India, July.

176. Titi, H. H., & Matar, M. G. (2018). Estimating resilient modulus of base aggregates for Mechanistic-Empirical pavement design and performance evaluation. Transportation Geotechnics, 17, 141-153.

177. Tohidi, M., Khayat, N., & Telvari, A. (2022). The use of intelligent search algorithms in the cost optimization of road pavement thickness design. Aim Shams Engineering Journal, 13(3), 101596.

178. Transportation Officials. (1993). AASHTO Guide for Design of Pavement Structures, 1993 (Vol. 1). AASHTO.
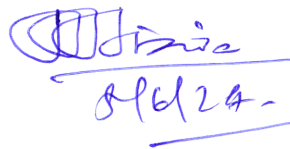
179. Tsiknas, A., Athanasopoulou, A., & Papa Georgiou, G. P. (2020, February). Evaluation of flexible pavement construction cost according to the design method. In Proceedings of the Institution of Civil Engineers-Transport (Vol. 173, No. 1, pp. 3-12). Thomas Telford Ltd.

180. Tutumluer, E., & Sarker, P. (2015). Development of improved overlay thickness design alternatives for local roads (No. FHWA-ICT-15-008). Illinois Center for Transportation.

181. Ullidtz P. "Modelling flexible pavement response and performance". Denmark: Tech Univ. of Denmark Polytekn; 1998.

182. URS Corp (2000), " Pavement performance prediction models." Interim Rep prepared for Kansas, Department of Transportation, Kansas Department of Transportation, Topeka, Kan.

183. US Army Engineer Waterways Experiment Station, Brown, D. N., & Ahlvin, R. G. (1961). Revised Method of Thickness Design for Flexible Highway Pavements at Military Installations.

184. Verstraeten, J. (1967, August). Stresses and Displacements in Elastic Layered Systems. General Theory-Numerical Stress Calculations in Four-Layered Systems with Continuous Interfaces. In Intl Conf Struct Design Asphalt Pvmts.

185. Von Quintus, H. L. (2001). Hot-mix asphalt layer thickness design for longer-life bituminous pavements. Transportation research circular, 503, 66-78.

186. Warren, H., & Dieckmann, W. L. (1963). Numerical computation of stresses and strains in a multiple-layer asphalt pavement system. International Report, Chevron Research Corporation, Richmond, CA.

187. Willis, J.R. (2009). Field-based strain thresholds for flexible perpetual pavement design.

188. Witczak, M. W. (1978). Determination of Flexible Pavement Life. Executive Summary, Vol. I. FHWA Rep. No. FHWA/MD.

189. Xiao, Y., Zhang, Z., Chen, L., & Zheng, K. (2018). Modeling stress path dependency of cyclic plastic strain accumulation of unbound granular materials under moving wheel loads. Materials & Design, 137, 9-21.

190. Yang, Y., Gao, X., Lin, W., F, D. H., Priest, A. L., Huber, G. A., & Andrewski, D. A. (2005). Perpetual pavement design in China. In International Conference on F Pavement, Ohio Research Institute for Transportation and the Environment.

191. Yoder et al. (1975): "Principle of Pavement Design". Wiley, New York (1975).

192. Yoder, E. J., &Witczak, M. W. (1991). "Principles of pavement design". John Wiley & Sons.

193. Yoder, E. J., and Witczak, M. W. (1975). "Principles of pavement design." Second Ed., John Wiley and Sons, New York, N.Y.

194. Zhang, W., & Macdonald, R. A. (2000). Modeling pavement response and estimating pavement performance. In Proceedings of the First International Conference on Accelerated Pavement Testing, Reno, NV.

195. Zofka, A., Sudyka, J., & Sybilski, D. (2017). Assessment of pavement structures at traffic speed. In Bearing Capacity of Roads, Railways and Airfields (pp. 585-588). CRC Press.

Dr. Partha Pratim Biswas
Professor
Department of Construction Engineering
Jadavpur University